Extrinsic and intrinsic factors regulate the spatio-temporal localisation of the Arabidopsis circadian component ELF3

James Ronald

Doctor of Philosophy

University of York

Biology

March 2021

Abstract

Circadian clocks are biological timekeeping mechanisms that integrate environmental signals to coordinate internal responses to occur at the most optimal time of the day. The plant circadian clock is composed of a series of autoregulatory feedback loops. Within these loops, EARLY FLOWERING3 (ELF3) has emerged as a critical regulatory hub. ELF3 recruits ELF4 and LUX ARRYTHMO (LUX) to form the evening complex (EC), a protein complex that represses gene expression. The EC is essential for the functionality and integration of environmental stimuli into the plant circadian clock. In recent years, we have developed a strong understanding of how the EC represses gene expression. In contrast, how the activity of the EC is regulated has remained poorly understood.

Changing the localisation of proteins within the cell is an emerging regulatory mechanism in light, temperature and circadian signalling in plants. In this thesis, I explored how the cellular dynamics of ELF3 are regulated. I found that the nuclear and sub-nuclear localisation of ELF3 is responsive to red (RL), blue and far-red light and warm temperature pulses. Further analysis of how RL-pulses controlled ELF3 localisation revealed two separate signalling pathways, one which is dependent on phytochromeB (phyB), while the other occurs independently of phyB.

I also investigated the contribution of ELF4 in controlling the localisation of ELF3 in response to light and warm temperature pulses. For all pulses that were tested, I observed no specific requirement for ELF4. However, I did find that ELF4 has a general role in promoting both the nucler and sub-nuclear localisation of ELF3. The importance of ELF4 was tissue-specific, with ELF4 having a more critical role in hypocotyl nuclei than root nuclei. Together, this thesis provides a new interface to understand how environmental signals are integrated into the oscillator and regulate the activity of plant circadian clock components.

Lists of Contents

Lists of Figures

List of Tables

Acknowledgements

I would like to formally thank the BBSRC Whiterose DTP and the University of York Biology Department for providing funding and access to facilities, respectively, during this PhD. I would also like to extend my thanks to members of staff within the York Biology Imaging and Cytometry, and Genomics technology facilities for their training, technical support and invaluable experimental advice. Finally, I would also like to thank the Biology Horticulture team for all their assistance throughout the last ~4.5 years. Who knew growing Arabiodpsis, a weed after all, could be so troublesome in controlled conditions.

I would also like to thank the people who have made this PhD possible. Firstly, to my primary supervisor Prof. Seth Davis, thank you for your endless patience, guidance and off-track discussions. I'm especially grateful for you allowing me the opportunity to carry out my research without boundaries or restrictions. To my co-supervisor Prof. Tony Wilkinson, I'm grateful for all your continued support and guidance throughout the PhD even though this thesis may have drastically changed from what we both originally invisaged at the beginning. Having you as a non-plant scientist sounding board has improved my research and writing for the better. I would also like to thank my thesis advisory panel members Prof. Bob White and Prof. Katherine Denby for their feedback throughout my PhD.

To the members of the Davis, Harper, Mackinder and Ezer groups who I have met and worked alongside in the last ~4.5 years, thank you for making L2 a pleasant working environment. In particular, Mandi, thank you for your endless patience in the face of what must have seemed never ending questions in the early period of my PhD. Your advice and technical support was invaluable, while the endless supply of sugary food was a much appreciated added bonus. Sarah and Liam, as well, thank you for making our corner of L2 an enjoyable location to work from.

To family and friends, I'm grateful for your support throughout. In particular, Chloe, thank you for your never ending support and bountyless patience in listening to

me talk endlessly about elves, lights and all other manner of PhD-related nonsense for the last ~4.5 years. You have made this process far easier. Nicola and Lewis, the PhD would have been a much worse experience without your friendship. Thank you both for the providing the room to vent and get grumpy when things stopped working.

Finally, this work is dedicated to the memory of three people for without whom it would have been impossible for me to even consider doing a BSc or masters, let alone a PhD. Thank you.

Authorship Declaration

Some of the work in this thesis has been adapted from peer-reviewed work that I have published or have submitted for publication during my PhD. I was solely responsible for writing the manuscripts, with the other listed authors responsible for providing edits to the manuscript. Other than these situations listed below, I declare that this thesis is a presentation of original work and I am the sole author. This work has not previously been presented for an award at this, or any other, University. All sources are acknowledged as references.

Chapter 1

Some of the work in this chapter has been adapted from peer-reviewed review articles that I published during my PhD. The sections that were adapted from the respective manuscripts for this introduction are:

1.3.1, 1.3.2 and 1.6.: Ronald, J & Davis. SJ. 2017. Making the Clock Tick: The Transcriptional Landscape of the Plant Circadian Clock. *F1000 Reports*. DOI: 10.12688/f1000research.11319.1

1.5 and 1.7: Ronald, J & Davis, SJ. 2019. Focusing on the nuclear dynamics of light and circadian signalling. Plant, Cell and Environment. DOI: 10.1111/pce.13634

Chapter 2

Some of the work in this chapter has been adapted from a book chapter I wrote during my PhD. This book chapter has been accepted and is in press at the time corrections to this thesis were submitted (30th June 2021). The following sections were adapted from this book chapter:

2.2.1 and 2.2.3 – Ronald, J and Davis, SJ. (2020) Measuring Hypocotyl Length in Arabidopsis. In: Davis, A, Davis S and Staiger, D (eds). Circadian Protocols. Methods in Molecular Biology (In Press).

Chapter 5

The work in this chapter was originally submitted for publication in March 2021 as a letter in Plant Physiology. This manuscript has now been provisionally accepted pending minor revision at the time corrections were made to the thesis (30th June 2021). Chapter 5 is a direct replica of the manuscript that was submitted to Plant Physiology for consideration. I note that the Plant Physiology letter includes no distinct sections, and that format has been kept for chapter 5.

The contributions to this manuscript were as followed:
James Ronald (JR), Professor Anthony Wilkinson (AJW), and Professor Seth Davis (SJD) conceived the original research plans; AJW and SJD supervised the experiments; JR performed the experiments; JR wrote the article with contributions of all the authors.

Chapter 1 - Introduction

1.1 Circadian rhythms are a ubiquitous feature of life

The daily rotation of the Earth generates predictable *diel* oscillations in light and temperature. Circadian clocks are internal biological timekeeping mechanisms that have evolved to facilitate the coordination of internal physiological responses to these daily changes in the external environment. This coordination allows biological processes to be precisely timed so that they occur at the most optimal time of the day. The first documentation of circadian rhythms in the scientific literature was in the 18th century, when leaf movements were reported to persist in constant darkness (McClung, 2006). Circadian rhythms have since been documented in bacteria, archaea, protozoa and animals.

The ubiquitous nature of circadian rhythms across all domains of life highlights their critical role in maximising an organism's fitness and productivity. In *Arabidopsis thaliana* (Arabidopsis henceforth), having a circadian clock with an internal cycle length that closely matches the external environment (~24 hours) results in enhanced photosynthetic output, ability to resist pathogen infection and faster growth (Dodd et al., 2005, Wang et al., 2011a). Similar benefits of having a circadian clock are now being described in humans. Our circadian clock defines all aspects of our daily lives, from controlling our sleep-wake cycles, to our periods of maximum physical and cognitive functions. Accordingly, defects in our circadian clock are now causatively linked to increasing our susceptibility to all forms of cancer, diabetes, cardiovascular disease and dementia (Roenneberg and Merrow, 2016). Circadian rhythms also provide fitness benefits to cyanobacteria and there have been reports of circadian rhythms in non-photosynthetic bacteria (Cohen and Golden, 2015, Saini et al., 2019, Eelderink-Chen et al., 2021). Therefore, circadian rhythms may provide a fitness benefit to organisms across multiple different domains of life.

Three properties are used to define the presence of a circadian rhythm in an organism (McClung, 2006). Firstly, circadian clocks must maintain robust rhythms that have an approximate period length of ~24 hours for several days under constant environmental conditions. The second property of a circadian clock is that it must be

entrainable, *i.e.,* circadian clocks must re-set their internal rhythm to match changes in the external environment (for example, changes in the timing of dawn). Entrainment of the circadian clock primarily occurs through detection of the light-dark, warm-cold cycles caused by the daily rotation of the Earth. However, other stimuli that have predictable *diel* oscillations can also entrain the oscillator (Webb et al., 2019, Xie et al., 2019). Finally, the pace of the circadian clock must be buffered against changes in physiological temperature. This process, called temperature compensation, results in circadian clocks maintaining a relatively constant period length of ~24 hours across a range of physiologically relevant temperatures (Kidd et al., 2015). In contrast, normal enzymatic reactions speed up as temperature increases. Together, these three principles are used to establish whether an internal rhythm is circadian or just *diel*.

Though the molecular and biochemical structure of circadian clocks are highly divergent across the domains and kingdoms of life, all circadian clocks can be viewed as composed of three integral parts **(Figure 1.1).** The first part of this three-part system are inputs called *zeitnehmers* (timekeepers). *Zeitnehmers* are sensors that are responsive to daily changes in environmental or internal stimuli called *zeitgebers* (time givers). The stimuli that these *zeitnehmers* respond to include light, temperature, metabolites and ions (Webb et al., 2019, Xie et al., 2019). In plants, the primary *zeitgebers* are light and temperature (Millar, 2004). The detection and response by *zeitnehmers* to changes in *zeitgebers* defines the process of entrainment, whereby the internal circadian cycle is bought into phase alignment with the external environmental cycle. *Zeitnehmers* can either be a core component of the clock or an intermediary receptor that acts as an interface between the circadian clock and the entraining stimuli.

The second element of a circadian clock is the oscillator, the biochemical mechanism that drives circadian rhythms. Circadian oscillators vary in complexity, at their simplest they can be two genes arranged into an autoregulatory feedback loop, while more complex oscillators involve multiple genes arranged into an interconnected network of autoregulatory feedback loops. The mechanisms used to generate circadian

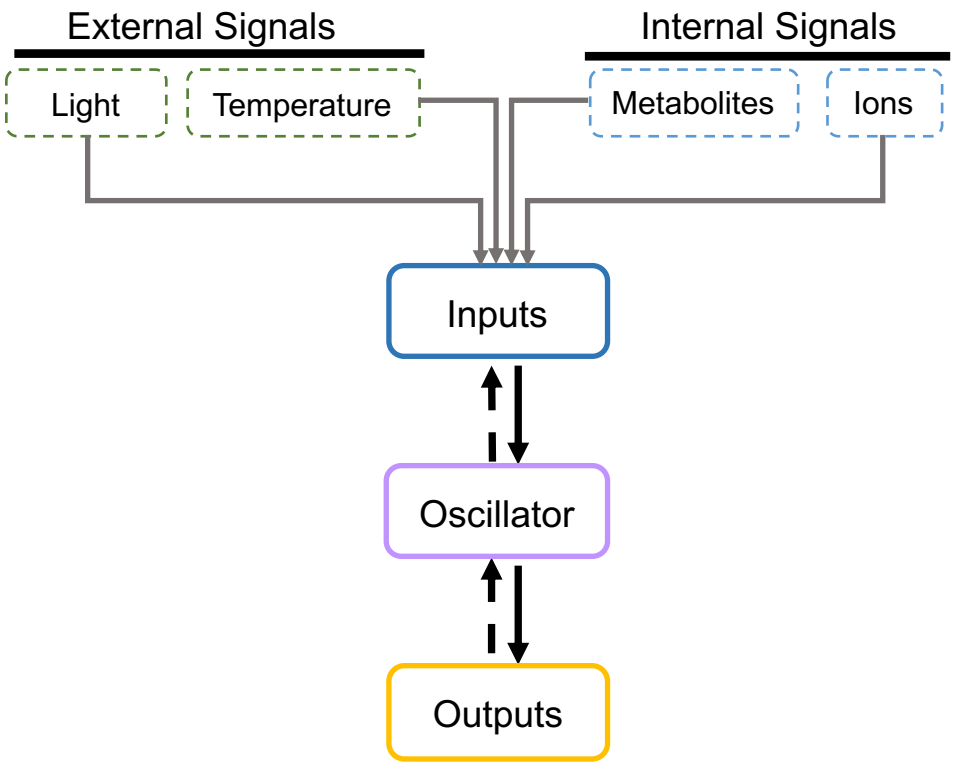

Figure 1.1 - The simplified structure of a circadian system

Circadian clocks can be largely simplified to a three-part system. Inputs (blue) are sensors that recognise external (*e.g.*, light and temperature) or internal (*e.g.*, metabolites and ions) stimuli. The inputs then entrain the oscillator (pink), which then regulates a series of outputs (yellow). A circadian system is usually not a unidirectional system, with outputs reciprocally regulating the oscillator, and the oscillator regulating inputs. This is de-noted by the dashed arrow. It should also be noted that in some circadian systems, inputs can be a part of the oscillator (not showed).

rhythms are highly diverse and have likely evolved independently multiple times. Oscillators can be composed of transcriptional-translational feedback loops (TTFLs) and/or post-translational feedback loops (PTFLs) (Saini et al., 2019). Redox cycles may also represent a secondary, ancestral circadian clock that occurs independently of transcription (O'Neill and Reddy, 2011).

The final component of the circadian clock are outputs. Outputs are unique to each organism, but universal processes under the control of the circadian clock include growth, the response to stress and reproduction (Saini et al., 2019). Circadian systems are not typically a unidirectional system. In many cases, outputs feedback to regulate the activity of the oscillator, while many of the photo- and thermoreceptors that entrain

the oscillator are themselves regulated by the circadian clock (Millar, 2004, Webb et al., 2019). This interconnected nature of the circadian system likely facilitates greater coordination between the clock and environment, maximising the organism's fitness and productivity.

1.2 **Measuring circadian rhythms**

A variety of methods have now been developed to measure circadian rhythms. The primary tool used to investigate circadian rhythms is a genetic construct composed of a circadian regulated gene promoter fused to the firefly LUCIFERASE (LUC) enzyme (henceforth referred to as *pro::LUC)* (Millar et al., 1992, Kondo et al., 1993). The use of *pro::LUC* assays in the circadian community has allowed large advances in understanding circadian rhythms in many different organisms. *pro::LUC* constructs can be transfected or transformed into cells or whole organisms to non-invasively measure circadian rhythms under a wide-range of entrainment and free-running conditions (Millar et al., 1992, Kondo et al., 1993, Feeney et al., 2016). Once the experiment has been set-up, automated data collection allows *pro::LUC* experiments to run for consecutive days with minimal manual involvement. Where not suitable, or to complement *pro*::*LUC* experiments, circadian rhythms at the transcriptional level can also be investigated through techniques such as reverse-transcriptase (RT)-qPCR or RNA-seq. RNA-based analysis methods have the drawback of being both manually intensive (*i.e.,* sample collecting, processing and analysing) and invasive compared to *pro::LUC* assays.

Alongside assays that measure circadian rhythms at the transcriptional level, experimental approaches have also been designed that allow non-invasive measurements of post-translational circadian rhythms. These assays utilise a genetic construct composed of a constitutive promoter (*e.g.,* the *35S* or ubiquitin promoter in plants) fused to the gene of interest and either the LUC enzyme or a fluorescent protein tag (*e.g.,* green fluorescent protein, GFP) (Gould et al., 2018, Kim and Somers, 2019). By driving the expression of a circadian-regulated gene under the control of a non-native promoter, it allows the uncoupling of circadian rhythms at the transcriptional level from

post-translational circadian regulation. Rhythmic accumulation of the protein-LUC fusion protein can be measured in the same manner as *pro::LUC* assays, while protein-GFP signal is measured through the use of confocal microscopy. The use of confocal microscopy also allows the measurement of circadian rhythms in protein localisation, a further level of post-translational regulation within circadian clocks (Kim et al., 2013b, Anwer et al., 2014, Öllinger et al., 2014). These approaches can be coupled with western blots, an invasive technique that quantifies protein accumulation. As with RT-qPCR and RNA-seq, however, the use of western blots has the drawback of being manually intensive. Finally, circadian rhythms can also be measured in the outputs of the oscillator. In plants, such measurement include delayed fluorescence or leaf movement assays (Gould et al., 2009).

To analyse these datasets, software such as Biological Rhythm Analysis Software (BRASS) and Biological Data Repository (BIODARE) have been developed (Zielinski et al., 2014). These software packages measure circadian datasets collected from transcriptional, post-translational or output assays. Four circadian parameters are of primary interest when measuring circadian rhythms **(Figure 1.2)**: 1. *Phase*: the relative timepoint in the circadian cycle when a specific event occurs, *e.g.,* dawn. 2. *Period*: the amount of time taken to reach the same phase in a circadian cycle. The period determines the speed of the circadian clock. 3. *Amplitude*: Defined as half the value between the peak and trough in a circadian cycle. 4. *Robustness*: A measurement of the accuracy of circadian oscillations. Robustness is scored by the relative amplitude error (R.A.E). R.A.E is calculated by dividing the amplitude error by the amplitude value. An R.A.E closer to 0 highlights a more precise and robust rhythm, while scores closer to 1 indicate a less precise rhythm. For the plant circadian clock, an R.A.E score greater than 0.5 is typically used as the cut-off point to indicate arrhythmicity (Kolmos et al., 2011).

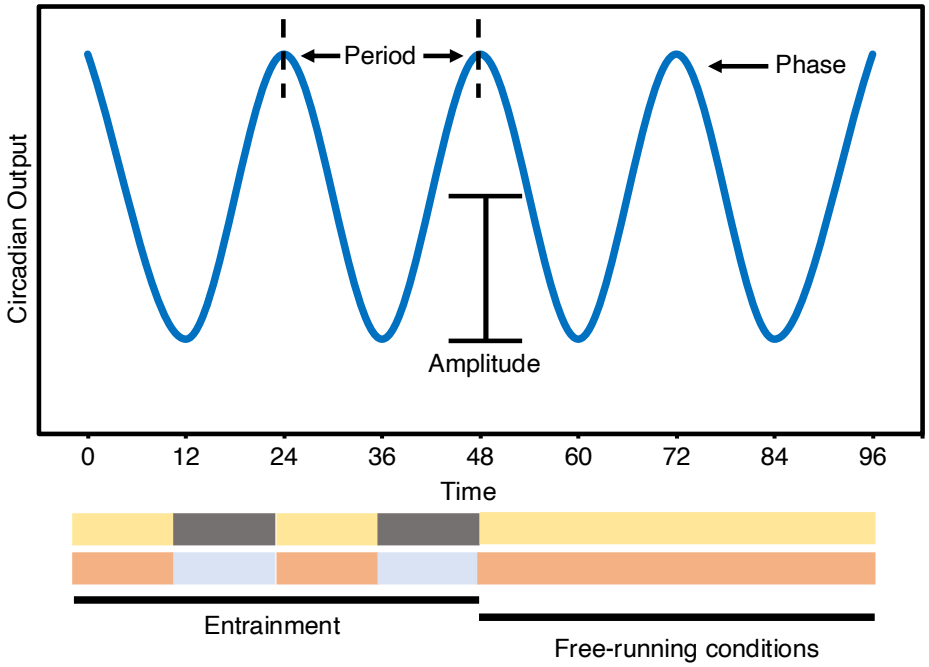

Figure 1.2 - Parameters used in measuring circadian rhythms

A circadian output has four measured properties. 1. Phase: the relative time a circadian event happens *e.g.*, dawn. 2. Period: the amount of time taken to reach the same phase in a circadian cycle, this is typically ~24 hours. 3. Amplitude: half the difference between the peak and trough of the output in a circadian cycle. 4. Robustness: a measurement of the accuracy of the circadian rhythms (not shown on this model). Circadian experiments start under entraining conditions *i.e.*, light/dark (illustrated by the yellow and grey boxes, respectively) and/or warm/cold (illustrated by the orange and blue boxes, respectively) cycles before they are released into free-running conditions (here, constant light and warm temperature). Circadian experiments are measured in *zeitgeber* time (ZT).

1.3 The plant circadian oscillator

The plant circadian clock provides a key benefit to the growth and fitness of Arabidopsis (Dodd et al., 2005). Since this work, the plant circadian clock has now been shown to enhance the fitness of other monocot and dicot crop plants (Bendix et al., 2015). The plant circadian clock is believed to be present in all plant cells, and it is generally accepted that the core structure of the plant clock has minimal variation between different plant organs (Bordage et al., 2016, Chen et al., 2020). However, the sensitivity of the circadian clock to light and temperature stimuli is tissue-specific (Bordage et al., 2016, Nimmo, 2018, Chen et al., 2020, Nimmo et al., 2020). Accordingly,

the circadian clock runs at differences paces throughout the plant, generating detectable waves of circadian rhythms (Gould et al., 2018).

Our understanding of the structure of the plant circadian clock has primarily come from research in Arabidopsis. From these works, the plant circadian clock has been established as a series of interconnected feedback loops that function at the transcriptional, translational and post-translational level to generate and sustain circadian rhythms (Ronald and Davis, 2017, Ronald and Davis, 2019). In the following sections, I will discuss our current knowledge of these regulatory feedback loops. This discussion is framed exclusively in the context of research that has been carried out in Arabidopsis. However, at least some aspect of these regulatory loops is likely to be conserved across embryophytes and potentially charophytic algae as well (Linde et al., 2017).

1.3.1 **The transcriptional network of the Arabidopsis circadian clock**

At the centre of the transcriptional loops of the plant circadian clock are the morning expressed, partially redundant MYB domain transcription factors (TFs) CIRCADIAN CLOCK ASSOCIATED1 (CCA1) and LATE ELONGATED HYPOCOTYL (LHY) **(Figure 1.3)**. *CCA1* and *LHY* are expressed at dawn and the expression of both genes is light responsive (Martínez-García et al., 2000, Más et al., 2003). CCA1/LHY directly repress the expression of most clock genes through binding to the evening element (EE) or CCA1 BINDING SITE (CBS) motif within the target promoter (Adams et al., 2015, Kamioka et al., 2016). The primary circadian target of CCA1/LHY repressive activity is *TIMING OF CAB EXPRESSION1* (*TOC1*, also known as *PSEUDO RESPONSE REGULATOR1*) (Alabadi et al., 2001). CCA1/LHY repressive activity restricts *TOC1* expression to a window around dusk. At dusk, TOC1 accumulates and reciprocally represses *CCA1*/*LHY* expression in addition to the expression of other clock genes (Gendron et al., 2012). This mutual antagonism between CCA1/LHY and TOC1 defines the central transcriptional loop of the plant circadian clock.

Additional interconnected loops subsequently regulate the activity of the central loop **(Figure 1.3)**. At dawn, the TFs TEOSINTE BRANCHED CYCLOPEDIA-PCF20/22 (TCP20/22) recruit the co-activator LIGHT REGULATED WD1 (LWD1) to activate *CCA1*/*LHY* expression (Wu et al., 2016). LWD1, and its homolog LWD2, also activate the expression of *PRR5*, *PRR7* and *PRR9* (Wang et al., 2011b). PRR5/7/9 independently bind to the *CCA1/LHY* promoter and repress *CCA1*/*LHY* expression (Nakamichi et al., 2010, Wang et al., 2013). *PRR9*, *PRR7* and *PRR5* are sequentially expressed, generating a wave of repressive activity. *PRR9* expression starts in the early morning, followed by *PRR7* in the late morning and *PRR5* in the afternoon (Matsushika et al., 2000). This repressive wave is further promoted by the CCA1-related MYB TF REVEILLE8 (RVE8) and its associated homologs, RVE6 and RVE4. RVEs activate the expression of *PRR9*, *PRR5, TOC1*, *LUX ARRYTHMO* (*LUX*) and *EARLY FLOWERING4* (*ELF4*) (Hsu et al., 2013). RVEs activate gene expression by recruiting the transcriptional co-activators NIGHT LIGHT-INDUCIBLE AND CLOCK REGULATED1/2 (LNK1/LNK2) to the target promoter (Xing et al., 2015). In the evening, LUX, ELF3 and ELF4 associate to form the evening complex (EC) (Nusinow et al., 2011, Herrero et al., 2012). The EC represses the expression of the morning-phased *PRR7* and *PRR9*, and evening-phased *GI*, *LUX* and *TOC1* (Kolmos et al., 2011, Lee et al., 2019b). LUX and ELF3 have also been recently shown to bind to the promoter of *LNK1*/*2*, highlighting another potential target of the EC (Xing et al., 2015). Together, this interconnected network of activators and repressors drives rhythmic gene expression within the plant oscillator.

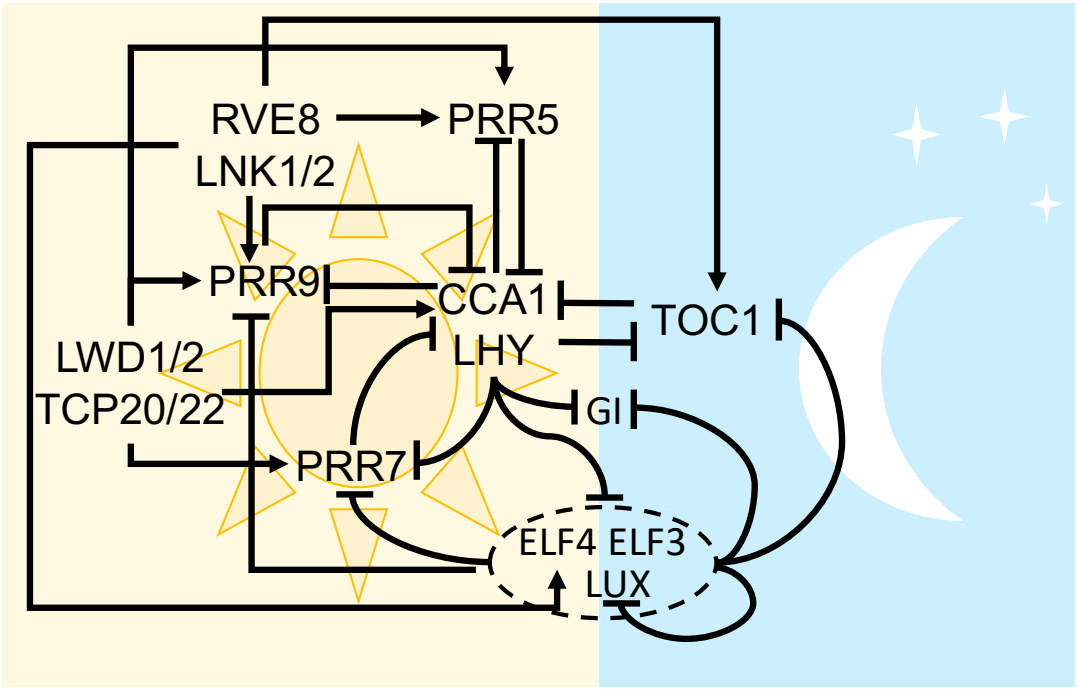

Figure 1.3 - A model of the transcriptional loops in the Arabidopsis circadian clock

At the centre of these transcriptional loops are the morning expressed *CCA1/LHY* and evening expressed *TOC1*. CCA1/LHY and TOC1 mutually repress each other's expression. Further loops include the morning to afternoon phased PRR9, PRR7 and PRR5 which repress *CCA1/LHY* expression. LWD1 and TCP20/22 form a transcriptional regulatory complex to activate the expression of the morning components (*CCA1/LHY*, *PRR9* and *PRR7*), while RVE8 and LNK1/2 form a complex to activate the expression of the morning (*PRR9*) and afternoon/evening (*TOC1*, *PRR5* and *ELF4*) phased genes. Finally, the evening complex (ELF3, ELF4 and LUX, dashed circle) closes the transcriptional loops by repressing the expression of *TOC1*, *LUX*, *GI*, *PRR9* and *PRR7* in the early evening. The position of the gene does not reflect their phase of expression.

1.3.2 Chromatin Remodelling

Underpinning these transcriptional oscillations are *diel* modifications of histones subunits that are wrapped around DNA. Histone subunits can be post-translationally modified through a suite of chromatin remodelling enzymes to generate what is collectively called the histone code (Venkatesh and Workman, 2015). These modifications regulate the accessibility of the DNA wrapped around the histone octamer through opening, compacting or moving the histone, replacing a histone sub-unit, or by providing a binding site for other proteins that recognise histone modifications.

Modifications associated with transcriptional activation include the acetylation of H3 lysine residues (H3Ac) or tri-methylation of H3K4 (H3K4me3), while repressive markers include the tri-methylation of H3K9 (H3K9me3) and H3K27 (H3K27me3) (Jiang and Berger, 2017).

The promoters of *CCA1*, *LHY*, *TOC1*, *GI*, *PRR9* and *LUX* all display *diel* changes in histone modifications. The levels of histone marks commonly associated with transcriptional activation such as H3K9Ac, H3K14Ac, H3K56Ac and H3K4m3 peak within the respective circadian gene promoter at the time of maximum gene expression (Perales and Mas, 2007, Malapeira et al., 2012, Song and Noh, 2012, Hemmes et al., 2012). Conversely, modifications associated with transcriptional repression increase as gene expression declines. These include a reduction in H3Ac, demethylation of H3K4m3 and an increase in H3K36me2 methylation. Therefore, post-translational modification of histones has a fundamental role in driving rhythmic patterns of gene expression within the plant circadian clock.

A large amount of progress has been made in understanding the chromatin remodelling enzymes that are responsible for these *diel* histone modifications. At the centre of the plant circadian clock, CCA1/LHY-mediated repression of *TOC1* is dependent on LYSINE-DEMETHYLASE1 (LSD1)-LIKE 1 (LDL1) and LDL2. LDL1/LDL2 directly recruit HISTONE DEACETYLASE6 (HDA6) to repress the expression of *TOC1* (Hung et al., 2018). TOC1 reciprocally recruits LDL1/LDL2 to repress *CCA1/LHY* expression (Hung et al., 2019). However, unlike CCA1/LHY mediated repression of *TOC1*, LDL1/LDL2 alone cannot fully explain all of TOC1's repressive effect on *CCA1/LHY* expression.

PRR5, PRR7 and PRR9 repress *CCA1/LHY* expression by recruiting the Groucho/Tup1 co-repressor TOPLESS (TPL) through an ETHYLENE AMPHIPHILIC REPRESSION (EAR) domain (Wang et al., 2013). TPL belongs to a multi-gene family of co-repressors which recruit HDA19 and/or the closely related HDA6 to facilitate gene silencing (Zhu et al., 2010). TOC1 does not have an EAR domain and was subsequently

found to not interact with TPL (Wang et al., 2013). Therefore, TOC1 must facilitate gene repression via a separate mechanism alongside recruiting LDL1/LDL2-HDA6.

1.4 Post-transcriptional regulatory mechanisms in the plant circadian clock

So far, most research on the plant circadian clock has focused on investigating the transcriptional network that contributes to the generation of circadian rhythms in plants. However, there are multiple further regulatory layers within the circadian clock at the translational and post-translational level that provide further precision to these transcriptional feedback loops. In the following section, I will discuss the recent advances made in understanding these additional regulatory mechanisms.

1.4.1 Splicing

Splicing has emerged as critical regulatory process within the plant circadian clock. Splicing is the mechanism whereby one precursor-mRNA (pre-mRNA) can produce multiple different transcripts through recognition of different acceptor or donor splice sites within the pre-mRNA. Mutations in the spliceosome cause alterations to the free-running period of Arabidopsis circadian clock, emphasising the importance of splicing in controlling circadian rhythms (Wang et al., 2012). Most genes of the core oscillator have now been shown to undergo alternative splicing: *CCA1*, *LHY*, *PRR9*, *PRR7*, *PRR5*, *PRR3*, *TOC1, ELF3* and *ZEITLUPE* (*ZTL*) pre-mRNA can produce multiple splice isoforms (James et al., 2012, Kwon et al., 2014). These alternative transcripts are usually non-functional and antagonise the activity of the primary transcript. For example, alternative splicing of CCA1 pre-mRNA produces a protein called CCA1β (Seo et al., 2012). The CCA1β protein is truncated so that it no longer bind to DNA but still retains the ability to interact with CCA1α (full-length CCA1) and LHY. The subsequent interactions between CCA1β and CCA1α or LHY decreases the association of CCA1 and LHY to DNA, reducing the transcriptional activity of CCA1/LHY (Seo et al., 2012). The splicing of circadian genes is responsive to the external environment, with

temperature particularly having a key role in regulating the isoform that is produced (James et al., 2018). However, light-dependent splicing of circadian genes has also been described (Shikata et al., 2014). Therefore, temperature and light-dependent alternative splicing of pre-mRNAs provides an additional interface through which the environment can regulate the activity of the plant circadian oscillator.

1.4.2 **Protein stability**

Alongside rhythmic patterns of expression, circadian proteins also display oscillations in protein turnover that closely follows their mRNA accumulation profiles. In recent years, we have begun to develop an understanding of how the stability of some circadian proteins is regulated and these can be arranged into a PTFL **(Figure 1.4)**.

At the centre of this PTFL is ZTL and the closely related FKF1 (FLAVIN-BINDING KELCH REPEAT F-BOX PROTEIN 1) and LKP2 (LOV KELCH PROTEIN 2). ZTL/FKF1/LKP2 form a small family of LOV-KELCH domain proteins that function as blue light (BL) receptors. BL promotes the activity and stability of ZTL, FKF1 and LKP2 (Kiba et al., 2007, Baudry et al., 2010). *ZTL* does not have *diel* changes in gene expression and only shows circadian oscillations at the protein level, with ZTL protein levels peaking in the afternoon (Kim et al., 2007). ZTL protein oscillations are dependent on at least two separate mechanisms. The first mechanism to be reported was HEAT SHOCK PROTEIN90 (HSP90)-mediated maturation and stabilisation of ZTL (Kim et al., 2011, Cha et al., 2017). In the absence of HSP90 functional activity, ZTL protein levels fail to oscillate across the day/night cycle and stay at a suppressed level (Kim et al., 2011). ZTL protein accumulation is also promoted by UBIQUITIN SPECIFIC PROTEASE12 (UBP12) and UBP13 independently of HSP90 (Lee et al., 2019a). UBP12/13 promotes the de-ubiquination of ZTL during the light phase of the *diel* cycle.

Neither HSP90 nor UBP12/13 directly interact with ZTL. Instead, the plant-specific protein GI facilitates the ZTL-HSP90 and ZTL-UBP12/13 interaction (Cha et al., 2017, Lee et al., 2019a). As the expression of *GI* is under circadian control and phased to the afternoon, ZTL protein accumulation subsequently mirrors the expression and

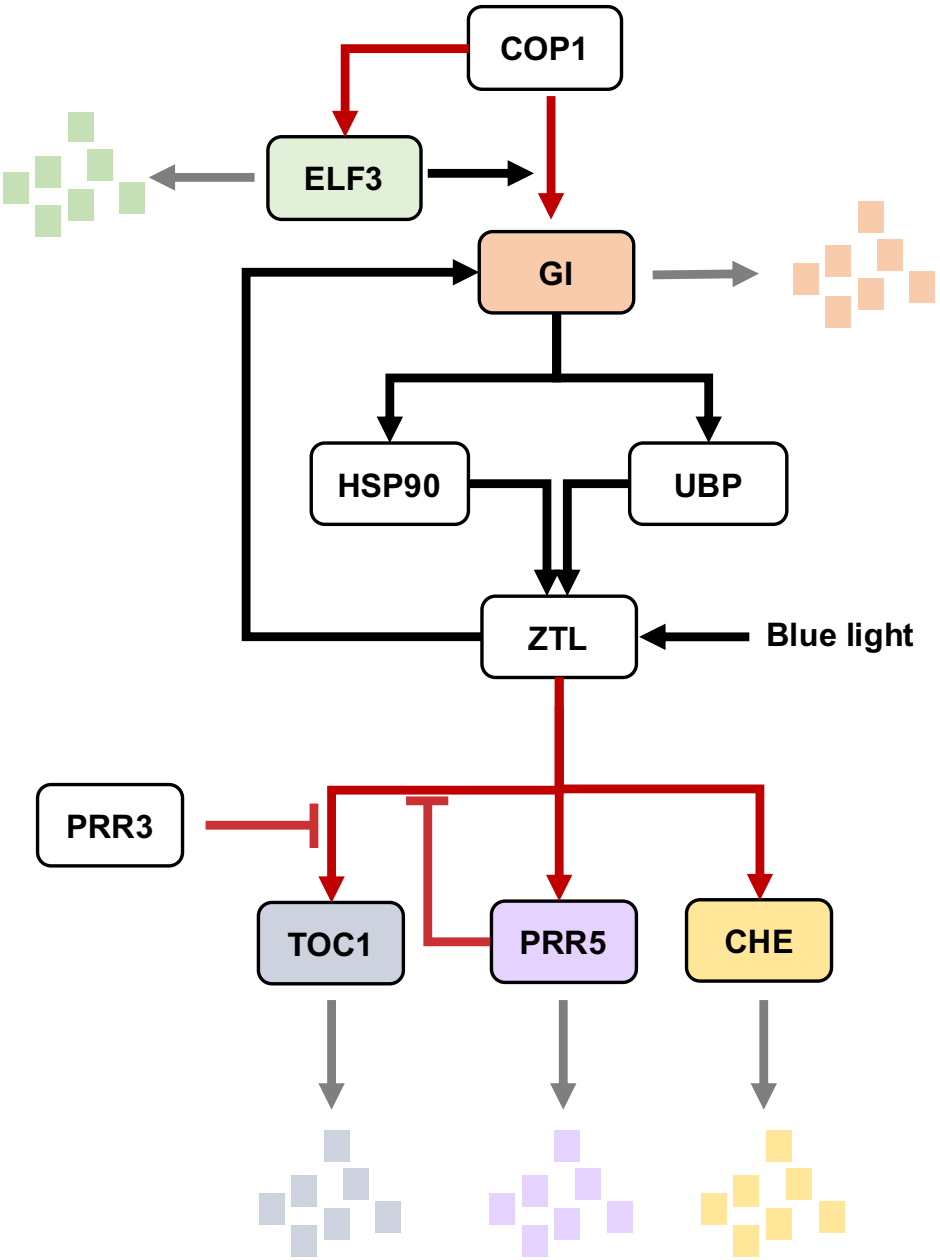

Figure 1.4 - Emerging post-translational loops in the plant circadian clock

ZTL directly promotes the degradation of PRR5, TOC1 and CHE by interacting with an SCF complex (not shown). The stability and activity of ZTL is promoted by BL and through GI. GI stabilises ZTL by facilitating the interaction between ZTL and HSP90, and UBP12/13 (UBP). ZTL reciprocally stabilises GI. PRR5 and PRR3 independently inhibit ZTL degradation of TOC1. GI is targeted for degradation by the activity of COP1. The interaction between GI and COP1 is dependent on ELF3. However, the ELF3-COP1 interaction also leads to the degradation of ELF3. Not shown are FKF1 and LKP2, two proteins related to ZTL and that are believed to function in a mostly redundant manner with ZTL in the circadian clock. Red arrows highlight a negative interaction (flat arrow heads are an inhibitory effect) black arrows highlight an interaction and grey arrows indicate the degrdation of a protein. Proteins in colour are those that are degraded in this feedback loop.

protein profile of GI (Kim et al., 2007). Once expressed and stabilised, ZTL recpriocally stabilsies GI by retaining GI in the cytoplasm (Kim et al., 2013a) **(Figure 1.4)**.

ZTL is an F-box substrate adaptor that facilitates the degradation of other circadian proteins by associating with an E3 ligase Skp/Cullin/F-box (SCF) complex (Kiba et al., 2007). ZTL functions redundantly with FKF1 and LKP2 within the circadian clock but only *ztl* single mutants have a circadian phenotype, highlighting the primacy of ZTL amongst the LOV-KELCH domain proteins in the circadian clock (Baudry et al., 2010). The circadian targets of ZTL are TOC1, PRR5 and CCA1 HIKING EXPEDITION (CHE) (Mas et al., 2003, Kiba et al., 2007, Lee et al., 2018) **(Figure 1.4)**. CHE is a transcriptional co-factor that aides TOC1 transcriptional activity (Pruneda-Paz et al., 2009). FKF1 and LKP2 also target PRR5 and TOC1 for degradation, while it remains to be tested whether FKF1 or LKP2 promote the degradation of CHE (Para et al., 2007, Lee et al., 2018).

The stability of TOC1 is promoted by physical interactions with PRR5 and PRR3 (Para et al., 2007, Baudry et al., 2010). PRR3 interacts with the N-terminus of TOC1 and therefore blocks the interaction between ZTL and TOC1 (Para et al., 2007). In contrast, it has remained unknown how PRR5 stabilises TOC1. PRR5 promotes the phosphorylation and the nuclear accumulation of TOC1 (Wang et al., 2010). As ZTL is localised to the cytoplasm, it possible that PRR5 mobilisation of TOC1 to the nucleus indirectly promotes the stability of TOC1 but this remains to be tested. Finally, the PTFLs are closed by ELF3 in the evening **(Figure 1.4)**. ELF3 acts a scaffold to facilitate the interaction between GI and the E3 ligase CONSTITUTIVE PHOTOMORPHOGENIC1 (COP1) (Yu et al., 2008). COP1 promotes the ubiquination of GI, leading to the degradation of GI by the proteasome pathway. The interaction between ELF3 and COP1 also results in ELF3 being ubiquinated and degraded by the proteasome pathway. Combined, these interactions have begun to explain how protein turnover is regulated in the plant circadian clock.

1.5 **The cellular dynamics of the plant circadian clock**

Regulating where in a cell a protein is localised has emerged as a critical regulatory mechanism across eukaryotic organisms in multiple diverse cellular signalling processes, including the plant circadian clock. Changing a protein's cellular or sub-cellular localisation can change the activity and/or stability of the protein, or separately facilitate the promotion or inhibition of protein-protein, protein-DNA or protein-RNA interactions (Kaiserli et al., 2018).

The nucleus is the site within the cell that is responsible for DNA replication, transcription, ribosomal synthesis and RNA processing. Within the nucleus, proteins, DNA and RNA can localise in sub-nuclear structures called nuclear bodies (Lamond and Sleeman, 2003). The formation of these sub-nuclear structures is proposed to enhance protein activity by condensing proteins, DNA and RNA together (Matera et al., 2009). Some of these nuclear bodies are conserved throughout eukaryotic nuclei. These include the nucleolus, cajal bodies and speckles, which mediates ribosome synthesis, RNA processing and splicing, respectively (Kaiserli et al., 2018). However, some of the nuclear sub-structures are kingdom specific. For example, the plant nucleus contains photobodies, while the animal nucleus contains promyelocytic leukemia protein (PML) bodies (Kaiserli et al., 2018).

Most plant circadian clock components are transcription factors (TOC1, LUX, PRR5/7/9, TCP20/22, RVE4/6/8, CCA1 and LHY) or transcriptional co-regulators (ELF4, GI, ELF3, LNK1/2 and LWD1/2). Accordingly, these proteins have been shown to display nuclear localisation either in transient expression systems or in stable Arabidopsis lines (Yu et al., 2008, Yakir et al., 2009, Wang et al., 2010, Herrero et al., 2012, Wang et al., 2013, Xie et al., 2014, Wu et al., 2016). For the LOV-KELCH domain proteins, only *ztl* single mutants have a circadian phenotype and ZTL is localised to the cytoplasm (Kim et al., 2013a). Therefore, the circadian function of the LOV-KELCH domain proteins likely occurs in the cytoplasm, while the nuclear localisation of FKF1 and LKP2 reflects unique functions of these two proteins (Zoltowski and Imaizumi, 2014). Below I will discuss the work that has provided insights into the cellular dynamics of CCA1, TOC1, PRR5 and

GI. The cellular dynamics of ELF3, ELF4 and LUX are discussed in section 1.6. For PRR7/9, LHY, RVE4/6/8, LNK1/2, LWD1/2 and TCP20/22 though these proteins have been shown to be nuclear localised, the nuclear dynamics of these proteins has not yet been investigated and are therefore not discussed.

CCA1 intrinsically localises to the nucleus and this occurs rapidly upon translation (Yakir et al., 2009). The kinetics of CCA1 localisation did not change in plants exposed to light or kept in the dark, suggesting that CCA1 nuclear dynamics are not influenced by light. There was also no report of CCA1 localising to nuclear foci in this report (Yakir et al., 2009). TOC1 also intrinsically localises to the nucleus through a NLS in the C-terminus (Wang et al., 2010). TOC1 nuclear localisation is enhanced by PRR5-mediated phosphorylation of TOC1, a function unique to PRR5 amongst the PRRs (Wang et al., 2010). PRR5 intrinsically localises to nuclear bodies, while TOC1 when expressed alone displays a diffuse nuclear localisation (Wang et al., 2010). However, TOC1 can localise to nuclear bodies when co-expressed with PRR5. It is unknown what role these nuclear bodies have in facilitating TOC1 or PRR5 activity.

The circadian function of GI occurs in the cytoplasm and nucleus. In the cytoplasm, GI interacts with HSP90 to stabilise ZTL, while in the nucleus GI directly and indirectly regulates gene expression (Kim et al., 2007, Sawa and Kay, 2011, Nohales et al., 2019, Anwer et al., 2020). GI was proposed to intrinsically localise to the nucleus and this was dependent on four stretches of basic amino acids that resemble an NLS within a 250 amino acid (aa) region in the centre of GI (Huq et al., 2000). However, the interaction between ZTL and GI sequesters GI to the cytoplasm, inhibiting the nuclear circadian function of GI (Kim et al., 2013a) **(Figure 1.5)**. It is unclear how GI overcomes ZTL-sequestration and translocates to the nucleus to regulate the gene expression.

Once in the nucleus, GI localises to sub-nuclear bodies **(Figure 1.5)**. The formation of these nuclear bodies is time-of-day dependent, with peak accumulation of nuclear bodies occurring at or just after dusk in long-day photoperiods when GI would typically have maximum accumulation (Kim et al., 2013b). ELF4 promotes the localisation of GI to these sub-nuclear structures, resulting in the inhibition of GI from

binding to DNA (Kim et al., 2013b). Seperately, GI was shown to localise with ELF3 and COP1 in nuclear bodies (Yu et al., 2008). The localisation of GI to these sub-nuclear structures with ELF3 and COP1 was proposed to lead to the degradation of GI. Therefore, the localisation of GI to sub-nuclear structures leads to the inhibition of GI function through two separate mechanisms.

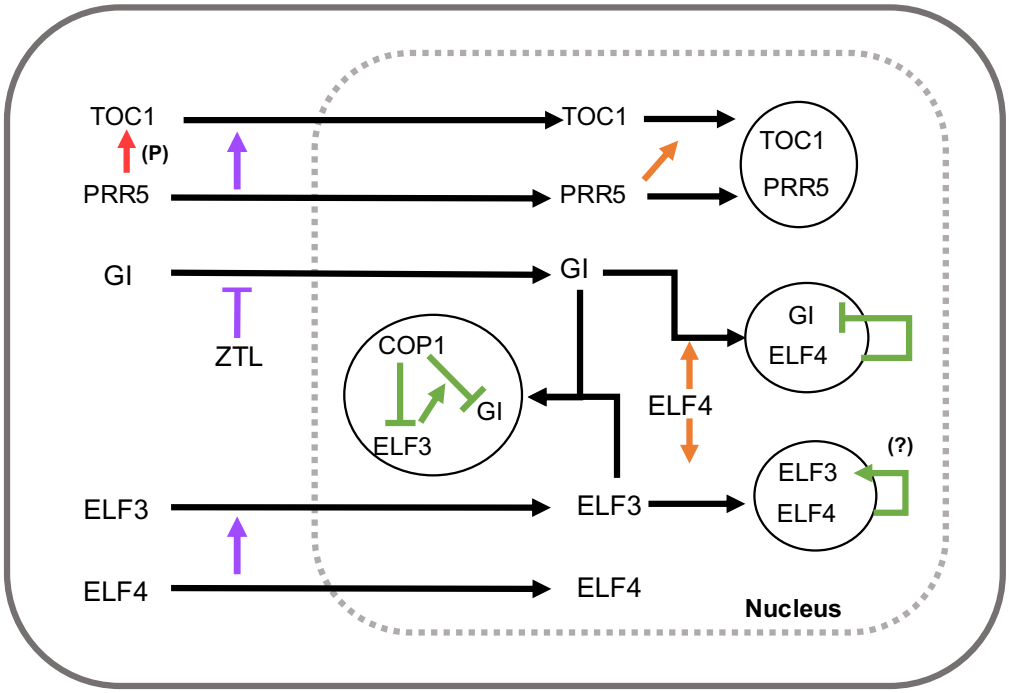

Figure 1.5 - The nuclear and sub-nuclear dynamics of the plant circadian clock

The localisation of TOC1 to the nucleus is promoted by PRR5, possibly through PRR5-mediated phosphorylation (P, red arrow) of TOC1. The localisation of PRR5 and TOC1 to the nucleus leads to the two proteins co-localising to sub-nuclear bodies together. The localisation of TOC1 to nuclear bodies is dependent on PRR5. GI intrinsically localises to the nucleus but this is inhibited by ZTL. Within the nucleus, GI localises to potentially two different populations of sub-nuclear structures, firstly with ELF4 and seperately with COP1 and ELF3. ELF3 can localise to the nucleus intrinsically but this is also promoted by ELF4. Within the nucleus, ELF3 localises to sub-nuclear structures with ELF4 and COP1/GI. Red arrows = post-translational modifications, purple arrows = cytoplasmic effect, orange arrows = nuclear effect and green arrows = sub-nuclear specific effect. Open arrowheads indicate a positive effect, straight arrowheads indicate repressive effect. Not shown are CCA1, LUX, PRR9/7, RVE8/6/4, LNK1/2, TCP20/22 and LWD1/2. These proteins all respectively localise to the nucleus but the nuclear dynamics of these proteins are unknown.

1.6 **The Evening Complex**

The EC is a tripartite protein complex composed of LUX, ELF3 and ELF4 (Nusinow et al., 2011, Herrero et al., 2012). Gene expression and protein levels of all three components peak approximately at dusk under all photoperiods. *elf3, lux* and *elf4* loss of function mutants share aberrantly elongated hypocotyls and photoperiodic insensitive flowering (Zagotta et al., 1996, Hazen et al., 2005, McWatters et al., 2007, Kolmos et al., 2011). Furthermore, a loss of any one of the EC components results in clock arrhythmia both under constant light and constant darkness (Hicks et al., 1996, Doyle et al., 2002, Hazen et al., 2005, Thines and Harmon, 2010, Herrero et al., 2012). This is a unique feature of the EC; the loss of any other oscillator gene does not cause circadian arrhythmia, emphasising the fundamental importance of the EC in the plant circadian clock.

The EC interacts with multiple chromatin remodelling enzymes to repress gene expression. In a mass-spectrometry screen for proteins that interacted with ELF3, MUT9 LIKE KINASE1-4 (MLK1-4) (now more commonly referred to as PHOTOREGULATORY PROTEIN KINASES, PPK) were found to co-precipitate with ELF3 (Huang et al., 2016). MLKs promote the phosphorylation of H3T3, a histone mark associated with heterochromatin formation and gene silencing (Wang et al., 2015b, Huang et al., 2016). *mlk* single and higher order loss of function mutants displayed a longer circadian period (Huang et al., 2016). In contrast, loss of function mutations in *elf3*, *elf4* or *lux* all display circadian arrhythmicity (Hazen et al., 2005, Herrero et al., 2012), suggesting that MLKs alone are not sufficient to explain all of the repressive activity of ELF3/EC.

Supporting the idea that EC utilises multiple mechanisms to repress gene expression, ELF3 was recently shown to physically interact with HDA9 to repress *GI* and *TOC1* expression and the SWI2/SNF2-RELATED (SWR1) complex to repress the expression of *PRR9* and *PRR7* (Lee et al., 2019b, Park et al., 2019, Tong et al., 2020). Mutations in either the *swr1* complex component that interacted with ELF3 (SERRATED LEAVES AND EARLY FLOWERING1, SEF1), or *hda9* did not cause circadian

arrhythmicity. Therefore, ELF3, and the EC, must sustain circadian rhythms through multiple, possibly partially redundant, chromatin remodelling mechanisms.

Alongside chromatin remodelling proteins, other proteins likely contribute to the activity of the EC. A genome wide analysis of the binding sites of the individual EC components revealed that G-box motifs were enriched underneath the DNA motifs that LUX binds to (Ezer et al., 2017a). G-box motifs are recognised by a diverse group of TFs, including those that function within the circadian clock (Ezer et al., 2017b). This suggests that the binding of the EC to DNA and/or activity of the EC could be facilitated by other TFs that bind in close proximity to the EC. Supporting this, a transcriptional co-regulator has now been described that promotes the activity of the EC. HIGH EXPRESSION OF OSMOTICALLY RESPONSIVE GENES (HOS15) was recently found to aid the binding of the EC to the *GI* promoter, and separately help recruit HDA9 to repress *GI* expression in an EC-dependent manner (Park et al., 2019). Therefore, though the EC in the literature and in this thesis refers to the EC as the tripartite ELF3/ELF4/LUX complex only, it is likely that the EC will be expanded to potentially include a range of new co-factors that facilitate the activity of the EC.

1.6.1 **ELF3**

ELF3 is a plant specific protein with no known functional domains **(Figure 1.6A)**. The presence of a proline-rich region, acidic residues, a threonine-rich region, a polymorphic glutamine stretch and a nuclear localisation signal (NLS) led to the proposal that ELF3 functions as a transcriptional regulator (Hicks et al., 2001). Work since has confirmed that ELF3 does function in transcriptional regulation but as a scaffold protein (Nusinow et al., 2011, Herrero et al., 2012, Huang et al., 2016). The role of the poly-Q domain in facilitating ELF3 transcriptional activity remains unclear. It was recently proposed that the poly-Q stretch may provide a direct mechanism to sense warm temperature (Jung et al., 2020). However, earlier work did not identify a requirement for the poly-Q domain in facilitating ELF3-dependent regulation of thermomorphogenesis (Press et al., 2016). Instead, the poly-Q domain was proposed to have a general function,

potentially as a domain to facilitate protein-protein interactions (Press et al., 2016, Press and Queitsch, 2017). The role of the other regions in facilitating ELF3 activity remain unclear; the importance of the proline-rich and acidic regions has remained untested, while the requirement of the NLS in facilitating the nuclear importation of ELF3 is debated (Saito et al., 2012).

ELF3 is required to recruit the other EC components and chromatin remodelling enzymes to repress gene expression (Nusinow et al., 2011, Huang et al., 2016, Lee et al., 2019b, Tong et al., 2020). Within the circadian clock, the established targets of the EC are *TOC1*, *PRR9*, *PRR7, LUX* and *GI* (Kolmos et al., 2011, Nusinow et al., 2011, Herrero et al., 2012, Lee et al., 2019b). However, the importance of the EC extends beyond the circadian clock, with the EC also required to regulate the expression of genes associated to development, hormone signalling and biotic and abiotic stress (Ezer et al., 2017a). The function of ELF3 is also not restricted to the EC. Independently of the EC, ELF3 promotes the degradation of GI by forming a ternary complex with COP1 and GI, and separately ELF3 can inhibit the activity of the TF PHYTOCHROME INTERACTING FACTOR4 (PIF4) from binding to DNA (Yu et al., 2008, Nieto et al., 2015).

ELF3 is functionally divided into three domains, the N-terminus (amino acid 1-261), the middle region (amino acid 262-484) and the C-terminus (amino acid 485-695) **(Figure 1.6A)**. These divisions were first defined in Liu *et al.,* (2001) and then later further refined in Herrero *et al.,* 2012. Though the N, M or C domain does not have a canonical protein domain, each region has at least one stretch of residues that are highly conserved throughout vascular plants and were proposed to provide an interface for protein-protein interactions (Herrero et al., 2012). Supporting this, the N, M and C domains have since been shown to directly facilitate protein interactions **(Figure 1.6A)** (Liu et al., 2001, Herrero et al., 2012, Nieto et al., 2015, Huang et al., 2016, Tong et al., 2020). Proteins that interact with ELF3 have subsequently been shown to connect ELF3 to a wider network of proteins, expanding the potential ELF3-interactome (Huang et al., 2016).

1.6.2 **ELF4**

ELF4 is a small, single domain protein that forms a homodimer and intrinsically localises to the nucleus via an NLS in the N-terminus of the ELF4 protein (Khanna et al., 2003, Kolmos et al., 2009, Herrero et al., 2012). ELF4 has a single protein domain of unknown function (DUF1313) that was proposed to facilitate protein-protein interactions (Kolmos et al., 2009) **(Figure 1.6B)**. Subsequently, ELF4 was found to interact with GI and ELF3 (Herrero et al., 2012, Kim et al., 2013b). Within the EC, ELF4 is proposed to function as an activator of EC activity (Kolmos et al., 2009, Kolmos et al., 2011) but the molecular basis of how ELF4 exerts this activity is unclear. Mutations in the ELF4 binding domain of ELF3 reduced the nuclear and sub-nuclear accumulation of ELF3 (Kolmos et al., 2011, Anwer et al., 2014), while ELF4 was also found to be required for the binding of the EC to DNA (Silva et al., 2020, Jung et al., 2020). Therefore, ELF4 may be a multi-functional activator of the EC; firstly, to promote the nuclear and sub-nuclear localisation of ELF3 **(Figure 1.5)** and secondly to help facilitate the binding of the EC to DNA. Highlighting the importance of ELF4 in activating the EC, mutations in *elf4* led to elevated expression of *LUX*, *PRR9*, *PRR7*, *TOC1* and *GI* (Kolmos et al., 2009).

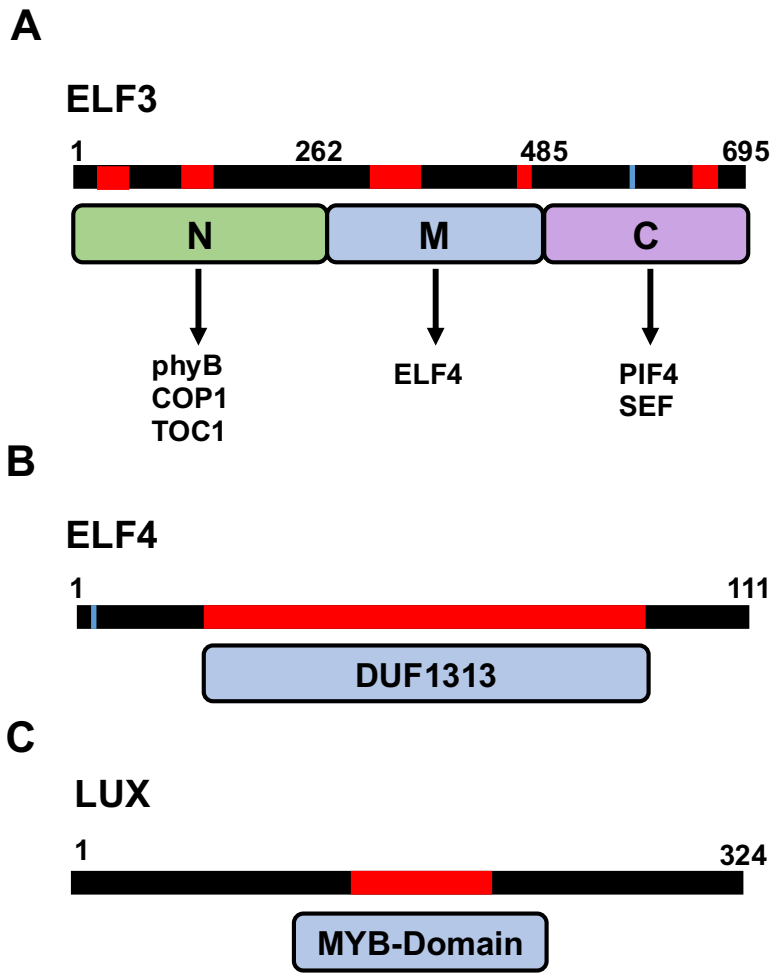

Figure 1.6 - Protein model of the evening complex components

(**A**) ELF3 is divided into three domains: N (1-261), M (262-484), and C (485-695) defined first in Liu et al., 2001 and then refined in Herrero et al., 2012. Each domain interacts with specific proteins. The N-terminus facilitates the phyB, COP1 and TOC1 interaction, the M-region facilitates the ELF4 interaction, while the C-terminus facilitates the PIF4 and SEF interaction. Within the N, M and C regions there are no conserved domains but highly conserved stretches of residues (red) that are present in all vascular plant ELF3 sequences and are partially conserved in bryophytes (mosses, liverworts, and hornworts). The small blue stretch defines the ELF3 NLS in the C-terminus. **(B)** ELF4 has one conserved domain (DUF1313) between regions of low complexity. The function of this domain is unknown but is likely a protein-protein interaction domain. The small blue region close to the N-terminus is the reported NLS. **(C)** LUX has a single conserved region, a MYB/GARP domain that facilitates the binding of LUX (and the EC) to DNA and the localisation of LUX to the nucleus. The conserved regions in (A), (B) and (C) are to scale for the respective size of the protein. Numbers above are the amino acids of ELF3, ELF4 and LUX, respectively

1.6.3 **LUX**

LUX (also known as PHYTOCLOCK1, PCL1) is a TF that belongs to the GARP/MYB family (Hazen et al., 2005, Onai and Ishiura, 2005). LUX intrinsically localises to the nucleus, via an NLS in the conserved GARP MYB-domain (Onai and Ishiura, 2005) **(Figure 1.6B)**. This GARP MYB-domain also facilitates the binding of LUX to DNA by recognising the LUX BINDING SITE (LBS) motif (GATWCG) in the promoter of target genes (Helfer et al., 2011, Silva et al., 2020). LUX has at least partial redundancy with a gene called BROTHER OF LUX ARRYTHMO (BOA, also referred to as NOX in the literature) (Dai et al., 2011, Chow et al., 2012). However, mutations in *lux* alone are sufficient to cause circadian arrhythmicity under free-running conditions and elevated expression of *PRR9* (Hazen et al., 2005, Helfer et al., 2011). This suggests that LUX shares minimal redundancy with BOA in the context of facilitating the binding of the EC to DNA. However, BOA interacts with ELF3 and artificial micro-RNA (amiRNA) gene silencing of *LUX* and *BOA* additively reduced the ability of ELF3 to bind to DNA (Chow et al., 2012). Thus, BOA can facilitate the binding of ELF3 to DNA. However, the importance of this in the context of EC function continues to be unclear.

1.7 Environmental signals entrain the oscillator

A key principle of all circadian systems is the requirement for the internal circadian rhythm to be reset everyday so that the internal cycle stays in alignment with daily and seasonal changes in the environment, a process called entrainment. Light and temperature stimuli are the primary entraining signals in the plant circadian clock (Millar, 2004). However, a number of other stimuli have now been described that also contribute to the process of entrainment in plants. These include *diel* changes in humidity, the availability of photosynthates and other metabolites (Mwimba et al., 2018, Webb et al., 2019). In recent years, it has become increasingly clear that entraining signals converge on a small number of components within the plant circadian clock (Webb et al., 2019).

The convergence of multiple signals on a small number of hubs within the circadian clock may facilitate greater synchrony between the circadian clock and the external environment.

1.7.1 **Principles of entrainment**

The mechanistic effect of entrainment refers to changing the phase of a circadian event so that it becomes coordinated with the external environment. Two independent mechanisms have been described to explain how these phase changes occur. Proposed by Pittendrigh (1964), non-parametric entrainment considers that the phase of the oscillator is adjusted "instantaneously" everyday upon exposure to an entraining signal (Pittendrigh and Minis, 1964). This instantaneous shift was proposed to be principally driven by daily changes in the time of dawn or dusk as the year progresses. Alternatively, Aschoff (1963) proposed parametric entrainment. In contrast to non-parametric entrainment, parametric entrainment considers entrainment to be continual processes whereby the oscillator is accelerating and de-accelerating throughout the *diel* cycle (Aschoff, 1963).

For the plant circadian clock, these two different mechanisms of entrainment have been joined together by a recent idea of the entrainment of the plant oscillator being in a dynamic state of flux (Webb et al., 2019). In this approach, the oscillator is viewed as undergoing continual parametric and non-parametric entrainment from different signals being integrated at multiple entry points throughout the day/night cycle. This is contrast to the idea of one principle entraining signal driving the phase and period of the oscillator (*i.e.,* time of dawn). By being in a state of flux rather than fixed, it is proposed to allow the oscillator to more rapidly respond to changes in the environment and subsequently provides the plant a greater fitness advantage.

1.7.2 **Light signalling**

The role of light in entraining the Arabidopsis circadian clock has so far been the best characterised. The total duration (daylength), direction, quality and wavelength composition of light all influence the Arabidopsis circadian clock (Oakenfull and Davis, 2017). Furthermore, all diurnal organisms are subjective to Aschoff's rules. Aschoff's first rule states that under constant conditions, the free-running period of a diurnal organism's circadian clock will progressively shorten as the intensity of light increases (Aschoff, 1960). In Arabidopsis, Aschoff's first rule has so far been observed under red (RL), BL, green (GL) and UV-B light (Covington et al., 2001, Feher et al., 2011, Battle and Jones, 2020).

Light signals are directly transmitted to the oscillator through the activity of photoreceptors. At least four classes of photoreceptors have been described to function in the entrainment of the Arabidopsis circadian clock: phytochromes (phys) signal RL, FRL and BL to the clock, cryptochromes (CRYs) detect BL, UV-B and GL, the LOV-KELCH family detect BL and UV RESISTANT LOCUS8 (UVR8) detects UV-A and UV-B light (Oakenfull and Davis, 2017, Battle and Jones, 2020). Light signals are also transmitted indirectly to the oscillator through the production of photosynthates (Haydon et al., 2013). Unlike the mammalian circadian system, plant photoreceptors are generally not viewed a core component of the plant circadian clock, although some models do place ZTL as part of the oscillator (Oakenfull and Davis, 2017).

Photoreceptors influence the circadian clock at the transcriptional, translational and post-translational level (Tepperman et al., 2001, Ito et al., 2003, Han et al., 2004, Li et al., 2011, Kim et al., 2013a, Yeom et al., 2014, Siddiqui et al., 2016, Hajdu et al., 2018, Nohales et al., 2019). Highlighting the importance of photoreceptors in mediating entrainment, mutations in photoreceptor genes cause alterations to the period, phase and amplitude of the circadian clock (Somers et al., 1998, Devlin and Kay, 2000, Yanovsky et al., 2000, Han et al., 2004, Feher et al., 2011).

1.7.3 **Temperature signalling**

A few degrees change in temperature across the day/night cycle is also sufficient in entraining the plant circadian clock (Thines and Harmon, 2010). In recent years, the identity of thermosensors in plants have begun to be uncovered. The expression and activity of the EC is directly regulated by cold and warm temperature (discussed in section **1.8**) (Mizuno et al., 2014, Box et al., 2015, Chow et al., 2014, Raschke et al., 2015, Ezer et al., 2017a, Chen et al., 2020, Jung et al., 2020, Silva et al., 2020). phyB, the primary RL receptor in Arabidopsis, is also a sensor for warm and cold temperatures (Legris et al., 2016, Jung et al., 2016, Jiang et al., 2020). Warm temperature represses phyB activity by promoting the photoconversion of phyB into an inactive isoform, while cold temperature promotes the stability of phyB (Legris et al., 2016, Jiang et al., 2020). Whether phyB's role as a sensor of warm or cold temperature has implications in the entrainment of the plant circadian clock to thermocycles remains to be tested. Finally, the chaperone protein HSP90 is important for the plant circadian clock to entrain to thermocycles (Davis et al., 2018). How HSP90 facilitates temperature entrainment of the circadian clock is unclear, but CCA1 and PRR7 were identified as components within this HSP90 signalling pathway (Davis et al., 2018).

Though small changes in temperature across the day/night cycle can entrain the clock, the circadian clock maintains a robust period of ~24 hr across a large range of physiological temperatures. This process is called temperature compensation (McClung, 2006). As with temperature entrainment, the signalling pathway(s) of temperature compensation has remained poorly understood. Mutations in the circadian components *gi*, *prr7*, *lhy* and *cca1* all respectively caused temperature compensation phenotypes (Gould et al., 2006, Salome et al., 2010). However, it is unclear how these genes contribute to the molecular mechanisms of temperature compensation. Furthermore, as CCA1 and PRR7 have been seperately linked to temperature entrainment of the oscillator (Davis et al., 2018), it is unclear the degree to which the process of temperature entrainment and compensation are independent of each other.

1.7.4 **Gating modulates the sensitivity of the oscillator to stimuli**

The senstivity of the oscillator to light, temperature and other *diel* signals across the day/night cycle is time-of-day dependent. Conversley, the circadian clock also regulates time of day sensitivity of physiological processes to environmental stimuli. Collectively, these two separate processes are called gating (Dowson-Day and Millar, 1999, McWatters et al., 2000, Covington et al., 2001, Rugnone et al., 2013, Zhu et al., 2020).. Gating allows the circadian clock to precisely time when environmental stimuli have their maximum effect (Millar, 2004). The best characterised example of gating in plants is light-gating of the photosynthetic gene *LIGHT HARVESTING CHLOROPHYLL A/B-BINDING PROTEIN1.1* (*LHCB1*, previously called *CHLOROPHYLL A/B-BINDING PROTEIN2 CAB2*). *LCHB1* expression is induced in a light-dependent manner at dawn. Outside of this small window around dawn, light pulses cause a much weaker induction of *LCHB1* expression in wild type Arabidopsis plants (McWatters et al., 2000, Covington et al., 2001). The EC is critical for light-gating of *LCHB1* expression; mutations in *elf3* or *elf4* caused acute induction of *LCHB1* expression in response to light pulses across the evening when the gate should be “closed” (McWatters et al., 2000, Covington et al., 2001, McWatters et al., 2007). Similar gating mechanisms have now been described for temperature and metabolic stimuli of the plant circadian clock (Webb et al., 2019). ELF3 is also required for gating the circadian clock to warm temperature pulses in the evening (Mizuno et al., 2014, Zhu et al., 2020). Therefore, ELF3 and the EC is an important hub for controlling the time-of-day sensitivity of the circadian clock to light and temperature signals.

1.8 **The Evening Complex is a hub for environmental signals**

Alongside attentuating the sensitivty of the circadian clock and physiological processes to the external environment, the EC itself has emerged as critical node within the circadian clock for integrating a myriad of different light and temperature stimuli. Here, I will briefly summarise the recent advancements made in understanding how the individual components of the EC are regulated by the environment.

1.8.1 **ELF3**

Light signalling indirectly regulates the expression of *ELF3* through CCA1. CCA1 directly binds to the CBS motif within the *ELF3* promoter, and this subsequently results in the repression of *ELF3* expression (Lu et al., 2012). The expression of *CCA1* is directly promoted by RL and this maximally occurs at dawn (Wang and Tobin, 1998). CCA1 also binds to CBS elements in the promoter of *ELF4* to repress *ELF4* expression (Li et al., 2011). Thus, dawn induction of *CCA1* can be seen as a mechanism to move the clock from the night-to-day phase of the clock by repressing the expression of the *EC* components.

Light signals also converge on ELF3 at the post-translational level. ELF3 physically interacts with phyB through the N-terminus of ELF3 and this interaction is dependent on a conserved stretch of residues within the first ~50 amino acids of the ELF3 N-terminus (Liu et al., 2001, Kim and Somers, 2019). The interaction between phyB and ELF3 connects ELF3 to other phys and a wider light signalling complex, although the functional significance of this remains unclear (Huang et al., 2016). Alongside potentially connecting ELF3 to a light signalling complex, Neito *et al.,* (2015) showed that phyB stabilised ELF3 in a light-dependent manner. It is unclear how phyB stabilises ELF3, but phyB could interfere with the interaction between ELF3 and COP1 (Nieto et al., 2015). COP1 also binds to the N-terminus of the ELF3 protein and this interaction leads to the degradation of ELF3 (Yu et al., 2008). Therefore, phyB and COP1 may compete for access to the ELF3 N-terminus to control the stability of ELF3 in a light-dependent manner.

phyB has also been proposed to inhibit the activity of ELF3 within the circadian clock (Kolmos et al., 2011, Herrero et al., 2012). Over-expressing phyB (*phyBox*) and ELF3 (*ELF3ox*) caused opposite effects on the period length of the circadian clock, with phyB shortening and ELF3 lengthening the circadian period respectively (Covington et al., 2001, Kolmos et al., 2011, Herrero et al., 2012). The ability of *ELF3ox* to lengthen the circadian period is dependent on the wavelength and intensity of light (Covington et

al., 2001); under white light (WL) and all tested intensities of BL, *ELF3ox* had a longer circadian period than wild type plants (Covington et al., 2001). In contrast, *ELF3ox* only lengthened the circadian period under medium to high intensities of RL (Covington et al., 2001). This inhibitory effect of RL on ELF3 repressive activity was alleviated by removing the N-terminus of ELF3, the domain of ELF3 that connects ELF3 to phyB (Liu et al., 2001, Herrero, 2011). Finally, over-expressing *phyA* or *phyB* enhanced the hypomorphic *elf3-12* circadian period phenotype in a light dependent manner (Kolmos et al., 2011). Together, the physical interaction between phyB and the N-terminus of ELF3 was proposed to act as a brake on ELF3 repressive activity within the circadian clock (Herrero et al., 2012).

Warm temperature has also been shown to influence ELF3 activity (Mizuno et al., 2014, Box et al., 2015, Raschke et al., 2015, Ezer et al., 2017a). Recently published work suggested that warm temperature directly repress ELF3 activity by promoting ELF3 to form non-functional nuclear condensates (Jung et al., 2020). The formation of these condensates was proposed to be dependent on a prion-like domain within the C-terminus of the ELF3 protein (Jung et al., 2020). Therefore, ELF3 represents a hub for integrating light and temperature signalling within the plant circadian clock **(Figure 1.7)**.

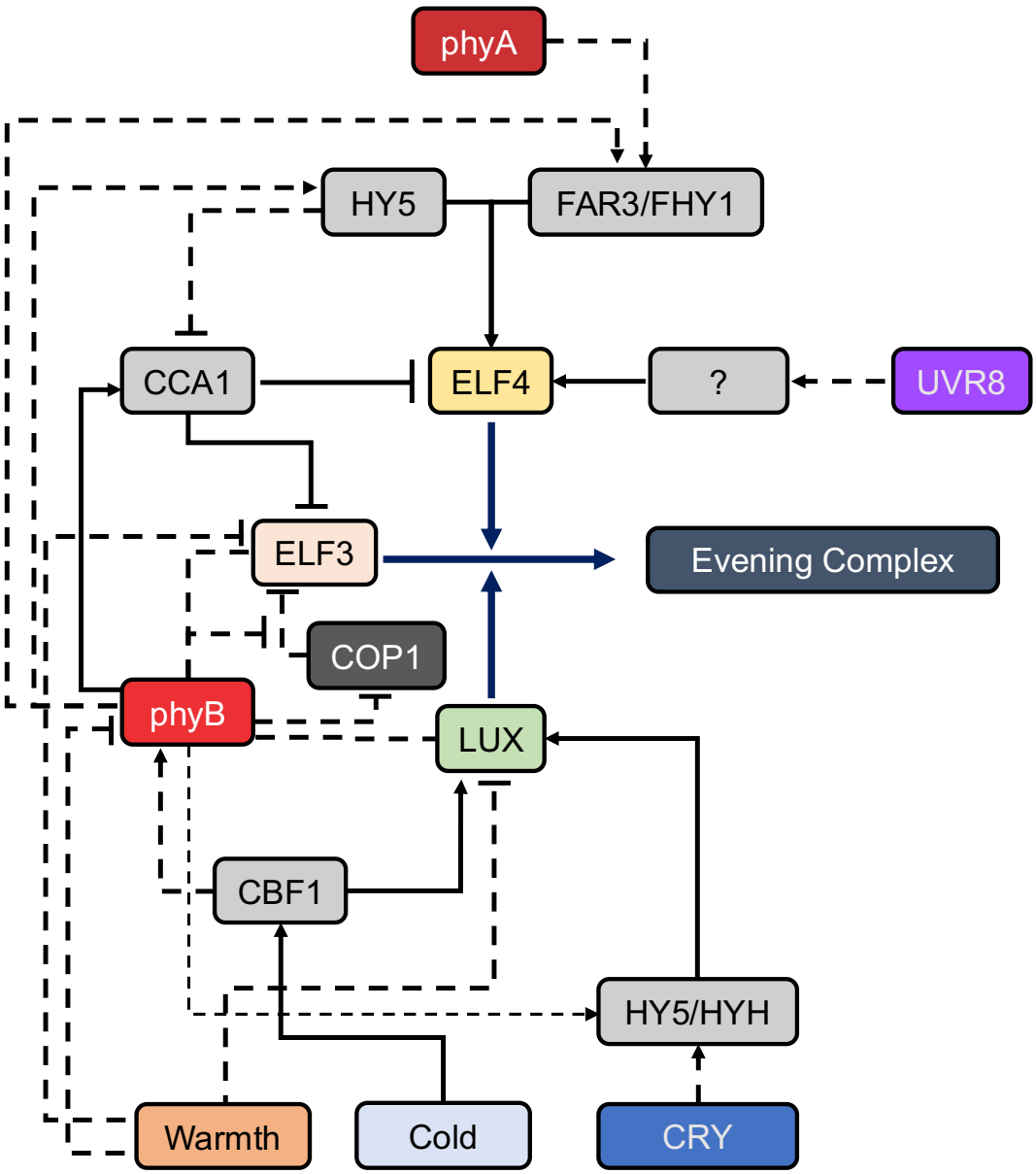

Figure 1.7 - The evening complex is a hub for environmental signals

ELF3, ELF4 and LUX expression and protein activity are independently regulated by light and temperature. The expression of *ELF3* is repressed by the transcription factor CCA1 whose expression is activated in turn by red light in a phyB dependent manner. phyB separately stabilise ELF3 by physically interfering with the ELF3-COP1 interaction. However, the ELF3-phyB interaction has also been proposed to repress ELF3 circadian function. Phytochrome signalling also activates and represses the expression of *ELF4*. Phytochromes directly activate *ELF4* expression through HY5/FAR3/FHY1 but represses *ELF4* indirectly through CCA1. UVR8 also activates the expression of *ELF4* in a UV-B dependent manner through an unclear signalling pathway. The expression of *LUX* is activated by cold temperatures, blue light and red light. The activation of *LUX* expression by blue and red light occurs through HY5. In this process, blue light has the major effect, while red light has a minor effect. Separately, the DNA binding activity of LUX is inhibited by warm temperatures. Finally, warm temperature represses ELF3 activity by

Figure 1.7 (Continued) - promoting ELF3 to form sub-nuclear condensates. Important signalling nodes (temperature, photoreceptors, COP1 and the evening complex) in this network are coloured, while signalling intermediaries are left in grey. Full lines indicate a transcriptional effect, dashed lines indicate a post-translational interaction. Full arrow heads indicate a positive effect, straight line arrow heads indicate a repressive effect. Thinner line width indicates a weaker effect in the network.

1.8.2 **ELF4**

Multiple light signalling pathways promote the expression of *ELF4* **(Figure 1.7)**. The UV-B photoreceptor UVR8 promotes the expression of *ELF4* through an unclear signalling pathway (Takeuchi et al., 2014). The expression of *ELF4* is also rapidly induced in response to FRL and RL in a phyA and phyB dependent manner, respectively (Tepperman et al., 2001, Siddiqui et al., 2016). The phytochrome-associated TFs FAR-RED IMPAIRED RESPONSE 1 (FAR1) and and FAR-RED ELONGATED HYPOCOTYL 3 (FHY3) are required to facilitate phyA and phyB activation of *ELF4* (Li et al., 2011, Siddiqui et al., 2016). FAR1/FHY3 directly bind to the FHY3-FAR1 BINDING SITE (FBS) motif within the *ELF4* promoter to activate *ELF4* expression. The ELONGATED HYPOCOTYL5 (HY5) TF was also found to directly bind to the *ELF4* promoter and is required along with FAR1/FHY3 to facilitate light induction of *ELF4* expression expression (Li et al., 2011).

RL induction of *ELF4* expression is restricted to occur only at dusk. This gating of *ELF4* expression was proposed to provide a mechanism through which plants can sense the changing time of dusk throughout the year (Siddiqui et al., 2016). However, it is unclear how light induction of *ELF4* at dusk is regulated. Light pulses still induced *ELF4* expression at dusk in the *fhy3, far1* or *fhy3/far1* mutants, although these mutants did show a decreased persistence of *ELF4* expression beyond dusk (Siddiqui et al., 2016). This suggests that other light-responsive TFs are required or work redundantly with FHY3/FAR1 to facilitate dusk induction of *ELF4*. HY5 can diretly bind to the promoter of *ELF4* through the ACGT-containing element (ACE) in the *ELF4* promoter and promotes *ELF4* expression in tandem with FHY3/FAR1 (Li et al., 2011). HY5 activity is also light-dependent. Therefore, HY5 could facilitate dusk induction of ELF4.

1.8.3 **LUX**

The expression and activity of LUX is directly regulated by temperature and light **(Figure 1.7)**. The cold-responsive TF C-REPEAT/DRE BINDING FACTOR1 (CBF1) directly promotes the expression of *LUX* by binding to COLD RESPONSIVE ELEMENTS (CORE) motif in the promoter of *LUX* (Chow et al., 2014). CBF1 activation of *LUX* is required for the circadian and growth response to cold temperatures. The DNA-binding activity of LUX is also highly sensitive to temperature, with warm temperatures (27°C) strongly reducing the DNA binding affinity of LUX *in vivo* (Ezer et al., 2017a). ELF4 was recently found to be essential for the binding of LUX and the EC to DNA at 27°C (Silva et al., 2020), but how ELF4 facilitates this process is unclear as ELF4 and LUX do not physically interact (Nusinow et al., 2011).

Light signalling also converges on LUX. The expression of *LUX*, and its homolog *BOA*, is activated by the HY5 transcription factor and its homolog HY5-HOMOLOG (HYH) (Hajdu et al., 2018). HY5/HYH activation of *LUX* and *BOA* was primarily dependent on a BL, signalling pathway but RL may have a small effect. RL signalling also converges on LUX at the post-translational level, with phyB shown to interact with LUX *in vitro* and *in vivo* (Yeom et al., 2014). However, the outcome of the phyB and LUX interaction has not yet been tested.

1.9 **Outputs of the circadian clock**

Circadian clocks allow organisms to precisely time biochemical or physiological processes on a daily and seasonal scale. Below, I will briefly discuss two physiological processes that have been the focus of investigations into outputs that are regulated by the plant circadian clock and are relevant to the work carried out in this thesis. However, these are only a brief insight and exclude many other outputs that the plant circadian clock controls. These other processes include other developmental processes (*e.g.,* root development), the response to biotic and abiotic stress, photosynthesis and metabolism (Bendix et al., 2015, Song et al., 2015).

1.9.1 **Hypocotyl elongation**

Changes in the length of the hypocotyl, or juvenile stem, is a commonly used tool by plant developmental biologists to understand the interplay between growth and a myriad of different external and internal signalling pathways in Arabidopsis. Light is a key regulator of hypocotyl elongation, with the extent of hypocotyl elongation dependent on both the quality, duration and the intensity of light. As the duration of light and/or intensity of light increases, hypocotyl elongation is progressively inhibited (Niwa et al., 2009). The principal promoters of hypocotyl growth are the basic-helix loop helix TF PIFs. Seven PIFs, PIF1/3/4/5/6/7/8, have now been described to regulate hypocotyl elongation in a largely redundant manner (Pham et al., 2018, Oh et al., 2020). Light, temperature, the circadian clock and hormone signalling pathways converge to regulate the expression and activity of PIFs, and subsequently control when and the degree to which the hypocotyl elongates.

Circadian control of hypocotyl elongation occurs primarily through the regulation of PIF4 and PIF5, but recently the circadian clock has also been shown to regulate *PIF7* expression (Nomoto et al., 2012, Jiang et al., 2019). *PIF4* and *PIF5* have *diel* changes in gene expression and the phase of the respective gene is dependent on the photoperiod. Under short-day (SD) photoperiods, *PIF4* and *PIF5* expression peaks in a narrow window around dawn, while under long-day (LD) photoperiods the expression of *PIF4* and *PIF5* is shifted to the early morning (Niwa et al., 2009). Maximal hypocotyl elongation occurs shortly after the expression of *PIF4/PIF5*. PIF4 promotes hypocotyl elongation by activating the expression of auxin biosynthesis enzymes (Franklin et al., 2011, Nomoto et al., 2012, Sun et al., 2012). Increased accumulation of auxin subsequently leads to increased hypocotyl elongation. Perception of the photoperiod by the circadian clock thus allows the plant to precisely time when hypocotyl elongation occurs.

Nearly all transcriptional components of the circadian clock have now been shown to directly regulate the expression of *PIF4* (Nusinow et al., 2011, Lu et al., 2012, Li et al., 2020a, Anwer et al., 2020). Separately, the circadian clock regulates PIF4

activity at the post-translational level. ELF3 physically interacts with PIF4 and this interaction secludes PIF4 from binding to DNA (Nieto et al., 2015). Similar regulatory mechanisms have also been described for TOC1 (Zhu et al., 2016). This combination of transcriptional and post-translational regulation of PIF4/5 by the circadian clock alongside the concerted activity of other signalling pathways allows the plant to precisely control the timing and extent of hypocotyl elongation.

1.9.2 **The floral transition**

The transition from vegetative to floral development is a key point in the life history of a plant. The initiation of flowering is regulated by environmental and intrinsic pathways that converge on a small number of genes called floral integrators. This co-regulation of a limited number of signal integrators allows the plant to co-ordinate flowering to only occur under the most optimal conditions (Srikanth and Schmid, 2011). A key driver of flowering in most plant species is the external photoperiod (daylength). Photoperiod-sensitive plants are divided into two categories: SD-plants flower when the daylength is below a critical threshold, while LD-plants flower when the daylength is above a critical threshold. SD and LD-plants are further divided into facultative (they will flower outside of the critical threshold but be greatly delayed) or obligate (the threshold must be met for flowering to commence) (Song et al., 2015). Photoperiod-sensitive plants use different mechanism to sense the photoperiod. Plants can either measure the total duration of the light or dark phase, or separately the presence of light or darkness at a critical point in the *diel* cycle is used to determine the daylength (Roden et al., 2002).

The primary entry point for the circadian clock in controlling flowering is through the photoperiodic pathway (Song et al., 2015). However, the circadian clock has now been shown to regulate flowering through other floral regulatory pathways such as gibberellin hormone signalling (Boden et al., 2014). In Arabidopsis, the circadian clock regulates the photoperiodic pathway by primarily controlling the timing of *CONSTANS* (*CO*) expression and protein accumulation (An et al., 2004). CO is a TF that promotes flowering by activating the expression of *FLOWERING LOCUS T* (*FT*) in leaf phloem

companion cells. FT protein then moves from the leaf to the shoot apical meristem where it triggers the initiation of flowering (Jaeger and Wigge, 2007). FT induces flowering as part of a complex with the TF FD and 14-3-3 proteins (Abe et al., 2005, Taoka et al., 2011). This complex, called the florigen-activation complex (FAC), directly activates the expression of *SUPPRESSOR OF CONSTANS1* (*SOC1*) and *APETALA1* (*AP1*) to trigger the induction of flowering.

The circadian clock in Arabidopsis controls the expression and stability of CO. During the morning and early afternoon, CYCLING DOF FACTORS (CDFs) repress the expression of *CO* (Sawa et al., 2007). The expression of CDFs is directly regulated by the circadian clock; CCA1/LHY activate *CDFs* in the morning, while PRR9/7/5 repress *CDFs* in the late afternoon (Nakamichi et al., 2007, Niwa et al., 2009). The circadian clock also regulates the stability of CDFs. In the late afternoon, FKF1 and GI form a protein complex that facilitates the ubiquination and degradation of CDFs in a BL-dependent manner (Sawa et al., 2007). The degradation of CDFs by FKF1/GI results in the expression of *CO* peaking in the light phase of the *diel* cycle. This coincidence of *CO* expression with the light-phase results in the stabilisation of CO protein through direct interactions with photoactivated CRY1/2 and phyA photoreceptors (Valverde et al., 2004). Stabilised CO subsequently promotes the expression of *FT.*

The ability of FKF1 and GI to promote the degradation of CDF1 is photoperiod dependent. In LD photoperiods, the expression of *FKF1* and *GI* is in phase with maximal expression of the two genes peaking in the afternoon (Sawa et al., 2007). Under SD conditions, the expression of *FKF1* and *GI* is out of phase and the FKF1/GI complex fails to accumulate during the daytime (Sawa et al., 2007). The failure of FKF1/GI complex to accumulate causes minimal degradation of CDF, delaying *CO* expression to the evening of SD photoperiods. CO was originally reported to be inactive in the dark due to being degraded by interactions with COP1 (Liu et al., 2008). However, recent work has suggested that CO is active in the night of SD but instead actively represses flowering by promoting the expression of *TERMINAL FLOWER1* (*TFL1*) (Luccioni et al., 2019). How CO has temporal- or light-dependent activator and repressor functions is unclear.

Furthermore, recent work has revealed further layers of circadian regulation that control the timing of *CO* expression, the stability of CO protein under LD and SD photoperiods and alternative entry points for the circadian clock downstream of *CO* (Shim et al., 2017). Together, the concerted regulation of CO at the transcriptional and post-translational level, in addition to other entry points in the photoperiodic and non-photoperiodic flowering pathways underpins how the circadian clock regulates flowering.

1.10 **Thesis Objectives**

In recent years, we have begun to develop a detailed understanding of ELF3's circadian and non-circadian functions. As part of the EC, ELF3 has been established as a critical component at the interface between environment and the circadian clock and as a core element of the plant circadian oscillator (Kolmos et al., 2011, Helfer et al., 2011, Herrero et al., 2012). The role of the EC has also been expanded to include coordinating juvenile and adult growth, the response to defence, senescence and hormone signalling (Ezer et al., 2017a). We have also begun to understand how ELF3 exerts its repressive activity both within the EC and independently of the EC (Yu et al., 2008, Nieto et al., 2015, Lee et al., 2019b, Park et al., 2019, Tong et al., 2020). In contrast, how the activity of ELF3 is regulated has remained relatively unclear. It has been proposed that phyB represses the circadian function of ELF3, while ELF4 activates ELF3 circadian function, but how phyB or ELF4 repress or promote ELF3 activity, respectively, has remained largely enigmatic (Kolmos et al., 2011, Herrero et al., 2012).

In this PhD, I aimed to determine how phyB and ELF4 regulate the activity of ELF3. Prior work has suggested that where, and when, ELF3 localises both within the cell and inside the nucleus are important factors in determining ELF3 activity and ELF4 may contribute to this process (Herrero et al., 2012, Anwer et al., 2014). Furthermore, an emerging mechanism of phy activity is controlling where proteins are localised in the cell to promote or repress their activity (Lu et al., 2015). Thus, the broad overarching hypothesis of this thesis was that phyB and ELF4 have antagonistic effects on where in the cell ELF3 is localised, and this subsequently controls ELF3 activity.

In chapter 3, I investigate whether the cellular localisation of ELF3 is responsive to light, and if there are competing effects of different light wavelengths on ELF3 cellular and sub-nuclear localisation. I also investigate the importance of phyB in facilitating light-dependent changes in the cellular localisation of ELF3, and the importance of phyB in regulating ELF3 activity. In chapter 4, I investigate the role of ELF4 in controlling the nuclear and sub-nuclear localisation of ELF3 in Arabidopsis, and the importance of ELF4 in promoting ELF3 repressive activity. Finally, in chapter 5 I investigate how warm temperatures changes the sub-nuclear localisation of ELF3 and the role of ELF4 within this. Collectively, this work provides a new understanding of how extrinsic and intrinsic factors regulate the spatio-temporal localisation of ELF3, and how ultimately this influences the activity of ELF3 in controlling gene expression and plant development.

Chapter 2 - Materials and Methods

2.1 **Materials**

2.1.1 **Plant Lines**

The Arabidopsis ecotype Wassilewskija-2 (Ws-2) with an *LHY::LUCIFERASE* (LUC) reporter was used as the wild type (WT) in this work (McWatters et al., 2007). The *CCR2::LUC* reporter present in some lines was first described in (Doyle et al., 2002). Unless otherwise stated, all mutant and transgenic lines used in this work are in the Ws-2 background. The mutant and transgenic lines used in the course of this work are described in table 2.1. The mechanism used to generate any new mutant or transgenic line during this project are also described in table 2.1. Primers used to genotype mutant and transgenic lines are described in table 2.2.

Table 2.1 Plant lines used in the course of this work.

Plant Line	**Reference**	**Luciferase Reporter**
Ws-2	McWatters et al., 2007.	LHY
elf3-4	Hicks *et al.,* 1996	LHY
elf3-4/elf4-1	Herrero *et al.,* 2012.	None
elf4-1	Doyle *et al.,* 2002	None
elf4-1	McWatters *et al.,* 2007.	LHY
phyB-10	Reed *et al.,* 1993.	CCR2
elf3-4/phyB-10	This study – crossed.	CCR2
elf3-4 35S::YFP:ELF3	Herrero *et al.,* 2012.	LHY
elf3-4 35S::YFP:ELF3MC	Herrero *et al.,* 2012.	LHY
elf3-4 35S::YFP:ELF3C	Herrero *et al.,* 2012.	LHY
elf3-4/elf4-1 *35S::YFP:ELF3*	This study – crossed.	LHY
elf3-4/phyB-10 *35S::YFP:ELF3*	This study – crossed.	Not determined

Table 2.2 - Genotyping primers used in this work.

Genotype	Sequence		Amplicon Size
elf3-4	F	TGCAGATAAAGGAGGGCCTA	Wild type: 146 bp Mutant: 140 bp
	R	ATGGTCCAGGATGAACCAAA	
phyB-10 (Exon 1)[1]	F	CTATGGGGAAGTCTCTGGTT	Wild type: 2 kb Mutant: No band
	R	CTAATATGGCATCATCAGCATC	
phyB-10 (Exon 4)[1]	F	AATGGCGTGTCCAGGTGAAG	256 bp
	R	CTAATATGGCATCATCAGCATC	
elf4-1 (WT)	F	GTCTTAATCTGTCATTAAGTACCTAC	Wild type: 1.3 kb Mutant: No band
	R	CTTAATTTGGACTGTGGTGGACATAAG	
elf4-1 (Mutant)	F	GTCTTAATCTGTCATTAAGTACCTAC	Wild type: No band Mutant: 1 kb
	R	TTTCTCCATATTGACCATCATACTCATTG	
35S::YFP:ELF3	F	GGGCATCGACTTCAAGGAGGAC	1307 bp
	R	ACAAAGCCACCTGACCTTGCA	
35S::YFP:ELF3MC	F	GGGCATCGACTTCAAGGAGGAC	1418 bp
	R	ATGGCCGAAAGGACTTGCTACC	
35S::YFP:ELF3C	F	GGGCATCGACTTCAAGGAGGAC	746 bp
	R	ATGGCCGAAAGGACTTGCTACC	

[1]*phyB-10* is a tDNA mutant, with the tDNA reported to be inserted between exon 3 and exon 4 of the *phyB* gene (Reed et al., 1993). However, there are no published primers available to genotype *phyB-10* and I was unable to find any tDNA-specific primers that amplified the tDNA insertion in the *phyB-10* mutant. To circumvent this problem, I designed a PCR that used a forward primer in either exon 1 or exon 4 of the *phyB* gene and a reverse primer at the 3' end of *phyB* exon 4. Two separate PCRs were then performed, using either the exon 1 or exon 4 forward primer and the exon 4 reverse primer. As the *phyB-10* tDNA insertion is between exon 3 and exon 4 of *phyB*, only WT plants produce a band when the exon 1 forward primer is used. The exon 4 forward primer is used as a positive control. This genotyping approach was validated by growing the purported *phyB-10* mutant under constant white light (CWL) to identify the elongated hypocotyl phenotype of *phyB* mutants under CWL (Reed et al., 1993).

Table 2.3 – *In planta* selection marker for transgenic lines.

Transgene	Selection marker
CCR2::LUC	Hygromycin
LHY::LUC	Hygromycin
35S::YFP:ELF3 (and fragments of)	Phosphinothricin (PPT)

Table 2.4 – Antibiotic stock and working concentrations used for *in planta* selection.

Antibiotic	Stock Concentration (Solvent)	Working Concentration
Hygromycin	30 mg/mL (ddH_2O)	15 µg/mL
PPT	12 mg/mL (ddH_2O)	12 µg/mL

All antibiotics were filtered sterilised with a 0.22 µM filter (Millex-GV, #SLGV033RS) before use.

2.1.2 Chemicals

2-Mercaptoethanol (Sigma, #M3148).

2-(N-morpholino)ethanesulfonic acid (MES) (Melford Biolaboratories, #M22040).

2-Propanol (Honeywell, #33539).

Agarose (Bio-Budget, #10-35-1020).

Boric acid (VWR Chemicals, #20185.297).

Chloroform (Fisher Chemicals, #C/4960/17).

Dimethyl sulfoxide (DMSO) (Fisher Chemicals, D/4121/PB08).

DL-Phosphinothricin (PPT) (Duchefa Biochemie, #P0159).

Ethylenediaminetetraacetic acid disodium salt (EDTA) (Merck-Sigma Aldrich, #E4884).

Ethanol (VWR Chemicals, #20821.330).

Ethidium bromide (Thermo Fisher, #17898).

Hydrochloric acid (HCL) (Merck-Sigma Aldrich, H1758).

Hygromyicin B (AppliChem PanReac, #A5347,0100).

Murashige and Skoog (MS) basal salt (Duchefa Biochemie, #M0222).

Phytoagar (Duchefa, Biochemie, #P1003).

Potassium hydroxide (KOH) (VWR Chemical, #26669.290).

Rifampicin (Melford, #R0146).

Select Agar (Invitrogen, #30391-023).

Sodium dodecyl sulfate (SDS) (Melford, #L22010).

Sucrose (Fisher Chemical #S860060).

Thin Bleach (Cleanline, #038000).

Tris base (Invitrogen, #15504-020).

Triton X-100 (Merck-Sigma Aldrich, #T8787).

2.1.3 **Reagents for each method**

General use

10x TE: 100 mM tris-HCL (pH 8), 10 mM EDTA. Diluted 1/10 in ddH_2O for experimental use. All stock and working solutions were autoclaved prior to use.

10x TBE: 121.1 g/L tris base, 61.8 g/L boric acid and 7.4 g/L EDTA. Diluted 1/10 in ddH_2O for experimental use.

DNA Ladders: GeneRuler 50 bp (Thermo Fisher, #SM0373).

GeneRuler 1KB ladder (Thermo Fisher, #SM0311).

TriTrack DNA Loading Dye (Thermo Fisher, #R1161).

Seed Sterilisation

Bleach/Triton X-100: 33% thick bleach, 0.02% Triton X-100 (v/v) in ddH_2O.

Agar Water: 0.1% select agar (w/v) in ddH_2O. Autoclaved prior to use.

Plant growth media & soil composition

MS**:** 4.4g/L MS basal salts, 2.5 g/L sucrose (0.25%), 0.5 g/L MES and 1.5% (w/v) phytoagar. The pH of the media was adjusted to ~5.7 with KOH. All media was autoclaved prior to use. This will be referred to as MS0.25 throughout this thesis to reflect the sugar concentration used.

Soil used for bulking and flowering time experiments: 1-part coir, 1-part F2+S, 1-part vermiculite and 0.7 g/L of osmocote® (East Riding Horticulture). No pesticide treatment was applied.

Plant DNA extractions

DNA Extraction Buffer: 200 mM Tris, 240 mM NaCl, 25 mM EDTA and 1% (w/v) SDS. The pH of the buffer was adjusted to 8 with HCl.

Plant genotyping

10x PCR buffer [15 mM $MgCl_2$] (Genaxxon, #M3001).

100 mM DNTPs (Merck Sigma-Aldrich, #DNTP100-1KT).

100 µM Primers (Merck Sigma-Aldrich). Sequences are in table 2.2. All genotyping primers were used at a 500 ng/µL concentration.

Taq DNA Polymerase S [high specificity] (Genaxxon, #M3001).

RNA Extractions and qPCR

RNeasy Plant Mini Kit (Qiagen, #74904).

RNA Clean & Concentrator Kits with DNAse (Zymo, #R1013).

SuperScript IV Reverse Transcriptase (Thermo Fisher Invitrogen, #18090010).

RNaseOUT™ Recombinant Ribonuclease Inhibitor (Thermo Fisher Invitrogen, #10777019).

Random Hexamers 50 µM (Thermo Fisher Invitrogen, #N8080127).

100 mM DNTPs (Merck Sigma-Aldrich, DNTP100-1KT).

Nuclease-Free Water (Thermo Fisher Invitrogen, #AM9932).

MicroAmp™ Optical 96-Well Reaction Plate (Thermo Fisher Applied Biosystems, #N8010560).

Fast SYBR™ Green Master Mix (Thermo Fisher Applied Biosystems, #4385612).

100 µM primers (Merck Sigma-Aldrich). Sequences are listed in table 2.5, primer concentrations and efficiencies are listed in table 2.11.

Table 2.5 - qPCR Primer sequences used in this study

Gene Target	Sequence		Source
PP2A	F	TATCGGATGACGATTCTTCGTGCAG	Herrero *et al.,* 2012.
	R	GCTTGGTCGACTATCGGAATGAGAG	
PRR9	F	GGAAGTGGTGCTCAGGCTAT	This study.
	R	GAGTGTGTTGGTCCTGAGC	
LUX	F	GCTTCGGATAAGCTCTTCTCTTC	Kolmos *et al.,* 2009.
	R	ATAAACTGGCATCTGCATCATCT	
TOC1	F	GTTGATGGATCGGGTTTCTC	Lee *et al.,* 2019.
	R	TCATGACCCCATGCATATAG	
GI	F	AGCAGTGGTCGACGGTTTATC	Nieto *et al., 2015*
	R	ATGGGTATGGAGCTTTGGTTC	

Microscopy

Glass slides (Thermo Scientific, #12372098).

Coverslips (Scientific Laboratory Supplies, #MIC3226).

2.2 Methods

2.2.1 Seed Sterilisation

Seeds were aliquoted into a 1.5 mL Eppendorf tube and washed in 0.75 mL of 100% ethanol for two minutes. Seeds were then spun down, the ethanol was decanted, and 0.75 mL of bleach/triton-X was added for two minutes. After two minutes, the bleach/triton-X solution was removed and replaced with 1 mL of sterile deionised water and spun down immediately. The wash step was repeated twice before seeds were re-suspended in 0.75 mL of agar-water. Seeds were then sown onto an MS0.25 plate.

2.2.2 Plant Genotyping

Leaf tissue from plants at the 6th leaf stage was harvested and placed into a 1.5 mL Eppendorf tube. To this eppendorf, 250 µL of DNA extraction buffer (DEB) was added and tissue was homogenised with a steel pestle attached to an IKA RW16 Basic Overhead Stirrer. Once the tissue was sufficiently homogenised, a further 250 µL of DEB

and 75 µL of chloroform was added. Samples were then vortexed for five minutes and then spun down at 14,000g for ten minutes. Following this, 300 µL of the top layer was then carefully removed and added to 300 µL of 100% isopropanol in a clean 1.5 mL Eppendorf. The tubes were inverted before being spun down again at 14,000g for ten minutes. The liquid was then decanted and 500 µL of 70% ethanol was added to the Eppendorf. Tubes were then vortexed briefly before being spun down for a further five minutes. The ethanol was then removed, and the tubes left to air dry at room temperature for one hour. After one hour, 100 µL of 1x TE was added to each Eppendorf to resuspend the DNA. Resuspended DNA was then stored at 4ºC until genotyped.

The default reaction mixes and cycle conditions for genotyping are described in table 2.6. The primers used for genotyping the respective mutant lines and the annealing temperature are described in table 2.2. PCR products were typically resolved on a 1.5% agarose gel (TBE) stained with ethidium bromide. However, a 3% agarose (TBE) gel was used if the resolved PCR fragment was under 200 bp in size (amplicon size is in **Table 2.2**). All PCR gels were imaged using a Biospectrum Geldoc (UVP, AnalytikJena) with VisionWorks LS software (V8.2).

Table 2.6 - PCR cycle conditions and reaction mix for Arabidopsis genotyping

Cycle Conditions	Reaction Mix (10 µL reaction)
1x:	
94ºC for 2.5 minutes	1 µL buffer
40x:	1 µL 2.5 mM DNTPs
95ºC for 30 seconds	0.5 µL 10 µM primer mix
56.5ºC for 45 seconds	1 µL template
72ºC for 1 minutes[1]	0.05 µL Genaxxon taq polymerase
1x:	6.45 µL water
72ºC for 10 minutes	

[1] For products over 1.5KB, 30 seconds was added for every additional KB.

2.2.3 **Photoperiodic Hypocotyl Assays**

Seeds were surfaced sterilised as described above before plated onto MS0.25 plates and stratified for three days at 4ºC (see chapter 3 and chapter 4 for specific details of lines used). After three days of stratification, all plates regardless of the photoperiod were germinated under 10 µmol/m^{-2}/s^{-1} of white light (WL) for three hours. After three hours, plates were transferred to appropriate photoperiod chamber. All chambers had a light intensity of 85 µmol/m^{-2}/s^{-1} and were kept at a constant temperature of 22ºC (± 1ºC). For constant darkness experiments, plates were immediately wrapped in foil after they had been exposed to WL for three hours and then placed into one of the photoperiod chambers for the duration of the experiment. Hypocotyl development was measured on the seventh day after transfer to the growth chamber. Hypocoty elongation was measured after seven days as hypocotyl growth has primarily ceased by this developmental point (Gendreau et al., 1997). All seedlings were measured before the start of the dark phase on the seventh day. Hypocotyl length was measured in imageJ (V1.51w). A minimum of two biological repeats were analysed for each photoperiod, with a minimum of 10 seedlings per repeat.

2.2.4 **Flowering Time Assays**

An adapted protocol first described in Kolmos et al., 2011 was followed to measure flowering time. In brief, aside from *elf3-4/phyB-10* (see below), seeds were surfaced sterilised as described above before being plated onto MS0.25 plates and stratified for three days at 4ºC. Specific details of the lines used are in chapter 3 and chapter 4, respectively. Seedlings were then grown for 12 days under a neutral day photoperiod (12/12 light/dark) with a constant temperature of 22ºC (± 1ºC). At day 12, seedlings were transferred to P40 trays filled with soil. Trays were then moved to a long- (16/8, LD) or short-day (8/16, SD) photoperiod growth chamber with a constant temperature of 22ºC (± 1.5ºC). Vented lids were placed over the seedlings and closed to maintain a high humidity for the first three days after seedlings were transferred to soil. Vents were then opened on the fourth day before the lids were removed on the fifth day. Plants were then monitored daily until the emergence of an inflorescence. Flowering was determined as the point at which the inflorescence was approximately ~1cm above the rosette. At this point, the number of rosette leaves and days taken to flower were recorded. Plant husbandry was carried out by the York Biology horticulture facility.

For *elf3-4/phyB-10*, seeds were stratified overnight in deionised water before being sown directly on P40 trays filled with soil. Trays were then moved to a neutral day cabinet for 12 days. On day 12, the *elf3-4/phyB-10* lines were thinned to ensure 1 seedling per P40 well and moved to the appropriate long- or short-day photoperiod chamber. This protocol was used to minimise the rapid desiccation of *elf3-4/phyB-10* seedlings that was observed when these seedlings were transferred from plates to soil. There was no discernible effect on *elf3-4/phyB-10* flowering time between seeds plated onto MS0.25 plates or sown directly onto soil (data not shown).

2.2.5 **Confocal Microscopy: Data collection, analysis and presentation**

Image Collection

For all experiments, the Leica Zeiss 710 confocal laser scanning microscope with Plan-Apochromat 63x/1.4 Oil DIC M27 objective and ZEN 2011 SP4 confocal software

(Leica) was used to collect images. Whole Arabidopsis seedlings were submerged in deionised water on clear white slides. For all YFP constructs, the fluorochrome was excited at 514 nm and emission detected between 525-615 nm. The CFP fluorochrome was excited at 488 nm and emission detected between 489-561 nm. The pinhole was set to airy one for all constructs. The same laser setting for each respective construct was used across all experiments **(Table 2.7)**. All images were collected as 512x512 Z-stacks, with a Z-stack slice depth of 0.4 μM.

Table 2.7 – Laser settings used in image capture

Construct	Laser (%)	Master Gain	Digital Gain	Digital Offset
35S::YFP:ELF3	4	695	2.60	23.40
35S::YFP:ELF3MC	3	758	1.90	8.04
35S::YFP:ELF3C	1	485	1	9
35S::YFP:ELF4	3	500	1.9	8.04
35S::ELF4:CFP	6	680	2.99	10

Data Analysis & Presentation

Measuring the cellular distribution of ELF3

The cellular distribution of full-length ELF3 and ELF3MC was measured from Arabidopsis hypocotyl cells (see Chapter 3, Figure 1A-B for representative images). For all images, Z-stacks were generated as described above and then compiled in ZEN-lite (Black Edition, version 2.3 SP1, Leica) and exported into imageJ (version 1.51w) for analysis. Image saturation was checked prior to analysis and any image that was saturated was discarded from the analysis. Images were also removed from the analysis if there was clearly more than one peak in the intensity plot when images were compiled in ZEN-lite. I then calculated the nuclear/cytoplasmic (N/C) ratio using the following approach:

1) Measure the total signal of the whole plant and the signal from each nuclei in that image using the imageJ polygon selection tool.

2) Calculate the average nuclear signal and average number of nuclei per image for each genotype under the respective condition (*e.g.,* full-length ELF3 in the dark at ZT10).
3) Divide the total image signal by the average number of nuclei for that genotype and condition. This I termed the “total” signal and used this as an approximation of the signal intensity per cell for that image.
4) Divide the average nuclear signal calculated in step 2 by the total signal calculated in step 3.
5) Calculate the average N/C ratio from the values of step 4.

All imaging was carried out on at least two separate occasions, with multiple seedlings imaged on each occasion. Each image that was collected was treated as a biological sample during the statistical analysis, although an average nuclei signal was calculated across all images to reduce variability betewen individual nuclei. Similar results were observed between images collected on different occasions. All presented images in this thesis are min/max projections that were compiled in ZEN-Lite (Black Edition, version 2.3 SP1, Leica edition). Further enhancements of image brightness were made in the Windows 10 Photo tool. Any adjustments that were made were applied consistently to all images of that particular figure.

Foci number and morphology measurements

ELF3 foci were manually counted from Z-stack compiled images of nuclei in the ZEN 2011 SP4 software. A min/max projection was generated for all images and the gamma was set arbitrarily to 2. The gamma was adjusted to 2 to reduce the intensity of the nucleoplasmic signal which in some instances hindered the distinguishment between foci and nucleoplasmic signal. Foci were then determined as any signal that generated clear signal peaks above the nucleoplasmic background in 2.5D projection plots. These counts were then validated by manually scanning through each image of that Z-stack for foci. All imaging was performed on at least two separate occasions. In total, foci were

counted in a minimum of 10 nuclei for each respective light treatment and genotype. Each nuclei was treated as an independent biological sample. Similar results were observed between images collected on different occasions.

To measure the morphology and number of ELF3C foci, Z-stacks of nuclei were compiled in ZEN-lite (Black Edition, version 2.3 SP1, Leica) before being exported into imageJ and converted into binary images. The number, intensity and dimensions of the foci were then automatically measured using the analyse particle tool within imageJ (version 1.51w). ELF3C foci were assumed to be spherical and the same fixed scale was used across all images. The minimum circularity was set to 0.55 to minimise the measurements of any non-spherical artefacts within each image. All ELF3C experiments were repeated twice, with a minimum of 6 images (>60 individual foci) analysed for each light condition. Any foci that moved during the collection of the Z-stacks was discarded from the morphology analysis but were included in the count of the number of foci per nucleus.

2.2.6 **Cellular Localisation Experiments**

Light Pulses Experiment

Full-length ELF3 (in the *elf3-4*, *elf3-4/elf4-1* or *elf3-4/phyB-10* background), ELF3MC and ELF3C seeds were surface sterilised as described above before being plated onto MS0.25 plates with the top quarter of agar removed. Seeds were stratified for three days before being grown vertically for seven days under SD photoperiods (8-hours light/16-hours dark) with a constant temperature of 22ºC and 85 µmol/m^{-2}/s^{-1} of white light (WL). On day 7, seedlings were transferred at ZT7 to a custom-built LED stack and pulsed with either BL, RL, FRL or WL **(Table 2.8)**. BL, RL and WL pulses were applied for three hours, while FRL pulses were applied for 15 minutes. Three hours of WL exposure has been previously described to promote the localisation of phys to their respective sub-nuclear bodies, while 15-minutes of FRL caused the rapid disassembly of phyB from these sub-nuclear bodies (Kircher et al., 2002, Van Buskirk et al., 2014). Thus, it was assumed a similar length of light exposure would be sufficient to promote

changes in ELF3 cellular localisation. As a control for the BL, RL and WL experiments, seedlings were moved to the dark at ZT7. For FRL experiments, a control plate of seedlings was kept under 85 μmol/m^{-2}/s^{-1} of WL for the duration of the FRL pulse. Light pulses and control plates were kept at 19ºC for the duration of the treatment. All seedlings were imaged immediately upon the end of the respective light treatment for up to one hour. Light intensity was measured with a Skye SpectroSense2 light sensor. Data was collected and analysed as described in section 2.2.5.

Table 2.8 - Light intensities used for confocal experiments.

Wavelength	**Blue light Intensity**	**Red light Intensity**	**Far-Red light Intensity**
Red Light (RL)		1-25 μmol/m^{-2}/s^{-1} (1)	
Blue Light (BL)	25 μmol/m^{-2}/s^{-1}		
White Light (+BL)	40 μmol/m^{-2}/s^{-1}	20 μmol/m^{-2}/s^{-1}	
White Light (+RL)	12 μmol/m^{-2}/s^{-1}	25 μmol/m^{-2}/s^{-1}	
White Light (BL=RL)	24 μmol/m^{-2}/s^{-1}	24 μmol/m^{-2}/s^{-1}	
Far-Red			110 μmol/m^{-2}/s^{-1}

[1]A range of RL intensities were used from 1 μmol/m^{-2}/s^{-1} up to 25 μmol/m^{-2}/s^{-1}. These are described in chapter 3.

[2] Wavelength spectrum: RL = 650 nm (20 nm bandwith), BL = 450 (20 nm bandwith) and FRL = 730 (20 nm bandwith).

Cellular and sub-nuclear localisation timecourse of ELF3.

Seeds of *35S::YFP:ELF3* in either the *elf3-4* or *elf3-4/elf4-1* mutant background were surfaced sterilised and plated onto MS0.25 plates before being stratified for three days. Seedlings were then grown vertically for six days under SD photoperiods (8/16) with a constant temperature of 22ºC and 85 μmol/m^{-2}/s^{-1} of WL. Imaging was started at ZT7 on day 7 and was carried out at ZT8, 12, 16, 20 and 24. Apart from ZT7 and ZT24, plates were kept in the dark until seedlings were imaged. For ZT7 and ZT24, seedlings were kept under 85 μmol/m^{-2}/s^{-1} of WL until they were imaged. The timecourse was repeated for both genotypes at least twice with a new plate of seedlings used for each

timepoint and multiple biological samples imaged at each ZT. The same microscope and laser settings **(Table 2.7)** was used regardless of the *ELF4* allele. All data was made relative to the values measured for ELF3 in the WT ELF4 background at ZT7. Data was collected and analysed as described in section 2.2.5.

ELF3 foci characterisation in root tissue

To characterise the foci dynamics of ELF3 in root tissue, *35S::YFP:ELF3* seeds in either the *elf3-4* or *elf3-4/4-1* background were plated onto MS0.25 plates. Plates were then stratified for the three days before being transferred to a SD chamber (8/16 LD) with a constant temperature of 22ºC and 85 µmol/m^{-2}/s^{-1} of WL. Seedlings were grown vertically for 6 days before the experiment was started at ZT7 on day 7. The number of foci per nucleus was measured at ZT7, ZT8 and ZT12 in the middle region of the root. A new plate of seedlings was used for each timepoint. For samples measured at ZT8, plates were transferred to the dark for five minutes before being imaged to provide a light-dark transition. These plates were then kept in the dark until they were imaged. All experiments were repeated at least twice and a new plate of seedlings was used for each timepoint. The microscope and laser settings for each respective construct are described in table 2.7. Foci were measured as described in section 2.2.5.

ELF3 foci and nuclear characterisation in response to heat stress

To investigate the responsiveness of ELF3 foci to heat stress, *35S::YFP:ELF3* seeds with a WT or mutant allele of *ELF4* were plated onto MS0.25 plates with the top quarter of the agar removed and then stratified for three days as described above. Seedlings were then grown vertically for 6 days under SD photoperiods with a constant temperature of 22ºC and 85 µmol/m^{-2}/s^{-1} of WL. At ZT6 on day 7, seedlings were transferred to either a 22ºC or 27ºC chamber for two hours until they were imaged at ZT8. A 2-hour heat pulse was applied to copy the duration of heat pulse applied in the work of Jung et al., (2020). However, the authors did not include the timing of their heat pulse. I reasoned as ELF3 is expresed and accumulates at dusk (Liu et al., 2001,

Nusinow et al., 2011), a pre-dusk pulse would elicit the strongest response For both temperatures pulses, seedlings were kept under 25 μmol/m^{-2}/s^{-1} of WL until lights were turned off at ZT8 to ensure the seedlings underwent a light-dark transition. Seedlings were then kept at the respective temperature in the dark until they were imaged to ensure there was no rapid reversion in foci dynamics in the absence of the heat pulse. Seeds from the two genotypes were plated onto the same plate to minimise heat or light gradients in the chamber.

Foci were measured in the nuclei of hypocotyl and upper to middle root tissue on at least two separate occasions with multiple biological samples used each time. The microscope and laser settings are as described in table 2.7, while foci were measured as described in section 2.2.5. The nuclear signal was measured by compiling Z-stacks in ZEN-lite (Black Edition, version 2.3 SP1, Leica) and exporting images (default intensity projection) into imageJ (version 1.51w). The nuclear signal data presented in chapter 5 is integrated density. Integrated density was used to account for variation in the size of nuclei between images.

2.2.7 **Gene expression analysis**

RNA Extraction and cDNA Synthesis

Approximately 100 mg of Arabidopsis seedlings were collected for each RNA extraction. Seeds were surface sterilised as described above and stratified for three days at 4ºC. Seedlings were then grown under SD (8/16) photoperiods with a constant of temperature of 22ºC and 85 μmol/m^{-2}/s^{-1} of WL for 6 days until they were harvested on day 7. See chapter 3 and chapter 4 for the specific details on the genotypes, light conditions and timepoints used. All tissue was flash-frozen in liquid nitrogen before being stored at -80ºC. RNA was extracted with the RNeasy Plant Mini Kit (Qiagen) following manufacturer's instructions. RNA was eluted in 50 μL of nuclease-free water. 5 μL of this elution was run on a 1.5% agarose gel (TBE) stained with ethidium bromide to confirm that the RNA extractions were successful and was not degraded. The remaining 45 μL of RNA was immediately stored at -80 until DNase treated.

DNase treatment was performed off-column following manufactures (Zymo) instructions apart from increasing the DNase incubation time from 15 to 25 minutes. After DNase treatment, RNA was cleaned using the Zymo clean and concentrator kit following manufactures instructions. Final RNA was eluted in 15 µL of nuclease-free water. The quality and quantity of RNA was checked by nanodrop ($A_{260}/A_{280} > 2$, $A_{260}/A_{230} > 2.1$). To confirm the integrity of the RNA, 1 µL of extracted RNA was loaded onto a 1.5% agarose gel (TBE) stained with ethidium bromide. RNA with the required quality and integrity was subsequently stored at -80 until cDNA was generated. 0.25 to 1 µg of cDNA was synthesised using SuperScriptIV (ThermoFisher Invitrogen) following manufactures instructions. Synthesised cDNA was diluted to a concentration of 1.25 ng/µL and then frozen at -20ºC.

qPCR

All qPCR reactions were performed on an ABI StepOnePlus™ (StepOne Plus Version 2.3 software) in a 20 µL reaction volume **(Table 2.9**, **Table 2.10)**. The concentration of primers used is described in table 2.11. All samples had two biological replicas, with at least two technical replicas per biological repeat. No template controls (NTCs) and no reverse-transcriptase controls (NRTCs) in duplicates were run in parallel alongside cDNA samples. qPCR cycle conditions are described in table 2.17. A melt-curve (cycle conditions in **Table 2.10**) was performed to ensure specific target amplification. All data is presented as the change in target transcript abundance relative to the transcript abundance of *PROTEIN PHOSPHATASE2A* (*PP2A*) in the respective genotype and experimental conditions, following the example described in previous studies (Kolmos et al., 2009).

Table 2.9 - qPCR reaction set-up

Reagent	**Quantity (20 µL volume**)
SYBR-Green	10 µL
Nuclease-free water (not DEPC treated)	1.5 µL
cDNA template (1.25 ng/µL)	7.5 µL
Primer Mix (Varying concentrations)[1]	1 µL

[1] See table 2.11 for primer concentration used.

Table 2.10 - qPCR cycle conditions

Condition	**Stage**
1x 94°C for 20 seconds **40x** 95°C for 3 seconds 60°C for 30 seconds	qPCR reaction
95°C for 15 seconds 60°C for 60 seconds[1] 95°C for 15 seconds	Melt curve

[1]Temperature was increased in 0.3 °C increments

qPCR Primer Efficiency Tests

The amplification efficiency of all primers used for qPCR (sequences in **Table 2.5**) was prior tested before any experiments were performed. Firstly, a non-quantitative PCR (reaction set-up described in **Table 2.6**) was carried out to confirm that the amplicons produced by the respective primers were of the expected size and did not generate visible primer dimers. Next, a serial-dilution qPCR reaction with a melt curve was carried out to determine amplification efficiency of the primers. A three-fold, 1:10 serial-dilution of cDNA (starting at 5 ng/µL) generated from RNA harvested from ten-day old WT Ws-2 seedlings at dawn and dusk was used as a template. The cycle conditions are described in table 2.9. All primers were optimised until an $R^2 > 0.98$ and a M of between -3.2 and -3.6 was achieved **(Table 2.11)**. NTCs and NRTCs were run in parallel to identify primer dimers and genomic DNA

contamination respectively. Any primers with non-specific amplification or primer dimers were discarded.

Table 2.11 - qPCR optimised primer standard curve values

Gene Target	Concentration (nM)	Efficiency	R^2	M
PP2A	250	1.02	0.987	-3.26
LUX	350	0.93	0.999	-3.58
TOC1	200	0.90	0.990	-3.6
PRR9	250	0.93	0.985	-3.51
GI	250	0.93	0.999	-3.5

2.2.8 **Bioinformatics**

Two separate protein alignments were carried out to investigate the ubiquity of the Arabidopsis ELF3 nuclear localisation signal (NLS). The first alignment used sequences orthologous to Arabidopsis ELF3 from across the tracheophyte (vascular) plant clade. The second alignment used ELF3 orthologs exclusively from monocotyledon (grasses) plants. Sequences with homology to *Arabidopsis thaliana* ELF3 were retrieved from Phytozome (https://phytozome.jgi.doe.gov/, version 12.1) using a BASIC LOCAL ALIGNMENT SEARCH TOOL PROTEOME (BLASTP) search in November 2020. All BLASTP parameters were set at their default setting. The reference Arabidopsis ELF3 protein used in these BLASTP searches was accessed from TAIR (https://www.arabidopsis.org/) in October 2016. The plant species used in the alignments are listed in table 2.12, while the full sequence of each ELF3 ortholog used in the tracheophyte and monocot-specific analysis is available in appendix 1 and appendix 2, respectively.

All protein alignments were carried out using the online version of MAFFT (https://mafft.cbrc.jp/alignment/software/, version 7). All parameters were set to their default settings for the monocotyledon alignment. For the tracheophyte alignment, the

iterative refinement E-INSI-i method was used and the “leave gappy regions” selected. This approach was adopted to circumvent the large stretches of low-complexity regions that were interspersed between short regions of high conservation in the ELF3 orthologs. Aligned sequence were exported as FASTA files before being imported into Jalview (https://www.jalview.org/, version 2.11) to visualise the alignment. These alignments were exported from Jalview as a .png image and then imported into InkScape (version 1) for visual enhancement. Putative NLS sequences were identified through the NLS database (NLSdb) online search tool (https://rostlab.org/services/nlsdb/).

Table 2.12 – Plant species used in the bioinformatic analysis.

Species	Number of sequences	Genome version	Analysis*
Arabidopsis thaliana	1[+]	TAIR10	T
Arabidopsis lyrata	1[$]	2.1	T
Oryza sativa	2[$]	7 JGI	B
Zea mays	2	Ensembl-18	B
Populus trichocarpa	2	3.0	T
Medicago truncatula	3[$]	Mt4.0v1	T
Brassica rapa	2[$]	FPsc v1.3	T
Sorghum bicolor	2	3.1.1	B
Solanum lycopersicum	3[$]	iTAG2.4	T
Eucalyptus grandis	2	2.0	T
Brachypodium distachyon	1	3.1	B
Selaginella moellendorffi	2	1	T
Hordeum vulgare	1	R1[^]	M
Setaria italica	2	2.2	M
Panicum virgatum	2[$]	1.1	M
Panicum hallii	2	2.0	M
Oropetium thomaeum	2	1	M

[*] Species were included in either the: tracheophyte alignment only (T), both alignments (B) or monocot alignment only (M).

[+] In Arabidopsis thaliana, a secondary protein called ESSENCE of ELF3 CONSENSUS (EEC) has been reported (Liu et al., 2001). EEC was not included in this analysis.

[$] Protein fragments were identified in the BLASTP searches that had partial homology to ELF3. However, the homology to *Arabidopsis thaliana* (A.T) ELF3 was restricted to 20 to 160 amino acid fragments which aligned primarily to the middle region or C-terminus of A.T ELF3 (as defined in Liu et al., 2001). These ELF3-fragments were excluded here.

^ The *Hordeum vulgare* (Barley) genome version is a pre-release.

Chapter 3 - The cellular localisation of ELF3 is dynamically regulated by light

3.1 Introduction

The perception and integration of light signals to the circadian clock is important for entrainment. Entrainment is the process whereby the phase of the circadian clock is aligned with the external environment so that internal physiological responses are coordinated to occur at the most optimal time of the day (Millar, 2004). Light signals are transmitted to the oscillator through the activity of photoreceptors. Phys are the principal photoreceptors that signal RL and FRL to the circadian clock (Somers et al., 1998). Phys exist in two forms, the inactive Pr and the active PFr (Rockwell et al., 2006). Exposure to RL promotes the conversion of phys from the Pr to PFr isoform. The reversion from the PFr back to the Pr isoform is promoted by a pulse of FRL or through thermal relaxation in response to elevated temperature and prolonged darkness (Klose et al., 2015, Legris et al., 2016).

In Arabidopsis, there are five phys: the light labile phyA, and the light stable phyB-E (Clack et al., 1994). phyA is the primary sensor of FRL and dim RL (RL intensities under 1 $\mu mol/m^{-2}/s^{-1}$), while phyB primarily facilitates RL entrainment above RL intensities of 10 $\mu mol/m^{-2}/s^{-1}$ (Somers et al., 1998). phyA also contributes to low intensity BL entrainment, while phyC-E function redundantly with phyB in facilitating RL entrainment (Somers et al., 1998, Jones et al., 2015). A key target of phy signalling activity within the circadian clock is the EC. The expression of *ELF4* is directly induced in response to FRL and RL in a phyA and phyB-dependent manner, respectively (Tepperman et al., 2001, Khanna et al., 2003, Siddiqui et al., 2016). Separately, phyB has been demonstrated to directly interact with LUX and ELF3 *in vitro* and *in vivo* (Liu et al., 2001, Yeom et al., 2014). So far, the outcome of the phyB-LUX interaction has remained untested, while the phyB-ELF3 interaction has been remained enigmatic. It has been proposed that the physical interaction between ELF3 and phyB inhibits the function of ELF3 within the circadian clock (Herrero et al., 2012). However, it has unknown how the interaction between phyB and ELF3 could lead to the inhibition of ELF3 function.

Controlling the spatial and temporal localisation of proteins to a specific cellular or sub-cellular compartment is an emerging mechanism in controlling a protein's activity (Ronald and Davis, 2019). Previous reports have highlighted the importance of the nuclear and sub-nuclear localisation of ELF3 in facilitating ELF3 circadian function (Kolmos et al., 2011, Herrero et al., 2012, Anwer et al., 2014). Separately, phyB has been described to regulate the spatial localisation of proteins to control their activity and stability (Al-Sady et al., 2006, Kaiserli et al., 2015, Lu et al., 2015). Therefore, I hypothesised that phyB regulates ELF3 activity by changing the cellular and/or sub-nuclear distribution of ELF3.

In this chapter I investigated whether the cellular localisation of ELF3 is responsive to light and the role of phyB in facilitating light-dependent changes in ELF3 localisation. I have found that different wavelengths of light dynamically regulate the cellular localisation of ELF3 within the cell, and for RL the effect is dependent on the intensity of light and domain of ELF3 analysed. Furthermore, I have characterised the requirement for phyB in facilitating RL-dependent changes in the cellular localisation of ELF3. Finally, I investigated the role of phyB in controlling ELF3 repressive activity. Together, this work provides a new understanding of how light signalling pathways regulate ELF3 activity.

3.2 Results

3.2.1 The cellular and sub-nuclear distribution of ELF3 is responsive to red light

To determine whether phyB regulated the cellular localisation of ELF3, I examined the effect of a RL-pulse on the cellular and sub-nuclear localisation of ELF3. Arabidopsis seedlings expressing *35S::YFP:ELF3* (first described in Herrero et al., 2012 and henceforth referred to as ELF3) were either transferred to the dark as a control or pulsed for three hours with 25 $\mu mol/m^{-2}/s^{-1}$ of RL at ZT7 (1-hour before dusk, short-day (SD) photoperiods) before being imaged immediately at ZT10. The *35S* promoter was chosen over the native *ELF3* promoter to remove any indirect of RL on *ELF3* transcription (Lu et al., 2012).

ELF3 has previously shown to localise to the cytoplasm and nucleus (Herrero et al., 2012). As a result, I assumed all non-nuclear signal measured here represented the cytoplasmic pool of ELF3 and is henceforth referred to as such. ELF3 was localised between the cytoplasm and nucleus of Arabidopsis hypocotyl cells regardless of the light treatment **(Figure 3.1A-B)**. However, the nuclear-cytoplasmic (N/C) ratio of ELF3 was lower in RL-pulsed samples than in the dark **(Figure 3.1C)**. ELF3 is stabilised in the light and this is facilitated by a physical interaction with phyB (Nieto et al., 2015). Therefore, these observed changes in the N/C ratio of ELF3 could reflect changes in the stability of ELF3. To test this, I analysed the relative nuclear and total signal under the different light regimes. A pulse of RL reduced the relative nuclear signal of ELF3, while there was no change in the relative total signal between the different light treatments **(Figure 3.1D-E)**. The reduction in the nuclear signal (-9.3%) was similar to the reduction in the N/C ratio (-8.4%) of ELF3 following a RL-pulse. Combined, this suggests that RL may directly regulate the cellular localisation of ELF3.

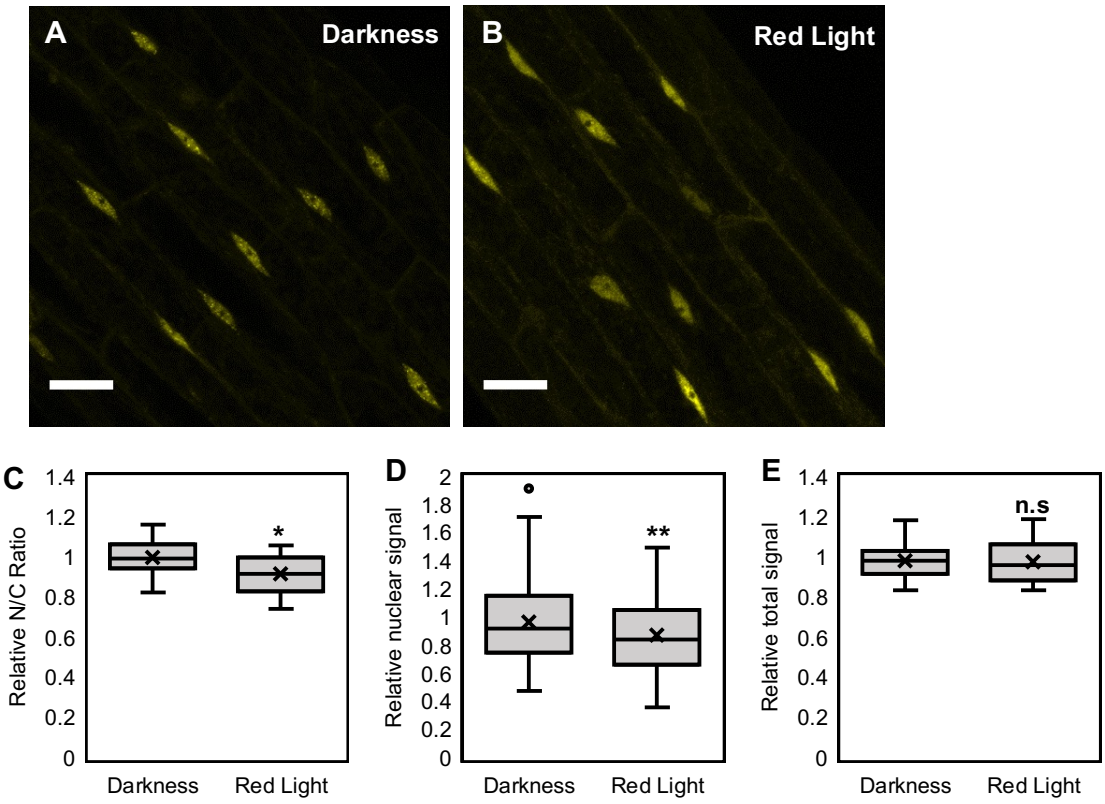

Figure 3.1 - Red light influences the cellular distribution of ELF3.

The cellular distribution of ELF3 was imaged in seven day old seedlings expressing *35S::YFP:ELF3* at ZT10 after being either transferred to the (**A**) dark or (**B**) pulsed with 25 μmol/m^{-2}/s^{-1} of red light (RL) for three hours starting at ZT7 (1-hour before dawn, short day photoperiods). Scale bars are 25 μm. Relative (**C**) nuclear/cytoplasmic (N/C) ratio (**D**) nuclear and **(E)** total signal of ELF3 under the different light regimes. All data was made relative to the values of ELF3 in the dark at ZT10. In total, for darkness 18 images were captured totalling 160 individual nuclei being measured. For red light, 14 images were captured totalling 125 individual nuclei being measured. Significance was determined by an unpaired two-way t-test, * = $p < 0.05$, ** = $p < 0.01$ and n.s = no significance.

Within the nucleus ELF3 associates to small, sub-nuclear structures previously called foci (Herrero et al., 2012, Anwer et al., 2014). Here, I will continue to refer to these sub-nuclear structures using this general name. The role of foci in facilitating ELF3 activity remains unknown. ELF3 interacts with different proteins that independently associate to sub-nuclear structures with distinct properties. For example, the localisation of phyB to sub-nuclear domains is dependent on RL and the size of these structures increases with the duration and intensity of the RL-pulse (Chen et al., 2003). Therefore,

understanding the physiological changes in number and morphology of ELF3 foci under different light conditions may in turn provide insights into the significance of these structures in facilitating ELF3 activity.

Regardless of the light treatment, there was at least one focus per nucleus in all nuclei that were imaged (data not shown). In the dark, there was approximately 13 foci per nucleus **(Figure 3.2A,C)**. The size of these foci was highly variable both within and across the different nuclei that were imaged. A RL-pulse reduced the number of foci per nucleus, resulting in approximately 6 foci per nucleus. This decrease was mirrored by an increase in nucleoplasmic signal **(Figure 3.2A-C)**. As with seedlings transferred to the dark, the size of foci was highly variable in RL-pulsed seedlings. However, foci did appear smaller after a RL-pulse. Direct measurements of foci morphology was attempted but it was not possible to accurately resolve the boundary between the nucleoplasm and focus for either samples in the dark or those pulsed with RL. Therefore, quantification of full-length ELF3 foci was not attempted further. In summary, RL can regulate the cellular and sub-nuclear distribution of ELF3.

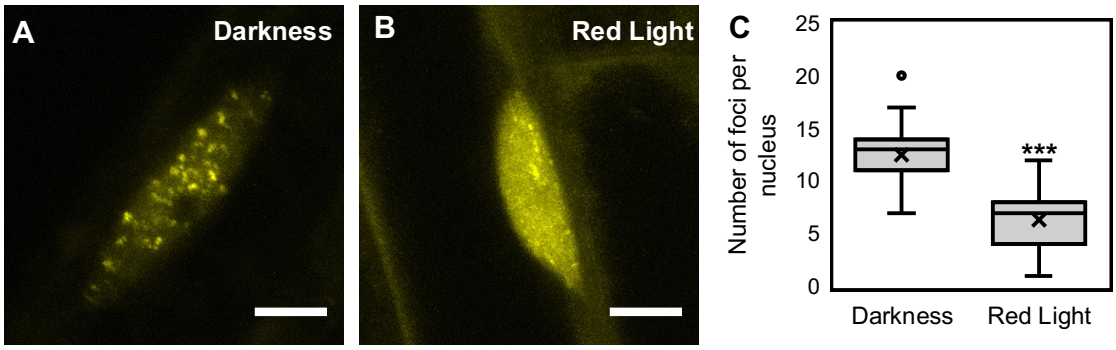

Figure 3.2 - Red light influences the sub-nuclear distribution of ELF3

Hypocotyl nuclei of 7-day old seedlings expressing *35S::YFP:ELF3* were imaged at ZT10 after being either transferred to the (**A**) dark or (**B**) pulsed with 25 μmol/m^{-2}/s^{-1} of red light (RL) for three hours starting at ZT7 (1-hour before dawn, short day photoperiods). Scale bars are 5 μm. (**C**) The number of foci per nucleus. In total, 40 nuclei images were analysed for darkness, while 47 nuclei images were analysed for RL. Significance was determined by an unpaired T-test, *** = $p < 0.001$. The darkness and RL data are re-used in further figures of this work.

3.2.2 **Light has wavelength-specific effects on ELF3 localisation**

To understand whether other wavelengths of light also influenced the cellular or sub-nuclear localisation of ELF3, I investigated the localisation of ELF3 after a pulse of BL. Using the same ELF3 line as before, seedlings were either transferred to the dark or pulsed for three hours with 25 μmol/m^{-2}/s^{-1} of BL at ZT7 before being imaged immediately at ZT10. As observed previously, ELF3 was distributed between the nucleus and cytoplasm but there was a greater nuclear localisation of ELF3 after a BL-pulse **(Figure 3.3A-C)**. Analysing the relative nuclear signal confirmed that the nuclear pool of ELF3 increased following a BL-pulse **(Figure 3.3D)**. However, the normalised total signal also increased after a BL-pulse **(Figure 3.3E)**. Therefore, BL promotes both the nuclear localisation and stability of ELF3.

Within the nucleus, ELF3 remained distributed between the nucleoplasm and foci. However, there was a large increase in the number of foci per nucleus following a BL-pulse **(3.3F-H)**. In contrast to the effect of RL, this change in the sub-nuclear distribution of ELF3 did not correlate with a change in the amount of nucleoplasmic signal compared to samples transferred to the dark. Furthermore, there was no consistently observable effect of the BL-pulse on the morphology of ELF3 foci compared to those in the dark. Again, direct quantification was not possible for the reasons discussed above. In conclusion, these results show that the cellular and sub-nuclear localisation of ELF3 is responsive to multiple wavelengths of light.

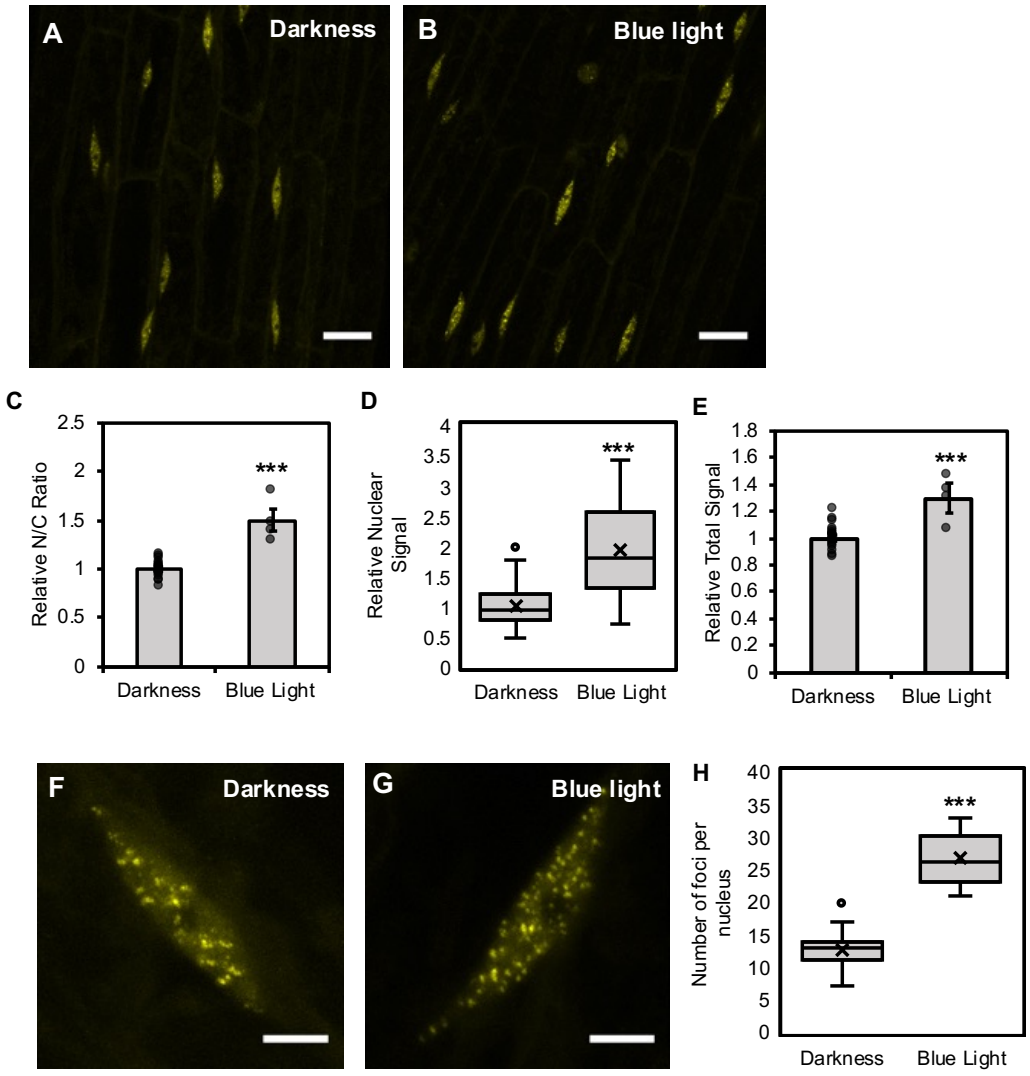

Figure 3.3 - Blue light regulates the cellular localisation of ELF3

The cellular distribution of ELF3 was imaged in 7-day old seedlings expressing *35S::YFP:ELF3* at ZT10 after being either transferred to the (**A, F**) dark or (**B, G**) pulsed with 25 μmol/m^{-2}/s^{-1} of BL for three hours starting at ZT7 (1-hour before dawn, short day photoperiods). Scale bars in (**A, B**) are 25 μm and in (**F, G**) 5 μm. The relative **(C)** nuclear/cytoplasmic (N/C) ratio, (**D**) nuclear and **(E)** total signal of ELF3 under the different light regimes. Data was made relative to the values of ELF3 in the dark. (**H**) The number of foci per nucleus in the dark or after a BL-pulse. For both treatments, images were collected on at least four separate occasions. In total, for darkness: **(C-E)** 18 images were captured, totalling 160 individual nuclei and **(H)** 40 images for the foci count. For blue light: **(C-E)** four images were captured totalling 45 individual nuclei and **(H)** nine images for foci counts. Significance was determined by an unpaired t-test, *** = $p < 0.001$. Errors bars are standard error of the mean, circles are datapoints. The blue light data is re-used in further figures in this work. The darkness data is the same as presented in figure 3.1 and figure 3.2.

3.2.3 **Different wavelengths of light have a competitve effect on ELF3 sub-nuclear localisation**

As RL and BL caused opposite effects on the localisation of ELF3, I investigated whether there was competition between RL and BL on regulating the localisation of ELF3. As the effect of both RL and BL was more strongly observed on ELF3 sub-nuclear dynamics, I focused on the response of ELF3 foci to different pulses of WL-pulses with varying spectral ratios of RL and BL. Seedlings were pulsed with equal ratios of RL and BL (25 μmol/m^{-2}/s^{-1} of each), predominantly blue (40 μmol/m^{-2}/s^{-1}BL:20 μmol/m^{-2}/s^{-1}RL) or predominantly RL (25 μmol/m^{-2}/s^{-1}RL:12 μmol/m^{-2}/s^{-1}BL) light. These were termed WL(=), WL(BL+) and WL(RL+), respectively. The timing and duration of the light pulses was carried out as described above.

ELF3 was localised between the nucleoplasm and foci regardless of the spectral composition of the WL-pulse. However, the RL:BL ratio did influence the number of foci that were observed **(Figure 3.4)**. In samples pulsed with WL(=) the number of foci was similar number to the foci observed in nuclei of seedlings transferred to the dark **(Figure 3.4A, 3.4D, 3.4G)**. However, there was a large amount of variation in the number of foci after a WL(=)-pulse. The source of this variation was unclear; foci formation after the WL(=)-pulse was highly variable both within and across different biological samples that were measured on separate occasions. The number of foci observed following a WL(=)-pulse reflected the spectrum of responses seen in nuclei pulsed with monochromatic RL or BL, or in those transferred to the dark **(Appendix 3, Figure 1)**.

After a WL(RL+)-pulse, the number of foci per nucleus was strongly reduced and the nucleoplasmic signal increased **(Figure 3.4C, 3.4G)**. The effect of a WL(RL+)-pulse was similar to the effect of a monochromatic RL-pulse **(Figure 3.4B-C)**. To confirm that the BL intensity used in the WL(RL+) was capable of promoting foci formation, I analysed the number of foci per nucleus after a 12 μmol/m^{-2}/s^{-1} monochromatic BL-pulse. As with a 25 μmol/m^{-2}/s^{-1}monochromatic BL-pulse, a 12 μmol/m^{-2}/s^{-1} monochromatic BL-pulse promoted ELF3 foci formation and there was no significant difference in the effect between the two BL intensities **(Appendix 3, Figure 2)**. This suggests that RL supress

the effect of BL on promoting ELF3's localisation to foci. Supporting this, the number of foci after a WL(BL+) was slightly, but not significantly, reduced compared to samples transferred to the dark **(Figure 3.4E, 3.4G)**. As with a 12 or 25 µmol/m^{-2}/s^{-1} pulse of BL, a 40 µmol/m^{-2}/s^{-1} monochromatic BL-pulse was sufficient to promote ELF3 foci formation **(Appendix 3, Figure 2)**. Thus, RL suppress the effect of BL on the sub-nuclear localisation of ELF3.

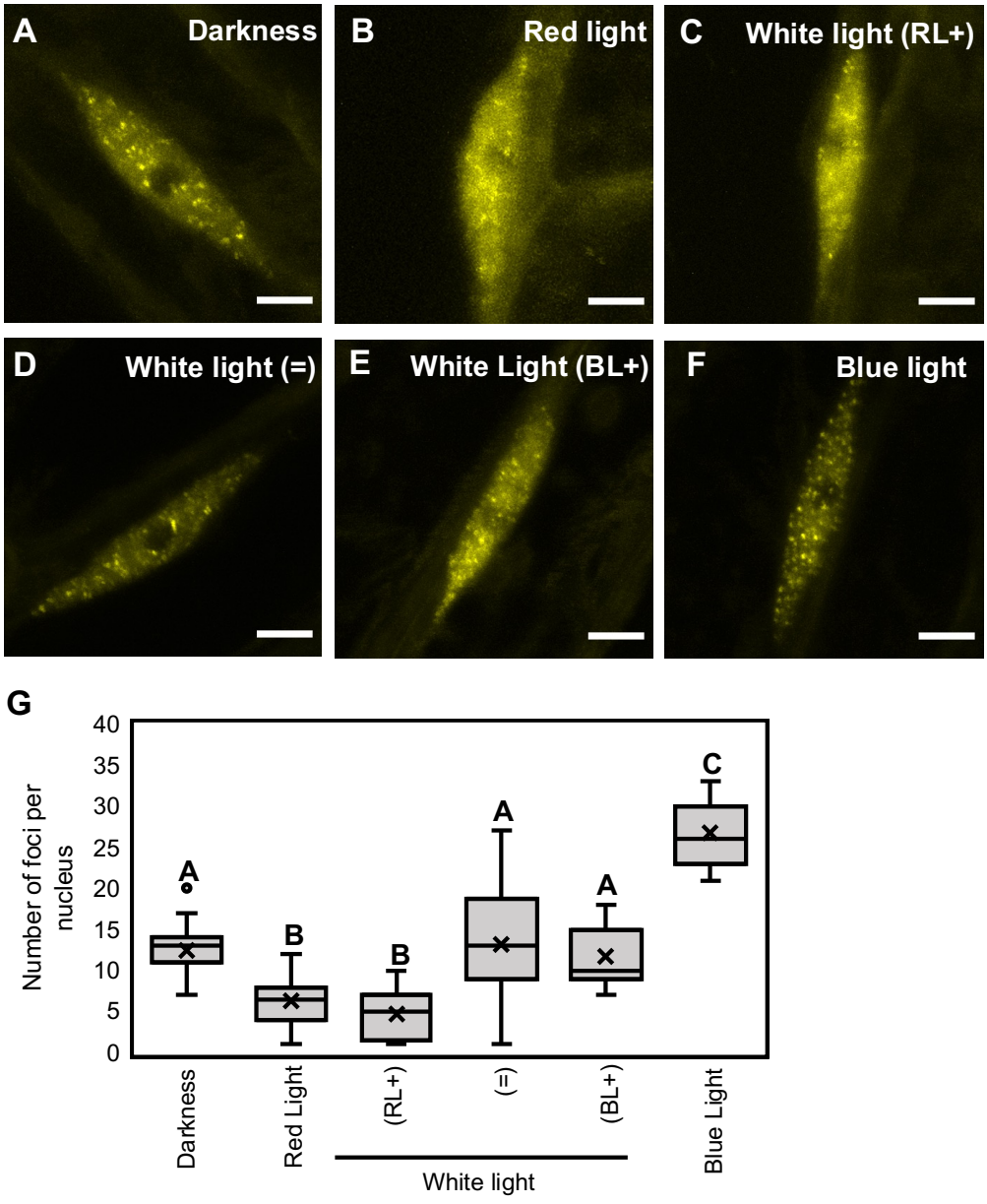

Figure 3.4 - Light has a competitive effect on the sub-nuclear localisation of ELF3

Hypocotyl nuclei of seedlings expressing *35S::YFP:ELF3* under different light treatments at ZT10 (short-day 8/16 photoperiods). **(A)** Darkness, **(B)** 25 μmol/m^{-2}/s^{-1} red light (RL)**, (C)** white light: 25 μmol/m^{-2}/s^{-1} of RL & 12 μmol/m^{-2}/s^{-1} of blue light (BL), **(D)** white light: 25 μmol/m^{-2}/s^{-1} of RL and 25 μmol/m^{-2}/s^{-1} of BL, **(E)** white light: 20 μmol/m^{-2}/s^{-1} of RL and 40 μmol/m^{-2}/s^{-1} of

Figure 3.4 (continued) - BL and **(F)** 25 μmol/m^{-2}/s^{-1} BL. Scale bars are 5 μm. **(G)** Number of foci per nucleus under the respective light treatments. All light pulses were applied for three hours starting at ZT7. All experiments were repeated twice, with at least 12 nuclei imaged and counted in total. Significance was determined by a one-way ANOVA with a tukey HSD posthoc test. Letters signify significant difference of $p < 0.001$, same letters indicate no significant difference. The darkness and RL25 datasets are the same as presented in figure 3.2, while the BL25 dataset is the same as presented in figure 3.3.

3.2.4 ELF3 has a domain specific response to red and blue light

The N-terminus region of the ELF3 protein (amino acid residues 1-261) connects ELF3 to light signalling directly through physical interactions with phyB and COP1 (Liu et al., 2001, Yu et al., 2008). However, the middle (amino acid residues 262-484) and C-terminus region (amino acid 485-695) of ELF3 facilitates interactions with other proteins also associated directly or indirectly connected with light signalling. Therefore, it is important to understand the importance of the ELF3 N-terminus in facilitating light-dependent changes in the cellular and sub-nuclear localisation of ELF3.

To investigate the requirement of the ELF3 N-terminus in facilitating light-dependent changes in ELF3 localisation, I tested the effect of RL and BL-pulses on the localisation of the previously described *35S::YFP:ELF3MC* and *35S::YFP:ELF3C* (Herrero et al., 2012). Arabidopsis seedlings expressing the respective *ELF3MC* or *ELF3C* constructs were pulsed with either 25 µmol/m^{-2}/s^{-1} BL or RL or transferred to the dark as a control. The timing and duration of the light pulse were carried as described above.

As previously reported, ELF3MC was localised between the nucleus and cytoplasm **(Figure 3.5A-C)** (Herrero et al., 2012). There was no change in the N/C partitioning of ELF3MC after a RL-pulse. However, both the relative nuclear and normalised total signal was reduced by a RL-pulse **(Figure 3.5F)**, suggesting that RL-pulses de-stabilise ELF3MC. A BL-pulse increased the nuclear localisation of ELF3MC, the same effect as was observed with full-length ELF3 **(Figure 3.3, Figure 3.5A-E).** Unlike full-length ELF3, there was no change in the normalised total signal of ELF3MC after a BL-pulse **(Figure 3.5F)**, suggesting that BL can directly promote the nuclear

localisation of ELF3. Within the nucleus, ELF3MC was predominantly localised to the nucleoplasm with foci infrequently observed in some nuclei. There was no clear effect of either RL or BL on the frequency of nuclei containing a focus or the number of foci per nuclei (data not shown).Taken together, this suggests that the N-terminus is required for RL-dependent changes in the localisation of ELF3 and BL-dependent changes in the stability of ELF3, while BL promotes the nuclear localisation of ELF3 through the M or C domain.

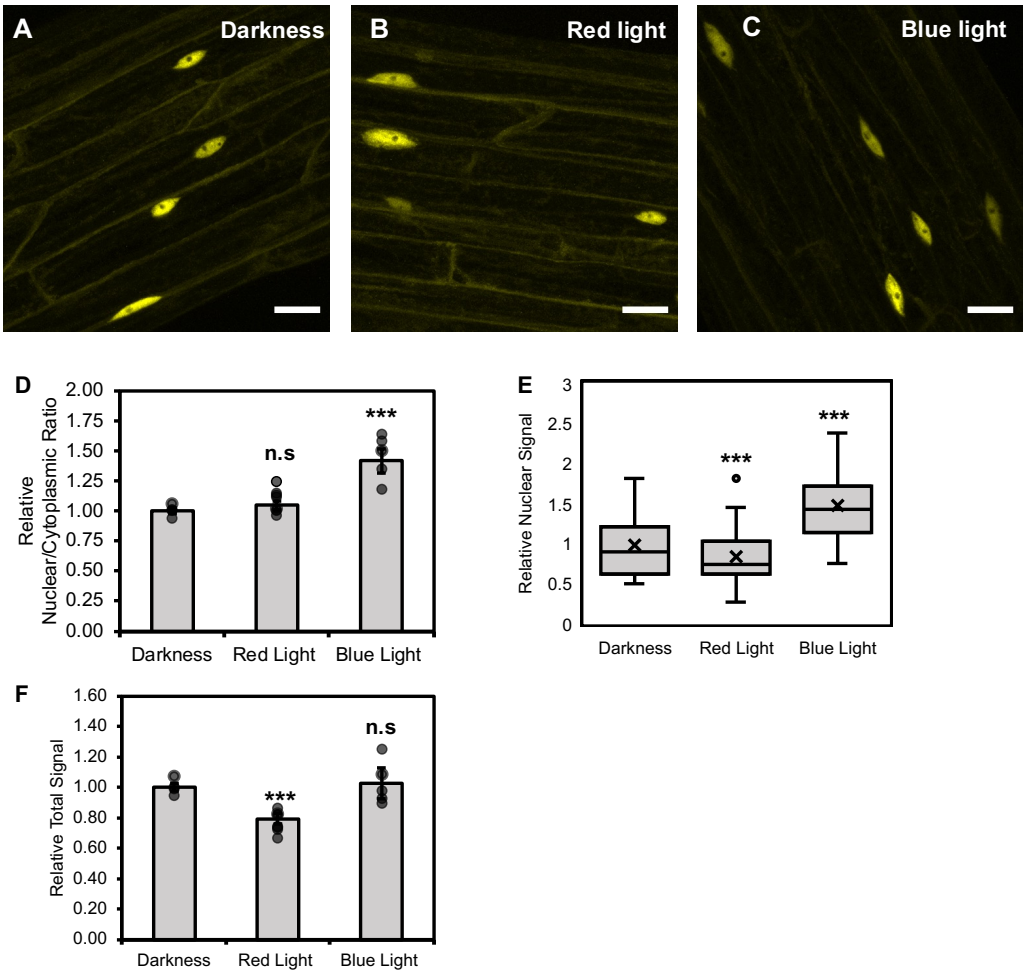

Figure 3.5 - The localisation of ELF3 has a domain dependent response to light

The cellular distribution of *35S::YFP:ELF3MC* (ELF3MC) in 7-day old seedlings either transferred to (**A**) the dark or pulsed with 25 μmol/m^{-2}/s^{-1} pulse of (**B**) red or (**C**) blue light. Light pulses were applied for three hours starting at ZT7 (1 hour before dusk, short-day photoperiods). Scale bars in A-C are 25 μm. (**D**) The relative nuclear/cytoplasmic (N/C) ratio, (**E**) relative nuclear and (**F**) relative total signal of ELF3MC under the different light treatments. Data was made relative to the values of ELF3MC in the dark at ZT10. In total, for the dark four images were collected, totalling 20 nuclei, for RL seven images were collected totalling 35 foci and for

Figure 3.5 (continued) - BL five images were collected, totalling 26 nuclei. Significance was determined by an unpaired T-test. The Bonferroni correction was applied to account for multiple T-tests. n.s = no significant difference, *** = $p < 0.005$. Error bars represent standard error of the mean (SEM).

ELF3C was previously found to exclusively localise to foci within the nuclei of tobacco mesophyll cells and Arabidopsis hypocotyl cells (Herrero et al., 2012). Congruent with this, I observed that ELF3C exclusively localised to nuclear foci in samples transferred to the dark **(Figure 3.6A-C, Appendix 3 Figure 3A-B)**. ELF3C foci were larger but fewer in number than full-length ELF3 foci. A RL-pulse had no effect on the number of ELF3C foci, although there was more variability in the number of foci per nucleus compared to those measured in the dark **(Figure 3.6A-B, 3.6D)**. There was also no effect of RL on the size or signal intensity of these foci **(Figure 3.6E-G).** Combined, this suggests that RL does not control the foci dynamics of ELF3C.

In contrast to RL, BL did have an effect on ELF3C foci dynamics **(Figure 3.6C, Table 3.1)**. The number of foci increased after a BL-pulse, although this increase was not significant due to the high variability in the number of foci per nucleus after the BL-pulse **(Figure 3.6D)**. BL also caused a significant decrease in the diameter, volume and signal intensity of ELF3C foci **(Figure 3.6E-G)**. This decrease was not caused by a consistent reduction in the size of foci following a BL-pulse. Instead, the decrease was caused by the presence of a population of foci that had a volume under 50 nm^3 or a diameter under 400 nm **(Appendix 3 Figure 3C-D)**. After a BL-pulse, 38.5% and 45.7% of foci had a volume or diameter under 50 nm^3 or 400 nm, respectively, while in the dark, only 9.8% or 13.1% of foci with a volume or diameter under 50 nm^3 or 400 nm, respectively. The size distribution of foci after a RL-pulse was similar to samples transferred to the dark: 11.9% and 16.4% of foci had a volume or diameter under 50 nm^3 or 400 nm, respectively (**Appendix Figure 3 Figure 3C-D**). Of foci with a larger volume or diameter than 50 nm^3 or 400 nm there was no consistent difference between the different light pulses tested here.

A BL-pulse also resulted in some ELF3C nuclei having nucleoplasmic signal **(Appendix 3 Figure 3E-F)**. Nuclei with nucleoplasmic signal still had foci but these foci were smaller than foci in nuclei with no nucleoplasmic signal. As with full-length ELF3, direct measurements of ELF3C foci in nuclei with nucleoplasmic signal was not possible due to the overlap between the nucleoplasm and focus. Hence, these foci were not included in the foci measurements dataset presented here **(Figure 3.6)**. In conclusion, BL can regulate the sub-nuclear dynamics of ELF3 through the C-terminus of ELF3.

Table 3.1– ELF3C foci measurements under different light conditions.

The number, volume (nm^3), diameter (nm) and relative signal intensity (arbituary units) of *35S::YFP:ELF3C* foci at ZT10. Samples were prior transferred to the dark or pulsed with 25 $\mu mol/m^{-2}/s^{-1}$ of red light or 25 $\mu mol/m^{-2}/s^{-1}$ of blue light for three-hours. All light-pulses were started at ZT7 (short-day, 8/16). Standard error of the mean (SEM) is in circle brackets. Significance (square brackets) was determined by an ANOVA, with significance determined by a Tukey HSD posthoc test. Astrik (**) indicates significance of $p < 0.01$.

Light Treatment	Number of foci	Volume (nm^3)	Diameter (nm)	R.S.I (arb.units)
Darkness	9 (0.87)	224.62 (21.2)	710.39 (23.3)	107.60 (6.9)
Red Light	9.90 (1.46) [n.s]	223.01 (20.9) [n.s]	685.42 (22.8) [n.s]	110.92 (6.6) [n.s]
Blue Light	12.50 (1.15) [n.s]	199.97 (20.8) [**]	614.08 (27.6) [**]	95.5 (11.5) [**]

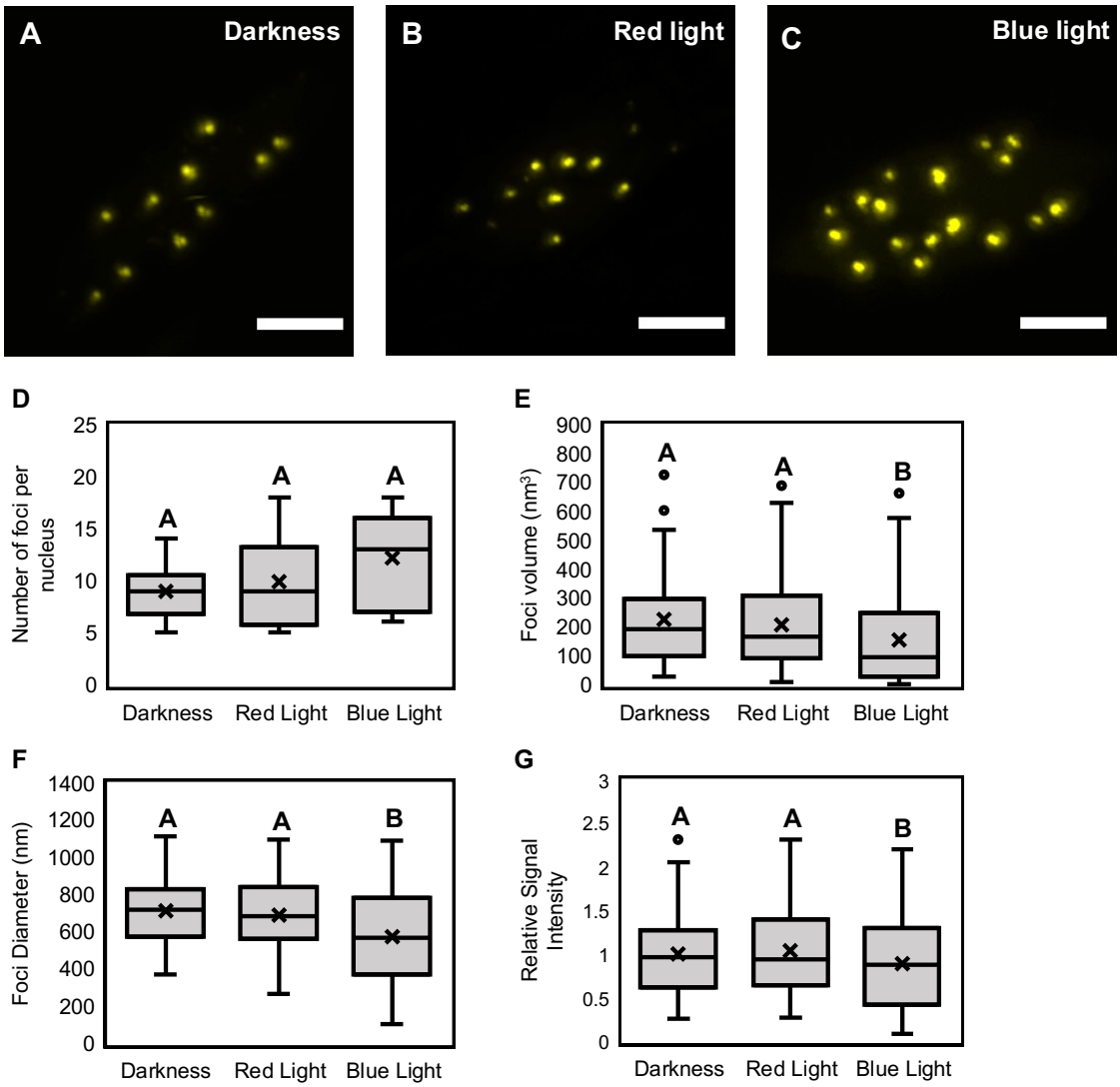

Figure 3.6 - The sub-nuclear localisation of ELF3 has a domain specific response to light

The cellular distribution of *35S::YFP:ELF3C* in 7-day old seedlings either transferred to (**A**) the dark or pulsed with **(B)** 25 μmol/m^{-2}/s^{-1} red light (RL) or **(C)** 25 μmol/m^{-2}/s^{-1} blue light. Light pulses were applied for three hours starting at ZT7 (1 hour before dusk, short-day photoperiods). Scale bars in A-C are 5 μm. (**D**) The number of foci per nucleus, (**E**) foci volume (nm^3), (**F**) foci diameter (nm) and (**G**) relative signal intensity under the different light treatments. Data was made relative to the values of ELF3C foci in the dark. All experiments were repeated at least twice, with multiple biological samples imaged on each occasion. In total, 60 foci were measured for each light treatment. Due to intercellular movement, not all foci that were included in the foci count were included in the measurement of foci volume or diameter. Significance was determined by an ANOVA, with significance determined by a Tukey HSD posthoc test. Letters indicates significance of $p < 0.01$.

3.2.5 Red light regulates ELF3 localisation in an intensity-dependent manner

As ELF3 has been previously connected to RL through phyB while no BL photoreceptor has so far been linked to ELF3 (Liu et al., 2001, Huang et al., 2016), I focused on further characterising the role of phyB in regulating ELF3 cellular and sub-nuclear localisation. The *phyB* circadian phenotype is dependent on the intensity of RL. Below RL intensities of 10 μmol/m^{-2}/s^{-1}, the *phyB* mutant has no circadian phenotype, while increases in the intensity of RL above 10 μmol/m^{-2}/s^{-1} progressively increases the severity of the *phyB* phenotype (Somers et al., 1998). To determine whether the cellular or sub-nuclear localisation of ELF3 was responsive to different intensities of RL, I investigated the localisation of ELF3 after a three-hour long pulse of 1, 10 or 15 μmol/m^{-2}/s^{-1} of RL. The timing and duration of the light pulse was carried out as described above.

At all tested intensities of RL, ELF3 was distributed between the cytoplasm and nucleus, and within the nucleus remained localised to either the nucleoplasm or foci. However, the intensity of the RL-pulse did influence the cellular and sub-nuclear distribution of ELF3. A 1 μmol/m^{-2}/s^{-1} pulse of RL increased the nuclear localisation of ELF3 **(Figure 3.7A**, **3.8A-B)**. Accordingly, the N/C ratio and relative nuclear signal of ELF3 was greater in samples pulsed with 1 μmol/m^{-2}/s^{-1} compared to those transferred to the dark **(Figure 3.F-G)**. However, this increase in nuclear signal did not lead to an increase in the number of foci. Instead, the number of foci per nucleus decreased slightly after a 1 μmol/m^{-2}/s^{-1} RL-pulse **(Figure 3.8A-B, 3.8F)**. Thus, changes in the nuclear localisation of ELF3 alone cannot necessarily explain subsequent changes in the sub-nuclear localisation of ELF3. Finally, the total signal after a 1 μmol/m^{-2}/s^{-1} RL-pulse decreased relative to samples in the dark **(Figure 3.7H)**. This suggests that i) nuclear localised ELF3 may be more unstable than cytoplasmic ELF3, and/or ii) low-light intensity light de-stabilises ELF3.

A 10 or 15 μmol/m^{-2}/s^{-1} RL-pulse had no effect on the N/C partitioning or the total signal of ELF3 **(Figure 3.7A, 3.7C-H)**. However, both a 10 and 15 μmol/m^{-2}/s^{-1} RL-pulse caused a reduction in the number of foci per nucleus **(Figure 3.8C-D)**. A 10

μmol/m^{-2}/s^{-1} RL-pulse only caused a small decrease relative to samples in the dark, while a 15 μmol/m^{-2}/s^{-1} RL-pulse caused a much greater reduction in the number of foci **(Figure 3.8F)**. The number of foci per nucleus following a 15 μmol/m^{-2}/s^{-1} pulse of RL was comparable to the effect caused by a 25 μmol/m^{-2}/s^{-1} pulse of RL (15 μmol/m^{-2}/s^{-1} pulse = 7 (± 0.76) foci, 25 μmol/m^{-2}/s^{-1} pulse = 6.3 (± 0.42) foci) **(Figure 3.8E-F)**. In summary, the cellular and sub-nuclear localisation of ELF3 is responsive to the intensity of RL. Low intensities of RL promote the nuclear localisation of ELF3 before increasing intensities of RL firstly inhibit the localisation of ELF3 to foci and then inhibit the nuclear accumulation of ELF3.

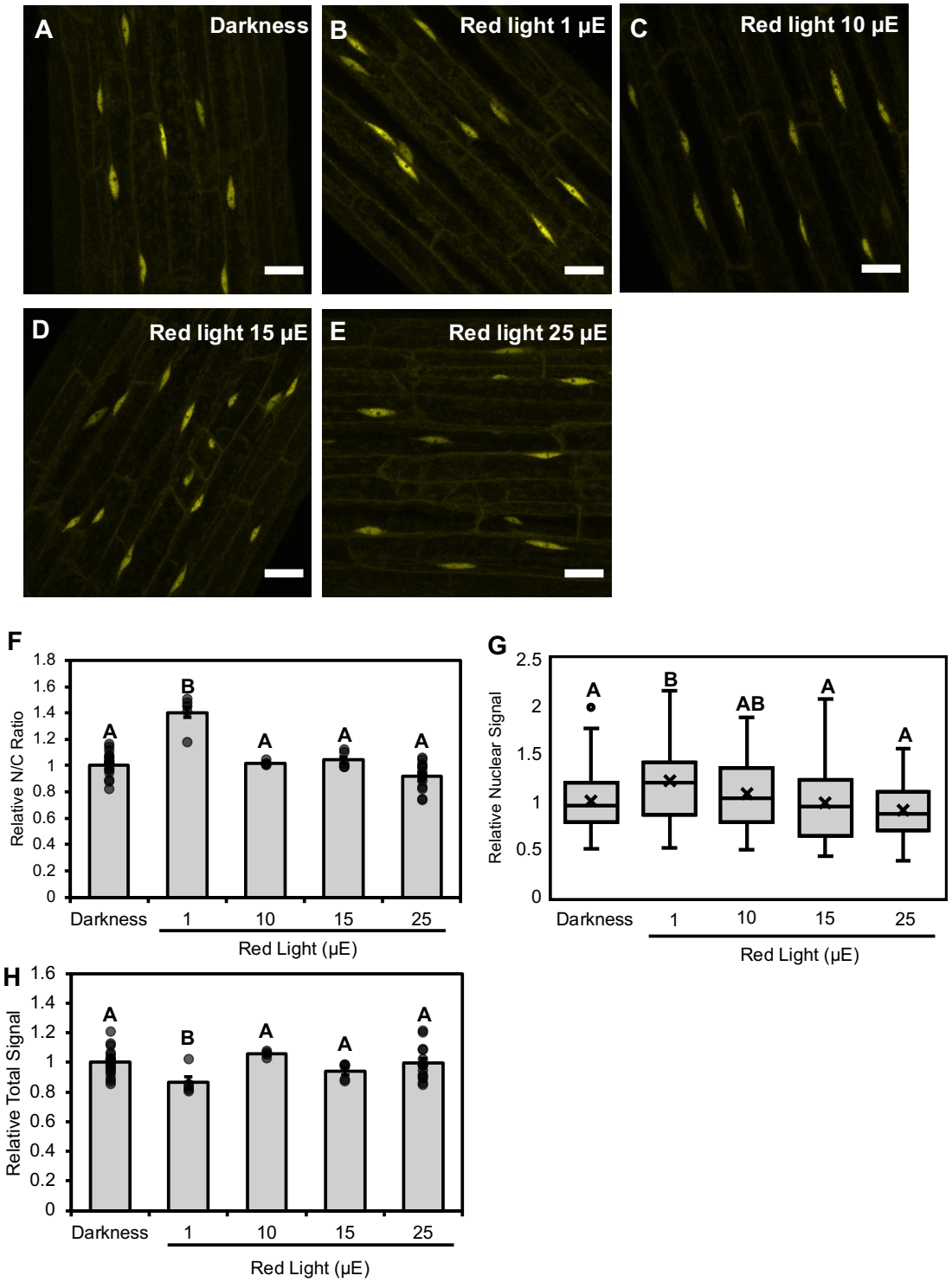

Figure 3.7 - The cellular localisation of ELF3 is responsive to red light in a dosage-dependent manner

The cellular localisation of *35S::YFP:ELF3* (*elf3-4*) in the **(A)** dark, or after a **(B)** 1, **(C)** 10, **(D)** 15 or **(E)** 25 μmol/m^{-2}/s^{-1} RL-pulse. Scale bars are equal to 25 μm. **(F)** The relative nuclear/cytoplasmic (N/C) ratio, **(G)** relative nuclear signal and **(H)** relative total signal of *35S::YFP:ELF3* (*elf3-4*) under the respective light treatments. All light pulses were started at ZT7 (8/16 short-days) and carried out for three-hours before seedlings were imaged at ZT10. All imaging was repeated twice, with a minimum of 10 images collected and analysedin total.

Figure 3.7 (continued) - Significance was determined by an one-way ANOVA with a tukey HSD posthoc test. Different letters signify a significance of $p < 0.01$, while same letters indicate no significant difference. The data for darkness and RL25 is the same as first presented in figure 3.1.

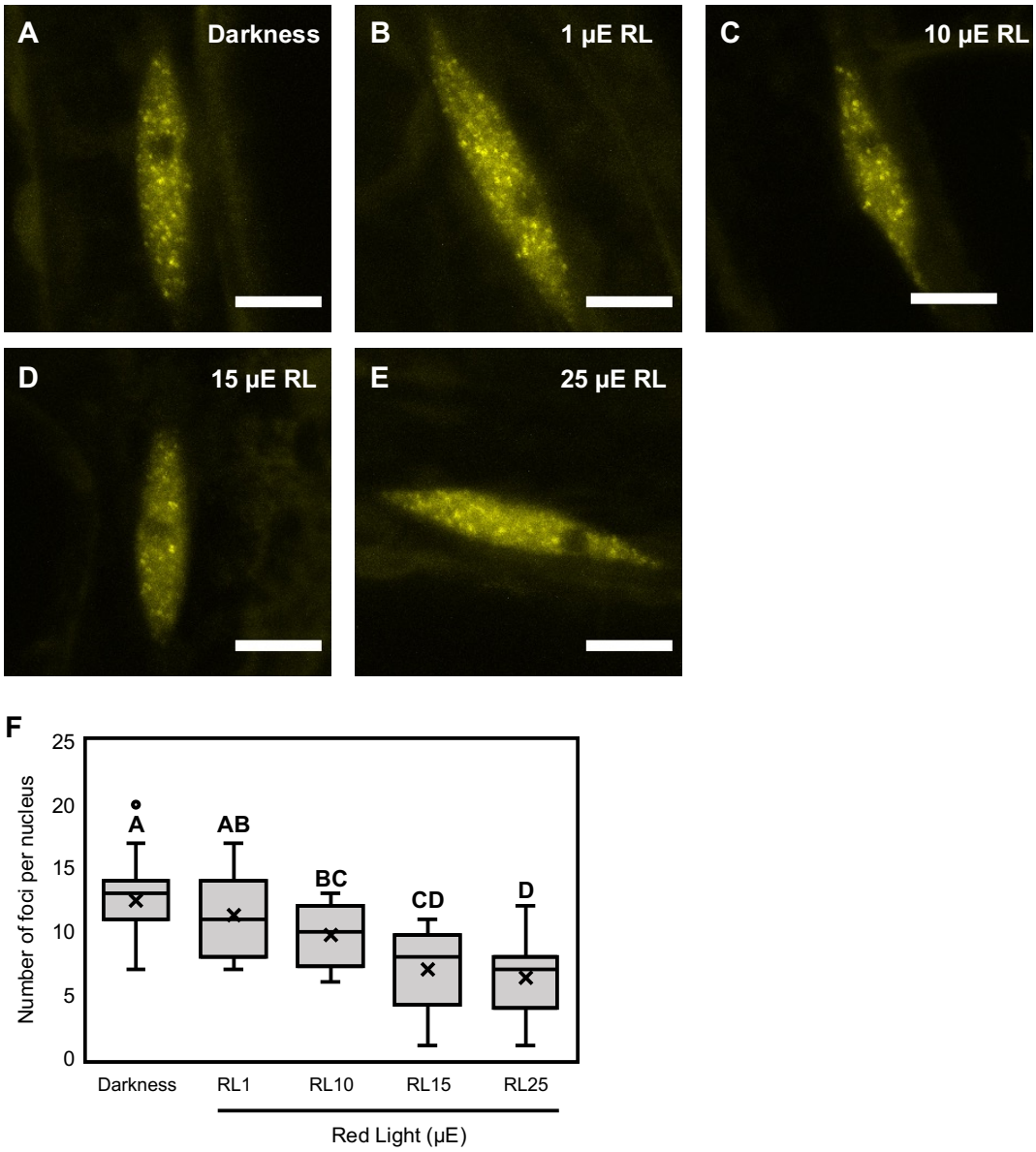

Figure 3.8 - The sub-nuclear localisation of ELF3 is responsive to red light in a dosage-dependent manner

The nuclear localisation of *35S::YFP:ELF3* (*elf3-4*) in the **(A)** dark, or after a **(B)** 1, **(C)** 10, **(D)** 15 or **(E)** 25 μmol/m^{-2}/s^{-1} RL-pulse. Scale bars equal 5 μm. **(F)** The number of foci per nucleus for *35S::YFP:ELF3* (*elf3-4*) under the respective light treatments. All light pulses were started at ZT7 (short-days) and carried out for three-hours before seedlings were imaged at ZT10. All imaging was repeated twice, with a minimum of 10 images collectedand analysed in total. Significance was determined by an one-way ANOVA with a tukey HSD posthoc test. Different

Figure 3.8 (continued) - letters signify a significance of $p < 0.01$, while same letters indicate no significant difference. The data for darkness and RL25 is the same as first presented in figure 3.2.

3.2.6 **Photoactivated phys regulate ELF3 cellular localisation at dusk**

A pulse of FRL converts photostable phys from the biologically active PFr state to the biologically inactive Pr state (Kircher et al., 1999). If phyB in the PFr conformer is inhibiting the nuclear accumulation of ELF3, an end of day (EOD) pulse of FRL should promote the nuclear accumulation of ELF3. To test this, ELF3 seedlings were pulsed with 110 $\mu mol/m^{-2}/s^{-1}$ of FRL for fifteen minutes at ZT7 (1-hour before dusk) and imaged immediately. As a control, seedlings were kept under WL for the duration of the FRL pulse. Under WL and FRL, ELF3 was localised between the cytoplasm and nucleus but, the nuclear accumulation of ELF3 was reduced by a FRL-pulse **(Figure 3.9A-D)**. There was no change in the normalised total signal between the two light treatments (**Figure 3.9E**), suggesting that a FRL-pulse directly represses the nuclear accumulation of ELF3. Comparing the average change in the cellular distribution of ELF3 after a 25 $\mu mol/m^{-2}/s^{-1}$ RL or 110 $\mu mol/m^{-2}/s^{-1}$ FRL-pulse, revealed FRL had a much greater effect on reducing the nuclear accumulation of ELF3 than a RL-pulse did **(Table 3.2)**.

Within the nucleus, ELF3 was distributed to the nucleoplasm and foci under WL and FRL but the number of foci was reduced following a FRL-pulse **(Figure 3.9F-H)**. In contrast to changes in the NC ratio, a FRL pulse had a weaker inhibitory effect on ELF3 foci association than a 25 $\mu mol/m^{-2}/s^{-1}$ RL pulse **(Table 3.2)**. Comparing the morphology of foci between WL and FRL-pulsed samples revealed no clear differences between the two light treatments. However, for both WL and FRL, ELF3 foci at ZT7 were smaller and less bright than the foci that were observed at ZT10 **(Figure 3.2, 3.3, 3.9F-H).** Together, this suggests that photoactivated phys are required to promote the nuclear and sub-nuclear localisation of ELF3 at dusk.

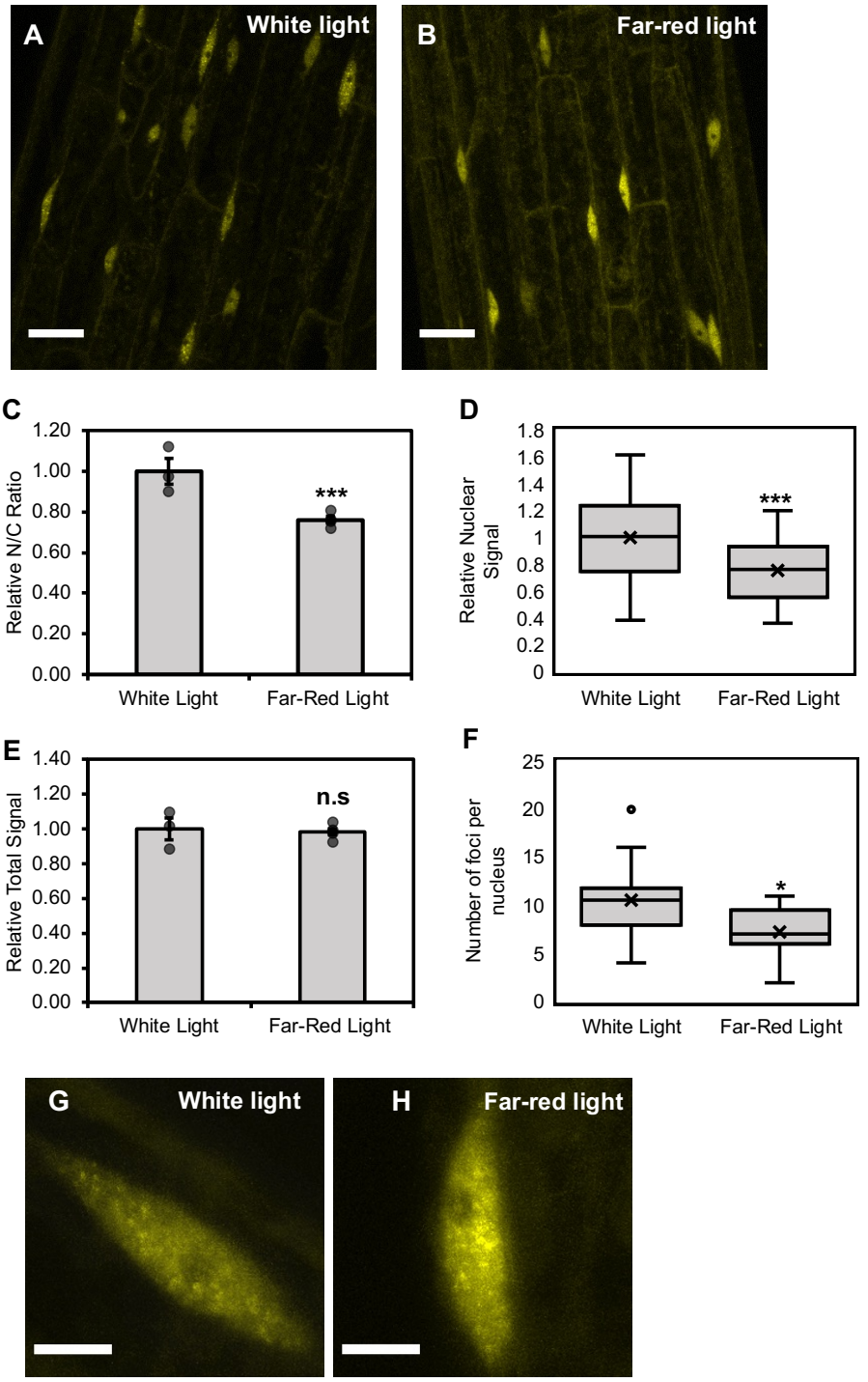

Figure 3.9 - A far-red light pulse suppresses the nuclear and sub-nuclear accumulation of ELF3

The localisation of *35S::YFP:ELF3* at ZT7 after either exposure to (**A, G**) 85 µmol/m^{-2}/s^{-1} of white light (WL) or (**B, H**) a 110 μmol/m^{-2}/s^{-1} far-red light (FRL)-pulse. The FRL-pulse was started at ZT7 (one-hour before dawn, 8/16 photoperiods) and carried out for 15 minutes. Seedlings were then immediately imaged for up to one-hour. Scale bars in **(A, B)** are 25 μm, while scale bars in **(G, H)** are 5 μm. **(C)** The relative nuclear/cytoplasmic (N/C) ratio, **(D)** relative nuclear signal, **(E)** relative total signal and **(F)** number of foci per nucleus under the respective light treatments. All experiments were repeated twice, with the presented data a combination of

Figure 3.9 (continued) - the two repeats. For white light (**C-E**) three images were analysed totalling 34 nuclei and (**F**) 12 nuclei were counted. For far-red light: (**C-E**) four images were analysed totalling 35 nuclei and (**F**) 13 nuclei were counted. Significance was determined by an unpaired, two-tailed T-test. n.s = no significance, * = $p < 0.05$ and *** = $p < 0.001$.

Table 3.2 - The change in ELF3 cellular and sub-nuclear accumulation after a red light or far-red light pulse.

The percentage change in the average nuclear-cytoplasmic (N/C) ratio, nuclear signal, total signal and number of foci per nucleus after a RL or FRL pulse. The percentage change is relative to the control group at the two respective timepoints; for RL this is samples that were transferred to the dark at ZT7, while for FRL controls samples were transferred to WL for the 15-minute duration of the FRL pulse that was started at ZT7.

Treatment	N/C Ratio	Nuclear	Total Signal	Number of foci
Red light (ZT10)	-8.3%	-9.3%	-0.01%	-49.2%
Far-red light (ZT7)	-23.5%	-24.5%	0.03%	-31.1%

3.2.7 phyB directly regulates the cellular and sub-nuclear distribution of ELF3

To understand the role of phyB in regulating the cellular localisation of ELF3, the *phyB-10* mutant was introgressed into the *35S::YFP:ELF3 elf3-4* transgenic line to generate a stable *35S::YFP:ELF3 elf3-4/phyB-10* line. This line will henceforth be referred to as ELF3 (B-), while the line with a wild type *phyB* allele will be referred to as ELF3 (B+). The cellular and sub-nuclear localisation of ELF3 was then imaged in seedlings either transferred to the dark or pulsed with 25 $\mu mol/m^{-2}/s^{-1}$ RL following the approach described above.

As with ELF3 (B+), ELF3 (B-) was localised to the cytoplasm and nucleus in the dark. However, the nuclear accumulation of ELF3 was severely compromised by the *phyB* mutation. The N/C ratio of ELF3 (B-) in the dark was decreased by ~40% compared to ELF3 (B+) **(Figure 3.10A, 3.10C)**. The localisation of ELF3 (B-) remained responsive to RL but displayed the opposite response to ELF3 (B+). Instead of decreasing, the nuclear localisation of ELF3 (B-) increased after a RL-pulse **(Figure 3.10B, 3.10D-E)**.

The N/C ratio of ELF3 (B-) following a RL-pulse was comparable to the N/C ratio of ELF3 (B+) after a RL-pulse. However, the relative nuclear signal of ELF3 (B-) after a RL-pulse was greater than the nuclear signal of ELF3 (B+) samples in the dark **(Figure 3.10F)**. The disparity in the N/C ratio and nuclear signal of ELF3 (B-) was caused by changes in the total signal of ELF3 (B-). In the dark and after a RL-pulse, the relative total signal of ELF3 (B-) was greater than ELF3 (B+) **(Figure 3.10G)**. ELF3 (B-) total signal in the dark only displayed a small increase (~15%), while a RL-pulse caused a large increase (~71%) relative to the total signal of ELF3 (B+) in the dark, respectively.

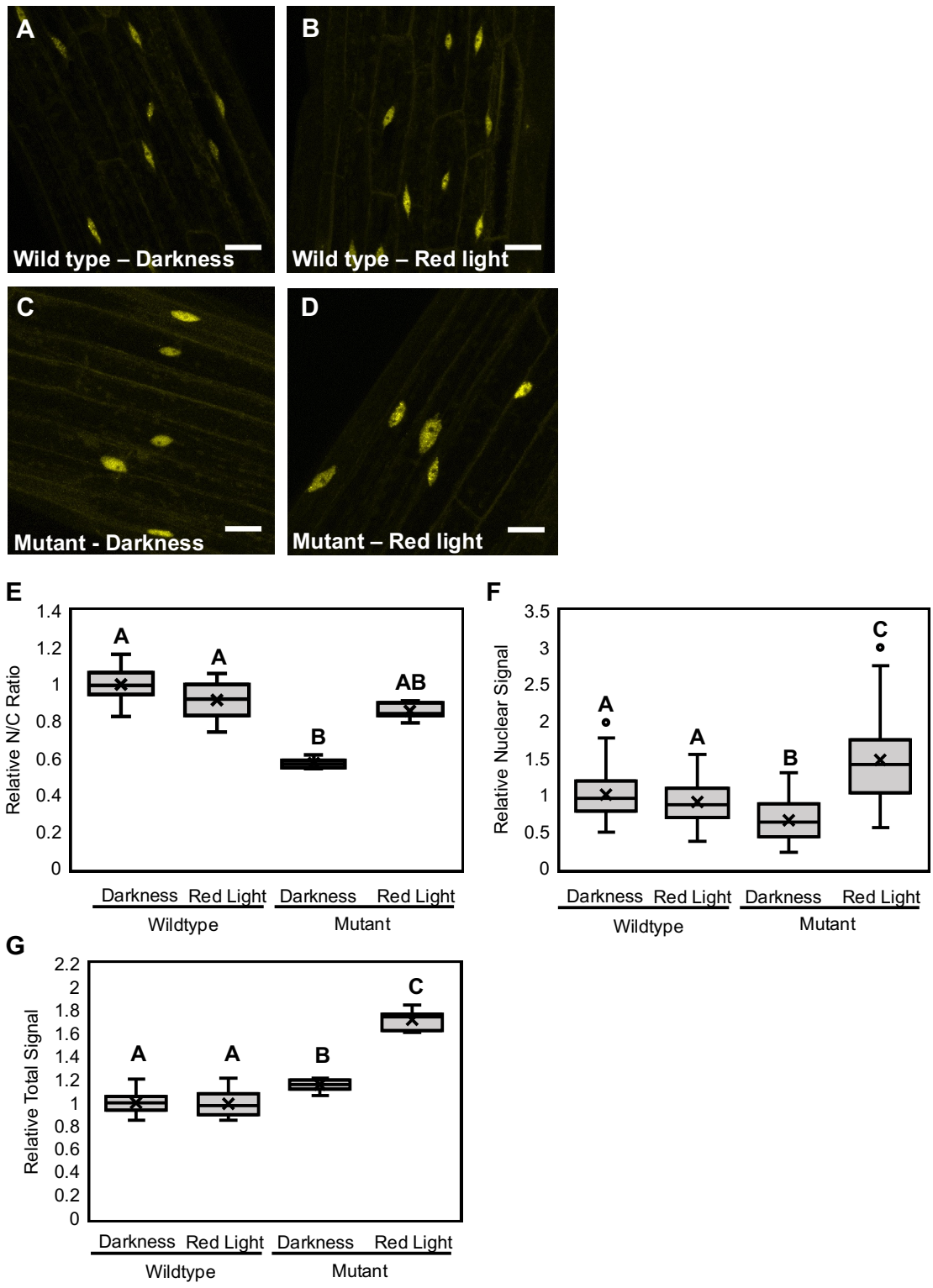

Figure 3.10 - phytochromeB promotes the nuclear localisation of ELF3

The localisation of *35S::YFP:ELF3* in the **(A-B)** *elf3-4* or **(C-D)** *elf3-4/phyB-10* background in the **(A, C)** dark or **(B, D)** after a 25 μmol/m^{-2}/s^{-1} red light (RL)-pulse. Light pulses were started at ZT7 before images were collected at ZT10. Scale bars represent 25 μm. (**E**) The nuclear/cytoplasmic (N/C) ratio, (**F**) relative nuclear signal and (**G**) relative total signal of the respective constructs in the dark or after a 25 µmol/m^{-2}/s^{-1} RL pulse. The nuclear and total signal was made relative to the nuclear and total signal of *35S::YFP:ELF3* (*elf3-4*) in the dark at ZT10.

Figure 3.10 (continued) - For *35S::YFP:ELF3 (elf3-4/phyB-10)* a minimum of four images were collected in total. The values for *35S::YFP:ELF3* (*elf3-4*) are the same as first presented in figure 3.1. Different letters signify significance difference ($p < 0.01$) as determined by an one-way ANOVA with a tukey HSD posthoc test.

The *phyB-10* mutation also had a strong phenotypic effect on the localisation of ELF3 to foci **(Figure 3.11)**. In the dark, ELF3 (B-) was predominantly localised to the nucleoplasm **(Figure 3.11A, 3.11C, 3.11E)**. When foci were observed, the number of foci per nucleus was strongly reduced. Excluding the 50% of nuclei (n = 12) that had no focus, there was ~2 foci per nucleus for ELF3 (B-) in the dark. In comparison, ELF3 (B+) had ~13 and ~6 foci per nucleus in the dark or after a RL-pulse, respectively. Alongside reducing the number of foci, ELF3 (B-) foci were also smaller and less bright than ELF3 (B+) both in the dark and after a RL-pulse **(Figure 3.10A-C)**.

As with the cellular localisation, the sub-nuclear localisation of ELF3 (B-) remained responsive to RL but again displayed the opposite response to ELF3 (B+) **(Figure 3.10D)**. Both the frequency of nuclei with one focus and the number of foci observed per nucleus increased after a RL-pulse: 89% of all nuclei had at least one focus following a RL-pulse (n=18), while the average number of foci per nucleus increased to ~5. However, the number of foci per nucleus after a RL-pulse was highly variable for ELF3 (B-), with the number of foci varying from 1 to 12 per nucleus **(Figure 3.10E)**. ELF3 (B-) foci after a RL-pulse were also larger and brighter than those observed in the dark. Combined, this suggests that RL may regulate the cellular and sub-nuclear localisation of ELF3 through phyB-dependent and phyB-independent pathways.

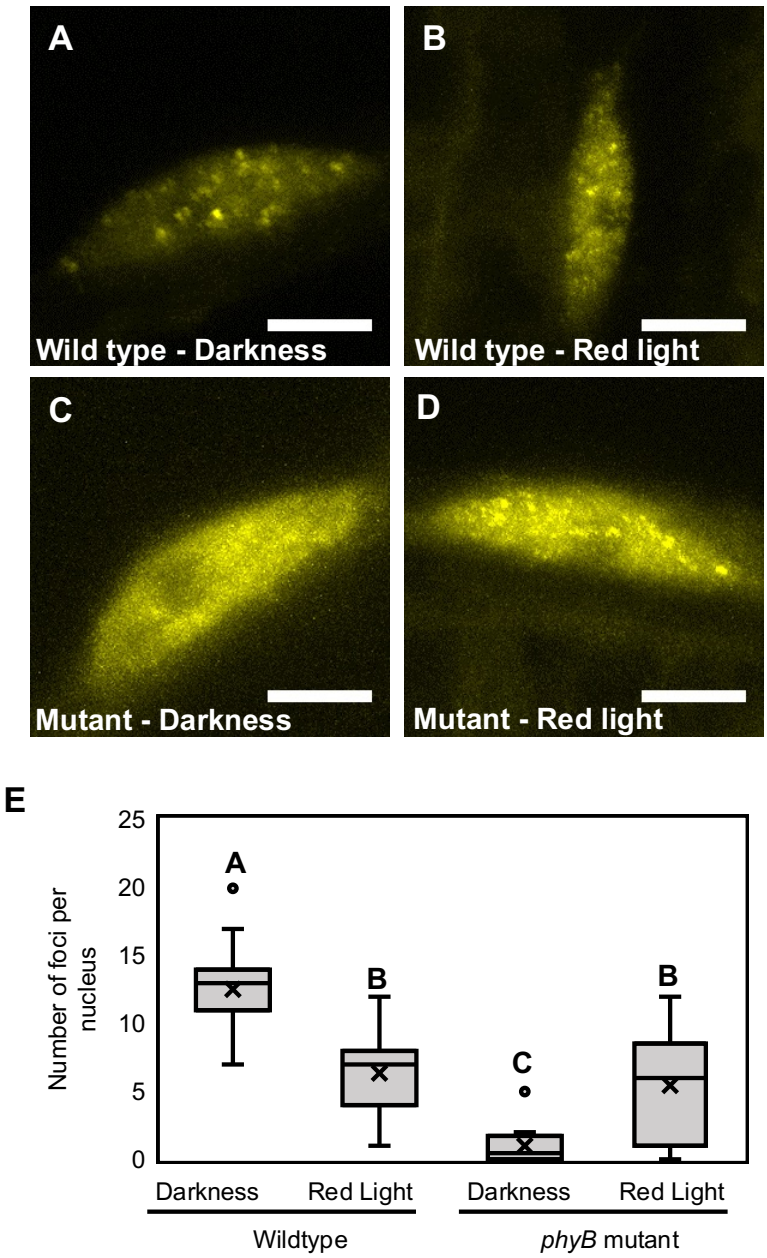

Figure 3.11 - phytochromeB is required for ELF3 to localise to foci

The localisation of *35S::YFP:ELF3* in the **(A-B)** *elf3-4* or **(C-D)** *elf3-4/phyB-10* background in either the **(A, C)** dark or **(B, D)** after a 25 μmol/m^{-2}/s^{-1} red light (RL)-pulse. Light pulses were started at ZT7 before images were collected at ZT10. Scale bars represent 5 μm. (**E**) Number of foci per nucleus for the respective constructs and light treatments. For *35S::YFP:ELF3* (*elf3-4/phyB-10*) all experiments were repeated twice, with 10 images collected in total.. The values for *35S::YFP:ELF3* (*elf3-4*) are the same as first presented in figure 3.2. Significance was determined by a one-way ANOVA with a tukey HSD posthoc test to determine significance. Different letters signify a significant difference of $p < 0.05$.

The role of phyB in regulating ELF3 transcriptional activity

To understand whether the changes in the localisation of ELF3 following the RL pulse and *phyB* mutation correlated with changes in the functional activity of ELF3, I measured the transcript abundance of genes that have been established as targets of ELF3/EC in the ELF3 (B+) and ELF3 (B-) background at ZT10 either in the dark or after a 25 μmol/m^{-2}/s^{-1} RL-pulse. The RL pulse was applied as described previously.

I first focused on the transcript abundance of *PRR9*, as it has been suggested that phyB could inhibit ELF3's ability to repress the expression of *PRR9* (Herrero et al., 2012). At ZT10 in the dark, there was no change in the transcript abundance of *PRR9* in either ELF3 (B+) or ELF3 (B-) compared to WT, consistent with previous work (Nieto et al., 2015) **(Figure 3.12A)**. The transcript abundance of *PRR9* was strongly induced in WT by a RL-pulse. In contrast, the transcript abundance of *PRR9* was not induced by a RL-pulse in either the ELF3 (B+) or ELF3 (B-) background. Instead, the transcript abundance of *PRR9* decreased following the RL-pulse in both backgrounds **(Figure 3.12E)**. Furthermore, there was no difference in the relative change of *PRR9* transcript abundance between ELF3 (B+) and ELF3 (B-). Therefore, phyB does not seem to inhibit ELF3 repression of *PRR9* transcript abundance in the evening.

ELF3/EC also regulates the expression of other genes that are also light responsive. Amongst these is *GIGANTEA* (*GI*), an evening phased gene whose expression was found to be induced by RL (Molas et al., 2006, Mizuno et al., 2014, Park et al., 2019). The transcript abundance of *GI* was repressed in ELF3 (B+) compared to WT at ZT10 in the dark **(Figure 3.12B)**. *GI* transcript abundance was also repressed in ELF3 (B-) but this repressive effect was weaker than ELF3 (B+). As previously reported, a RL-pulse strongly promoted the transcript abundance of *GI* in WT **(Figure 3.12B)** (Molas et al., 2006). The transcript abundance of *GI* was also induced in response to the RL-pulse in ELF3 (B+), but not ELF3 (B-) where *GI* transcript abundance remained unchanged relative to the transcript abundance of GI in the dark **(Figure 3.12E)**. Comparing the relative change in *GI* transcript abundance in response to RL between WT and ELF3 (B+) revealed a similar degree of induction in the two backgrounds **(Figure**

3.12E). This suggests that RL induction of *GI* is dependent on phyB and ELF3 does not inhibit this process.

I also measured the transcript abundance of *LUX* and *TOC1*, further direct targets of ELF3/EC (Helfer et al., 2011, Lee et al., 2019b). As previously reported, the transcript abundance of *TOC1* was repressed in ELF3 (B+) **(Figure 3.12C)** (Lee et al., 2019b). *TOC1* transcript abundance was also repressed in ELF3 (B-) and there was no significant difference in the repressive activity when compared to ELF3 (B+). A RL-pulse strongly repressed the transcript abundance of *TOC1* in WT and ELF3 (B-), while RL had a weaker repressive effect in the ELF3 (B+) background **(Figure 3.12E)**. The transcript abundance of *LUX* was also repressed in ELF3 (B+) and ELF3 (B-) compared to WT in the dark. Here, ELF3 (B-) exerted a stronger repressive effect than ELF3 (B+) on repressing *LUX* transcript abundance **(Figure 3.12D)**. The transcript abundance of *LUX* was weakly induced by a RL-pulse in WT and ELF3 (B+), while the transcript abundance of *LUX* decreased slightly in ELF3 (B-) following a RL-pulse **(Figure 3.12E)**. Together, these results highlight a complex role for phyB in regulating the transcriptional activity of ELF3 in the evening.

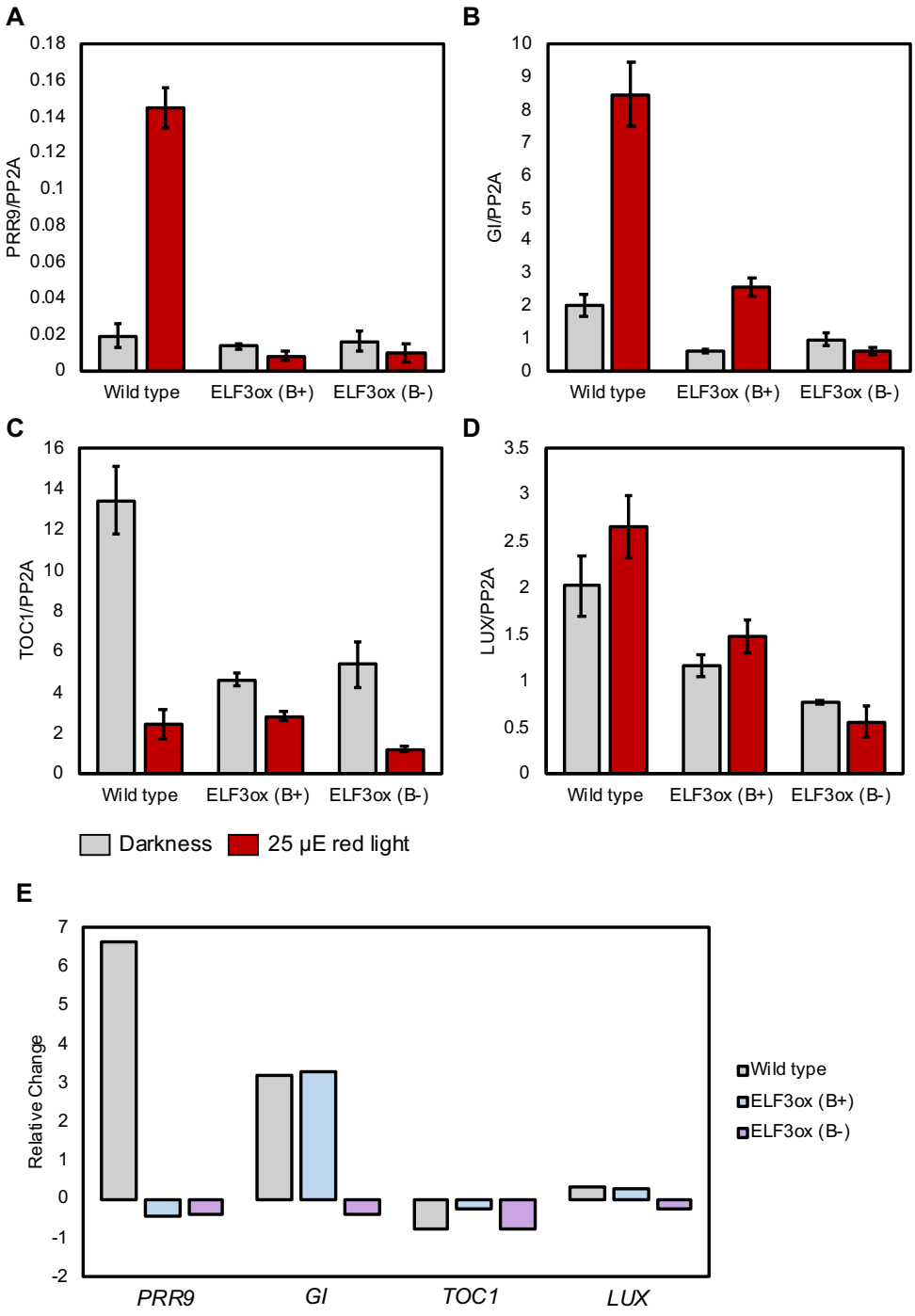

Figure 3.12 - Complex effect of phyB in regulating ELF3 transcriptional activity

The transcript abundance of (**A**) *PSEUDO RESPONSE REGULATOR9* (*PRR9*) (**B**) *GIGANTEA* (*GI*) (**C**) *TIMING OF CAB1 TRANSCRIPT ABUNDANCE* (*TOC1*) and (D) *LUX ARRYTHMO* (*LUX*) was measured in wild type (Ws-2), *35S::YFP:ELF3 elf3-4* (ELF3 B+) or *35S::YFP:ELF3 elf3-4/phyB-10* (ELF3 B-) at ZT10. Respective lines were either prior pulsed with 25 μmol/m^{-2}/s^{-1} of red-light (RL, red bars) or transferred to the dark (grey bars) at ZT7. Data was normalised to the transcript abundance of *PROTEINPHOSPHATASE SUBUNIT2A* (*PP2A*). Presented data is the average of at least two technical replicas. Error bars indicate standard deviation amongst the

Figure 3.12 (continued) - technical replicas. **(E)** The relative change in the transcript abundance of *PRR9*, *GI, TOC1* and *LUX* following a RL-pulse compared to the transcript abundance of the gene in the dark.

3.2.8 ELF3 inhibition of hypocotyl development under white light is independent of phyB

Though phyB and ELF3 are proposed to function antagonistically within the circadian clock, both proteins repress juvenile and adult photoperiodic growth in Arabidopsis and share common regulatory targets (Shim et al., 2017, Pham et al., 2018). Furthermore, recent mass-spectrometry analysis revealed that the phyB-ELF3 interaction connected ELF3 to a wider network of light-signalling associated proteins (Huang et al., 2016). This expanded network of interactors included chromatin remodelling enzymes and transcriptional co-regulators. Therefore, phyB could facilitate or promote some aspects of ELF3 function.

During seedling development, ELF3 and phyB inhibit hypocotyl elongation via repressing PIF4 activity (Choi and Oh, 2016). Previously, ELF3 was not found to be required for phyB-dependent inhibition of hypocotyl elongation (Reed et al., 2000). However, whether phyB was required for ELF3 to repress hypocotyl elongation was not tested. To investigate this, I measured the hypocotyl length of WT, *elf3-4*, *phyB-10*, *elf3-4/phyB-10* and *ELF3ox* with or without the *phyB-10* mutation across a range of photoperiods. As before, ELF3 with a WT phyB allele will be referred to as ELF3 (B+) and ELF3 with the phyB mutation will be referred to as ELF3 (B-).

As previously established, hypocotyl elongation in WT seedlings was inversely correlated with daylength (Anwer et al., 2020). As the daylength increased, hypocotyl elongation in WT seedlings was progressively inhibited until a breakpoint was reached at 20-hours of light **(Figure 3.13)**. Further increases in the daylength did not cause any additional reduction in hypocotyl length past this breakpoint. The *elf3-4* mutant had a longer hypocotyl than WT under all *diel* photoperiods, although the severity of this phenotype was dependent on the extent of the dark-phase **(Figure 3.13)**. The *phyB-10*

single and *phyB-10/elf3-4* double mutant had a longer hypocotyl than WT plants under all *diel* photoperiods and constant light conditions **(Figure 3.13)**. In constant darkness, the *phyB-10* single mutant failed to germinate, while the *elf3-4/phyB-10* double mutant had a marginally longer hypocotyl compared to the other lines tested here. There was also an additive effect of the *elf3-4* and *phyB-10* mutations under *diel* conditions and constant light, with the *elf3-4/phyB-10* hypocotyl phenotype more pronouced than either respective single mutant across all photoperiods.

ELF3 (B+) fully rescued the *elf3-4* hypocotyl phenotype and had a shorter hypocotyl than WT under all photoperiods aside from constant conditions and 20-hours of light **(Figure 3.13)**. In contrast, ELF3 (B-) only partially rescued the *elf3-4/phyB-10* hypocotyl phenotype and had a longer hypocotly than WT under all photoperiods. Furthermore, the hypocotyl phenotype of *ELF3ox* (B-) mostly phenocopied the *phyB-10* hypocotyl phenotype under all *diel* and constant conditions. Together, this suggests that ELF3 and phyB are largely functioning independently in regulating hypocotyl elongation and phyB is not required for ELF3 to repress hypocotyl development under the conditions tested here.

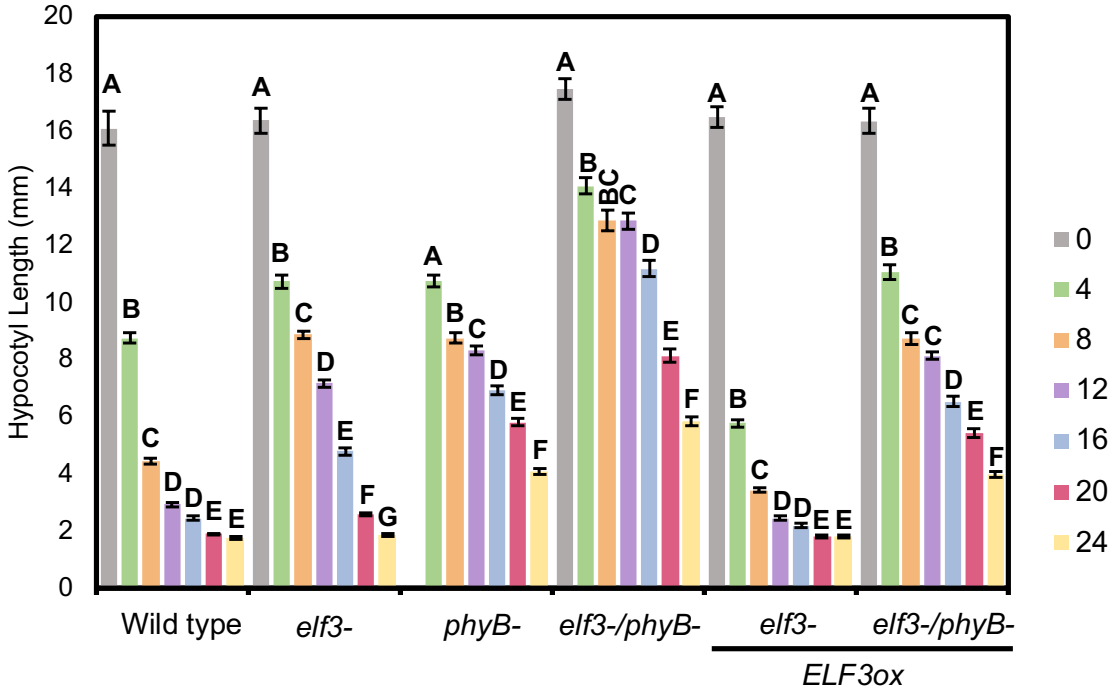

Figure 3.13 - phyB does not regulate activity ELF3 in controlling hypocotyl elongation under white light

The hypocotyl length of wild type (Ws-2), *elf3-4 (elf3-)*, *phyB-10 (phyB-)*, *elf3-4/phyB-10 (elf3-/phyB-)*, *ELF3ox* (*elf3-*) and *ELF3ox* (*elf3-/phyB-*) under different photoperiods (see legend for hours of light). Hypocotyls were measured at subjective dawn on day 7. All chambers had a light intensity of 85 μmol/m^{-2}/s^{-1} and a constant temperature of at 22ºC. A minimum of 10 seedlings were measured for each genotype under each respective photoperiod. Different letters signify significant differences ($p < 0.05$) within the respective genotype across the different photoperiods. Significance was determined by a one-way ANOVA with a tukey HSD posthoc test. Error bars represent standard error of the mean (SEM). For *phyB-10* there was no germination in the constant darkness photoperiod for both experimental repeats. All experiments were repeated twice with the presented data a combination an average of these two independent experiments.

3.2.9 **phyB and ELF3 independently regulate petiole elonga q qtion**

Alongside promoting hypocotyl elongation, PIFs also promote petiole elongation (Lorrain et al., 2008). Accordingly *elf3* and *phyB* loss of function mutants have elongated petioles **(Figure 3.14A1-2, B1-2 & C1-2)** (Reed et al., 2000). Visually analysing the petioles of the lines described above confirmed previous reports that *elf3* loss of function mutants have longer petioles than *phyB* under LD and SD photoperiods **(Figure 3.14B1-2, C1-2)**. However, in contrast to previous work (Reed et al., 2000), the petioles of the *phyB-10/elf3-4* double mutant were not visibly longer than the *elf3-4* single mutant under either LD or SD photoperiods **(Figure 3.14B1-2, D1-2)**. ELF3 (B+) fully rescued the petiole phenotype of the *elf3-4* mutant under LD and SD photoperiods **(Figure 3.14E1-2)**. In contrast, ELF3 (B-) was not capable of rescuing the petiole phenotype of the *phyB-10/elf3-4* double mutant under either photoperiod (**Figure 3.14F1-2)**. Instead, the petioles of ELF3 (B-) plants closely resembled the *phyB-10* single mutant **(Figure 3.14C1-2)**. Therefore, as with hypocotyl elongation, ELF3 and phyB likely regulate petiole elongation independently of each other.

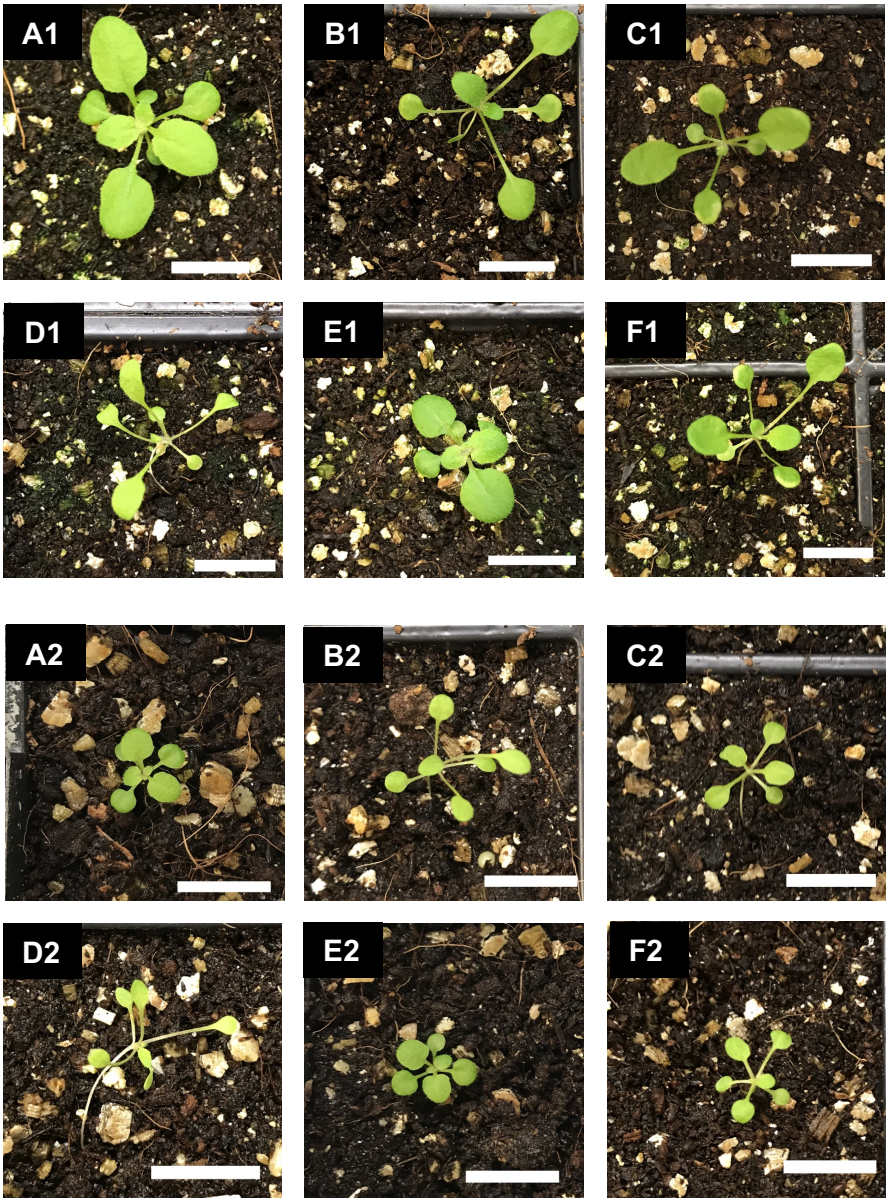

Figure 3.14 - Crosstalk between phyB and ELF3 in regulating petiole development

Twenty-day old (**A1, A2**) Wild type (Ws-2), (**B1, B2**) *elf3-4*, (**C1, C2**) *phyB-10*, (**D1, D2**) *elf3-4*/*phyB-10*, (**E1, E2**) *ELF3ox* (*elf3-4*) and (**F1, F2**) *ELF3ox* (*elf3-4*/*phyB-10*) plants. For (**1**) plants were grown under long-day photoperiods, while for (**2**) seedlings were grown under short-day photoperiods. The temperature was set at 22ºC for both photoperiods. Scale bars represent 2 cm.

3.2.10 **phyB inhibit ELF3's repressive effect on flowering time**

Alongside controlling hypocotyl and petiole development through repressing PIFs, ELF3 and phyB both repress the floral transition by regulating the expression and stability of the TF CONSTANS (CO) (Shim et al., 2017). To determine whether ELF3's repression of flowering time was regulated by phyB, I analysed the flowering time phenotype of the lines described above under long (LD)- and short-day (SD) photoperiods.

As previously reported, *elf3-4* and *phyB-10* flowered earlier than WT plants under SD and LD photoperiods **(Figure 3.15A-D, Appendix 3 Figure 4A-B)** (Reed et al., 2000). Under LD, the phenotype of the two single mutants was indistinguishable but under SD *elf3-4* flowered much earlier than *phyB-10*. The *elf3-4/phyB-10* double mutant flowered earlier than either respective single mutant under LD or SD, supporting previous work that used the Col-0 *elf3-1* and *phyB-9* alleles **(Figure 3.15A-D)** (Reed et al., 2000). ELF3 (B+) fully rescued the *elf3-4* early flowering phenotype under LD and SD photoperiods **(Figure 3.15A-D)**. Furthermore, ELF3 (B+) also delayed flowering under LD but not SD compared to WT, in agreement with previous work (Liu et al., 2001).

The early flowering phenotype of the *elf3-4/phyB-10* double mutant was also fully rescued by the over-expression of *ELF3* under LD and SD. As with ELF3 (B+), ELF3 (B-) flowered later than WT under LD photoperiods **(Figure 3.15A-B)**. Comparing the flowering time phenotype of ELF3 (B+) and ELF3 (B-) under LD revealed that ELF3 (B-) flowered later than ELF3 (B+) under LD **(Figure 3.15A, 3.15C, 3.15E, Appendix 3 Figure 4A-C)**. This phenotype was observed across three separate repeats, although for the second repeat the difference between ELF3 (B+) and ELF3 (B-) was smaller than in the first or third repeat **(Figure 3.15E)**. Under SD, the flowering time phenotype of ELF3 (B-) was dependent on the measurement of flowering time used. As measured by days to flower, ELF3 (B-) flowered later than WT or ELF3 (B+) **(Figure 3.15B)**. However, when measured by leaf count, ELF3 (B-) had the same number of leaves as WT and ELF3 (B+) **(Figure 3.15D)**. These differing phenotypes under SD could highlight a metabolic or a plastochron phenotype in the ELF3 (B-) background. Together, my results

suggest that phyB and ELF3 can regulate flowering independently of each other, but phyB may also antagonise the repressive effect of ELF3 on flowering under LD.

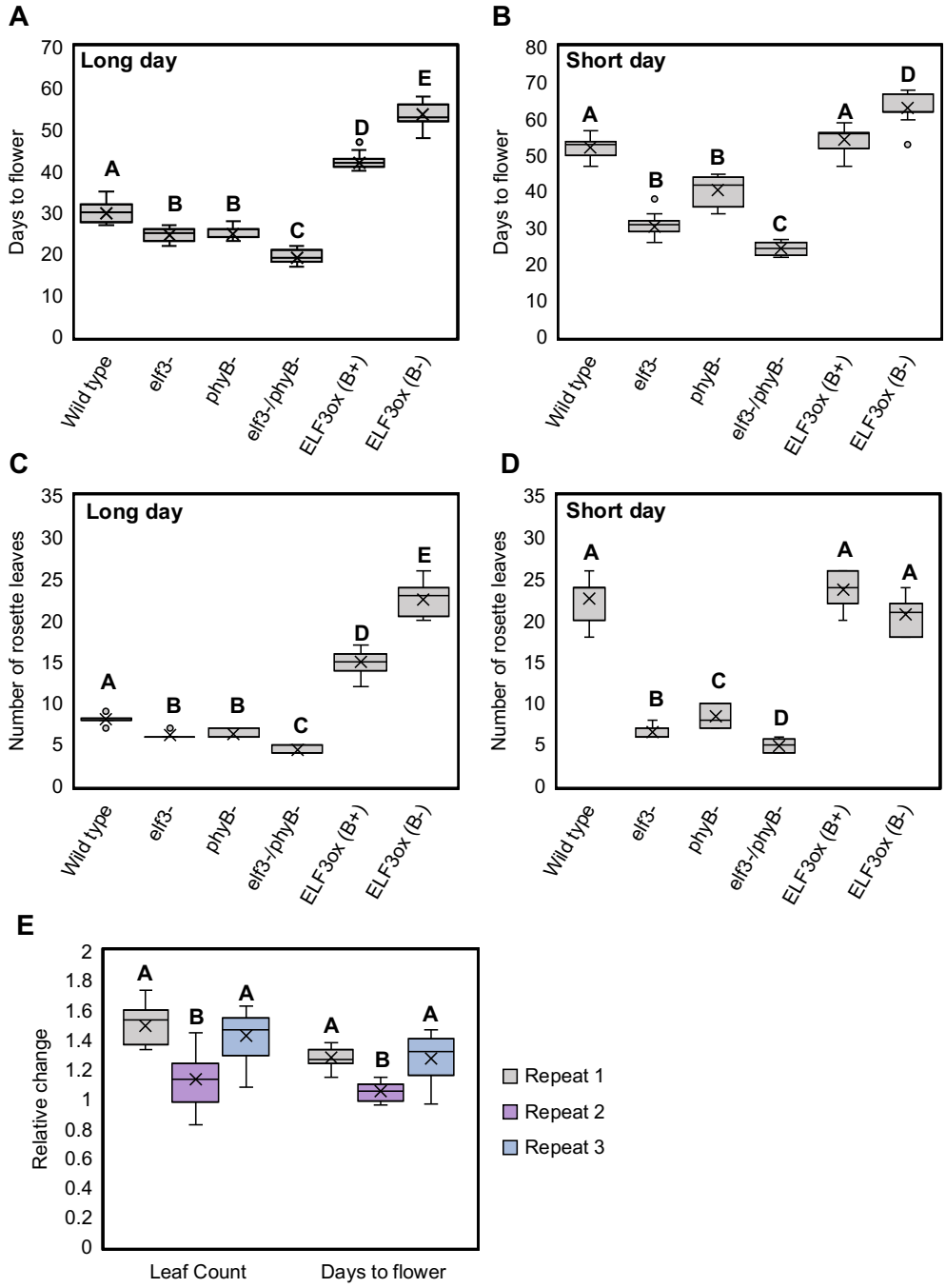

Figure 3.15 - phyB inhibits the repressive effect of ELF3 on flowering time under long day photoperiods

Flowering time in wild type (Ws-2), *elf3-4*, *phyB-10*, *elf3-4/phyB-10, ELF3ox elf3-* (ELF3 B+) and *ELF3ox elf3-4/phyB-10* (ELF3 B-) as measured by **(A-B)** days to flower or (**C-D**) number of rosette leaves under **(A, C**) long-days (LD) or **(B, D)** short-days (SD). Flowering was determined when the inflorescence bolt was ~1 cm above the rosette. **(E)** The change in rosette leaf number or day to flowers for ELF3ox (phyB-) relative to ELF3ox (phyB+) under LD photoperiods in

Figure 3.15 (continued) - three separate repeats. The data for repeat 2 and repeat 3 is included in Appendix 3, Figure 4. Letters signify significant difference ($p < 0.01$) as determined by a one-way ANOVA with a tukey HSD posthoc test. A minimum of eight plants were measured per genotype and photoperiod. For LDs, all experiments were repeated at least twice, while the SD experiment was performed once.

3.3 Discussion

Integrating light signals into the circadian clock is critical for entrainment and subsequent phase alignment between the internal cycle and the external environment. In this chapter, I have found that light-dependent regulation of circadians proteins may provide a new interface for integrating light signals into the oscillator. I observed that the cellular and sub-nuclear distribution of ELF3 was responsive to different wavelengths of light with RL, FRL and BL all regulating the localisation of ELF3 (**Figure 3.1-3.3, 3.8)**. Furthermore, there was also a competitive effect of RL and BL on the sub-nuclear localisation of ELF3, with the effect of RL suppressing the effect of BL **(Figure 3.4, Appendix 3 Figure 1)**. Therefore, multiple light signalling pathways may converge on ELF3 to competitively regulate where ELF3 is localised in the cell and ultimately control ELF3 functional activity.

ELF3 is a modular protein that is divided into three domains (N, M, C) that each independently facilitates protein-protein interactions (Liu et al., 2001, Herrero et al., 2012). ELF3 is directly connected to light signalling through a physical interaction with the primary RL photoreceptor phyB, which requires the N-terminus of ELF3 (Liu et al., 2001, Kim and Somers, 2019). Light signalling is further connected to the N-terminus of ELF3 through direct interactions with COP1 (Yu et al., 2008). Hence, the N-terminus of ELF3 has been viewed as the light-terminal of ELF3. However, my results suggest that light signalling converges on all domains of ELF3. The cellular localisation of ELF3 remained responsive to RL and BL in the absence of the N-terminus **(Figure 3.5)**, while the sub-nuclear localisation of ELF3-C was also responsive to BL **(Figure 3.6, Appendix 3 Figure 3)**. Thus, multiple proteins must transmit light signals to ELF3, and these potentially have competitive effects.

My results have also highlighted a potentially complex role for phyB in controlling the cellular and sub-nuclear localisation of ELF3. A FRL-pulse repressed the nuclear localisation of ELF3 at dusk **(Figure 3.9)**, suggesting that phys are requierd to promote the nuclear localisation of ELF3. Supporting this, the nuclear and sub-nuclear localisation of ELF3 was severly reduced in the *phyB* background **(Figure 3.10-11)**. However, RL-

pulses above 10 μmol/m^{-2}/s^{-1} decreased the abundance of ELF3 foci, while a 25 μmol/m^{-2}/s^{-1} RL pulse also suppressed the nuclear accumulation of ELF3 **(Figure 3.1, 3.8)**. Together, this suggests that phyB is required to both promote and repress the nuclear localisation of ELF3. How phyB could exert two opposite effects on ELF3 is discussed further in chapter 6.

Within the circadian clock, phyB was proposed to repress the activity of ELF3 (Hicks et al., 1996, Kolmos et al., 2011, Herrero et al., 2012). To test this I measured the effect of the *phyB* mutation on the ability of ELF3 to repress gene . However, this analysis did not reveal any clear, consistent effect of the *phyB* mutation on ELF3 repressive activity. The transcript abundance of *PRR9* and *TOC1* was similar in ELF3 (B+) and ELF3 (B-), while the transcript abundance of *GI* and *LUX* decreased and increased in ELF3 (B-) relative to ELF3 (B+), respectively **(Figure 3.12)**. Together, these results suggests that phyB does not necessarily antagonise ELF3 activity in the evening.

Previous work has highlighted that ELF3 has a critical role in repressing the input of light signals to the clock across the evening (Covington et al., 2001, Kolmos et al., 2011). Here, I observed that RL-induction of *PRR9* transcript abundance was inhibited by the over-expression of *ELF3* **(Figure 3.12)**. Furthermore, a RL-pulse increased the repressive effect of ELF3 on *PRR9* , indicating that a RL signalling pathway may re-enforce the repressive effect of ELF3 on *PRR9* transcript abundance in the evening. However, ELF3 did not repress RL induciton of *GI* **(Figure 3.12)**. Together, these results suggest that ELF3 may selectively inhibit light induction of morning, but not evening, expressed genes. The basis for such molecular specificity in gating the light sensitivity of certain genes is not clear and will need to be investigated further.

Alongside investigating the ability of phyB to regulate ELF3's ability to repress gene expression, I also examined whether phyB contributed to ELF3 function in repressing hypocotyl elongation, petiole elongation and the floral transition. For hypocotyl and petiole elongation, I observed no clear evidence that phyB regulated ELF3 activity in either developmental processes **(Figure 3.13 – 3.14)**. Instead, it seems ELF3 and phyB largely regulate these two processes independently of each other, in

agreement with the results of previous work (Reed et al., 2000). In contrast, for flowering time I observed that ELF3 (B-) flowered later than ELF3 (B+) under LD, suggesting that phyB antagonises ELF3 activity in controlling the floral transition under inductive conditions **(Figure 3.13 – 3.14, Appendix 3 Figure 4)**. How phyB may antagonise ELF3 activity is unclear, but ELF3 is hypothesised to function in the morning of LDs to bind and inhibit CO activity (Song et al., 2018). Thus, it is possible that the ELF3-phyB interaction may disrupt the ELF3-CO interaction and thereby promote CO activity in the morning.

In conclusion, my results highlight a complex effect of light on controlling the spatial localisation of ELF3 within the cell. phyB seems to be essential for the repressive but not positive effect of RL on the cellular localisation of ELF3. Therefore, other proteins must also transmit RL signals to ELF3 independently of phyB. The expression of *ELF4* is RL-responsive (Siddiqui et al., 2016) and ELF4 has been seperately proposed to promote the localisation of ELF3 to the nucleus and sub-nuclear bodies (Kolmos et al., 2011, Herrero et al., 2012, Anwer et al., 2014). In chapter 4, I test whether ELF4 regulates the localisation of ELF3 and the potential role of ELF4 in transmiting light signals to ELF3.

Chapter 4 - ELF4 regulates the nuclear and sub-nuclear accumulation of ELF3

4.1 Introduction

The recruitment of a protein to the nucleus can either occur intrinsically through a NLS present within the encoded protein, or the protein can be shuttled to the nucleus by interacting with a protein capable of self-localising to the nucleus (Ronald and Davis, 2019). Arabidopsis ELF3 is proposed to intrinsically localises to the nucleus through a NLS present within the C-terminus of the ELF3 protein (Liu et al., 2001). However, this NLS is only conserved amongst Brassicaceae ELF3 **(Appendix 4, Figure 1A)**. Monocotyledon ELF3 protein sequences contain a predicted NLS in the middle-region of the ELF3 protein **(Appendix 4, Figure 1B)**, while I could find no NLS motif in other angiosperms and more distantly related vascular plants (predicted through the NLS database: https://rostlab.org/services/nlsdb/). Therefore, other mechanisms must facilitate the nuclear localisation of ELF3.

One NLS-independent mechanism that could facilitate the nuclear localisation of ELF3 is through physical interactions with ELF4. ELF4 is a single domain protein that is proposed to function as an activator (Kolmos et al., 2009, Herrero et al., 2012). ELF4 intrinsically localises to the nucleus and contains a putative NLS within the N-terminus of the ELF4 protein (Khanna et al., 2003). ELF4 physically interacts with the middle domain of ELF3 (ELF3-M), and they co-localise together within sub-nuclear structures in tobacco cells (Herrero et al., 2012). Co-expressing *ELF4* and *ELF3-M* increased the nuclear localisation of ELF3-M in tobacco mesophyll cells. Furthermore, two separate point mutations have been identified in the ELF3-M region that reduced the nuclear accumulation of ELF3 (Kolmos et al., 2011, Anwer et al., 2014). Although there were no overt physiological phenotypes, both these *ELF3* alleles independently caused a shortening of the circadian period, highlighting a requirement for nuclear-localised ELF3 to regulate the plant circadian clock. Alongside ELF3, ELF4 has also been demonstrated to promote the localisation of GI to sub-nuclear bodies (Kim et al., 2013b). In contrast to ELF3, the recruitment of GI to these nuclear bodies was found to repress GI activity. Therefore, ELF4 seemingly regulates the cellular distribution of circadian proteins to control their functional activity.

So far, the role of ELF4 in facilitating the recruitment of ELF3 to the nucleus has only been shown in transient systems using a singular domain of ELF3 or indirectly inferred through mutations within the ELF4 binding region of ELF3 (Kolmos et al., 2011, Herrero et al., 2012, Anwer et al., 2014). To confirm that ELF4 directly regulates the nuclear accumulation of ELF3, in this chapter I characterised the cellular and sub-nuclear distribution of ELF3 across an evening in a wild type or mutant *elf4* background in Arabidopsis hypocotyl cells. I then tested the importance of ELF4 in facilitating the repressive activity of ELF3 in regards to controlling gene expression, hypocotyl elongation and the floral transition. Finally, I investigated whether the sub-nuclear dynamics of ELF3 was dependent on the tissue-type and the role of ELF4 within this.

4.2 Results

4.2.1 ELF4 is required for the nuclear localisation of ELF3

To determine the role of ELF4 in regulating the cellular and sub-nuclear localisation of ELF3, the *elf3-4/elf4-1* mutant was introgressed into the previously described *35S::YFP:ELF3* line (Herrero et al., 2012) to generate a homozygous *35S::YFP:ELF3 elf3-4/elf4-1* double mutant. The cellular and sub-nuclear localisation of ELF3 in hypocotyl cells was then imaged in these two backgrounds. Seedlings of the respective construct were grown under a short-day (SD) photoperiod before imaging was started at ZT7 (1-hour before dusk) on day 6. Seedlings were then imaged at ZT8 and then every four hours following this until dawn on day 7 (ZT24). *35S::YFP:ELF3* seedlings with a WT *ELF4* allele are referred to as ELF3 (4+), while *35S::YFP:ELF3* seedlings with a mutant *elf4* allele are called ELF3 (4-), respectively. All data was made relative to the values measured for ELF3 (4+) at ZT7.

ELF3 was localised between the cytoplasm and nucleus at all timepoints and in both respective backgrounds **(Figure 4.1A-C, Figure 4.2A-B)**. However, the extent of ELF3 nuclear localisation was dependent on both the time of day and the context of the *ELF4* allele. The nuclear/cytoplasmic (N/C) ratio of ELF3 (4+) peaked at dusk (ZT8) and remained unchanged at ZT12 **(Figure 4.1A, Figure 4.2A1-3)**. At ZT16, the N/C ratio of ELF3 (4+) declined and reached the lowest level of the timeseries **(Figure 4.2A4)**. The N/C ratio of ELF3 then subsequently recovered at ZT20 back to levels comparable with ZT7, before further increasing at ZT24 (dawn on day 7) **(Figure 4.1A, Figure 4.2A5-6)**. The relative nuclear signal of ELF3 (4+) closely followed the observed changes in N/C ratio **(Figure 4.1B)**, while the only change in total signal was at ZT8 and ZT20 where there was a ~15% reduction at both timepoints compared to ZT7 **(Figure 4.1C)**. The total signal otherwise remained relatively consistent across the timeseries for ELF3 (4+). Together, this indicates that the nuclear accumulation of ELF3 is time of day dependent.

There was no significant change in the N/C ratio of ELF3 (4-) at ZT7 compared to ELF3 (4+) **(Figure 4.1A)**. However, the N/C ratio of ELF3 did not peak at dusk or at ZT12, with the N/C ratio declining at ZT8 and then further declining at ZT12 **(Figure**

4.1A, Figure 4.2B1-3). Instead, the N/C ratio of ELF3 (4-) peaked at ZT16 but this peak was lower than the peak observed for ELF3 (4+) at ZT8 or ZT12 **(Figure 4.2B4)**. After peaking at ZT16, the N/C ratio of ELF3 (4-) then declined at ZT20 before further decreasing at ZT24 **(Figure 4.1A, Figure 4.2B5-6)**. The relative nuclear signal of ELF3 (4-) mostly followed the oscillations in N/C ratio, with the relative nuclear signal reaching its maxima and minima at ZT16 and ZT12, respectively **(Figure 4.1B)**. However, the relative nuclear signal of ELF3 (4-) at ZT8 and ZT24 did not show the same decrease as was observed in the N/C ratio. Instead, the relative nuclear signal remained unchanged or increased at ZT8 and ZT24 compared to ELF3 (4+) at ZT7, respectively **(Figure 4.1B)**.

These disparities between the N/C ratio and relative nuclear signal are likely caused by changes in the total signal of ELF3 (4-). Unlike the relative total signal of ELF3 (4+) which remained relatively consistent across the timecourse, the total signal of ELF3 (4-) did oscillate across the evening **(Figure 4.1C)**. At ZT8 and ZT12, the total signal of ELF3 (4-) increased above WT ZT7 levels, before declining at ZT16 and ZT20. The total signal of ELF3 (4-) then recovered at ZT24 and increased above WT ZT7 levels **(Figure 4.1C)**. Comparing the percentage difference between maximum and minimum total signal revealed that ELF3 (4-) had a ~51% change in total signal between peak and trough. In contrast there was only a ~20% change between the peak and trough in total signal for ELF3 (4+). This suggests that ELF4 may buffer the stability of ELF3 across the evening, alongside promoting the nuclear accumulation of ELF3.

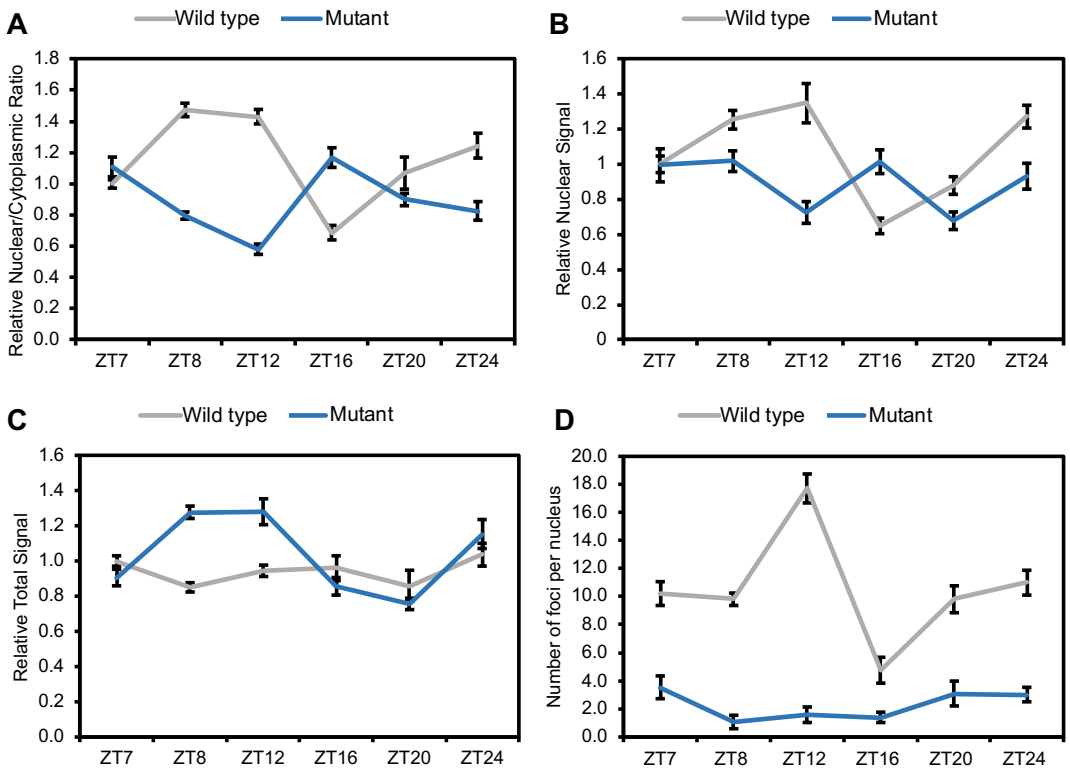

Figure 4.1 - The nuclear and sub-nuclear dynamics of ELF3 across a short-day evening

Oscillations in the nuclear and sub-nuclear localisation of *35S::YFP:ELF3* in the (**A**) *elf3-4* (grey, wild type) or (**B**) *elf3-4/elf4-1* (blue, mutant) background. (**A**) The relative nuclear/cytoplasmic ratio, (**B**) relative nuclear signal, (**C**) relative total signal and (**D**) the number of foci per nucleus of ELF3 in the two respective backgrounds. The data of (A-C) was made relative to the respective values of *35S::YFP:ELF3* (*elf3-4*) at ZT7. For all timepoints, imaging was repeated on at least two occasions.For (A-C), a minimum of four images were analysed for each timepoint in total, while for (D) a minimum of eight images were collected and analysed. Error bars represent standard error of the mean.

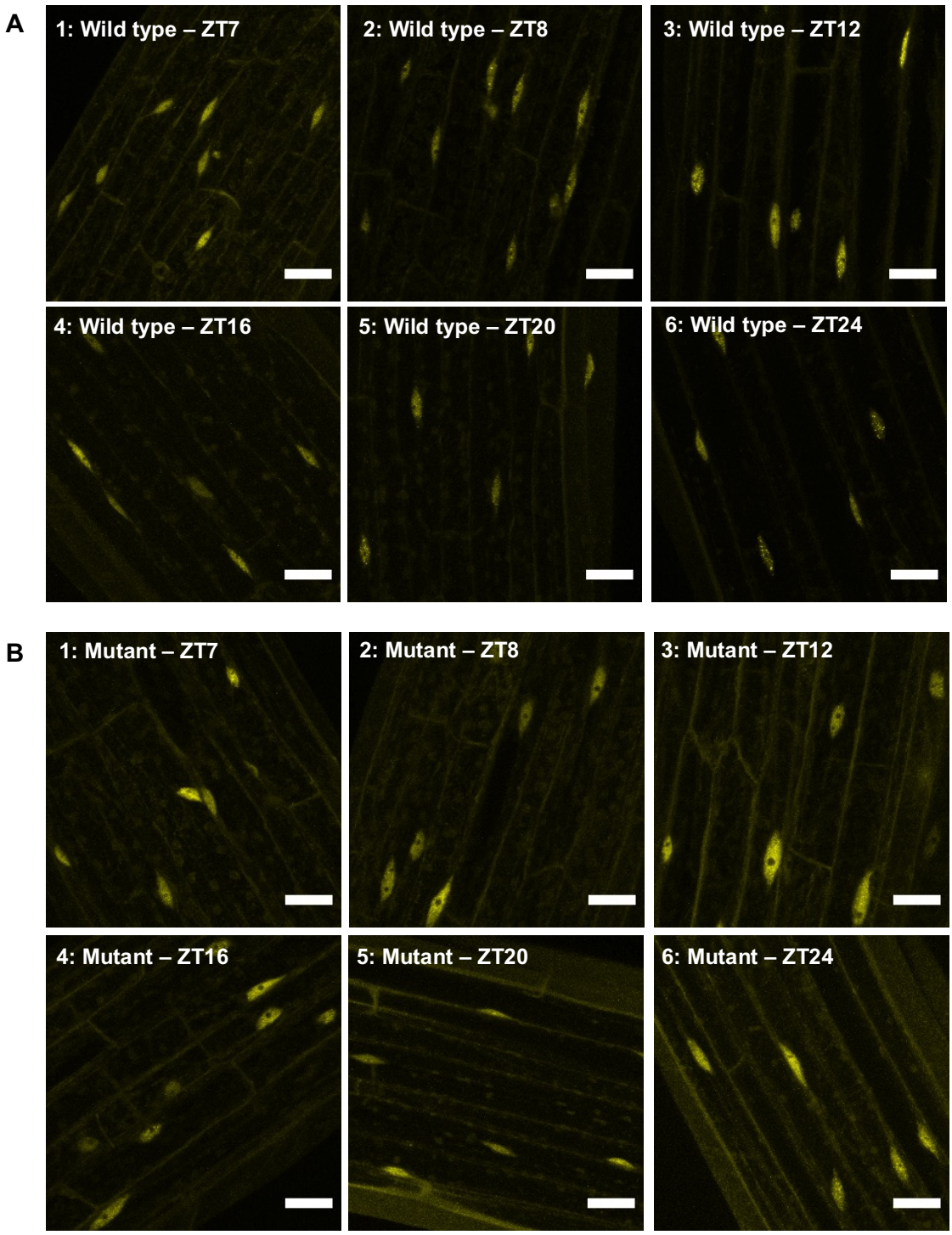

Figure 4.2 - The cellular localisation of ELF3 across the evening

The localisation of *35S::YFP:ELF3* in the **(A)** *elf3-4* (wild type) or **(B)** *elf3-4/elf4-1* (mutant) background at different timepoints in the evening of a short-day (8/16) photoperiod. Images are representative of the data presented in figure 4.1. For both backgrounds, all imaging were repeated twice. Scale bars are equal to 25 μm.

4.2.2 **ELF4 promotes the localisation of ELF3 to sub-nuclear structures**

I also found that the localisation of ELF3 to foci was dependent on both the time of day and the context of the *ELF4* allele **(Figure 4.1D, Figure 4.3A-B)**. Although the nuclear accumulation of ELF3 (4+) increased at ZT8 relative to ZT7, there was no change in the number of foci between the two timepoints **(Figure 4.1D, 4.3A1-2)**. Instead, ELF3 (4+) foci peaked at ZT12 before rapidly declining at ZT16 to the lowest value of the timeseries **(Figure 4.3A3-4)**. The number of foci then recovered back to ZT7 levels at ZT20 and then remained unchanged at ZT24 **(Figure 4.1D, 4.3A5-6)**. Alongside changes in number of foci, the morphology of ELF3 (4+) foci also changed across the night. At ZT7 and ZT8, ELF3 (4+) foci were largely indistinguishable from each other **(Figure 4.3A1-2)**. Foci then became larger and brighter at ZT12, before becoming smaller at ZT16 and ZT20 **(Figure 4.3A3-5)**. At dawn (ZT24), ELF3 (4+) foci increased in size and brightness, appearing similar to foci that were observed at ZT12 **(Figure 4.3A6)**.

The association of ELF3 to foci was strongly impaired in the *elf3-4/elf4-1* background. At all timepoints, ELF3 (4-) was predominantly localised to the nucleoplasm with foci infrequently observed **(Figure 4.3B1-6)**. When foci were observed, there were fewer foci per nuclei than observed for ELF3 (4+) **(Figure 4.1D)**. The phenotypic effect of the *elf4-1* mutation on the frequency of nuclei containing a focus and the number of foci per nuclei was particularly enhanced in the early evening (ZT8-12) **(Figure 4.1D, 4.3B1-3).** These results are similar to the phenotypic effect of the *elf4-1* mutation on the nuclear accumulation of ELF3 **(Figure 4.1A).** ELF3 (4-) foci also failed to display the same peak and trough in foci accumulation at ZT12 and ZT16 as observed for ELF3 (4+) **(Figure 4.1D)**. Instead, ELF3 (4-) foci peaked at ZT7 and reached a minimum at ZT8. ELF3 (4-) foci were also smaller and less bright than ELF3 (4-) at all timepoints and there was no observable change in the appearance of ELF3 (4-) foci across the timeseries **(Figure 4.3B1-6)**. In conclusion, ELF4 has a critical role in promoting the association of ELF3 to foci.

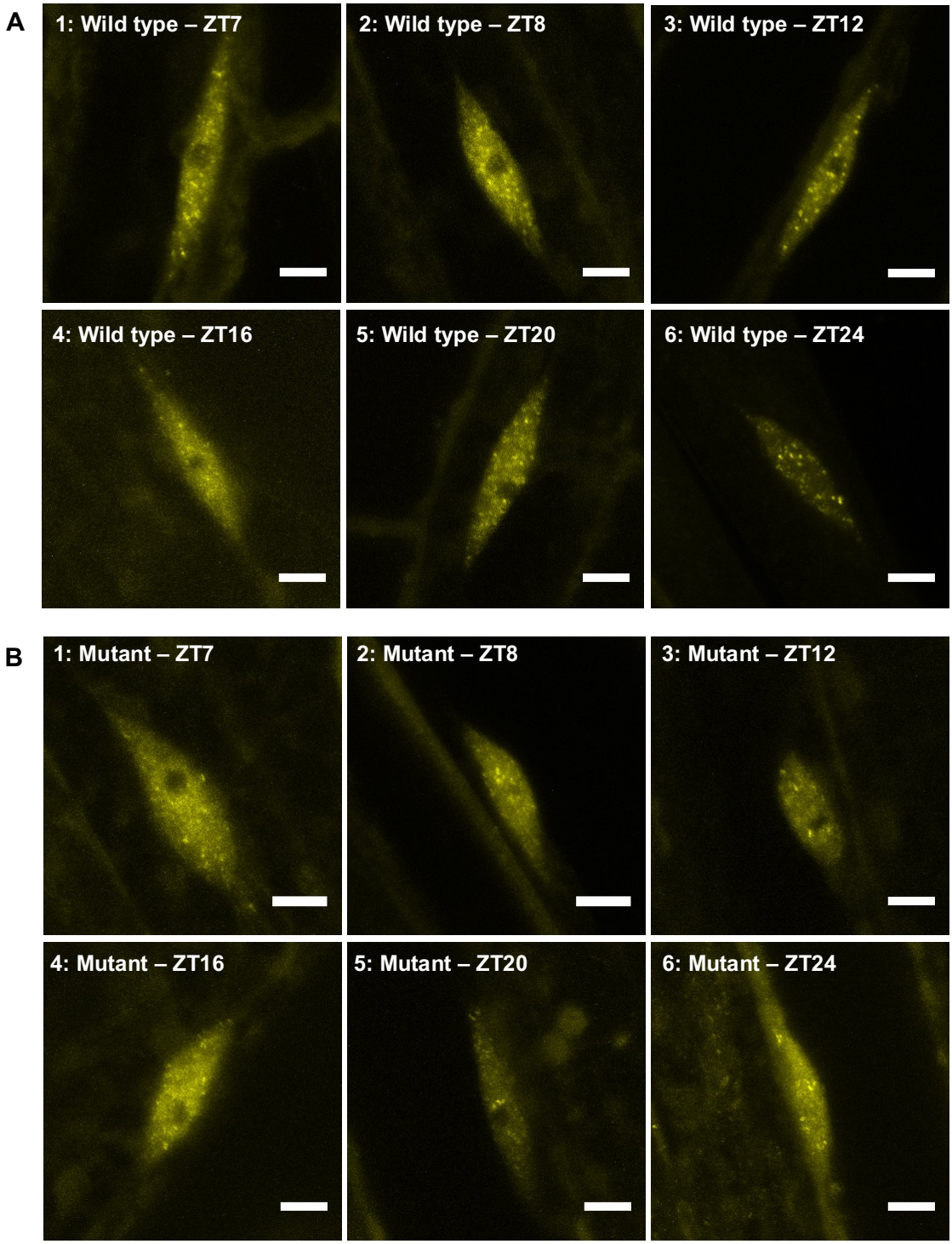

Figure 4.3 - The sub-nuclear localisation of ELF3 across the evening

The sub-nuclear localisation of *35S::YFP:ELF3* in the (**A**) *elf3-4* (wild type) or (**B**) *elf3-4/elf4-1* (mutant) background at different timepoints in the evening of a short-day (8/16) photoperiod. Images are representative of the data presented in figure 4.1. For both backgrounds, all imaging were repeated twice. Scale bars are equal to 5 μm.

4.2.3 **ELF4 is required for ELF3 to repress gene expression**

To understand how changes in the cellular localisation of ELF3 influenced ELF3 activity, I compared the transcript abundance of ELF3/EC targets in ELF3 (4+) and ELF3 (4-) at ZT12. ZT12 was chosen as this timepoint had the largest difference in the nuclear and sub-nuclear accumulation of ELF3 between the two respective backgrounds (**Figure 4.1A, 4.1D)**. I measured the transcript abundance of four genes, *PSEUDO RESPONSE REGULATOR9* (*PRR9*), *LUX ARRYTHMO* (*LUX*), *TIMING OF CAB1 EXPRESSION* (*TOC1*) and *GI.* All four are established targets of the EC (Herrero et al., 2012, Chow et al., 2012, Lee et al., 2019b, Park et al., 2019).

There was no change in the transcript abundance *PRR9*, *LUX*, *TOC1* or *GI* transcript abundance in ELF3 (4+) at ZT12 compared to WT **(Figure 4.4A-D)**. These results support earlier results that found no repressive effect of *ELF3ox* at ZT12 (Nieto et al., 2015). The transcript abundance of *PRR9* in ELF3 (4-) was similar to ELF3 (4+), being slightly elevated compared to WT **(Figure 4.4D)**. In contrast, the transcript abundance of *GI* and *LUX* was elevated in ELF3 (4-) when compared to WT and ELF3 (4+) **(Figure 4.4A-B)**. The transcript abundance of *TOC1* was also elevated in ELF3 (4-), although the difference in *TOC1* transcript abundance between ELF3 (4-) and WT/ELF3 (4+) was smaller than the difference for *GI* and *LUX* **(Figure 4.4C)**. Combined, these results suggest that ELF4 is required for ELF3 to repress the transcript abundance of *GI, LUX* and *TOC1* in the evening.

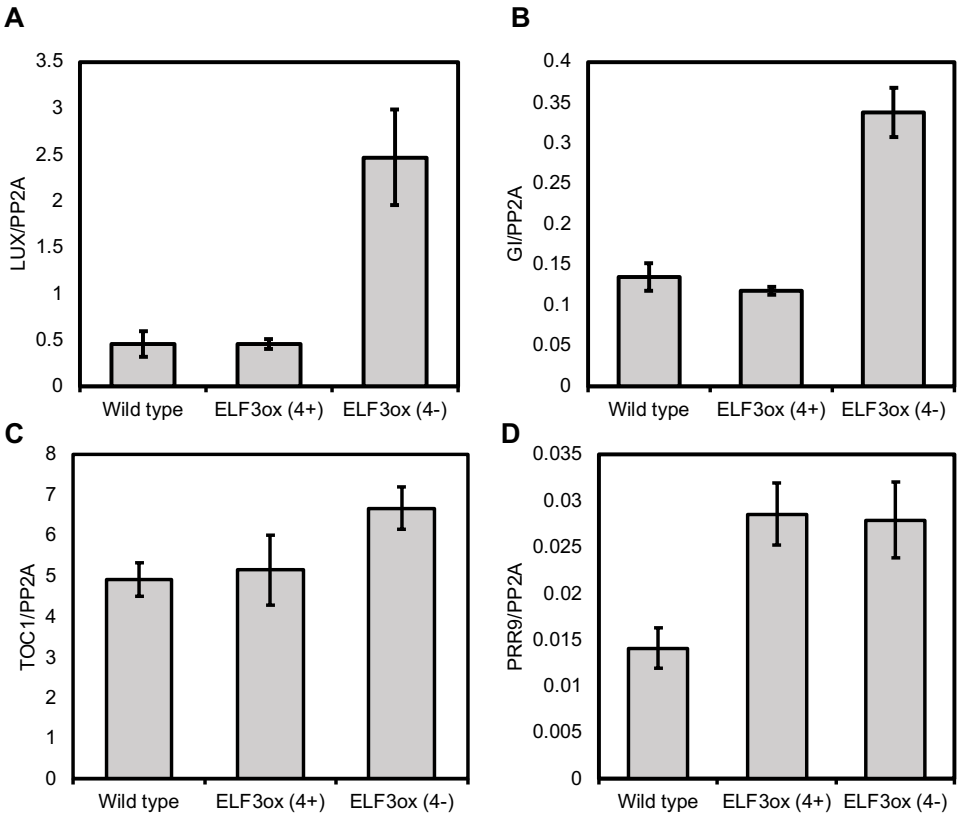

Figure 4.4 - ELF4 is required for ELF3 to repress evening-phased genes

The transcript abundance of (**A**) *LUX ARRHYTMO* (*LUX*), (**B**) *GIGANTEA* (*GI*), **(C)** *TIMING OF CAB EXPRESSION1* (*TOC1*) and **(D)** *PSEUDO RESPONSE REGULATOR9* (*PRR9*) in a wild type, *35S::YFP:ELF3 elf3-4* (ELF3 4+) or *35S::YFP:ELF3* (ELF3 (4-) background at ZT12 (short-day 8/16 photoperiods). Transcript abundance of the respective gene was standardised to the transcript abundance of *PROTEIN PHOSPHATASE2A* (*PP2A*). Presented data is the average of three technical replicas. Error bars are standard deviation of the technical replicas.

4.2.4 ELF4 promotes ELF3 inhibition of hypocotyl elongation in a photoperiod-dependent manner

Two separate studies have identified point mutations within the ELF4-binding domain of ELF3 that reduced ELF3 activity and subsequently caused a shortening of the circadian period (Kolmos et al., 2011, Anwer et al., 2014). However, neither point mutation caused significant changes to juvenile or adult plant development. To investigate the importance of ELF4 in facilitating ELF3's regulation of plant development, I measured hypocotyl elongation in WT, *elf3-4*, *elf3-4/elf4-1*, *35S::YFP:ELF3* (*elf3-4*) and *35S::YFP:ELF3* (*elf3-4/elf4-1*) seedlings. As before, *35S::YFP:ELF3* (*elf3-4*) and

35S::YFP:ELF3 (*elf3-4/elf4-1*) will be referred to as ELF3 (4+) and ELF3 (4-), respectively.

As in chapter 3, the hypocotyl length of WT seedlings was inversely related to the length of the photoperiod, with hypocotyl elongation progressively inhibited as the photoperiod was extended **(Figure 4.5A)**. *elf3-4* single mutants had longer hypocotyls than WT seedlings under all *diel* photoperiods as observed in chapter 3 **(Figure 4.5**, **Figure 3.13**). The *elf3-4* hypocotyl phenotype was again particularly enhanced in photoperiods with a neutral or extended dark phase. The *elf3-4/elf4-1* double mutant mostly phenocopied the hypocotyl phenotype of *elf3-4*, with the *elf3-4/elf4-1* mutant having an elongated hypocotyl phenotype that was most pronounced under short- and neutral-day photoperiods **(Figure 4.5A)**. However, the *elf3-4/elf4-1* mutant did have a long hypocotyl phenotype under constant white light (CWL) **(Figure 4.5A-B)**. Comparing the respective single mutants revealed that only *elf4-1* had a CWL hypocotyl phenotype, and this phenotype was similar in magnitude to the *elf3-4/elf4-1* double mutant **(Figure 4.5B)**. Taken together, this suggests that ELF4 may repress hypocotyl elongation under CWL independently of ELF3.

The *elf3-4* hypocotyl phenotype was fully rescued in ELF3 (4+) under all photoperiods. Furthermore, in photoperiods with a light phase less than 16-hours, ELF3 (4+) hypocotyls were shorter than WT seedlings. In contrast, ELF3ox (4-) only partially rescued the *elf3-4/elf4-1* phenotype. Under short-days and neutral days, the hypocotyl of ELF3 (4-) was longer than WT. The hypocotyl length of ELF3ox (4-) under these photoperiods was not as long as the *elf3-4/elf4-1* double mutant, indicating ELF3 retained some activity in the absence of *elf4*. For photoperiods with 16 or more hours of light, ELF3 (4-) had a similar hypocotyl length to WT and ELF3 (4+). This indicates that ELF4 may have a critical role in facilitating ELF3 activity in photoperiods with an extended dark phase.

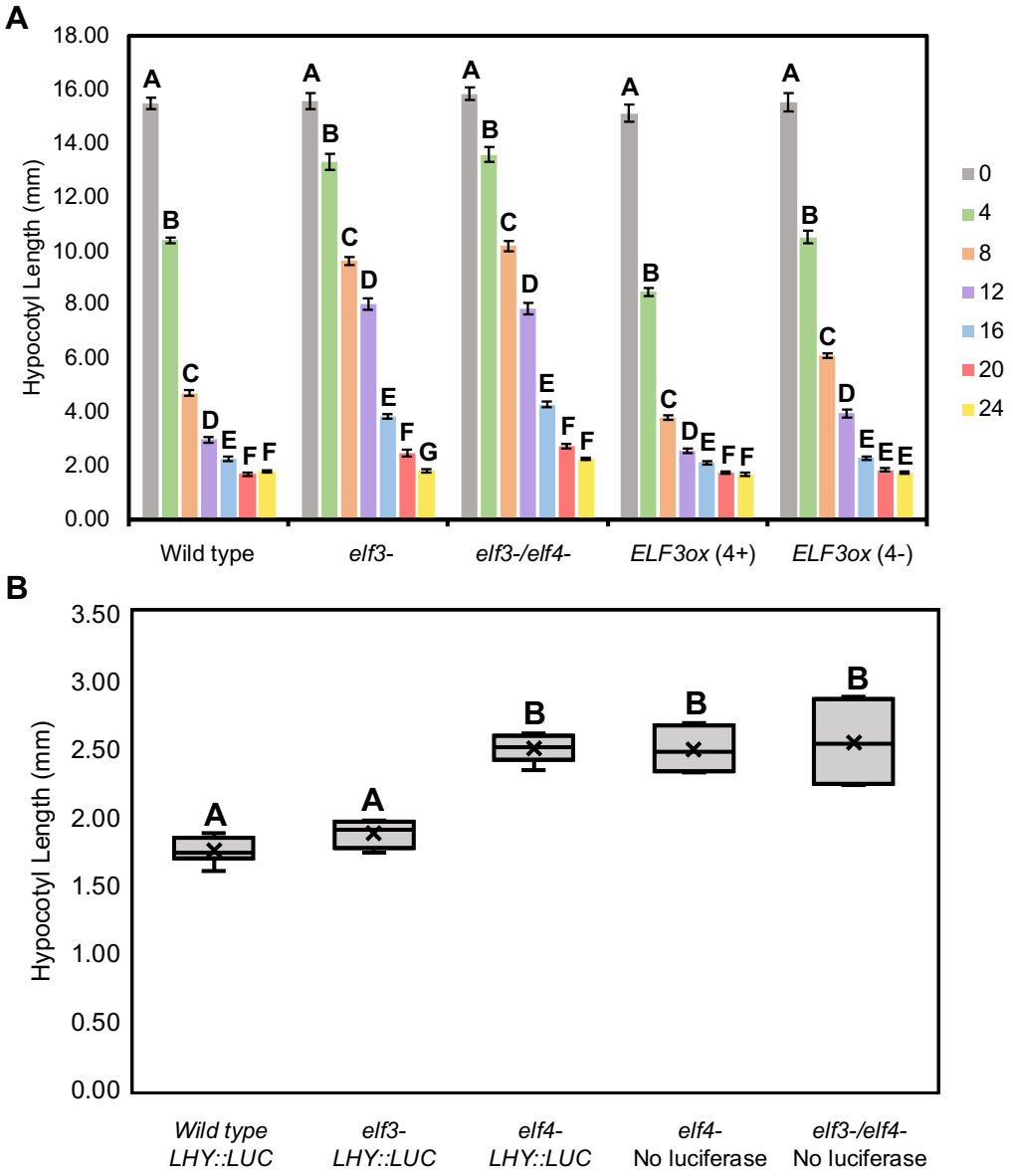

Figure 4.5 – ELF4 is required for ELF3 to regulate hypocotyl elongation

(A) Hypocotyl length in wild type (WT), *elf3-4* (*elf3-*), *elf3-4/elf4-1* (*elf3-/elf4-*), and *35S::YFP:ELF3* in either the *elf3-4* (ELF3 4+) or *elf3-4/elf4-1* (ELF3 4-) background under different photoperiods (see legend for duration of light). **(B)** Hypocotyl length for WT (*LHY::LUC*), *elf3-* (*LHY::LUC*), *elf4-* (*LHY::LUC*), *elf4-* (no luciferase) and *elf3-4/elf4-* (no luciferase) under constant light. Hypocotyl length was measured on day seven. All chambers had a light intensity of 85 μmol/m^{-2}/s^{-1} and a constant temperature of at 22ºC. A minimum of 10 seedlings were measured for each genotype under each respective photoperiod. For **(A)**, all experiments were repeated twice, with the presented data an average of the two repeats. For **(B)**, all experiments were repeated at least four times. Different letters signify significant differences ($p < 0.05$) either (A) within the respective genotype across the different photoperiods or (B) between genotypes. Significance was determined by a one-way ANOVA with a tukey HSD posthoc test. Error bars are standard error of the mean (SEM).

4.2.5 ELF4 is required for ELF3 to repress flowering in short day photoperiods

As ELF4 was required to facilitate ELF3's inhibition of hypocotyl elongation under shorter-day photoperiods, I investigated whether ELF4 had a similar function in repressing flowering time. Using the same lines as before, I tested flowering time under inductive long-days (LD) or non-inductive short-day (SD) photoperiods **(Figure 4.6)**.

As in chapter 3, the *elf3-4* single mutant had a photoperiod insensitive early flowering phenotype. Similarly, the *elf3-4/elf4-1* also had an early flowering phenotype that was insensitive to the photoperiod **(Figure 4.6A-D)**. There was no difference in the severity of the flowering time phenotype of the single or double mutant under LD or SD. Re-introducing ELF3 into the *elf3-4* and *elf3-4/elf4-*1 double mutant restored photoperiod sensitivity, with ELF3 (4+) and ELF3 (4-) both flowering later under SD than LD photoperiods **(Figure 4.6A-D)**. ELF3 (4+) flowered later than WT plants under LD photoperiods, while there was no significant difference between WT and ELF3 (4+) under SD **(Figure 4.6E-F)**. ELF3 (4-) flowered slightly later than WT plants under LD photoperiods, although this was not as late as ELF3 (4+) **(Figure 4.6A, 4.6C)**. Under SD, ELF3 (4-) only partially rescued the *elf3-4/elf4-1* early flowering phenotype, flowering earlier than WT and ELF3 (4+) **(Figure 4.6B, 4.6D, 4.6F)**. In summary, ELF4 seemingly has a critical role in facilitating ELF3 functional activity under photoperiods with a shorter light phase.

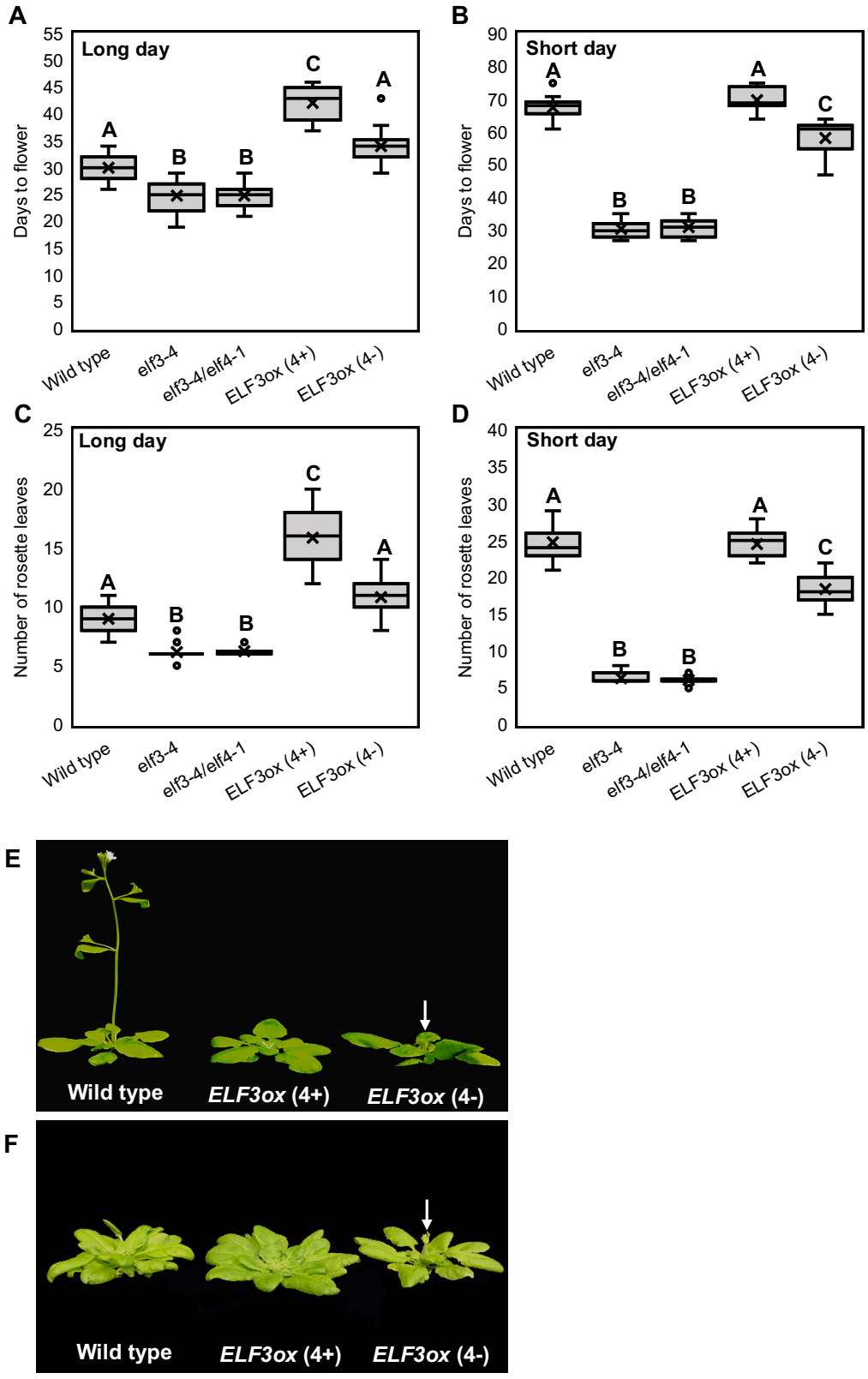

Figure 4.6 – ELF4 is required for ELF3 to repress flowering time under short-day photoperiod

Flowering time of Ws-2 (wild type), *elf3-4*, *elf3-4/elf4-1*, *35S::YFP:ELF3 elf3-4* (ELF3 4+) and *35S::YFP:ELF3 elf3-4/elf4-1* (ELF3 4-) under (**A, C, E**) long-days or **(B, D, F)** short-days. Flowering time was measured as (**A, B**) days to flower or the (**C, D**) number

Figure 4.6 (continued) - of rosette leaves. Flowering was determined when the inflorescence was ~1cm above the rosette. Representative images of WT, ELF3 4+ and ELF3 4- under (**E**) long-day or (**F**) short-day photoperiods. Arrow indicates the emergence of an inflorescence. Significance was determined with a one-way ANOVA with a tukey HSD posthoc test, letters indicate significance difference ($p < 0.001$).

4.2.6 Light dependent responses of ELF3 cellular localisation in the *elf4* mutant background

In chapter 3 I found that the cellular and sub-nuclear localisation of ELF3 was responsive to light. These light-dependent changes in ELF3 localisation were partially dependent on the N-terminus of ELF3 that facilitates the interaction between ELF3 and the primary RL receptor phyB (Liu et al., 2001). However, the cellular localisation of ELF3 was responsive to light in the absence of the domain of ELF3 that facilitates the phyB-ELF3 interaction **(Figure 3.5, 3.6, 3.10-11)**. Therefore, other proteins that interact with ELF3 must be capable of transmitting light signals to ELF3.

The expression of *ELF4* is directly induced by FRL, RL and UV-B light (Tepperman et al., 2001, Li et al., 2011, Takeuchi et al., 2014, Siddiqui et al., 2016). As ELF4 also regulates the localisation of ELF3 **(Figure 4.1-3)**, I tested whether ELF4 regulated light-dependent changes in the sub-nuclear localisation of ELF3. I pulsed ELF3 (4-) seedlings with 25 $\mu mol/m^{-2}/s^{-1}$ of RL or BL or transferred them to the dark at ZT7 for three hours. As a control, ELF3 (4+) seedlings were exposed to the same light treatments. As reported in chapter 3, the sub-nuclear localisation of ELF3 (4+) was responsive to light in a wavelength dependent manner. A pulse of RL reduced the association of ELF3 (4+) to foci, while a pulse of BL promoted the localisation of ELF3 (4+) to foci **(Figure 4.7A-C, 4.7G)**.

As observed in the timecourse, the localisation of ELF3 (4-) to foci was strongly impaired in the dark at ZT10. When foci were observed, these were smaller and less bright than ELF3 (4+) foci in the dark **(Figure 4.7A, 4.7D)**. There was no further reduction

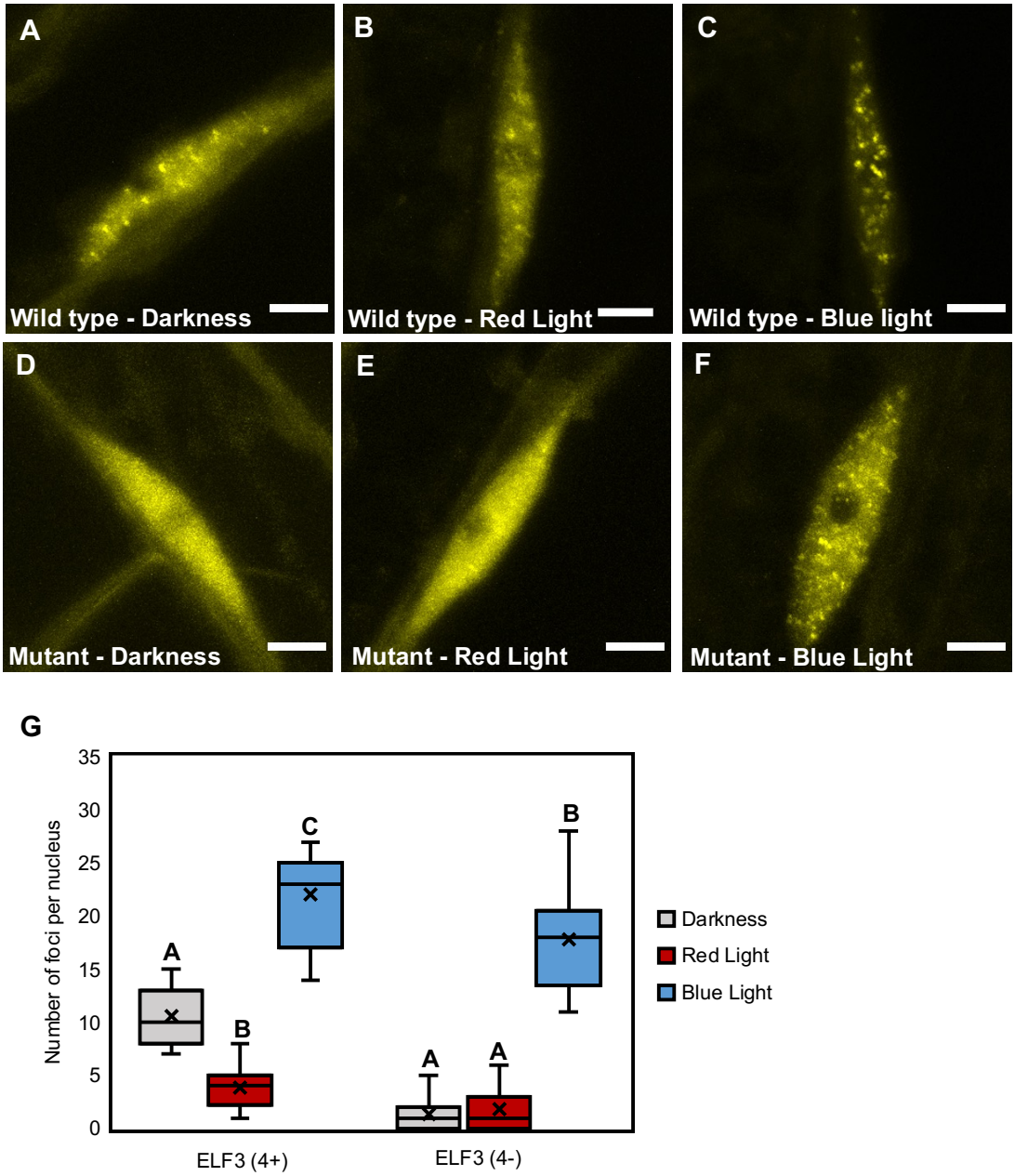

Figure 4.7 - Light responsiveness of ELF3 sub-nuclear localisation in the *elf4* mutant background

The localisation of (**A-C**) *35S::YFP:ELF3 elf3-4* (ELF3 4+, wild type) and (**D-F**) *35S::YFP:ELF3 elf3-4/elf4-1* (ELF3 4-, mutant) at ZT10 in the (**A, D**) dark of after a 3-hour long pulse of **(B, E)** 25 μmol/m^{-2}/s^{-1} red-light (RL) or (**C, F**) 25 μmol/m^{-2}/s^{-1} blue-light (BL) that was started at ZT7 (short-day, 8/16 photoperiod). Scale bars are 5 μm. (**G**) Quantification of the number of foci per nucleus after the respective light treatments in ELF3 4+ and ELF3 4-. All experiments were repeated at least twice. In total, a minimum of eight nuclei were analysed for each light treatment. Letters signify significance difference ($p < 0.001$) within the respective genotype as determined by a one-way ANOVA with a tukey HSD posthoc test.

in the number of ELF3 (4-) foci following a RL-pulse, although the frequency of nuclei containing at least one focus did increase (data not shown). As in the dark, ELF3 (4-) foci after a RL-pulse were smaller and less bright compared to ELF3 (4+) under the same light treatment. The sub-nuclear localisation of ELF3 (4-) foci was responsive to BL and retained the same response as ELF3 (4+), with the number of foci increasing following a BL-pulse **(Figure 4.F-G)**. However, the response of ELF3 (4-) foci to BL was more variable and overall weaker than the response of ELF3 (4+). As under the other light treatments, ELF3 (4-) foci were also smaller and less than bright than ELF3 (4+) foci after a BL-pulse **(Figure 4.C, 4.F)**. Together, these results suggest that BL and ELF4 regulate ELF3 foci dynamics independently of each other, while RL is potentially upstream of ELF4 in controlling the sub-nuclear distribution of ELF3.

4.2.7 **ELF3 foci have different temporal dynamics in roots and shoots**

Though the core structure of the Arabidopsis circadian clock is believed to be uniformly present across all plant cells, there is variation in the pace and accuracy of circadian rhythms in different tissue types (Gould et al., 2018). The source of this variation has been hypothesised to be caused by tissue-dependent changes in the sensitivity to entrainment stimuli and variation in the phase of circadian gene expression across the plant (Gould et al., 2018, Greenwood et al., 2019). However, another source of variation could be different cellular dynamics of circadian proteins in different tissue types.

To investigate whether ELF3 sub-nuclear dynamics had tissue-specific dynamics, I measured ELF3 foci accumulation in the roots of seedlings expressing *35S::YFP:ELF3* (*elf3-4*) at ZT7, ZT8 and ZT12. Seedlings were grown vertically under short-day (8/16) photoperiods and a constant temperature of 22ºC. These timepoints were chosen as it captures the light-to-dark transition (ZT7/ZT8) and the time at which ELF3 has maximal foci accumulation in hypocotyl tissue (ZT12). The root data was compared to the foci timecourse from hypocotyl nuclei that was presented earlier **(Figure**

4.1D). At ZT7 there was on average no change in the number of foci per nucleus between the two tissue types, while at ZT8 and ZT12 the average number of foci in root nuclei was higher and lower than in hypocotyl nuclei, respectively **(Figure 4.8A)**. Comparing the morphology of hypocotyl and root foci revealed that foci in root nuclei were usually larger and brighter than foci in hypocotyl nuclei at ZT7 and ZT8 **(Figure 4.9)**, while at ZT12 there was minimal difference in the size and brightness of foci between the two tissue types **(Appendix 4, Figure 2)**.

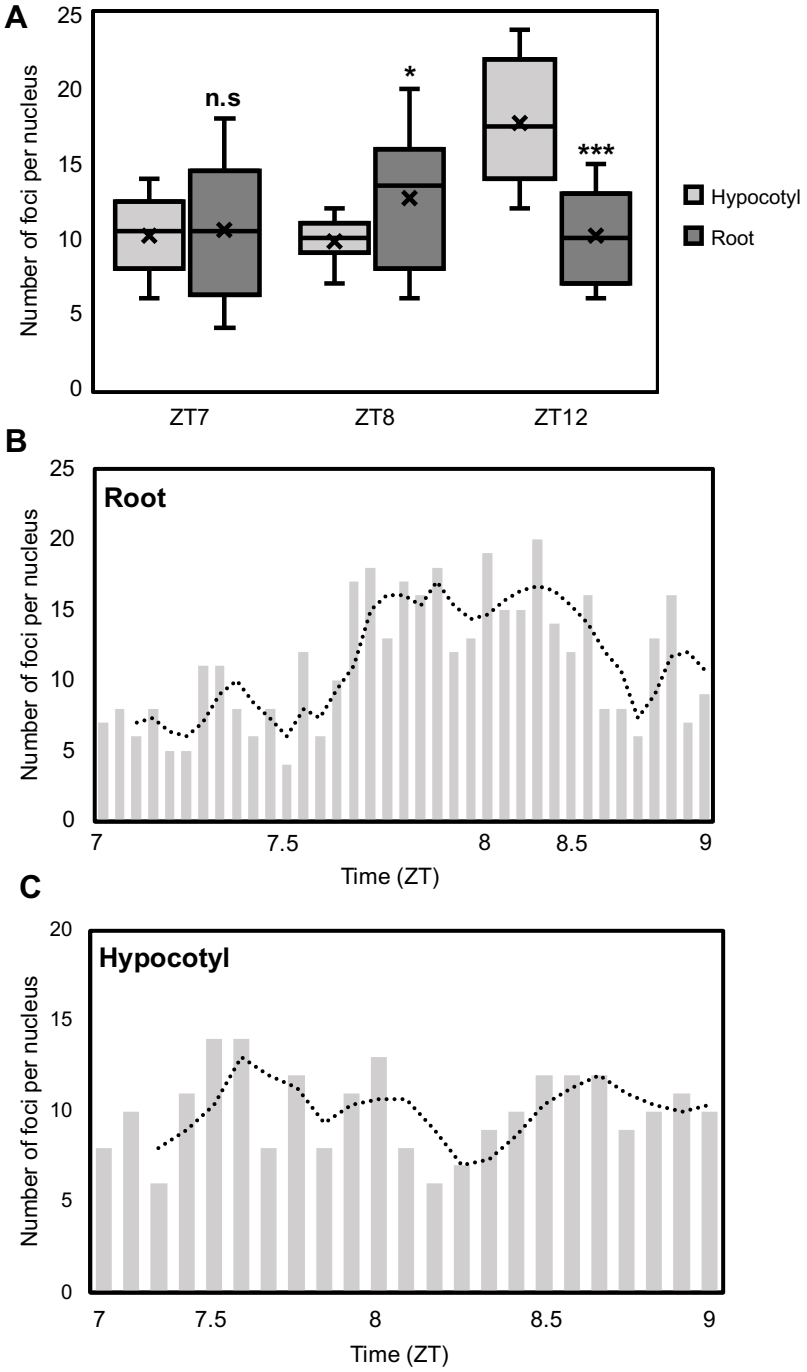

Figure 4.8 - ELF3 foci dynamics have a tissue-dependent response

Figure 4.8 (continued) (**A**) The localisation of *35S::YFP:ELF3* in the *elf3-4* background at ZT7, ZT8 and ZT12 (short-day, 8/16) in hypocotyl or root nuclei. The number of foci per nucleus for **(B)** root or **(C)** hypocotyl nuclei across ZT7 and ZT8. For (B, C) each bar represents an individual nucleus. Note, the nucleus was not re-imaged, with each bar representing a new nucleus. The dotted line is the rolling average across the timeseries. All experiments were repeated twice, with a total of 37 (root) or 23 (hypocotyl) images analysed across the timeseries. The hypocotyl data is the same as first presented in figure 4.1. Significance was determined by a two-way, unpaired T test. n.s = no significance, * = $p < 0.05$ and *** = $p < 0.001$.

I also observed that the number of foci in root nuclei at ZT7 and ZT8 was more variable than in hypocotyl nuclei **(Figure 4.8A)**. Analysing the data by the timepoint at which the image was captured revealed a strong oscillation in the number of ELF3 foci across the light-dark transition in root nuclei **(Figure 4.8B)**. Between ZT7 and ZT7.5, the number of foci per root nucleus was below the average for ZT7 timepoint **(Figure 4.9A, Table 1)**. However, from ZT7.5 onwards there was a large increase in the number of foci leading up to the light-dark transition at ZT8 **(Figure 4.9B, Figure 4.8B**, **Table 4.1)**. The number of foci then remained consistently elevated until ~ZT8.5 when the number of foci per nucleus began to decline below the average for the ZT8 timepoint **(Figure 4.9C-D, Table 4.1)**. Together, this suggests that the variability in the number of foci at ZT7 and ZT8 is caused by temporal oscillations in foci abundance across the light-dark transition.

I then looked to see whether there were similar temporal dynamics across the light-dark transition in hypocotyl nuclei **(Figure 4.8C, Table 4.1)**. As with root nuclei, the number of foci per hypocotyl nucleus did increase across ZT7 leading up to the light-dark transition **(Figure 4.9E-F)**. However, the number of foci then declined between ~ZT8 and ZT8.5 in hypocotyl nuclei, the opposite to what was observed in root nuclei **(Figure 4.8C, Figure 4.9G)**. The number of foci per hypocotyl nucleus then increased at ZT8.5 before remaining consistent for the remainder of the ZT8 timepoint **(Figure 4.9H)**. At ZT12, there was no clear oscillations in foci dynamics in either hypocotyl or root nuclei (data now shown). In conclusion, temporal oscillations in ELF3 foci dynamics around the light-dark transition may exist in hypocotyl and root nuclei, although the two tissue types have different responses, and the response is seemingly stronger in root nuclei.

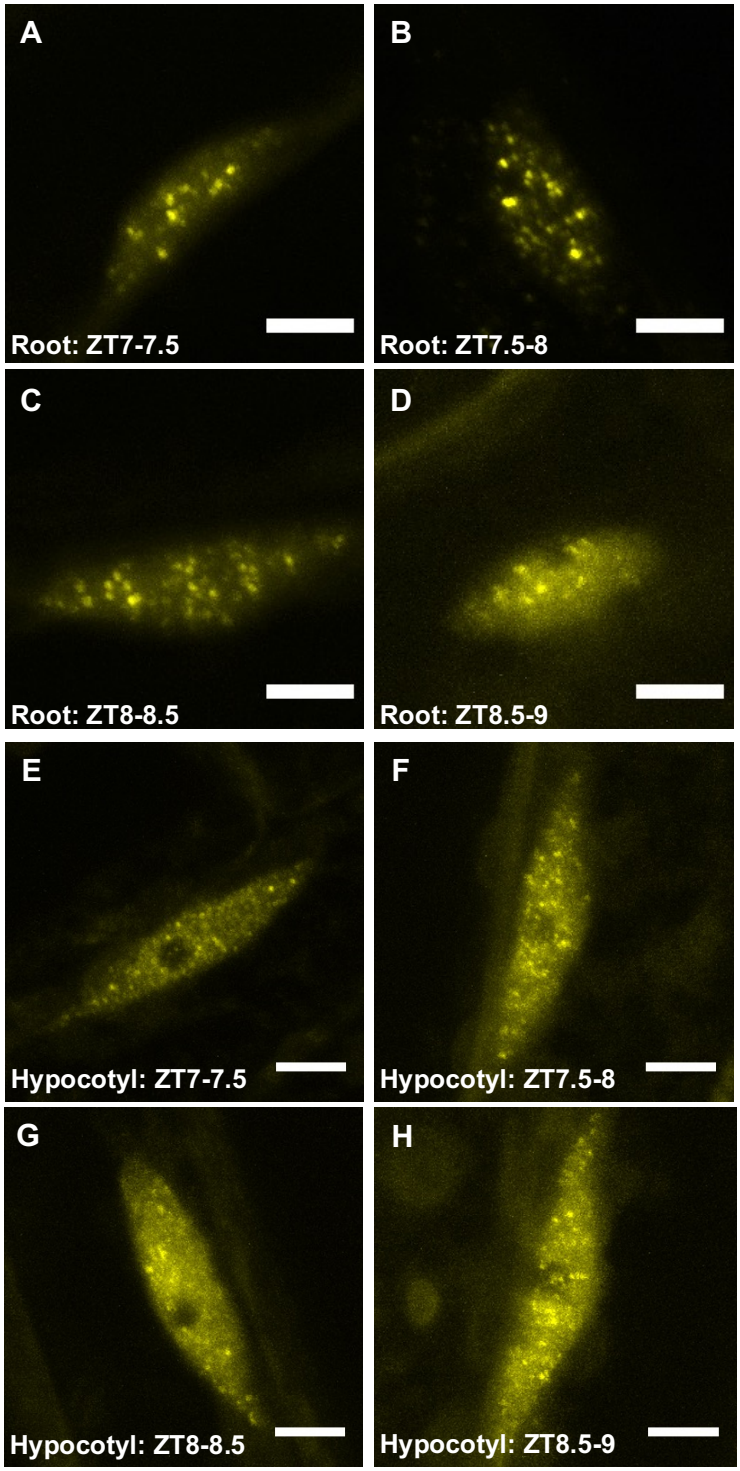

Figure 4.9 - The sub-nuclear localisation of ELF3 in root and hypocotyl nuclei

Changes in the sub-nuclear dynamics of *35S::YFP:ELF3* (*elf3-4*) across ZT7 and ZT8 in (**A-D**) root or (**E-H**) hypocotyl nuclei. Time window are broken down into 30 minute intervals: (A, E) ZT7 – ZT7.5, (B, F) ZT7.5 – ZT8, (C, G) ZT8 – ZT8.5 and (D, H) ZT 8.5 – ZT9. Seedlings were grown under a short-day (8/16 photoperiods). Scale bars are equal to 5 μm. Images are representative of the data presented in figure 4.8B-C.

Table 4.1 – Changes in the foci dynamics of ELF3 across ZT7 and ZT8.

The average number of ELF3 foci per nucleus at ZT7 and ZT8 or broken down into thirty minutes time-windows in hypocotyl or root nuclei. Images were collected under a short-day photoperiod. All images were collected on at least two separate occasions. The hypocotyl data was first presented in Figure 4.1. In brackets is the standard error of the mean for that respective timepoint.

Tissue	ZT7 Average	ZT7- ZT7.5	ZT7.5 - ZT8	ZT8 Average	ZT8 - ZT8.5	ZT8.5 - ZT9
Hypocotyl	10.2 (0.85)	8.6 (1.11)	11.2 (1.11)	9.92 (0.36)	8.6 (1.20)	10.8 (0.41)
Root	10.6 (0.93)	7.5 (0.93)	12.7 (0.68)	12.7 (1.20)	16.6 (1.21)	10.6 (1.27)

4.2.8 Tissue dependent requirement of ELF4 in promoting ELF3 localisation to foci

ELF4 is a mobile protein that moves from shoots to roots and this is movement is proposed to facilitate ELF3 activity in roots (Chen et al., 2020). However, the effect of the *elf4-1* mutation on regulating the nuclear or sub-nuclear localisation of ELF3 in root nuclei has remained untested. Here, I measured the foci dynamics of ELF3 (4-) in root nuclei of seedlings at ZT7 and ZT8 and compared it to the foci dynamics of ELF3 (4+).

As in hypocotyl nuclei, ELF3 (4-) formed fewer foci at ZT7 and ZT8 compared to ELF3 (4+) in root nuclei **(Figure 4.10A-B)**. However, the *elf4-1* mutation had a weaker phenotypic effect on foci abundance in root nuclei compared to hypocotyl nuclei at both timepoints. In root nuclei, the number of foci was reduced by ~52% and ~47% at ZT7 and ZT8 respectively, while in hypocotyl nuclei the number of foci was reduced by ~66% and ~89% at ZT7 and ZT8, respectively **(Table 4.2)**. Furthermore, ELF3 (4-) nuclei had at least one focus in all nuclei that were imaged at both timepoints, while in hypocotyl cells many ELF3 (4-) nuclei had no focus at either ZT7 or ZT8 (data not shown). Morphologically, ELF3 (4-) foci in root nuclei at ZT7 were smaller and less bright than ELF3 (4+) foci, while at ZT8 the foci from the two respective backgrounds were similar

(Figure 4.10A). The *elf4-1* mutation also disrupted the temporal dynamics of ELF3 foci across the light-dark transition. At both ZT7 and ZT8, the number of ELF3 (4-) foci was highly variable between nuclei and the peak in foci around the light-dark transition observed for ELF3 (4+) was not observable for ELF3 (4-) **(Figure 4.10C)**. In summary, ELF4 regulates ELF3 foci accumulation in root nuclei but has a weaker effect when compared to the effect of the *elf4* mutation on foci accumulation in hypocotyl nuclei.

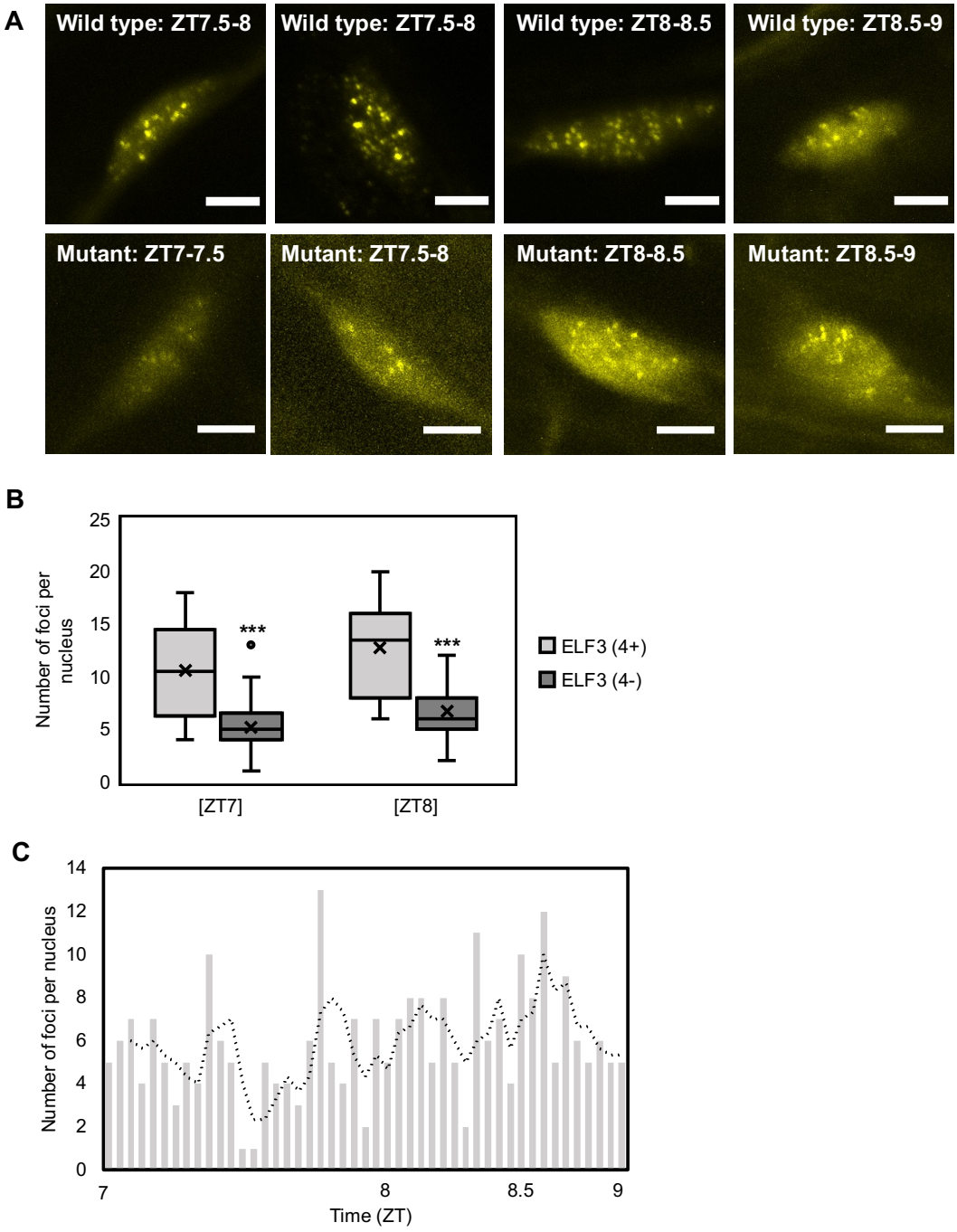

Figure 4.10 - ELF4 regulates ELF3 foci accumulation in root nuclei

Figure 4.10 (continued) - (A) The localisation of *35S::YFP:ELF3* in the *elf3-4* (wild type) or *elf3-4*/*elf4-1* (mutant) background between ZT7 and ZT9 (short-day 8/16 photoperiods). Scale bars are 5 μm. **(B)** The number of foci per root nucleus at ZT7 and ZT8 in the *elf3-4* (wild type) or *elf3-4*/*elf4-1* (mutant) background for *35S::YFP:ELF3*. The data and images of wild type in (A, B) were presented first in figure 4.8 and 4.9. **(C)** The number of foci per nucleus for *35S::YFP:ELF3* (*elf3-4*/*elf4-1*) across ZT7 – ZT9 in root nuclei. Each bar is an individual nucleus, with the dotted line the rolling average. All experiments were repeated twice, with the presented data a combination of these two repeats. Significance was determined with a two-tailed T test, *** = $p < 0.001$.

Table 4.2– ELF3 foci accumulation in hypocotyl and root nuclei in the *elf4* mutant

The average number of foci per nucleus for ELF3 (4+) and ELF3 (4-) at ZT7 and ZT8 in hypocotyl or root nuclei. Images were collected under a short-day (8/16) photoperiod. Images were collected on at least two separate occasions. The hypocotyl data for ELF3 (4+) and ELF3 (4-) was first presented in Figure 4.3, while the root data for ELF3 (4+) and ELF3 (4-) was presented in Figure 4.8 and 4.10, respectively. In brackets is the standard error of the mean (SEM).

Genotype	Hypocotyl ZT7	Root ZT7	Hypocotyl ZT8	Root ZT8
ELF3 (4+)	10.2 (0.9)	10.6 (0.93)	9.9 (0.6)	12.7 (1.20)
ELF3 (4-)	3.5 (0.8)	5.1 (0.52)	1.1 (0.5)	6.7 (0.51)

4.3 Discussion

Previous studies have suggested that ELF4 directly regulates the nuclear and sub-nuclear localisation of ELF3 (Kolmos et al., 2011, Herrero et al., 2012, Anwer et al., 2014). In this chapter, I directly tested this hypothesis by comparing the nuclear and sub-nuclear localisation of ELF3 in the *elf3*-or *elf3-/elf4*- background across a short-day evening **(Figure 4.1-3)**. These results revealed that the nuclear and sub-nuclear distribution of ELF3 in hypocotyl cells oscillates across the night, with the nuclear and sub-nuclear localisation of ELF3 peaking in the early evening before declining in the late evening **(Figure 4.1A, 4.1D)**. In the absence of *elf4*, these nuclear and sub-nuclear oscillations were strongly dampened. The nuclear localisation of ELF3 was delayed by the *elf4-1* mutation, with ELF3 nuclear accumulation not peaking until ~4 to 8 hours after ELF3 (4+) **(Figure 4.1, 4.2)**. Furthermore, the sub-nuclear localisation of ELF3 (4-) in hypocotyl nuclei failed to display any clear peaks unlike ELF3 (4+) **(Figure 4.1, 4.3)**.

The requirement of ELF4 in promoting the sub-nuclear localisation of ELF3 was not restricted to hypocotyl nuclei, with the sub-nuclear localisation of ELF3 also affected by the *elf4-1* mutation in root nuclei **(Figure 4.10)**. However, the phenotypic effect of the *elf4-1* mutation was weaker in root nuclei than hypocotyl nuclei **(Table 4.2)**, suggesting that the importance of ELF4 on regulating ELF3 localisation is partially dependent on the tissue-type. Combined, my results highlight a critical role for ELF4 in regulating the cellular localisation of ELF3.

ELF4 has emerged as a hub for light signalling, with the transcript abundance of *ELF4* directly regulated by RL, FRL and UV-B light signalling pathways (Tepperman et al., 2001, Li et al., 2011, Takeuchi et al., 2014, Siddiqui et al., 2016, Hajdu et al., 2018). As the sub-nuclear localisation of ELF3 is regulated by light **(Figure 4.7)**, I tested whether ELF4 facilitated light-dependent changes in the sub-nuclear distribution of ELF3. There was no additive effect of a RL-pulse and the *elf4-1* mutation on suppressing the localisation of ELF3 (4-) to foci, while a BL-pulse partially rescued the ELF3 (4-) foci phenotype **(Figure 4.7)**. However, the effect of BL on ELF3 (4-) foci association was highly variable between nuclei. A potential explanation for this variation is that foci in the

elf4 mutant background are more unstable. Though the mechanistic basis of ELF3 foci formation remains unknown, protein-protein interactions are critical for stabilising the formation of other nuclear bodies. For example, PHOTOPERIODIC HYPOCOTYL ELONGATION1 (PCH1) and the PCH1 homolog, PCH1-like, are essential for maintaining and stabilising phyB nuclear bodies (Enderle et al., 2017). Therefore, ELF4 could have a similar function in stabilising ELF3 foci.

Though *elf3* and *elf4* share abberantly elongated hypocotyls and photoperiod-insensitive early flowering (Hicks et al., 1996, Reed et al., 2000, Doyle et al., 2002, Khanna et al., 2003), ELF4 has been proposed to regulate flowering independently of ELF3 (Kim et al., 2013b), while ELF3 also regulates hypocotyl and flowering time independently of ELF4 and the EC (Yu et al., 2008, Nieto et al., 2015). Furthermore, point mutations in the ELF4 binding domain of ELF3 only caused a mild hypocotyl and flowering time phenotype (Kolmos et al., 2011, Anwer et al., 2014). Therefore, it was unclear what role ELF4 had in facilitating the non-circadian functions of ELF3.

Here, I observed that ELF4 has a important role in facilitating ELF3's inhibition of hypocotyl elongation and flowering time. However, the importance of ELF4 within this was dependent on the photoperiod. Under photoperiods with an extended dark phase, over-expressing ELF3 failed to rescue the early flowering or elongated hypocotyl phenotype of the *elf3-4/elf4-1* double mutant **(Figure 4.5, Figure 4.6)**. There was no additive effect of the *elf4-1* mutation on the *elf3-4* hypocotyl or flowering time phenotype under these photoperiods **(Figure 4.5, 4.6)**. Together, this suggests that the ELF3 (4-) phenotype is not a reflection of ELF4 regulating either process independently of ELF3 but rather reduced functional activity of ELF3 in the absence of *elf4*. As the photoperiod was extended to 16 or more hours of light, the ELF3 (4-) hypocotyl and flowering phenotype became indistinguishable from WT. It is unclear whether these results reflect a lesser-role for ELF4 in facilitating ELF3 activity or a weaker requirement of ELF3 itself and will need to be investigated further

A number of studies have recently begun to investigate the context of the plant circadian clock at a tissue or single cell level (Takahashi et al., 2015, Gould et al., 2018,

Greenwood et al., 2019). These studies have revealed that the plant circadian clock is not running at a consistent pace across an Arabidopsis plant. Instead, different tissues and even populations of cells within tissues have variations in the period of the circadian clock and the amplitude of circadian rhythms (Gould et al., 2018, Greenwood et al., 2019). The molecular basis of this has remained unclear, but tissue-dependent differences in the sensitivity of the circadian clock to *zeitgebers* (entrainment stimuli), strength of cell-to-cell coupling and differences in the transcript abundance patterns of circadian genes across different tissue-types are hypothesised to cause these differences in circadian parameters (James et al., 2008, Takahashi et al., 2015, Gould et al., 2018, Greenwood et al., 2019, Chen et al., 2020, Li et al., 2020b, Nimmo et al., 2020).

In this chapter, I have found that tissue-dependent changes in the cellular localisation of circadian proteins could also help explain why the properties of the plant circadian clock changes between different tissue types. In hypocotyl nuclei, ELF3 foci had maximal accumulation at ZT12, while in root nuclei ELF3 foci peaked earlier across the light-dark boundary (~ZT7.5 – ZT8.5) **(Figure 4.3, Figure 4.8-9)**. Furthermore, the *elf4* mutation was essential for ELF3 to localise to foci in hypocotyl nuclei, while in root nuclei the *elf4* mutation had a much weaker phenotypic effect **(Figure 4.10, Table 4.2**). Although the role of the EC within the root circadian clock is still debated (Chen et al., 2020, Nimmo et al., 2020), differences in when and where the EC localises in different tissue types could contribute to explaining tissue-specific variation in the plant circadian clock.

In conclusion, I have found that ELF4 has a critical role for regulating the cellular distribution of ELF3. Recently, ELF4 was found to have a secondary function in promoting ELF3 activity by facilitating the binding of the EC onto chromatin under warm temperatures (Silva et al., 2020). However, the molecular basis of such activity was not determined. Exposure to warm temperature caused ELF3 to localise to speckles, sub-nuclear condensates of inactive ELF3 (Jung et al., 2020). As ELF4 can regulate the sub-nuclear localisation of ELF3, I hypothesised that ELF4 inhibits the localisation of ELF3

to these speckle structures. Such a mechanism may preserve the ability of ELF3/EC to access chromatin at warmer temperatures. In chapter 5 I will test this hypothesis.

Chapter 5 – Arabidopsis ELF3 sub-nuclear localisation responds to warm temperature

5.1 Main text

Dear Editor,

Plants adapt their development to daily and seasonal ambient temperature fluctuations. Warming triggers a suite of molecular responses that leads to pronounced changes in plant development and architecture (Quint et al., 2016). Collectively, this response is called thermomorphogenesis. The evening complex (EC) is a transcriptional regulatory complex composed of EARLY FLOWERING3 (ELF3), ELF4, and LUX ARRYTHMO (LUX) that has emerged as a hub in the circadian clock and plant development (Nusinow et al., 2011, Herrero et al., 2012, Ezer et al., 2017a). The ability of the EC to bind to DNA is temperature-dependent, with warm temperature reducing the association of the EC to DNA (Raschke et al., 2015, Press et al., 2016, Ezer et al., 2017a, Silva et al., 2020). However, it is unclear how warm temperature inhibits the DNA binding ability of the EC. Previously, we observed that ELF3 localizes to sub-nuclear structures called foci (Herrero et al., 2012). Impaired localization of ELF3 to foci correlated with elevated expression of EC targets (Anwer et al., 2014), suggesting that foci could be sites where the EC binds to DNA and represses gene expression. Therefore, we hypothesized that warm temperatures inhibits EC function by reducing the localization of ELF3 to foci.

To test this, first we investigated whether warm temperature influenced the sub-nuclear localization of ELF3 in Arabidopsis. Using the previously described *35S::YFP:ELF3* (*elf3-4*) line (Herrero et al., 2012), we observed that a two-hour 27ºC temperature pulse resulted in fewer and smaller foci in hypocotyl nuclei (**Figure 5.1A, 5.1C, 5.1E**). ELF4 was found to be required for ELF3 to these localize to foci (Kolmos et al., 2011, Herrero et al., 2012, Anwer et al., 2014) and was also proposed to have a warm temperature specific function in the EC (Jung et al., 2020, Silva et al., 2020). Therefore, we investigated whether ELF4 regulated the sensitivity of ELF3 foci to warm temperature. We introgressed the *35S::YFP:ELF3* line into the *elf3-4/elf4-1* mutant. This line will be referred to as ELF4 (4-), while the original line will be called ELF3 (4+). The

localization of ELF3 (4-) to foci was impeded at 22ºC **(Figure 5.1B)** and this was further reduced by a 27ºC pulse **(Figure 5.1D-E)**. However, the relative change in the number of foci for ELF3 (4-) in response to the 27ºC pulse was similar to ELF3 (4+) **(Figure 5.1F)**. Together, warm temperatures suppress the localization of ELF3 to foci and ELF4 has a limited role within this.

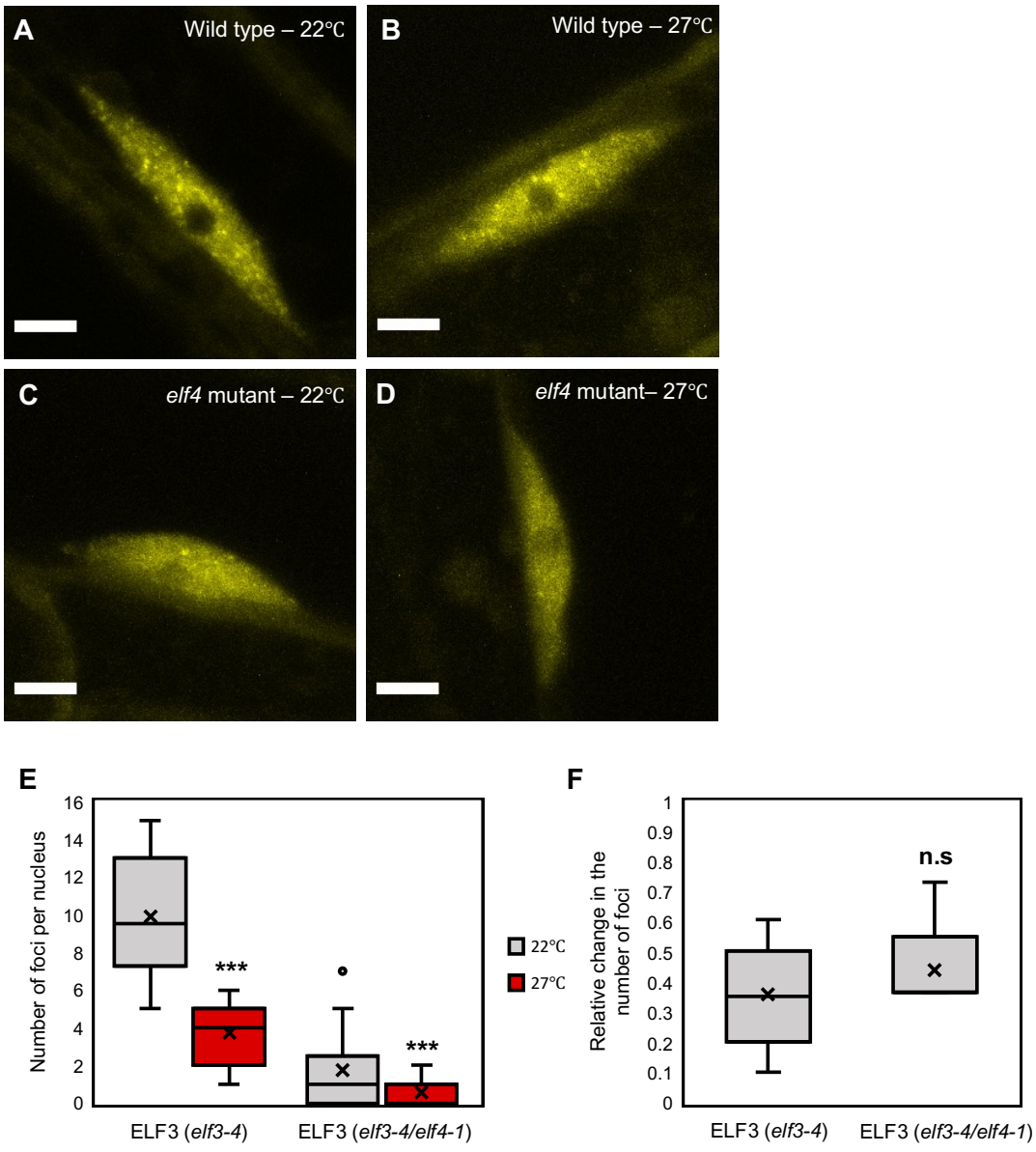

Figure 5.1 - Elevated temperature reduces the association of ELF3 to foci in hypocotyl nuclei

The localisation of ELF3 at dusk in hypocotyl nuclei of **(A-B)** *35S::YFP:ELF3 elf3-4* or **(C-D)** *35S::YFP:ELF3 elf3-4/elf4-1* plants. Images were taken at (**A, C**) 22ºC or **(B, D)** after a two-hour 27ºC pulse started at ZT6 (short-day 8/16 photoperiods). (**E**) Number of foci per nucleus under the respective treatment. (**F**) Relative change in the number of ELF3 foci following a temperature pulse in the *elf3-4* or *elf3-4/elf4-1* mutant. Data was made relative to the respective genotype at

Figure 5.1 (continued) - 22ºC. For *elf3-4*/*elf4-1*, nuclei with no focus were removed this from calculation. Images were collected on two occasions. Significance was determined by a T-test: n.s = no significance, *** = $p < 0.001$. Scale bars are 5 μm.

To understand if the response of ELF3 foci to temperature was tissue-dependent, we investigated the effect of a 27ºC pulse on foci formation in root nuclei. As in hypocotyl nuclei, a 27ºC pulse suppressed the localization of ELF3 (4+) to foci in root nuclei and these foci were smaller and less bright than at 22ºC **(Figure 5.2A-B)**. There was no significant change in the magnitude of effect caused by the 27ºC pulse between the tissue types, with ELF3 (4+) foci reduced by 62% and 60% in hypocotyl and root nuclei, respectively. Therefore, ELF3 foci do not have a tissue-dependent response to warm temperature.

As ELF4 protein moves from shoot to root tissue, and this movement is temperature sensitive (Chen et al., 2020), we examined the requirement of ELF4 in regulating the thermal responsiveness of ELF3 foci in root nuclei. As with ELF3 (4+), ELF3 (4-) localized to foci in root nuclei and these foci were larger and brighter than those in hypocotyl nuclei **(Figure 5.1C, 5.2C)**. The phenotypic effect of the *elf4-1* mutation on ELF3 foci abundance was weaker in root nuclei, with foci only reduced by 52% compared to an 81% reduction in hypocotyl nuclei at 22ºC. ELF3 (4-) foci in root nuclei were also reduced by a 27ºC temperature pulse **(Figure 5.2D-E)**. However, this effect was more variable and on average weaker than the response of ELF3 (4+) foci to the 27ºC pulse **(Figure 5.2F)**. As with ELF3 (4+), ELF3 (4-) foci appeared smaller and less bright after a 27ºC pulse in root nuclei **(Figure 5.2C-D)**. Combined, ELF4 does not have a critical role in buffering ELF3 foci against warming temperatures in either hypocotyl or root nuclei.

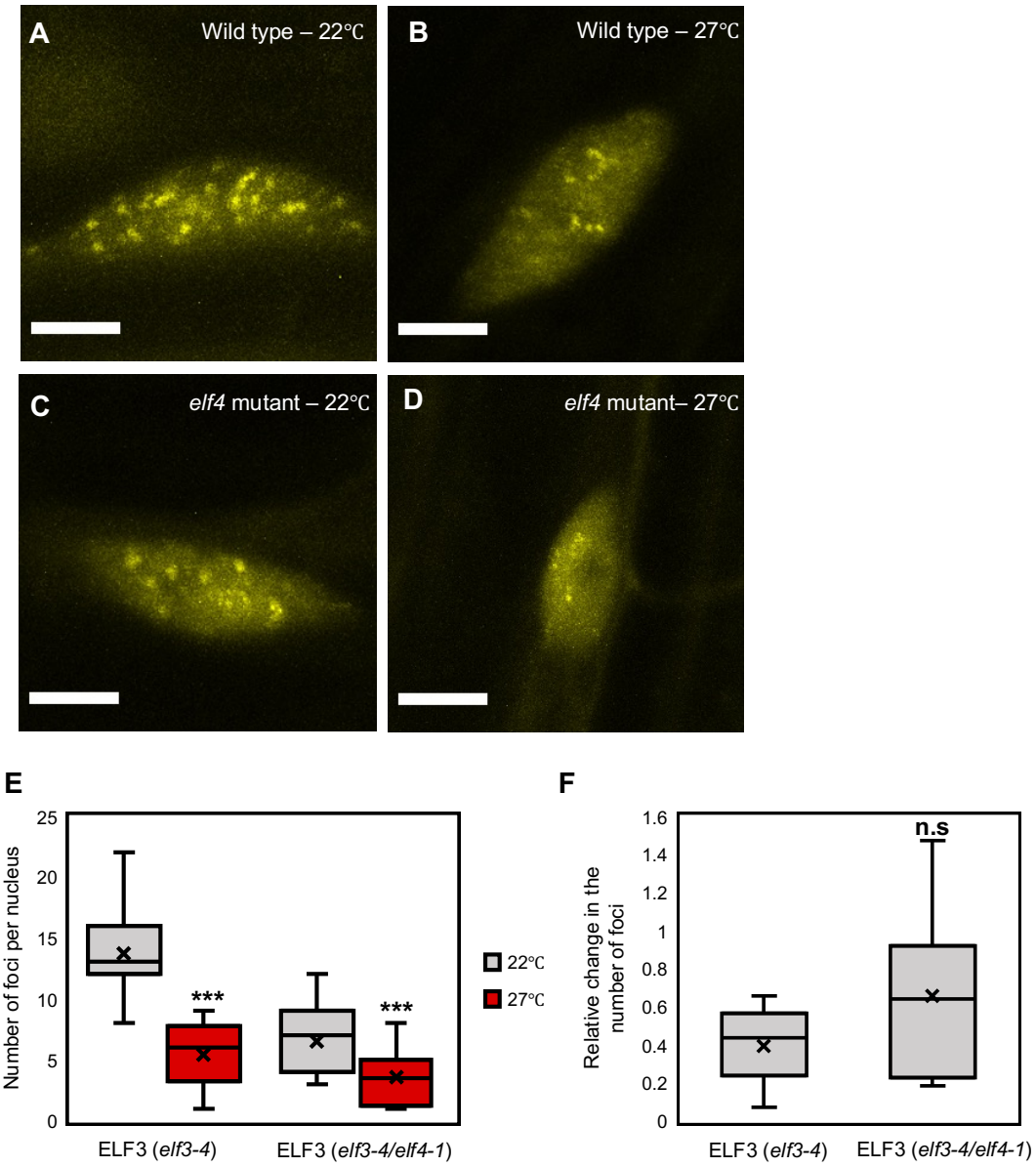

Figure 5.2 - A 27ºC pulse inhibits the association of ELF3 to foci in root nuclei

The localisation of ELF3 at dusk in root nuclei of **(A-B)** *35S::YFP:ELF3 elf3-4* or **(C-D)** *35S::YFP:ELF3 elf3-4/elf4-1*. Images were taken at (**A, C**) 22ºC or **(B, D)** after a two-hour 27ºC pulse started at ZT6 (short-day 8/16 photoperiods). (**E**) Number of foci per nucleus under the respective treatment. (**F**) Relative change in the number of ELF3 foci following a temperature pulse in the *elf3-4* or *elf3-4/elf4-1* background. Data was made relative to the respective genotype at 22ºC. Images were collected on two occasions. Significance was determined by an unpaired T-test: n.s = no significance, *** = $p < 0.001$. Scale bars are 5 μm.

The decrease in foci number following a 27ºC pulse could reflect changes in the nuclear accumulation of ELF3. To investigate this, we measured ELF3 (4+) and ELF3 (4-) nuclear signal at 22ºC and 27ºC in hypocotyl and root nuclei. As we have reported previously, ELF4 was required for the nuclear accumulation of ELF3 (**Figure 5.3**).

Regardless of the temperature, ELF3 (4-) had a lower nuclear accumulation than ELF3 (4+) in hypocotyl and root nuclei. The 27ºC pulse also strongly reduced the nuclear accumulation of ELF3 (4+) in hypocotyl nuclei **(Figure 5.3A)**. Furthermore, there was an additive effect of the 27ºC pulse and the *elf4-1* mutation on the nuclear accumulation of ELF3 in hypocotyl nuclei. A similar response to the 27ºC pulse was seen in root nuclei for both ELF3 (4+) and ELF3 (4-) **(Figure 5.3B)**. As with hypocotyl nuclei, the 27ºC pulse and the *elf4-1* mutation had an additive effect on ELF3 nuclear accumulation **(Figure 5.3B)**. The reduced nuclear accumulation of ELF3 at 27ºC is consistent with a recent report that ELF3 is degraded by BBX18 and XBAT31 at warm temperatures (Zhang et al., 2021).

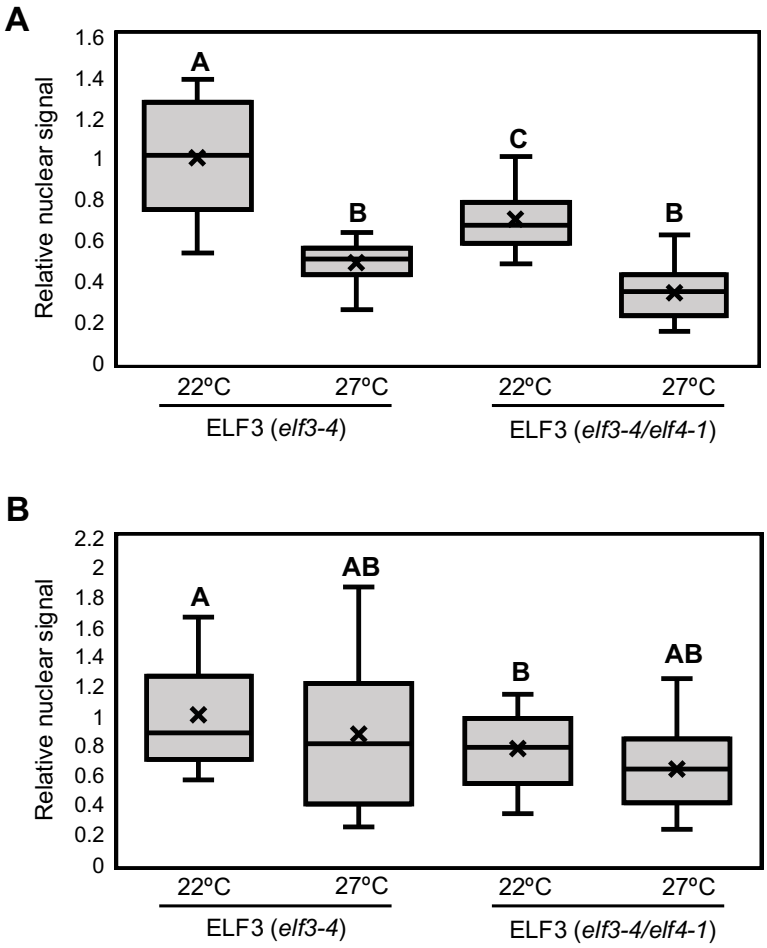

Figure 5.3 – Elevated temperature reduces the nuclear accumulation of ELF3

The relative nuclear signal of ELF3 in (**A**) hypocotyl or (**B**) root nuclei. Nuclear signal was quantified using the images collected for the foci counts of figure 5.1 and figure 5.2, respectively. The nuclear signal was made relative to the nuclear signal of ELF3 in the *elf3-4* background at

Figure 5.3 (Continued) - 22ºC for each respective tissue type. Images were collected on two separate occasions with a combined n of 12 or more images analyzed for each respective genotype and temperature treatment. Significance was calculated using a one-way ANOVA with a tukey HSD posthoc test. Different letters signify a significance of $p < 0.05$.

In summary, we have observed that the localization of ELF3 to foci is suppressed by warm temperature and ELF4 does not seem to regulate this process. Thus, ELF4 must stabilize the function of the EC at warm temperatures through a separate mechanism. As the localization of ELF3 to foci was associated with increased transcriptional activity of ELF3, a reduction in foci may contribute to the weaker EC function at warm temperatures that has been previously reported.

We also highlight a recent report that observed ELF3 localizing to sub-nuclear structures called speckles in response to warming. It is unclear why our results diverge from the results of earlier work (Jung et al., 2020). Jung *et al.,* (2020) used a native promoter of *ELF3*, while here a *35S* promoter was used to drive *ELF3* transcript abundance. We consider it unlikely that the use of a *35S* promoter has driven aberrant foci formation as previous work that used a native promoter of *ELF3* also observed foci at 22ºC (Anwer et al., 2014). Further differences in the genetic constructs between the two pieces of work include the source of the ELF3 sequence. Our *ELF3* sequence was cloned from the Arabidopsis accession Ws-2 (Herrero et al., 2012), while the *ELF3* sequence of Jung *et al.,* (2020) was cloned from Col-0. Ws-2 and Col-0 ELF3 sequences have differing poly-Q lengths, and the poly-Q stretch of ELF3 was reported to be part of the prion-like domain (Tajima et al., 2007, Undurraga et al., 2012, Jung et al., 2020). However, previous work found no role for the poly-Q domain in ELF3 temperature signaling (Press et al., 2016). Finally, it is possible that we are observing different sub-nuclear structures. ELF3 has been reported to localize to sub-nuclear structures with proteins that have different temporal transcript abundance or accumulation patterns (Yu et al., 2008, Herrero et al., 2012, Kaiserli et al., 2015, Huang et al., 2016). Our heat-pulse was applied at ZT6 (2-hours before dusk, see supplementary methods), while it is unclear when the heat-pulses were applied in the work of Jung et al., (2020). Therefore,

it is possible that the cellular response of ELF3 to temperature is dependent on when the heat pulse is applied due to different proteins interacting with ELF3.

Chapter 6 - General Discussion

6.1 Summary

At the beginning of this thesis, we had a poor understanding of how the activity of ELF3 was regulated. It was hypothesised that ELF4 and phyB competitively regulate ELF3 activity, but the mechanistic basis of this activity was unclear. Therefore, the aim of this thesis was to understand how ELF3 activity is regulated and how phyB and ELF4 contribute to this process. Here, I have found that ELF4 and phyB both regulate the cellular and sub-nuclear distribution of ELF3. The effect of phyB on ELF3 activity is complex, with both an inhibitory and positive effect, while ELF4 promotes both the nuclear and sub-nuclear localiation of ELF3. My results also suggest that other proteins function alongside ELF4 and phyB to control the spatio-temporal distribution of ELF3. Below, I contextualise the findings of my thesis and provide insights into the direction of future work.

6.2 Unravelling the complex role of phyB in regulating ELF3 activity

I have identified a complex mechanistic role for phyB in regulating the nuclear and sub-nuclear localisation of ELF3. In the absence of *phyB*, the nuclear and sub-nuclear localisation of ELF3 was severely reduced **(Figure 3.10-11)**. Furthermore, de-activating photoactivated phys at dusk with a FRL pulse also suppressed the nuclear accumulation of ELF3 **(Figure 3.9)**, while low intensity RL-pulses promoted the nuclear localisation of ELF3 **(Figure 3.7-8)**. Together, this suggests that RL promotes the nuclear and sub-nuclear localisation of ELF3.

My results also have highlighted an inhibitory effect of RL, however. A 10 $\mu mol/m^{-2}/s^{-1}$ RL-pulse reduced the sub-nuclear accumulation of ELF3 and this inhibitory effect was further increased by a 15 $\mu mol/m^{-2}/s^{-1}$ RL-pulse. A 25 $\mu mol/m^{-2}/s^{-1}$ RL-pulse also reduced the nuclear accumulation of ELF3, in addition to suppressing the localisation of ELF3 to foci **(Figure 3.1-2, 7-8)**. The repressive effect of RL on the nuclear accumulation of ELF3 was alleviated by removing the N-terminus of ELF3 **(Figure 3.5)**, the domain that mediates the ELF3-phyB interaction (Liu et al., 2001). Furthermore, the repressive effect of RL on the nuclear and sub-nuclear accumulation of ELF3 was also not observed

in the *phyB* mutant background. Instead, RL promoted the nuclear localisation of ELF3 in the absence of *phyB* **(Figure 3.10-11)**. Together, this suggests that RL can promote and repress the nuclear and sub-nuclear accumulation of ELF3.

The activity of ELF4 may help explain these contradictory effects. ELF4 promotes the nuclear and sub-nuclear localisation of ELF3 **(Figure 4.1-3, 5.1-3)** and the expression of *ELF4* is directly activated by RL in a phyB-dependent manner via the FAR3/FHY1 TFs (Siddiqui et al., 2016). This leads to a model where phyB directly represses the nuclear and sub-nuclear localisation of ELF3 via a physical interaction with the ELF3 N-terminus, while indirectly promoting the nuclear and sub-nuclear accumulation of ELF3 via activating *ELF4* expression at dusk **(Figure 6.1)**. This model can be tested by investigating the localisation of ELF3 in the *elf4/phyB* mutant background and determining whether the localisation of ELF3 remains responsive to RL in the absence of *phyB* and *elf4*.

These two separate roles of phyB in regulating ELF3 localisation would explain the results of earlier reports that suggested phyB can activate and repress ELF3 function (Kolmos et al., 2011, Herrero et al., 2012, Nieto et al., 2015, Ezer et al., 2017a). It was initially proposed that phyB represses the circadian function of ELF3 by physically interacting with the N-terminus of ELF3 (Kolmos et al., 2011, Herrero et al., 2012). However, subsequent analysis revealed that the targets of the EC were mis-expressed in the *phyABCDE* quintuple mutant background in the evening, but not the day (Ezer et al., 2017a). This led to the suggestion that phys promote EC activity. Both results are explainable by the proposed dual function of phyB, whereby phyB physically represses ELF3, while indirectly activating ELF3 via ELF4. In the absence of *phy* function in the *phyABCDE* background, it would be expected that the expression of *ELF4* does not peak at dusk, inhibiting the nuclear localisation of ELF3 and subsequent formation of the EC. Subsequently, the expression of EC targets would be elevated in the *phyABCDE* background as observed in Ezer *et al.*, (2017a).

In conclusion, I propose that phyB directly represses ELF3 activity, while indirectly activating ELF3 in the e vening by promoting the expression of ELF4.

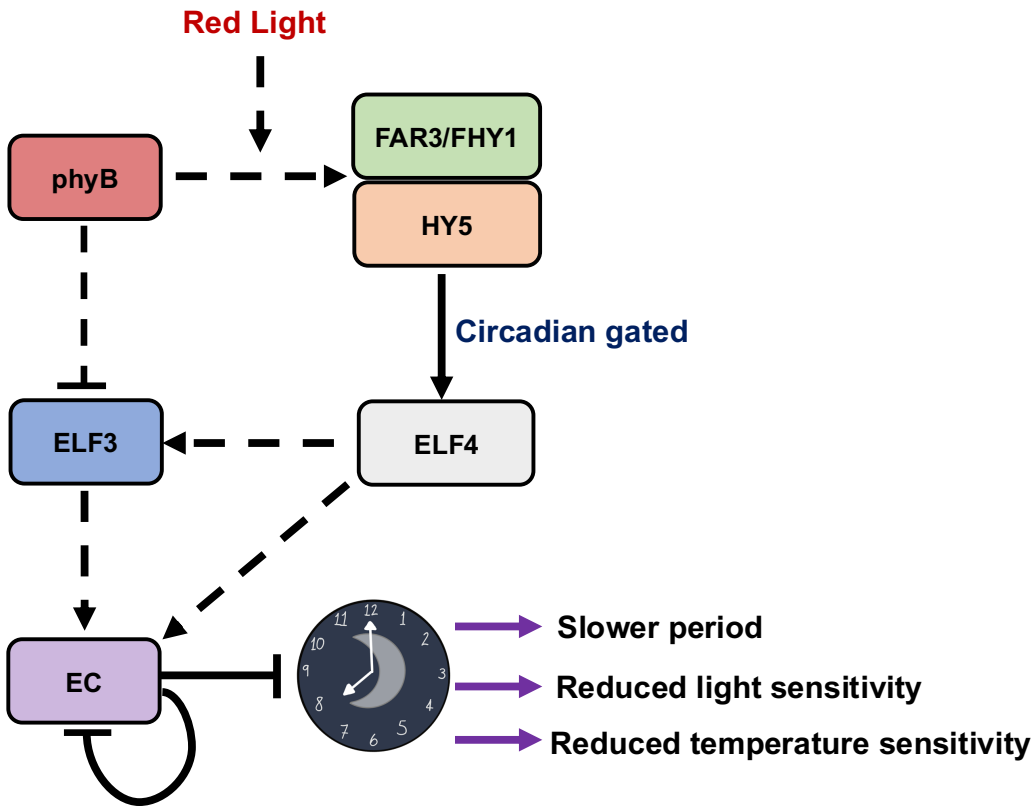

Figure 6.1 – Proposed dual model of phyB activity in regulating ELF3

phyB directly represses the activity of ELF3 by physically interacting with ELF3. Separately, phyB indirectly promotes ELF3 activity by facilitating the activity of the FAR3/FHY1 and HY5 transcription factors in a red-light dependent manner. FAR3/FHY1 and HY5 activate the expression of *ELF4* at dusk. This process is controlled by the circadian clock through an unclear mechanism. ELF4 subsequently activates ELF3 function by promoting the nuclear and sub-nuclear localisation of ELF3 and separately by promoting the assembly of the EC onto chromatin. The EC then represses the expression of genes within circadian clock, leading to an oscillator running in a slower state and one that is less sensitive to light and temperature. The EC also represses its own expression, completing the feedback loop. Full arrows indicate a transcriptional effect, dotted arrows indicate a post-translational effect.

6.3 A cellular tug-of-war to control ELF3 activity

What remains unanswered from my thesis is where does phyB and ELF4 exert their activity on ELF3, does this occur in the cytoplasm or nucleus?

ELF3 was initially proposed to localise to the nucleus intrinsically through an NLS motif within the C-terminus of the Arabidopsis ELF3 protein (Liu et al., 2001, Herrero et

al., 2012). However, multiple lines of evidence suggest that ELF3 may be shuttled to the nucleus via interactions with other proteins. Firstly, the reported NLS of ELF3 is only present in the Brassica ELF3 sequences. Though I identified a monocot specific NLS sequence, all other vascular ELF3 protein sequences I analysed had no identifiable NLS motif **(Appendix 4, Figure 1A-B)**. Furthermore, previous work found that the NM and M domains of Arabidopsis ELF3 were capable of localising to the nucleus in the absence of an NLS signal in both tobacco and Arabidopsis nuclei (Herrero et al., 2012). Therefore, NLS-independent mechanisms must also facilitate the localisation of ELF3 to the nucleus.

Here, I propose that ELF4 actively shuttles ELF3 from the cytoplasm to the nucleus at dusk. At ZT7 (one hour before dusk), the nuclear signal of ELF3 in the WT and *elf4* background was similar. However, at ZT8 the nuclear signal of ELF3 (4+) increased, while the nuclear signal of ELF3 (4-) remained unchanged from ZT7 **(Figure 4.1)**. The peak nuclear signal of ELF3 (4-) was then delayed until ~ZT16, four to eight hours after the peak in ELF3 (4+) nuclear signal. This indicates that although ELF3 can localise to the nucleus independently of ELF4, ELF4 seemingly increases the speed at which ELF3 localises to the nucleus. Supporting a role for ELF4 in promoting the nuclear accumulation of ELF3, the nuclear pool of the ELF3 middle region (ELF3M) was increased when co-expressed alongside ELF4 (Herrero et al., 2012). Together, these results suggst that ELF4 directly shuttles ELF3 into the nucleus at dusk to rapidly form the formation of the EC. Once in the nucleus, ELF4 may also promote the localisation of ELF3 to sub-nuclear structures **(Figure 6.2)**. The importance of this is discussed in section 6.5.

It is less clear where phyB regulates ELF3 activity. Although the activity of phyB is typically associated with the translocation of phyB to the nucleus in response to light, not all of phyB's, and other phys', activity can be explained by the localisation of phys to the nucleus (Rösler et al., 2010). Therefore, it has been proposed that phys have nuclear and cytoplasmic functions. Similarly, phyB may have nuclear and cytoplasmic functions in circadian signalling. Analysis of a constitutitvely active allele of *phyB* (termed YHB)

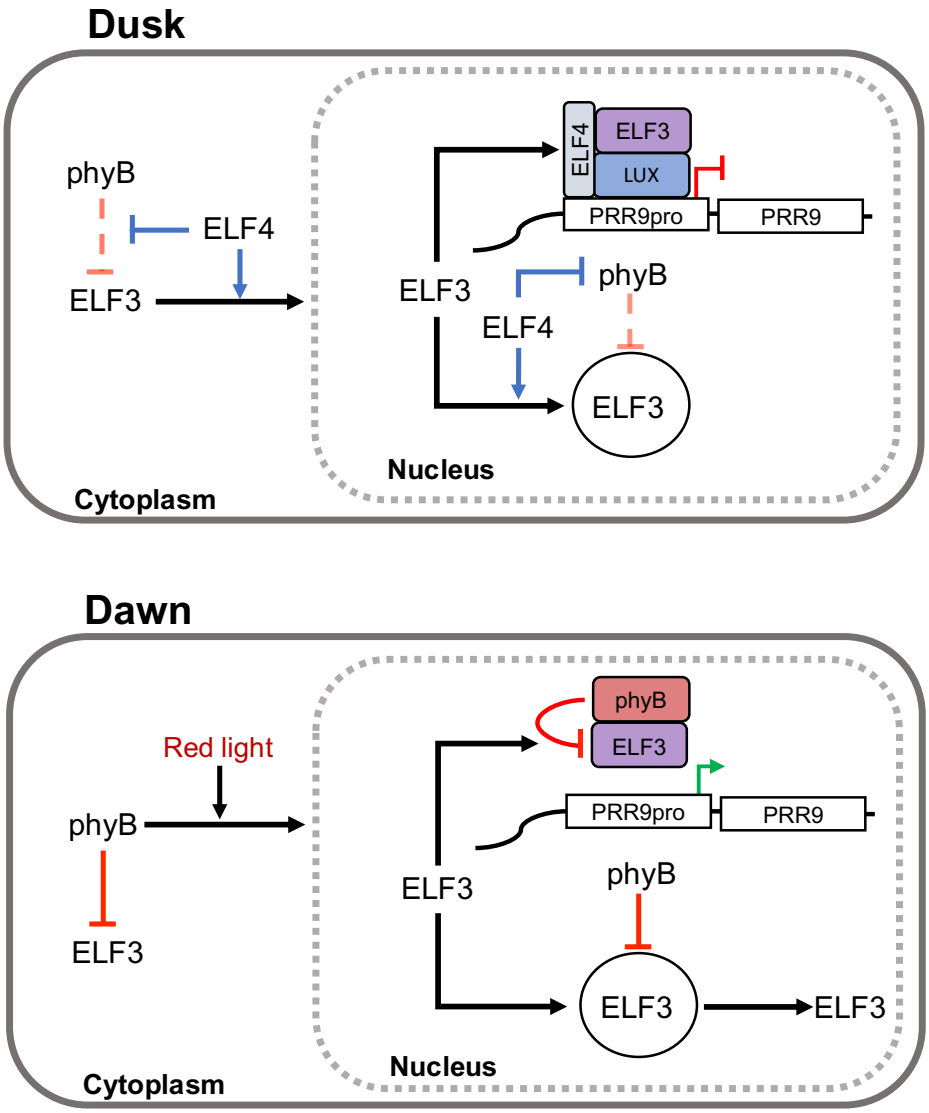

Figure 6.2 - A cellular tug-of-war between phyB and ELF4 in controlling ELF3 activity

A cellular model of the hypothesised tug-of-war between ELF4 and phyB. At dusk (top panel), the accumulation of ELF4 facilitates the localisation of ELF3 to the nucleus, potentially by inhibiting the sequestration of ELF3 in the cytoplasm by phyB. Once in the nucleus, ELF4 assembles with ELF3 and LUX on the promoter of EC targets, here the *PRR9* promoter, to repress gene expression. Separately, ELF4 promotes the localisation of ELF3 to foci, potentially by inhibiting the repressive activity of phyB. Conversely, from just before dawn (bottom panel) phyB sequesters ELF3 in the cytoplasm. In the nucleus phyB displaces ELF3 from foci and sequesters ELF3 from binding to chromatin, alleviating the repressive effect of ELF3 on gene expression. This subsequently re-sensitise the promoter of morning phased genes such as *PRR9*, illustrated by the green arrow.

that was mutated so that it could no longer localise to the nucleus, revealed that this mutated *YHB* allele failed to accelerate the circadian period and amplify circadian rhythms in the dark unlike the WT *YHB* allele (Jones et al., 2015). However, this mutated *YHB* allele was still capable of advancing the phase of *PRR9* expression, suggesting that cytoplasmic localised phyB may have some circadian function (Jones et al., 2015).

PRR9 is a direct target of ELF3/EC (Herrero et al., 2012) and ELF3 can interact with the Pr isoform of phyB that is localised to the cytoplasm (Liu et al., 2001, Yeom et al., 2014). Therefore, phyB may sequester ELF3 in the cytoplasm to inhibit ELF3 from localising to the nucleus and subsequently forming the EC and repressing the expression of *PRR9*. The accumulation of ELF4 at dusk would alleviate the repressive effect of phyB on ELF3, potentially by disturbing the phyB-ELF3 interaction **(Figure 6.2)**. Subsequently, ELF4 would shuttle ELF3 to the nucleus, thereby allowing the formation of the EC and the repression of *PRR9* and other EC-targets.

A repressive effect of phyB on ELF3 exclusively in the cytoplasm cannot sufficiently explain all of the effects that RL has on the localisation of ELF3 that I have observed here, however. A 10 $\mu mol/m^{-2}/s^{-1}$ and 15 $\mu mol/m^{-2}/s^{-1}$ pulse of RL was able to suppress the sub-nuclear accumulation of ELF3 but had no effect on the nuclear pool of ELF3 **(Figure 3.7-8)**. This suggests that nuclear localised phyB must also disrupt foci localised ELF3 or otherwise inhibit the localisation of ELF3 to foci, as well regulating the nuclear/cytoplasmic distribution of ELF3. The role of foci in facilitating ELF3 activity continues to remain enigmatic. Therefore, it is unclear exactly what effect phyB-dependent inhibition of ELF3 to foci would have on ELF3 activity.

A final site of the ELF4-phyB competition in controlling ELF3 activity may be at the gene promoter. The binding of phyB to DNA was found to overlap with binding sites of the EC, including at the *PRR9* promoter (Ezer et al., 2017a). Though the significance of the overlap between phyB and ELF3 on chromatin has yet to be tested, ELF4 was shown to be essential for the EC to assembly onto DNA *in vitro* (Silva et al., 2020). Therefore, phyB and ELF4 may competitively control the assembly of ELF3 onto chromatin, thereby controlling the repressive activity of the EC. Here, ELF3/EC would

assemble onto chromatin at dusk and in the early evening when ELF4 has maximal protein accumulation. The assembly of the EC to DNA would subsequently lead to the recruitment of chromatin remodelling enzymes to repress gene expression (Lee et al., 2019b, Park et al., 2019, Tong et al., 2020). Conversely at dawn and in the early morning when phyB accumulates in the nucleus in response to light, phyB would disrupt the association of ELF3 from chromatin **(Figure 6.2)**. This in turn would re-sensitise the circadian clock to light and temperature signals that are inhibited by ELF3/EC repressive activity during the evening (Covington et al., 2001, Mizuno et al., 2014, Zhu et al., 2020).

6.4 Testing the cellular tug-of-war hypothesis

To further investigate the relationship between ELF4 and phyB in controlling where ELF3 is in the cell and the potential antagonism between ELF4 and phyB, it would be insightful to image ELF3, ELF4 and phyB across the day-night cycle. To do this, ELF3 and phyB could be placed under the control of their own respective promoter and tagged with a FRET-compatible pairing (*e.g.,* YFP and CFP). ELF4 would then be placed under the control of an inducible estradiol promoter with an RFP-derivative tag. The localisation of ELF3 and phyB can then be imaged across the day with differing levels of ELF4 induction. This would provide insights into where and when ELF3 and phyB interact in the cell and how the induction of *ELF4* expression modulates the ELF3-phyB interaction. The system could also be inverted so that the expression of phyB is made inducible and ELF4 is placed under its own native promoter.

It will also be important to understand how the promoter occupancy of ELF3 is controlled by phyB. Directly comparing the promoter occupancy of ELF3 in a WT or mutant *phyB* background may generate complex results due to the proposed dual effects of phyB on promoting and repressing ELF3 activity **(Figure 6.1)**. Instead, the chromatin occupancy of full-length ELF3 (ELF3F) and the ELF3MC construct could be compared via ChIP-PCR in the *elf3-4* background. ELF3MC rescues the *elf3-4* arrhythmic phenotype, indicating that this construct is fully functional within the circadian clock (Herrero et al., 2012). However, ELF3MC cannot interact with phyB, phenomimicking a

phyB mutant in regard to the direct phyB-ELF3 interaction, while still maintaining the indirect connection between phyB and ELF3 through ELF4. If phyB does disrupt the localisation of ELF3 to DNA in response to light, it would be expected that ELF3MC would have increased chromatin occupancy at the *PRR9* promoter compared to ELF3F at dawn or in response to prolonged light exposure.

6.5 The role of foci in regulating ELF3 activity

Though ELF3 has been shown to associate to sub-nuclear structures for more than 10 years, it has remained largely unknown what functions these structures have in facilitating ELF3 activity. Originally, ELF3 was found to co-localise with COP1 and GI in sub-nuclear structures and this co-localisation was proposed to lead to the degradation of GI and ELF3 (Yu et al., 2008). ELF3 foci were also proposed to be sites where the EC may assemble to repress gene expression (Herrero et al., 2012, Anwer et al., 2014). However, the data I have generated in this thesis and the results that other research groups have published in the last few years (Ezer et al., 2017a) would suggest that foci are not sites of ELF3/EC transcriptional activity.

In chapter 4, I observed that the peak accumulation of ELF3 occurred at ZT12 under SD (8/16 photoperiods) **(Figure 4.1-3)**. The association of ELF3 to DNA is so far exclusively dependent on the transcription factor LUX and the LUX-homolog BOA (Chow et al., 2012). The binding of LUX to DNA shows a strong time-of-day dependency, with the association of LUX to DNA much weaker at ZT12 than at ZT8 or ZT10 under SD (Ezer et al., 2017a). This association pattern of LUX strongly follows the reported protein accumulation of LUX, which shows a strong decline between ZT8 and ZT12 (Nusinow et al., 2011). Therefore, the peak association of ELF3 to foci does not correlate with the accumulation and subsequent binding of LUX to DNA. Accordingly, I found that the expression of *TOC1, LUX*, *GI* and *PRR9* were all unchanged in the *ELF3ox* compared to WT at ZT12 **(Figure 4.1-3)**. In comparison, *ELF3ox* repressed *TOC1, LUX* and *GI* transcript abundance at ZT10 relative to WT **(Figure 3.12)**, consistent with the DNA-binding activity of LUX reported in Ezer *et al.,* (2017). Comparing foci accumulation of

ELF3 at ZT10 and ZT12 revealed that ELF3 forms comparatively fewer foci at ZT10 than at ZT12 (ZT12 average = 17.7 [± 1], ZT10 average = 12.5 [± 0.43]). Thus, the maximal accumulation of ELF3 in foci is not synchronous with the accumulation or activity of LUX, or the repressive activity of ELF3.

Further support for a non-transcriptional function of ELF3 foci was observed in chapter 3. A RL-pulse strongly reduced the association of ELF3 to foci at ZT10 **(Figure 3.2, 3.8)**. However, there was no clear inhibitory effect of a RL-pulse on ELF3's ability to repress gene expression. In fact, a pulse of RL increased the repressive effect of *ELF3ox* on *PRR9* transcript abundance **(Figure 3.13)**. Furthermore, I observed that ELF3 (B-) exerted the same repressive effect on *LUX*, *PRR9* and *TOC1* as ELF3 (B+) even though the association of ELF3 (B-) to foci was strongly impaired in the dark **(Figure 3.13)**. ELF3 (B-) also fully rescued the early flowering phenotype of the *elf3-4/phyB*-10 double mutant under long-day and short-day photoperiods and even exerted a greater repressive effect on flowering time under LD than ELF3 (B+) **(Figure 3.15)**. Combined, it is unlikely that foci are sites where ELF3/EC repress gene expression.

Instead, ELF3 foci could function indirectly as a storage site for ELF3 protein. ELF3 protein is less stable in the dark and shows a strong decline across the subjective evening (Liu et al., 2001). The degradation of ELF3 in the dark is mediated by interactions with the E3-ligase COP1 (Yu et al., 2008). ELF3 interacts with COP1 directly via the N-terminus of ELF3 and indirectly via interactions with the adaptor protein B-BOX19 (BBX19) (Wang et al., 2015a). Other BBX proteins have been described to have a similar function under warm temperature conditions (Ding et al., 2018). As ELF3 is required to function in the dark, mechanisms must exist to protect ELF3 from degradation by BBX/COP1.

The localisation of phyB to nuclear bodies was hypothesised to stabilise phyB against dark and thermal reversion (Van Buskirk et al., 2012). My results suggest that ELF3 foci may provide a similar protective role for ELF3. Warm temperature suppressed the localisation of ELF3 to foci and accordingly the nuclear signal of ELF3 was strongly reduced **(Figure 5.1-3)** Furthermore, I observed that a pulse of BL increased the total

signal of ELF3, but this increase in total signal was dependent on BL promoting the localisation of ELF3 to foci **(Figure 3.3)**. When the effect of BL on promoting the localisation of ELF3 to foci was suppressed by combining the BL-pulse with a RL-pulse, there was no longer an increase in the total signal of ELF3 **(Figure 6.3)**. There was also no effect of BL on increasing the total signal of ELF3MC, as would be expected as ELF3MC cannot localise to foci **(Figure 3.5)**. Separately, the total signal of ELF3 (4-) strongly declined towards the end of the evening before recovering at dawn, while the total signal of ELF3 (4+) remained relatively constant across the evening **(Figure 4.1)**. A similar observation was made for the protein accumulation of ELF3-Sha which displayed a strong decline in late subjective evening in the dark but not the light (Anwer et al., 2014). Both ELF3 (4-) and ELF3-Sha have impaired localisation to foci due to the absence or decreased interaction with ELF4, respectively. Therefore, the reduced accumulation of ELF3 (4-) and ELF3-Sha towards the end of the evening may be caused by ELF3 localising to fewer foci and being more rapidly degraded by interactions with BBX proteins and/or COP1.

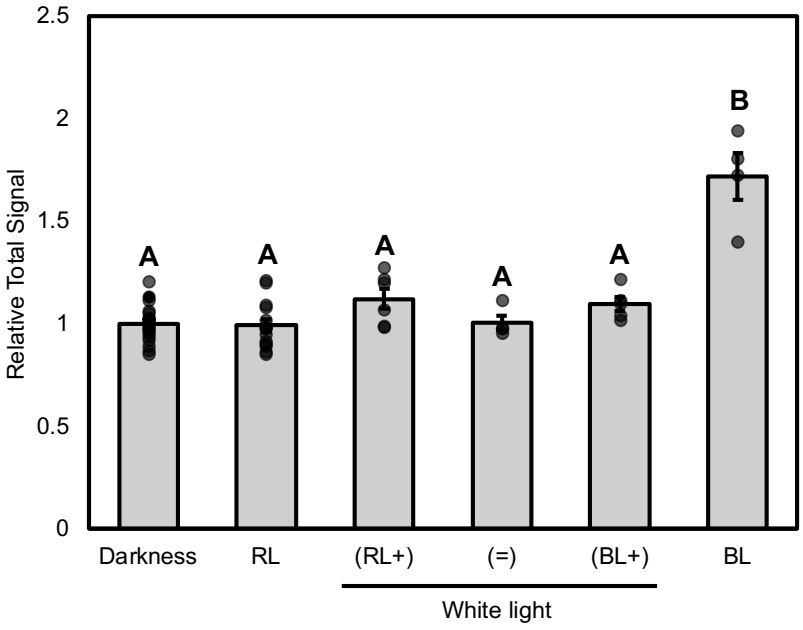

Figure 6.3 – The total signal of ELF3 under different light treatments at ZT10

The total signal of *35S::YFP:ELF3* (*elf3-4*) at ZT10 in the dark or under different intensities of monochromatic red light (RL), blue light (BL) or different spectral combinations of RL and BL (termed white light). RL+ indicates a greater proportion of RL compared to BL in the WL-pulse *etc*., See chapter 2 table 2.8 for exact light ratios. Pulses were started at ZT7 and applied for

Figure 6.3 (continued) - three-hours. Imaging was repeated on two occasions with the presented data a combination of these individual repeats. Significance was determined by a one-way ANOVA with a tukey HSD posthoc test. Different letters signify a significant difference of $p < 0.001$.

6.6 Focusing in on ELF3 protein-protein interactions in the nucleus

To better understand the function of foci in ELF3 activity, it will be necessary to determine what proteins localise with ELF3 in foci. So far, we have a relatively poor understanding of what proteins co-localise in foci. ELF3 was first shown to localise with GI and COP1 in sub-nuclear structures (Yu et al., 2008). Alongside, GI and COP1, ELF4 was also shown to co-localise with ELF3 in tobacco mesophyll nuclei (Herrero et al., 2012). Furthermore, ELF4 co-localised with GI in sub-nuclear structures in tobacco mesophyll nuclei cell (Kim et al., 2013b). However, in Arabidopsis hypocotyl nuclei ELF4 only displayed a diffuse nuclear localisation (Herrero et al., 2012).

Why ELF4 has a different sub-nuclear localisation in tobacco mesophyll and Arabidopsis hypocotyl nuclei has remained unresolved. To further investigate this, I analysed the localisation of a new ELF4 construct that was tagged at the C-terminus with a CFP fluorochrome **(6.4A-B)**. I then compared the localisation of this construct to the localisation of the originally described YFP:ELF4 construct. As reported previously, I found that YFP:ELF4 only had a diffuse nuclear localisation (Herrero et al., 2012) (**Figure 6.4C, 6.4E**). In comparison, in two independent transgenic I observed that ELF4:CFP localised to foci in hypocotyl and root nuclei **(Figure 6.4D, 6.4F-H)**. These ELF4:CFP foci also showed *diel* oscillations (data not shown), suggesting that these foci are biologically active. Further investigations are needed to understand why ELF4:CFP but not YFP:ELF4 can localise to foci in Arabidopsis nuclei.

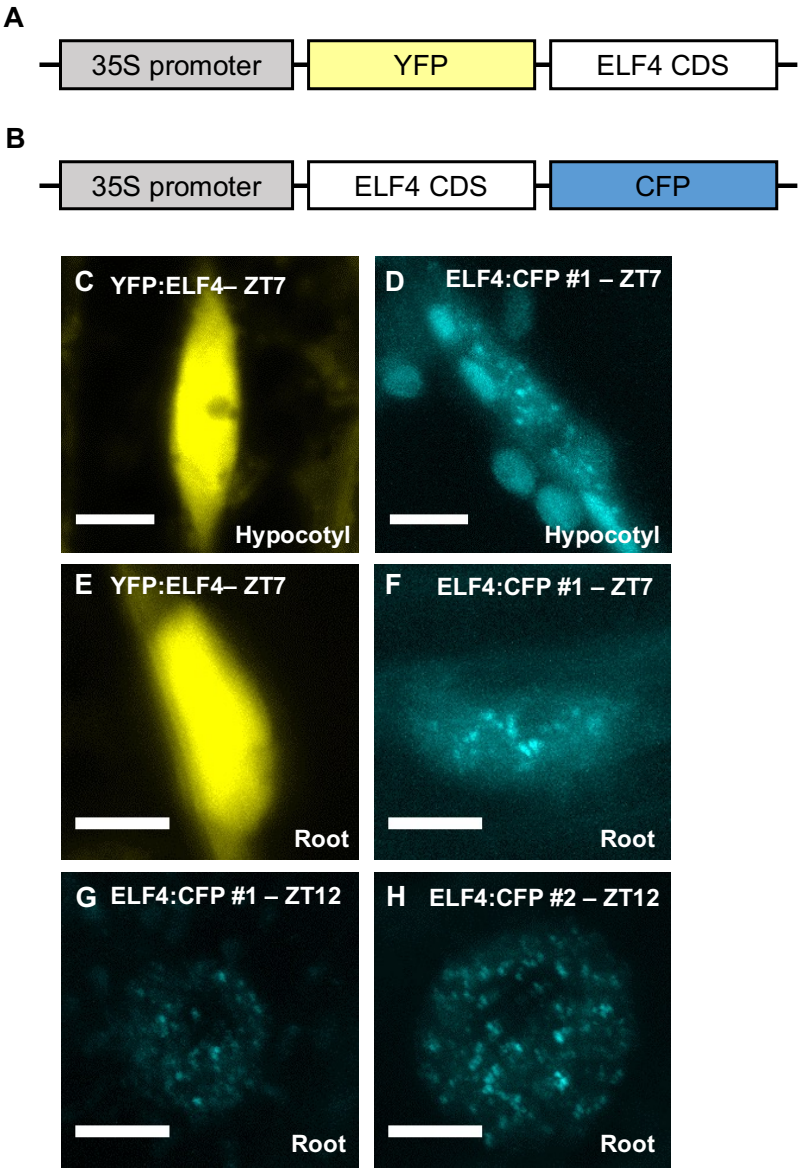

Figure 6.4 - ELF4:CFP but not ELF4:YFP localises to foci in Arabidopsis nuclei

Schematic of either **(A)** the original *YFP:ELF4* construct described in Herrero *et al*., 2012 or **(B)** the new ELF4:CFP construct tested here. CDS = coding domain sequence. The cellular localisation of (**C, E**) *35S::YFP:ELF4* or (**D, F-H**) *35S::ELF4:CFP* in Arabidopsis was imaged in (**C-D**) hypocotyl or (**E-H**) root nuclei at various timepoints in a short-day (8/16) photoperiod. The *35S::YFP:ELF4* construct was first described in Herrero et al., 2012. Scale bars are 5 μm.

Other proteins that interact with ELF3 have been separately described to localise to nuclear bodies. The best characterised of these is phyB, which localises to sub-nuclear structures called photobodies in response to RL (Chen et al., 2003). Comparing the different responses of ELF3 foci and phyB photobodies to RL would suggest that phyB and ELF3 localise to different sub-nuclear structures. For example, a 10 µmol/m^{-}

$^{2}/s^{-1}$ pulse of RL promotes the localisation of phyB to large photobodies (Chen et al., 2003), while I observed that a 10 10 µmol/$m^{-2}/s^{-1}$of RL suppressed the localisation of ELF3 to foci **(Figure 3.8)**. Thus, it would seem unlikely that ELF3 and phyB can co-localise together in sub-nuclear structures. However, work by Kaiserli *et al.,* (2015) observed that ELF3 co-localises with the TF TZP to nuclear bodies in tobacco mesophyll cells (Kaiserli et al., 2015). The localisation of TZP to these sub-nuclear structures is dependent on RL and phyB was observed to have an essential role in facilitating the localisation of TZP to these sub-nuclear structures (Kaiserli et al., 2015). Furthermore, phyB co-localised with TZP within these structures, suggesting it is possible that ELF3 and phyB co-localises together with TZP in light-dependent nuclear bodies. The functional importance of this co-localisation is unknown.

In conclusion, ELF3 may localise to foci with multiple proteins creating complexity in ascribing exclusively one function to these sub-nuclear structures **(Figure 6.5)**. By determining where and when proteins localise with ELF3 in the cell, the importance of these nuclear bodies in facilitating ELF3 activity can be better understood.

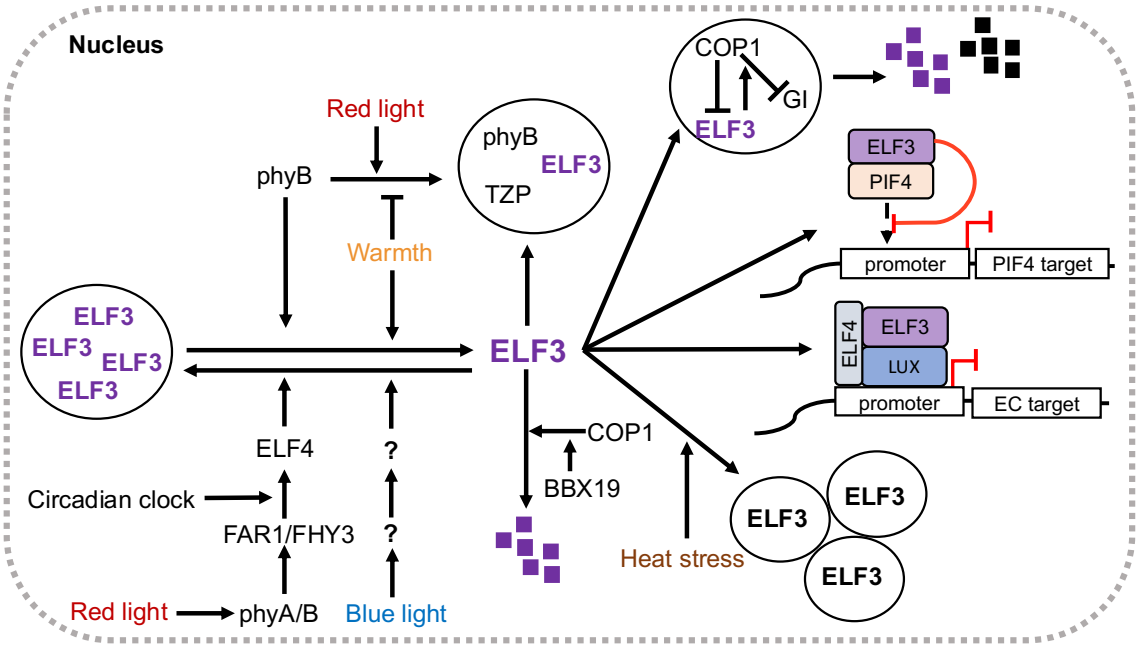

Figure 6.5 – Proposed nuclear and sub-nuclear dynamics of ELF3

A proposed model of ELF3 interactions and compartments within the nucleus. Nuclear localised ELF3 is either localised freely in the nucleoplasm or localised to sub-nuclear structures. In the

Figure 6.5 (continued) - nucleoplasm, COP1 and BBX19 promotes the degradation of ELF3. ELF4 and blue light independently inhibit this process by promoting the localisation of ELF3 to foci, stabilising ELF3. *ELF4* expression is promoted by the FAR1/FHY3 and HY5 (not shown) transcription factors in a signalling pathway, with phyB and possibly phyA upstream of FAR1/FHY3 and HY5. The activity of FAR1/FHY3 is also controlled by the circadian clock, gating the expression of *ELF4* and subsequently the formation of ELF3 foci to dusk. The removal of ELF3 from these structures is promoted directly by phyB and warmth. Nucleoplasmic ELF3 can also localise to nuclear structures with GI and COP1, leading to the degradation of both GI and ELF3. ELF3 may also localise with TZP and phyB in nuclear bodies from the early morning. Separately, heat stress promotes the reversible condenstation of ELF3 into sub-nuclear structures called speckles (based on the work of Jung et al., 2020). Finally, the formation of the EC and subsequent repression of gene expression, and the sequestration of PIF4 from binding to chromatin by ELF3 may occur diffusely in the nucleoplasm. I also highlight that many of the proteins that interact with ELF3 in the nucleus could also interact with ELF3 in the cytoplasm. The potential effects of these cytoplasmic interactions are not considered in this model.

6.7 Towards a structural understanding of ELF3 foci formation

Alongside developing our understanding of what proteins localise with ELF3 in sub-nuclear structures, experimental approaches will need to be designed so that the function of these structures can be investigated. Of all the approaches I tested here (light, temperature and genetic manipulation), only a 10 $\mu mol/m^{-2}/s^{-1}$and 15 $\mu mol/m^{-2}/s^{-1}$ of RL-pulse reduced the sub-nuclear localisation of ELF3 without causing a similar reduction in the nuclear pool of ELF3. However, if ELF3 can localise to nuclear structures with phyB, utilising RL-pulses to suppress the localisation of ELF3 to sub-nuclear structures may cause experimental artefacts. Instead, it is important that we understand the intrinsic mechanisms that facilitates the localisation of ELF3 to foci.

Of the domains of ELF3 (N, M and C), only ELF3-C localises to foci in the nucleus (Herrero et al., 2012). Therefore, the protein sequence responsible for the localisation of ELF3 to foci is likely within the C-terminus of the ELF3 protein. ELF3 does not have defined protein domains, instead it has stretches of conserved residues interspersed within long regions of low complexity. Within the C-terminus (defined as residue 485-695 by Herrero *et al.,* 2012), there is one stretch of residues towards the C-terminal (amino acid 661-687 in Arabidopsis) that was conserved amongst all embryophyte (land plants)

ELF3 sequences I analysed (data not shown). Therefore, this stretch of conserved residues is a promising target to mutate and determine whether this stretch of conserved sequences facilitates the localisation of ELF3 to foci.

It will also be of interest to determine whether or not this mutated ELF3 protein is still capable of dimerising. The proposed dimerization domain of ELF3 is within the C-terminus (Liu et al., 2001). Protein dimerization has been previously shown to be critical for the localisation of phyB to sub-nuclear bodies (Qiu et al., 2017) and other proteins in plants and animals (Odaka et al., 2000, Wang et al., 2017). Therefore, the dimerization domain of ELF3 may contribute to the localisation of ELF3 in sub-nuclear compartments.

6.8 New photoreceptor signalling pathways to control ELF3 activity

Light signalling has been directly connected to ELF3 via the interaction between the ELF3-N terminus and phyB (Liu et al., 2001). However, my results suggest that other RL photoreceptors must also signal to ELF3. In the absence of *phyB*, the cellular localisation of ELF3 remained responsive to RL but had the opposite effect compared to seedlings with a WT allele of *phyB* **(Figure 3.1-2, 3.10-11)**. As discussed above, it is likely that a RL-signalling pathway that activates *ELF4* expression is mediating these RL phyB-independent effects.

How RL activates *ELF4* expression in the absence of *phyB* is unclear. In Ws-2 (the Arabidopsis accession used in this work), the *phyD* allele is naturally mutated (Aukerman et al., 1997). Hence, only phyA, phyC and phyE can transmit RL signals to ELF3 in the Ws-2 background. The functional activity of phys is dependent on their dimerization (Klose et al., 2015). phyC and phyE are proposed to not form homodimers *in vivo* and instead exclusively heterodimerise with phyB or phyD (Sharrock and Clack, 2004, Clack et al., 2009). Therefore, is unlikely that phyC or phyE have functional activity in the absence of *phyB* or *phyD*.

Instead, it is more likely that phyA is transmitting RL signals to ELF3 in the *phyB* mutant background. phyA is active under RL, although less stable, and works redundantly with phyB in RL entrainment of the circadian clock (Devlin and Kay, 2000).

phyA can also form functional homodimers, unlike phyC or phyE. To test the role of phyA in transmitting RL signals to ELF3, it will be necessary to image the localisation of ELF3 in response to a RL-pulse in the *phyA/phyB* background. If phyA is transmitting RL signals to ELF3 redundantly with phyB, the localisation of ELF3 should be unresponsive to RL in the *phyA/B* background.

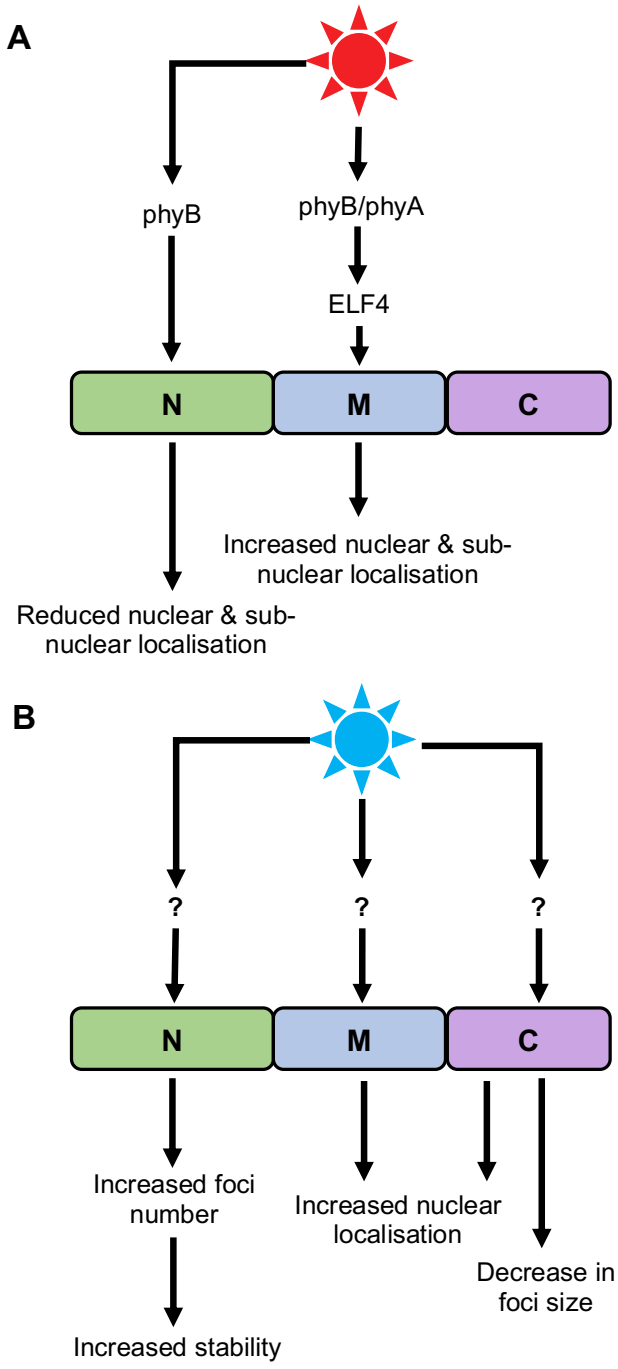

Figure 6.6 – Domain-dependent effect of red and blue light signalling pathways in controlling ELF3 activity

Figure 6.6 (continued) - (A) Red light signals to ELF3 via the N-terminus of ELF3 which mediates the phyB-ELF3 interaction. This interaction subsequently supresses the nuclear and sub-nuclear accumulation of ELF3. Separately, phyB and potentially phyA indirectly transmit RL signals to ELF3 via ELF4. ELF4 promotes the nuclear and sub-nuclear accumulation of ELF3 through interactions with the middle domain of ELF3. **(B)** Blue light (BL) likely controls the cellular and sub-nuclear distribution of ELF3 via all three domains of ELF3. The BL receptors and proteins downstream of these BL receptors are, however, yet to be determined.

It is unclear how BL signals control the localisation of ELF3. No BL-receptor was identified in a mass-spectrometry screen of proteins that interact with ELF3 (Huang et al., 2016). Therefore, it is more likely that BL regulates ELF3 indirectly via other protein that interacts with ELF3. As the response of ELF3 to BL was dependent on the domain of ELF3 analysed **(Figure 3.3, Figure 3.5, Figure 3.6)**, it is likely that multiple proteins are transmitting BL signals to ELF3 **(Figure 6.6B)**. The expression of *ELF4* was previously found to be promoted by BL (Hajdu et al., 2018). However, I found that BL still promoted the localisation of ELF3 to foci in the absence of *elf4* **(Figure 4.7)**. Furthermore, preliminary work revealed that BL also promoted the nuclear accumulation of ELF3 in the *elf4* background **(Figure 6.7A-B)**. Therefore, other BL-responsive proteins must be capable of promoting the nuclear localisation of ELF3 independently of ELF4.

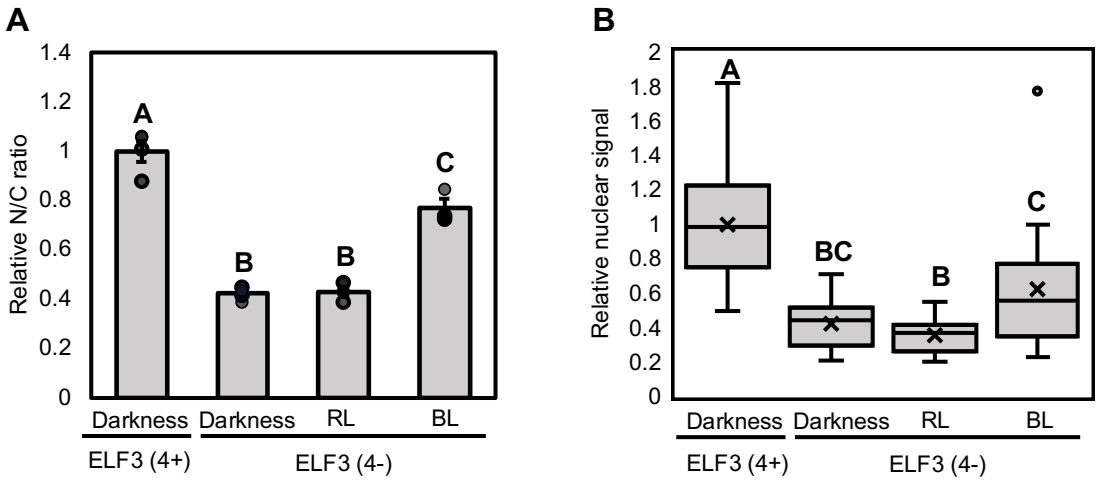

Figure 6.7 – Blue light promotes the nuclear localisation of ELF3 independently of ELF4

The **(A)** relative nuclear/cytoplasmic (N/C) ratio or **(B)** relative nuclear signal of *35S::YFP:ELF3 elf3-4* (ELF3 4+) or *35S::YFP:ELF3 elf3-4/elf4-1* (ELF3 4-) in the dark or for ELF3 (4-) after a 25 μmol/m^{-2}/s^{-1} pulse of red light (RL) or blue light (BL) at ZT10. Light pulses were started at

Figure 6.7 (continued) - ZT7 and applied for three-hours (short-day 8/16 photoperiods). Data was made relative to the values of ELF3 (4+) at ZT10 in the dark. All imaging was repeated twice, with the presented data a combination of these two repeats. Letters signify significant difference ($p < 0.05$), determined by a one-way ANOVA with Tukey HSD posthoc test.

Other proteins connected to BL signalling that have also been shown to interact with ELF3 include *LUX*, *BOA*, *TOC1* and *GI* (Baudry et al., 2010, Kim et al., 2013a, Hajdu et al., 2018). Whether these proteins can regulate ELF3 localisation is unknown and will need to be investigated. Furthermore, it'll be important to understand the photoreceptor upstream of these proteins that are transmitting BL signals to ELF3. Within the circadian clock, the primary BL receptors are CRYs and LOV-KELCH proteins (Oakenfull and Davis, 2017). phyA has also been linked to BL entrainment of the circadian clock, although the BL intensities used here (12 – 40 μmol/m^{-2}/s^{-1}) are far greater than the light intensities the *phyA* mutant had a circadian phenotype at (2 – 4 μmol/m^{-2}/s^{-1}) (Devlin and Kay, 2000). Therefore, it is unlikely that phyA is responsible for the observed BL-response of ELF3. Instead, CRYs and/or LOV-KELCH domain proteins are more likely to be transmitting BL signals to ELF3. This can be directly tested by incorporating mutants of the respective genes into the *YFP:ELF3* background and investigating how the cellular localisation of ELF3 responds to BL in these mutant backgrounds.

6.9 Is regulating the spatio-temporal distribution of ELF3 a mechanism of entrainment?

Entrainment is the process whereby the internal cycle is synchronised with the external environment. Two mechanisms of entrainment were originally proposed; non-parametric entrainment states that entrainment occurs "instantaneously" at one-off points in the *diel* cycle (Pittendrigh and Minis, 1964). In contrast, the mechanism of parametric entrainment argues that the circadian clock is being continuously adjusted throughout the *diel* cycle by incorporating stimuli that increase or decrease the velocity of the oscillator (Aschoff, 1963).

Both mechanisms of entrainment are dependent on the integration of *zeitgebers* (time-givers) by *zeitnehmers* (timekeepers). ELF3 has been established as a *zeitnehmer* of light and temperature entrainment of the plant circadian (Covington et al., 2001, Anwer et al., 2020, Zhu et al., 2020). However, the molecular mechanism of how ELF3 functions as a *zeitnehmer* for either light or temperature has remained unclear. My results suggest that light and temperature *zeitgebers* are incorporated by ELF3 via protein-protein interactions that control the spatio-temporal localisation of ELF3. By controlling the localisation of ELF3, light and temperature signalling pathways subsequently control ELF3 activity. This regulatory interface thus determines when ELF3 represses the circadian period and the duration of this repressive activity (Covington et al., 2001).

In this proposed entrainment pathway, the activity of phyB and ELF4 is principally important. phyB has *diel* accumulation in gene expression and protein accumulation, with both peaking around dawn (Bognár et al., 1999). In the natural environment, the gradual increase in RL intensity around the dark-to-light transition at dawn would slowly lead to the activation of phyB until phyB becomes saturated in the active PFr conformer in the early morning. This process would therefore gradually alleviate the repressive activity of ELF3 by antagonising the nuclear and sub-nuclear accumulation of ELF3, and possibly the chromatin occupancy of ELF3 **(Figure 6.2)**. The daily shift in the timing of dawn would subsequently control when phyB begins to accumulate and inhibit ELF3's repressive activity, leading the circadian clock to transition into a "day-phase".

Conversely, the accumulation of ELF4 at dusk would lead to the antagonism of phyB-inhibition of ELF3 function in the cytoplasm and nucleus **(Figure 6.1, 6.2).** ELF3 would subsequently form the EC and recruit chromatin remodelling enzymes to repress gene expression. This activity would lead to the clock transitioning into an "evening-phase". The converge and competition between other environmental stimuli that also provide time-of-day information such as BL (a dusk and twilight signal) **(Figure 3.3, 3.5, 3.6)** and warm temperature (a day-time signal) **(Figure 5.1-5.2)** on regulating the sub-nuclear localisation of ELF3 would further contribute to determining the duration of ELF3

repressive activity across the evening and when the oscillator transitions between these "day" and "evening" phases.

Possible targets for ELF3 in this entrainment pathway are the morning phased genes *PRR9* and *PRR7*. The *prr9/prr7* double mutant has a long circadian period under free-running conditions, phenocopying the *ELF3ox* long-period phenotype (Covington et al., 2001, Farré et al., 2005). The expression of *PRR9* and *PRR7* is also directly repressed by the EC, although the repressive effect of the EC is seemingly greater on *PRR9* than *PRR7* (Herrero et al., 2012, Tong et al., 2020). The expression of *PRR9* and *PRR7* is also regulated by the external environment. *PRR9* expression is directly induced by RL and UV-B (Ito et al., 2003, Takeuchi et al., 2014), while the expression of *PRR7* is activated by bZIP63 in response to low sugar levels (Frank et al., 2018). Furthermore, both *PRR9* and *PRR7* are directly activated by a warm temperature pulse at dawn (Mizuno et al., 2014). In chapter 3, I observed that ELF3 directly represses the ability of RL to induce the expression of *PRR9* **(Figure 3.12)**, while other studies have reported that the EC represses temperature induction of *PRR7* (Mizuno et al., 2014). It has yet to be tested whether ELF3 contributes to metabolic regulation of *PRR7* expression or temperature induction of *PRR9*, respectively. Therefore, entrainment pathways that converge on ELF3, may in turn control the sensitivity of other entrainment pathways within the oscillator. This would further increase the synchronicity of the internal cycle with the external environment.

In conclusion, I propose an entrainment pathway whereby light and temperature *zeitgebers* control the cellular dynamics of ELF3. This would determine the ability of ELF3 and the EC to not only repress the expression of *PRR9* and *PRR7* but also de-sensitise the promoter of both genes to environmental stimuli. Such a model of entrainment is not easily defined as either parametric or non-parametric entrainment, as the cellular localisation of ELF3 is seemingly highly dynamic and responds rapidly to multiple light and temperature pulses of different wavelengths and durations at different points in the day. Instead, my results more closely agree with the recent idea that the

plant oscillator is being continuously adjusted throughout the day in response to the changing internal and external environment (Webb et al., 2019).

Chapter 7 - References

ABE, M., KOBAYASHI, Y., YAMAMOTO, S., DAIMON, Y., YAMAGUCHI, A., IKEDA, Y., ICHINOKI, H., NOTAGUCHI, M., GOTO, K. & ARAKI, T. 2005. FD, a bZIP protein mediating signals from the floral pathway integrator FT at the shoot apex. *Science,* 309**,** 1052-6.

ADAMS, S., MANFIELD, I., STOCKLEY, P. & CARRE, I. A. 2015. Revised Morning Loops of the Arabidopsis Circadian Clock Based on Analyses of Direct Regulatory Interactions. *PLOS ONE,* 10**,** e0143943.

AL-SADY, B., NI, W., KIRCHER, S., SCHAFER, E. & QUAIL, P. H. 2006. Photoactivated phytochrome induces rapid PIF3 phosphorylation prior to proteasome-mediated degradation. *Mol Cell,* 23**,** 439-46.

ALABADI, D., OYAMA, T., YANOVSKY, M. J., HARMON, F. G., MAS, P. & KAY, S. A. 2001. Reciprocal regulation between TOC1 and LHY/CCA1 within the Arabidopsis circadian clock. *Science,* 293**,** 880-3.

AN, H., ROUSSOT, C., SUAREZ-LOPEZ, P., CORBESIER, L., VINCENT, C., PINEIRO, M., HEPWORTH, S., MOURADOV, A., JUSTIN, S., TURNBULL, C. & COUPLAND, G. 2004. CONSTANS acts in the phloem to regulate a systemic signal that induces photoperiodic flowering of Arabidopsis. *Development,* 131**,** 3615-26.

ANWER, M. U., BOIKOGLOU, E., HERRERO, E., HALLSTEIN, M., DAVIS, A. M., VELIKKAKAM JAMES, G., NAGY, F. & DAVIS, S. J. 2014. Natural variation reveals that intracellular distribution of ELF3 protein is associated with function in the circadian clock. *eLife,* 3**,** e02206.

ANWER, M. U., DAVIS, A., DAVIS, S. J. & QUINT, M. 2020. Photoperiod sensing of the circadian clock is controlled by EARLY FLOWERING 3 and GIGANTEA. *Plant J,* 101**,** 1397-1410.

ASCHOFF, J. 1960. Exogenous and endogenous components in circadian rhythms. *Cold Spring Harb Symp Quant Biol,* 25**,** 11-28.

ASCHOFF, J. 1963. Comparative physiology: diurnal rhythms. *Annu Rev Physiol,* 25**,** 581-600.

AUKERMAN, M. J., HIRSCHFELD, M., WESTER, L., WEAVER, M., CLACK, T., AMASINO, R. M. & SHARROCK, R. A. 1997. A deletion in the PHYD gene of the Arabidopsis Wassilewskija ecotype defines a role for phytochrome D in red/far-red light sensing. *The Plant Cell,* 9**,** 1317-1326.

BATTLE, M. W. & JONES, M. A. 2020. Cryptochromes integrate green light signals into the circadian system. *Plant Cell Environ,* 43**,** 16-27.

BAUDRY, A., ITO, S., SONG, Y. H., STRAIT, A. A., KIBA, T., LU, S., HENRIQUES, R., PRUNEDA-PAZ, J. L., CHUA, N. H., TOBIN, E. M., KAY, S. A. & IMAIZUMI, T. 2010. F-box proteins FKF1 and LKP2 act in concert with ZEITLUPE to control Arabidopsis clock progression. *The Plant Cell,* 22**,** 606-22.

BENDIX, C., MARSHALL, C. M. & HARMON, F. G. 2015. Circadian Clock Genes Universally Control Key Agricultural Traits. *Mol Plant,* 8**,** 1135-52.

BODEN, S. A., WEISS, D., ROSS, J. J., DAVIES, N. W., TREVASKIS, B., CHANDLER, P. M. & SWAIN, S. M. 2014. EARLY FLOWERING3 Regulates Flowering in Spring Barley by Mediating Gibberellin Production and FLOWERING LOCUS T Expression. *The Plant Cell,* 26**,** 1557-1569.

BOGNÁR, L. K., HALL, A., ÁDÁM, É., THAIN, S. C., NAGY, F. & MILLAR, A. J. 1999. The circadian clock controls the expression pattern of the circadian input photoreceptor, phytochrome B. *Proc Natl Acad Sci U S A,* 96**,** 14652-14657.

BORDAGE, S., SULLIVAN, S., LAIRD, J., MILLAR, A. J. & NIMMO, H. G. 2016. Organ specificity in the plant circadian system is explained by different light inputs to the shoot and root clocks. *New Phytol,* 212**,** 136-49.

BOX, M. S., HUANG, B. E., DOMIJAN, M., JAEGER, K. E., KHATTAK, A. K., YOO, S. J., SEDIVY, E. L., JONES, D. M., HEARN, T. J., WEBB, A. A. R., GRANT, A., LOCKE, J. C. W. & WIGGE, P. A. 2015. ELF3 controls thermoresponsive growth in Arabidopsis. *Curr Biol,* 25**,** 194-199.

CHA, J. Y., KIM, J., KIM, T. S., ZENG, Q., WANG, L., LEE, S. Y., KIM, W. Y. & SOMERS, D. E. 2017. GIGANTEA is a co-chaperone which facilitates maturation of ZEITLUPE in the Arabidopsis circadian clock. *Nat Commun,* 8**,** 3.

CHEN, M., SCHWAB, R. & CHORY, J. 2003. Characterization of the requirements for localization of phytochrome B to nuclear bodies. *Proc Natl Acad Sci U S A,* 100**,** 14493-8.

CHEN, W. W., TAKAHASHI, N., HIRATA, Y., RONALD, J., PORCO, S., DAVIS, S. J., NUSINOW, D. A., KAY, S. A. & MAS, P. 2020. A mobile ELF4 delivers circadian temperature information from shoots to roots. *Nat Plants,* 6**,** 416-426.

CHOI, H. & OH, E. 2016. PIF4 Integrates Multiple Environmental and Hormonal Signals for Plant Growth Regulation in Arabidopsis. *Molecules and cells,* 39**,** 587-593.

CHOW, B. Y., HELFER, A., NUSINOW, D. A. & KAY, S. A. 2012. ELF3 recruitment to the PRR9 promoter requires other Evening Complex members in the Arabidopsis circadian clock. *Plant Signal Behav,* 7**,** 170-3.

CHOW, B. Y., SANCHEZ, S. E., BRETON, G., PRUNEDA-PAZ, J. L., KROGAN, N. T. & KAY, S. A. 2014. Transcriptional regulation of LUX by CBF1 mediates cold input to the circadian clock in Arabidopsis. *Curr Biol,* 24**,** 1518-24.

CLACK, T., MATHEWS, S. & SHARROCK, R. A. 1994. The phytochrome apoprotein family in Arabidopsis is encoded by five genes: the sequences and expression of PHYD and PHYE. *Plant Mol Biol,* 25**,** 413-27.

CLACK, T., SHOKRY, A., MOFFET, M., LIU, P., FAUL, M. & SHARROCK, R. A. 2009. Obligate heterodimerization of Arabidopsis phytochromes C and E and interaction with the PIF3 basic helix-loop-helix transcription factor. *The Plant Cell,* 21**,** 786-799.

COHEN, S. E. & GOLDEN, S. S. 2015. Circadian Rhythms in Cyanobacteria. *Microbiol Mol Biol Rev,* 79**,** 373-85.

COVINGTON, M. F., PANDA, S., LIU, X. L., STRAYER, C. A., WAGNER, D. R. & KAY, S. A. 2001. ELF3 Modulates Resetting of the Circadian Clock in Arabidopsis. *The Plant Cell,* 13**,** 1305-1316.

DAI, S., WEI, X., PEI, L., THOMPSON, R. L., LIU, Y., HEARD, J. E., RUFF, T. G. & BEACHY, R. N. 2011. BROTHER OF LUX ARRHYTHMO is a component of the Arabidopsis circadian clock. *The Plant Cell,* 23**,** 961-72.

DAVIS, A. M., RONALD, J., MA, Z., WILKINSON, A. J., PHILIPPOU, K., SHINDO, T., QUEITSCH, C. & DAVIS, S. J. 2018. HSP90 Contributes to Entrainment of the Arabidopsis Circadian Clock via the Morning Loop. *Genetics,* 210**,** 1383-1390.

DEVLIN, P. F. & KAY, S. A. 2000. Cryptochromes are required for phytochrome signaling to the circadian clock but not for rhythmicity. *The Plant Cell,* 12**,** 2499-2510.

DING, L., WANG, S., SONG, Z. T., JIANG, Y., HAN, J. J., LU, S. J., LI, L. & LIU, J. X. 2018. Two B-Box Domain Proteins, BBX18 and BBX23, Interact with ELF3 and Regulate Thermomorphogenesis in Arabidopsis. *Cell Rep,* 25**,** 1718-1728.e4.

DODD, A. N., SALATHIA, N., HALL, A., KEVEI, E., TOTH, R., NAGY, F., HIBBERD, J. M., MILLAR, A. J. & WEBB, A. A. 2005. Plant circadian clocks increase photosynthesis, growth, survival, and competitive advantage. *Science,* 309**,** 630-3.

DOWSON-DAY, M. J. & MILLAR, A. J. 1999. Circadian dysfunction causes aberrant hypocotyl elongation patterns in Arabidopsis. *Plant J,* 17**,** 63-71.

DOYLE, M. R., DAVIS, S. J., BASTOW, R. M., MCWATTERS, H. G., KOZMA-BOGNÁR, L., NAGY, F., MILLAR, A. J. & AMASINO, R. M. 2002. The ELF4 gene controls circadian rhythms and flowering time in Arabidopsis thaliana. *Nature,* 419**,** 74-77.

EELDERINK-CHEN, Z., BOSMAN, J., SARTOR, F., DODD, A. N., KOVÁCS, Á. T. & MERROW, M. 2021. A circadian clock in a nonphotosynthetic prokaryote. *Science Advances,* 7**,** eabe2086.

ENDERLE, B., SHEERIN, D. J., PAIK, I., KATHARE, P. K., SCHWENK, P., KLOSE, C., ULBRICH, M. H., HUQ, E. & HILTBRUNNER, A. 2017. PCH1 and PCHL promote photomorphogenesis in plants by controlling phytochrome B dark reversion. *Nat Commun,* 8**,** 2221.

EZER, D., JUNG, J. H., LAN, H., BISWAS, S., GREGOIRE, L., BOX, M. S., CHAROENSAWAN, V., CORTIJO, S., LAI, X., STOCKLE, D., ZUBIETA, C., JAEGER, K. E. & WIGGE, P. A. 2017a. The evening complex coordinates environmental and endogenous signals in Arabidopsis. *Nat Plants,* 3**,** 17087.

EZER, D., SHEPHERD, S. J. K., BRESTOVITSKY, A., DICKINSON, P., CORTIJO, S., CHAROENSAWAN, V., BOX, M. S., BISWAS, S., JAEGER, K. E. & WIGGE, P. A. 2017b. The G-Box Transcriptional Regulatory Code in Arabidopsis. *Plant Physiology,* 175**,** 628-640.

FARRÉ, E. M., HARMER, S. L., HARMON, F. G., YANOVSKY, M. J. & KAY, S. A. 2005. Overlapping and Distinct Roles of PRR7 and PRR9 in the Arabidopsis Circadian Clock. *Curr Biol,* 15**,** 47-54.

FEENEY, K. A., PUTKER, M., BRANCACCIO, M. & O'NEILL, J. S. 2016. In-depth Characterization of Firefly Luciferase as a Reporter of Circadian Gene Expression in Mammalian Cells. *Journal of Biological Rhythms,* 31**,** 540-550.

FEHER, B., KOZMA-BOGNAR, L., KEVEI, E., HAJDU, A., BINKERT, M., DAVIS, S. J., SCHAFER, E., ULM, R. & NAGY, F. 2011. Functional interaction of the circadian clock and UV RESISTANCE LOCUS 8-controlled UV-B signaling pathways in Arabidopsis thaliana. *Plant J,* 67**,** 37-48.

FRANK, A., MATIOLLI, C. C., VIANA, A. J. C., HEARN, T. J., KUSAKINA, J., BELBIN, F. E., WELLS NEWMAN, D., YOCHIKAWA, A., CANO-RAMIREZ, D. L., CHEMBATH, A., CRAGG-BARBER, K., HAYDON, M. J., HOTTA, C. T., VINCENTZ, M., WEBB, A. A. R. & DODD, A. N. 2018. Circadian Entrainment in Arabidopsis by the Sugar-Responsive Transcription Factor bZIP63. *Curr Biol,* 28**,** 2597-2606.e6.

FRANKLIN, K. A., LEE, S. H., PATEL, D., KUMAR, S. V., SPARTZ, A. K., GU, C., YE, S., YU, P., BREEN, G., COHEN, J. D., WIGGE, P. A. & GRAY, W. M. 2011. PHYTOCHROME-INTERACTING FACTOR 4 (PIF4) regulates auxin biosynthesis at high temperature. *Proc Natl Acad Sci U S A,* 108**,** 20231-20235.

GENDREAU, E., TRAAS, J., DESNOS, T., GRANDJEAN, O., CABOCHE, M. & HOFTE, H. 1997. Cellular Basis of Hypocotyl Growth in Arabidopsis thaliana. *Plant Physiology,* 114**,** 295-305.

GENDRON, J. M., PRUNEDA-PAZ, J. L., DOHERTY, C. J., GROSS, A. M., KANG, S. E. & KAY, S. A. 2012. Arabidopsis circadian clock protein, TOC1, is a DNA-binding transcription factor. *Proc Natl Acad Sci U S A,* 109**,** 3167-72.

GOULD, P. D., DIAZ, P., HOGBEN, C., KUSAKINA, J., SALEM, R., HARTWELL, J. & HALL, A. 2009. Delayed fluorescence as a universal tool for the measurement of circadian rhythms in higher plants. *Plant J,* 58**,** 893-901.

GOULD, P. D., DOMIJAN, M., GREENWOOD, M., TOKUDA, I. T., REES, H., KOZMA-BOGNAR, L., HALL, A. J. W. & LOCKE, J. C. W. 2018. Coordination of robust single cell rhythms in the Arabidopsis circadian clock via spatial waves of gene expression. *eLife,* 7**,** e31700.

GOULD, P. D., LOCKE, J. C., LARUE, C., SOUTHERN, M. M., DAVIS, S. J., HANANO, S., MOYLE, R., MILICH, R., PUTTERILL, J., MILLAR, A. J. & HALL, A. 2006. The molecular basis of temperature compensation in the Arabidopsis circadian clock. *The Plant Cell,* 18**,** 1177-87.

GREENWOOD, M., DOMIJAN, M., GOULD, P. D., HALL, A. J. W. & LOCKE, J. C. W. 2019. Coordinated circadian timing through the integration of local inputs in Arabidopsis thaliana. *PLOS Biology,* 17**,** e3000407.

HAJDU, A., DOBOS, O., DOMIJAN, M., BALINT, B., NAGY, I., NAGY, F. & KOZMA-BOGNAR, L. 2018. ELONGATED HYPOCOTYL 5 mediates blue light signalling to the Arabidopsis circadian clock. *Plant J,* 96**,** 1242-1254.

HAN, L., MASON, M., RISSEEUW, E. P., CROSBY, W. L. & SOMERS, D. E. 2004. Formation of an SCF(ZTL) complex is required for proper regulation of circadian timing. *Plant J,* 40**,** 291-301.

HAYDON, M. J., MIELCZAREK, O., ROBERTSON, F. C., HUBBARD, K. E. & WEBB, A. A. 2013. Photosynthetic entrainment of the Arabidopsis thaliana circadian clock. *Nature,* 502**,** 689-92.

HAZEN, S. P., SCHULTZ, T. F., PRUNEDA-PAZ, J. L., BOREVITZ, J. O., ECKER, J. R. & KAY, S. A. 2005. LUX ARRHYTHMO encodes a Myb domain protein essential for circadian rhythms. *Proc Natl Acad Sci U S A,* 102**,** 10387-92.

HELFER, A., NUSINOW, D. A., CHOW, B. Y., GEHRKE, A. R., BULYK, M. L. & KAY, S. A. 2011. LUX ARRHYTHMO encodes a nighttime repressor of circadian gene expression in the Arabidopsis core clock. *Curr Biol,* 21**,** 126-33.

HEMMES, H., HENRIQUES, R., JANG, I. C., KIM, S. & CHUA, N. H. 2012. Circadian clock regulates dynamic chromatin modifications associated with Arabidopsis CCA1/LHY and TOC1 transcriptional rhythms. *Plant Cell Physiol,* 53**,** 2016-29.

HERRERO, E. 2011. *A molecular basis of ELF3 action in the Arabidopsis circadian clock.* PhD, Universität of Köln.

HERRERO, E., KOLMOS, E., BUJDOSO, N., YUAN, Y., WANG, M., BERNS, M. C., UHLWORM, H., COUPLAND, G., SAINI, R., JASKOLSKI, M., WEBB, A., GONCALVES, J. & DAVIS, S. J. 2012. EARLY FLOWERING4 recruitment of EARLY FLOWERING3 in the nucleus sustains the Arabidopsis circadian clock. *The Plant Cell,* 24**,** 428-43.

HICKS, K. A., ALBERTSON, T. M. & WAGNER, D. R. 2001. EARLY FLOWERING3 encodes a novel protein that regulates circadian clock function and flowering in Arabidopsis. *The Plant Cell,* 13**,** 1281-92.

HICKS, K. A., MILLAR, A. J., CARRÉ, I. A., SOMERS, D. E., STRAUME, M., MEEKS-WAGNER, D. R. & KAY, S. A. 1996. Conditional circadian dysfunction of the Arabidopsis early-flowering 3 mutant. *Science,* 274**,** 790-2.

HSU, P. Y., DEVISETTY, U. K. & HARMER, S. L. 2013. Accurate timekeeping is controlled by a cycling activator in Arabidopsis. *Elife,* 2**,** e00473.

HUANG, H., ALVAREZ, S., BINDBEUTEL, R., SHEN, Z., NALDRETT, M. J., EVANS, B. S., BRIGGS, S. P., HICKS, L. M., KAY, S. A. & NUSINOW, D. A. 2016. Identification of Evening Complex Associated Proteins in Arabidopsis by Affinity Purification and Mass Spectrometry. *Mol Cell Proteomics,* 15**,** 201-17.

HUNG, F. Y., CHEN, F. F., LI, C., CHEN, C., CHEN, J. H., CUI, Y. & WU, K. 2019. The LDL1/2-HDA6 Histone Modification Complex Interacts With TOC1 and Regulates the Core Circadian Clock Components in Arabidopsis. *Front Plant Sci,* 10**,** 233.

HUNG, F. Y., CHEN, F. F., LI, C., CHEN, C., LAI, Y. C., CHEN, J. H., CUI, Y. & WU, K. 2018. The Arabidopsis LDL1/2-HDA6 histone modification complex is functionally associated with CCA1/LHY in regulation of circadian clock genes. *Nucleic Acids Res,* 46**,** 10669-10681.

HUQ, E., TEPPERMAN, J. M. & QUAIL, P. H. 2000. GIGANTEA is a nuclear protein involved in phytochrome signaling in Arabidopsis. *Proc Natl Acad Sci U S A,* 97**,** 9789-9794.

ITO, S., MATSUSHIKA, A., YAMADA, H., SATO, S., KATO, T., TABATA, S., YAMASHINO, T. & MIZUNO, T. 2003. Characterization of the APRR9 pseudo-response regulator belonging to the APRR1/TOC1 quintet in Arabidopsis thaliana. *Plant Cell Physiol,* 44**,** 1237-45.

JAEGER, K. E. & WIGGE, P. A. 2007. FT protein acts as a long-range signal in Arabidopsis. *Curr Biol,* 17**,** 1050-4.

JAMES, A. B., CALIXTO, C. P. G., TZIOUTZIOU, N. A., GUO, W., ZHANG, R., SIMPSON, C. G., JIANG, W., NIMMO, G. A., BROWN, J. W. S. & NIMMO, H. G. 2018. How does temperature affect splicing events? Isoform switching of splicing factors regulates splicing of LATE ELONGATED HYPOCOTYL (LHY). *Plant Cell Environ,* 41**,** 1539-1550.

JAMES, A. B., MONREAL, J. A., NIMMO, G. A., KELLY, C. L., HERZYK, P., JENKINS, G. I. & NIMMO, H. G. 2008. The Circadian Clock in Arabidopsis Roots Is a Simplified Slave Version of the Clock in Shoots. *Science,* 322**,** 1832.

JAMES, A. B., SYED, N. H., BORDAGE, S., MARSHALL, J., NIMMO, G. A., JENKINS, G. I., HERZYK, P., BROWN, J. W. & NIMMO, H. G. 2012. Alternative splicing mediates responses of the Arabidopsis circadian clock to temperature changes. *The Plant Cell,* 24**,** 961-81.

JIANG, B., SHI, Y., PENG, Y., JIA, Y., YAN, Y., DONG, X., LI, H., DONG, J., LI, J., GONG, Z., THOMASHOW, M. F. & YANG, S. 2020. Cold-Induced CBF–PIF3 Interaction Enhances Freezing Tolerance by Stabilizing the phyB Thermosensor in Arabidopsis. *Molecular Plant,* 13**,** 894-906.

JIANG, D. & BERGER, F. 2017. Histone variants in plant transcriptional regulation. *Biochim Biophys Acta Gene Regul Mech,* 1860**,** 123-130.

JIANG, Y., YANG, C., HUANG, S., XIE, F., XU, Y., LIU, C. & LI, L. 2019. The ELF3-PIF7 Interaction Mediates the Circadian Gating of the Shade Response in Arabidopsis. *iScience,* 22**,** 288-298.

JONES, M. A., HU, W., LITTHAUER, S., LAGARIAS, J. C. & HARMER, S. L. 2015. A Constitutively Active Allele of Phytochrome B Maintains Circadian Robustness in the Absence of Light. *Plant Physiology,* 169**,** 814-825.

JUNG, J.-H., DOMIJAN, M., KLOSE, C., BISWAS, S., EZER, D., GAO, M., KHATTAK, A. K., BOX, M. S., CHAROENSAWAN, V., CORTIJO, S., KUMAR, M., GRANT, A., LOCKE, J. C. W., SCHÄFER, E., JAEGER, K. E. & WIGGE, P. A. 2016. Phytochromes function as thermosensors in Arabidopsis. *Science,* 354**,** 886.

JUNG, J. H., BARBOSA, A. D., HUTIN, S., KUMITA, J. R., GAO, M., DERWORT, D., SILVA, C. S., LAI, X., PIERRE, E., GENG, F., KIM, S. B., BAEK, S., ZUBIETA, C., JAEGER, K. E. & WIGGE, P. A. 2020. A prion-like domain in ELF3 functions as a thermosensor in Arabidopsis. *Nature,* 585**,** 256-260.

KAISERLI, E., PALDI, K., O'DONNELL, L., BATALOV, O., PEDMALE, U. V., NUSINOW, D. A., KAY, S. A. & CHORY, J. 2015. Integration of Light and Photoperiodic Signaling in Transcriptional Nuclear Foci. *Dev Cell,* 35**,** 311-21.

KAISERLI, E., PERRELLA, G. & DAVIDSON, M. L. 2018. Light and temperature shape nuclear architecture and gene expression. *Curr Opin Plant Biol,* 45**,** 103-111.

KAMIOKA, M., TAKAO, S., SUZUKI, T., TAKI, K., HIGASHIYAMA, T., KINOSHITA, T. & NAKAMICHI, N. 2016. Direct Repression of Evening Genes by CIRCADIAN CLOCK-ASSOCIATED1 in the Arabidopsis Circadian Clock. *The Plant Cell,* 28**,** 696-711.

KHANNA, R., KIKIS, E. A. & QUAIL, P. H. 2003. EARLY FLOWERING 4 functions in phytochrome B-regulated seedling de-etiolation. *Plant Physiology,* 133**,** 1530-1538.

KIBA, T., HENRIQUES, R., SAKAKIBARA, H. & CHUA, N. H. 2007. Targeted degradation of PSEUDO-RESPONSE REGULATOR5 by an SCFZTL complex regulates clock function and photomorphogenesis in Arabidopsis thaliana. *The Plant Cell,* 19**,** 2516-30.

KIDD, P. B., YOUNG, M. W. & SIGGIA, E. D. 2015. Temperature compensation and temperature sensation in the circadian clock. *Proc Natl Acad Sci U S A,* 112**,** E6284.

KIM, J., GENG, R., GALLENSTEIN, R. A. & SOMERS, D. E. 2013a. The F-box protein ZEITLUPE controls stability and nucleocytoplasmic partitioning of GIGANTEA. *Development,* 140**,** 4060-9.

KIM, T. S., KIM, W. Y., FUJIWARA, S., KIM, J., CHA, J. Y., PARK, J. H., LEE, S. Y. & SOMERS, D. E. 2011. HSP90 functions in the circadian clock through stabilization of the client F-box protein ZEITLUPE. *Proc Natl Acad Sci U S A,* 108**,** 16843-8.

KIM, W. Y., FUJIWARA, S., SUH, S. S., KIM, J., KIM, Y., HAN, L., DAVID, K., PUTTERILL, J., NAM, H. G. & SOMERS, D. E. 2007. ZEITLUPE is a circadian photoreceptor stabilized by GIGANTEA in blue light. *Nature,* 449**,** 356-60.

KIM, Y., LIM, J., YEOM, M., KIM, H., KIM, J., WANG, L., KIM, W. Y., SOMERS, D. E. & NAM, H. G. 2013b. ELF4 regulates GIGANTEA chromatin access through subnuclear sequestration. *Cell Rep,* 3**,** 671-7.

KIM, Y. J. & SOMERS, D. E. 2019. Luciferase-Based Screen for Post-translational Control Factors in the Regulation of the Pseudo-Response Regulator PRR7. *Front Plant Sci,* 10**,** 667.

KIRCHER, S., GIL, P., KOZMA-BOGNÁR, L., FEJES, E., SPETH, V., HUSSELSTEIN-MULLER, T., BAUER, D., ADÁM, E., SCHÄFER, E. & NAGY, F. 2002. Nucleocytoplasmic partitioning of the plant photoreceptors phytochrome A, B, C, D, and E is regulated differentially by light and exhibits a diurnal rhythm. *The Plant Cell,* 14**,** 1541-1555.

KIRCHER, S., KOZMA-BOGNAR, L., KIM, L., ADAM, E., HARTER, K., SCHÄFER, E. & NAGY, F. 1999. Light Quality–Dependent Nuclear Import of the Plant Photoreceptors Phytochrome A and B. *The Plant Cell,* 11**,** 1445-1456.

KLOSE, C., VICZIAN, A., KIRCHER, S., SCHAFER, E. & NAGY, F. 2015. Molecular mechanisms for mediating light-dependent nucleo/cytoplasmic partitioning of phytochrome photoreceptors. *New Phytol,* 206**,** 965-71.

KOLMOS, E., HERRERO, E., BUJDOSO, N., MILLAR, A. J., TOTH, R., GYULA, P., NAGY, F. & DAVIS, S. J. 2011. A reduced-function allele reveals that EARLY FLOWERING3 repressive action on the circadian clock is modulated by phytochrome signals in Arabidopsis. *The Plant Cell,* 23**,** 3230-46.

KOLMOS, E., NOWAK, M., WERNER, M., FISCHER, K., SCHWARZ, G., MATHEWS, S., SCHOOF, H., NAGY, F., BUJNICKI, J. M. & DAVIS, S. J. 2009. Integrating ELF4 into

the circadian system through combined structural and functional studies. *HFSP J,* 3**,** 350-66.

KONDO, T., STRAYER, C. A., KULKARNI, R. D., TAYLOR, W., ISHIURA, M., GOLDEN, S. S. & JOHNSON, C. H. 1993. Circadian rhythms in prokaryotes: luciferase as a reporter of circadian gene expression in cyanobacteria. *Proc Natl Acad Sci U S A,* 90**,** 5672-6.

KWON, Y.-J., PARK, M.-J., KIM, S.-G., BALDWIN, I. T. & PARK, C.-M. 2014. Alternative splicing and nonsense-mediated decay of circadian clock genes under environmental stress conditions in Arabidopsis. *BMC plant biology,* 14**,** 136-136.

LAMOND, A. I. & SLEEMAN, J. E. 2003. Nuclear substructure and dynamics. *Curr Biol,* 13**,** R825-8.

LEE, C. M., FEKE, A., LI, M. W., ADAMCHEK, C., WEBB, K., PRUNEDA-PAZ, J., BENNETT, E. J., KAY, S. A. & GENDRON, J. M. 2018. Decoys Untangle Complicated Redundancy and Reveal Targets of Circadian Clock F-Box Proteins. *Plant Physiology,* 177**,** 1170-1186.

LEE, C. M., LI, M. W., FEKE, A., LIU, W., SAFFER, A. M. & GENDRON, J. M. 2019a. GIGANTEA recruits the UBP12 and UBP13 deubiquitylases to regulate accumulation of the ZTL photoreceptor complex. *Nat Commun,* 10**,** 3750.

LEE, K., MAS, P. & SEO, P. J. 2019b. The EC-HDA9 complex rhythmically regulates histone acetylation at the TOC1 promoter in Arabidopsis. *Commun Biol,* 2**,** 143.

LEGRIS, M., KLOSE, C., BURGIE, E. S., ROJAS, C. C., NEME, M., HILTBRUNNER, A., WIGGE, P. A., SCHAFER, E., VIERSTRA, R. D. & CASAL, J. J. 2016. Phytochrome B integrates light and temperature signals in Arabidopsis. *Science,* 354**,** 897-900.

LI, G., SIDDIQUI, H., TENG, Y., LIN, R., WAN, X. Y., LI, J., LAU, O. S., OUYANG, X., DAI, M., WAN, J., DEVLIN, P. F., DENG, X. W. & WANG, H. 2011. Coordinated transcriptional regulation underlying the circadian clock in Arabidopsis. *Nat Cell Biol,* 13**,** 616-22.

LI, N., ZHANG, Y., HE, Y., WANG, Y. & WANG, L. 2020a. Pseudo Response Regulators Regulate Photoperiodic Hypocotyl Growth by Repressing PIF4/5 Transcription. *Plant Physiology,* 183**,** 686-699.

LI, Y., WANG, L., YUAN, L., SONG, Y., SUN, J., JIA, Q., XIE, Q. & XU, X. 2020b. Molecular investigation of organ-autonomous expression of Arabidopsis circadian oscillators. *Plant Cell Environ,* 43**,** 1501-1512.

LINDE, A. M., EKLUND, D. M., KUBOTA, A., PEDERSON, E. R. A., HOLM, K., GYLLENSTRAND, N., NISHIHAMA, R., CRONBERG, N., MURANAKA, T., OYAMA, T., KOHCHI, T. & LAGERCRANTZ, U. 2017. Early evolution of the land plant circadian clock. *New Phytol,* 216**,** 576-590.

LIU, L. J., ZHANG, Y. C., LI, Q. H., SANG, Y., MAO, J., LIAN, H. L., WANG, L. & YANG, H. Q. 2008. COP1-mediated ubiquitination of CONSTANS is implicated in cryptochrome regulation of flowering in Arabidopsis. *The Plant Cell,* 20**,** 292-306.

LIU, X. L., COVINGTON, M. F., FANKHAUSER, C., CHORY, J. & WAGNER, D. R. 2001. ELF3 encodes a circadian clock-regulated nuclear protein that functions in an Arabidopsis PHYB signal transduction pathway. *The Plant Cell,* 13**,** 1293-304.

LORRAIN, S., ALLEN, T., DUEK, P. D., WHITELAM, G. C. & FANKHAUSER, C. 2008. Phytochrome-mediated inhibition of shade avoidance involves degradation of growth-promoting bHLH transcription factors. *Plant J,* 53**,** 312-23.

LU, S. X., WEBB, C. J., KNOWLES, S. M., KIM, S. H., WANG, Z. & TOBIN, E. M. 2012. CCA1 and ELF3 Interact in the control of hypocotyl length and flowering time in Arabidopsis. *Plant Physiology,* 158**,** 1079-88.

LU, X.-D., ZHOU, C.-M., XU, P.-B., LUO, Q., LIAN, H.-L. & YANG, H.-Q. 2015. Red-Light-Dependent Interaction of phyB with SPA1 Promotes COP1–SPA1 Dissociation and Photomorphogenic Development in Arabidopsis. *Molecular Plant,* 8**,** 467-478.

LUCCIONI, L., KRZYMUSKI, M., SANCHEZ-LAMAS, M., KARAYEKOV, E., CERDAN, P. D. & CASAL, J. J. 2019. CONSTANS delays Arabidopsis flowering under short days. *Plant J,* 97**,** 923-932.

MALAPEIRA, J., KHAITOVA, L. C. & MAS, P. 2012. Ordered changes in histone modifications at the core of the Arabidopsis circadian clock. *Proc Natl Acad Sci U S A,* 109**,** 21540-5.

MARTÍNEZ-GARCÍA, J. F., HUQ, E. & QUAIL, P. H. 2000. Direct Targeting of Light Signals to a Promoter Element-Bound Transcription Factor. *Science,* 288**,** 859-863.

MÁS, P., ALABADÍ, D., YANOVSKY, M. J., OYAMA, T. & KAY, S. A. 2003. Dual Role of TOC1 in the Control of Circadian and Photomorphogenic Responses in Arabidopsis. *The Plant Cell,* 15**,** 223-236.

MAS, P., KIM, W. Y., SOMERS, D. E. & KAY, S. A. 2003. Targeted degradation of TOC1 by ZTL modulates circadian function in Arabidopsis thaliana. *Nature,* 426**,** 567-70.

MATERA, A. G., IZAGUIRE-SIERRA, M., PRAVEEN, K. & RAJENDRA, T. K. 2009. Nuclear bodies: random aggregates of sticky proteins or crucibles of macromolecular assembly? *Dev Cell,* 17**,** 639-47.

MATSUSHIKA, A., MAKINO, S., KOJIMA, M. & MIZUNO, T. 2000. Circadian waves of expression of the APRR1/TOC1 family of pseudo-response regulators in Arabidopsis thaliana: insight into the plant circadian clock. *Plant Cell Physiol,* 41**,** 1002-12.

MCCLUNG, C. R. 2006. Plant circadian rhythms. *The Plant Cell,* 18**,** 792-803.

MCWATTERS, H. G., BASTOW, R. M., HALL, A. & MILLAR, A. J. 2000. The ELF3 zeitnehmer regulates light signalling to the circadian clock. *Nature,* 408**,** 716-20.

MCWATTERS, H. G., KOLMOS, E., HALL, A., DOYLE, M. R., AMASINO, R. M., GYULA, P., NAGY, F., MILLAR, A. J. & DAVIS, S. J. 2007. ELF4 is required for oscillatory properties of the circadian clock. *Plant Physiology,* 144**,** 391-401.

MILLAR, A. J. 2004. Input signals to the plant circadian clock. *Journal of Experimental Botany,* 55**,** 277-283.

MILLAR, A. J., SHORT, S. R., CHUA, N. H. & KAY, S. A. 1992. A novel circadian phenotype based on firefly luciferase expression in transgenic plants. *The Plant Cell,* 4**,** 1075-87.

MIZUNO, T., NOMOTO, Y., OKA, H., KITAYAMA, M., TAKEUCHI, A., TSUBOUCHI, M. & YAMASHINO, T. 2014. Ambient temperature signal feeds into the circadian clock transcriptional circuitry through the EC night-time repressor in Arabidopsis thaliana. *Plant Cell Physiol,* 55**,** 958-76.

MOLAS, M. L., KISS, J. Z. & CORRELL, M. J. 2006. Gene profiling of the red light signalling pathways in roots. *Journal of Experimental Botany,* 57**,** 3217-3229.

MWIMBA, M., KARAPETYAN, S., LIU, L., MARQUES, J., MCGINNIS, E. M., BUCHLER, N. E. & DONG, X. 2018. Daily humidity oscillation regulates the circadian clock to influence plant physiology. *Nat Commun,* 9**,** 4290.

NAKAMICHI, N., KIBA, T., HENRIQUES, R., MIZUNO, T., CHUA, N.-H. & SAKAKIBARA, H. 2010. PSEUDO-RESPONSE REGULATORS 9, 7, and 5 Are Transcriptional Repressors in the Arabidopsis Circadian Clock. *The Plant Cell,* 22**,** 594-605.

NAKAMICHI, N., KITA, M., NIINUMA, K., ITO, S., YAMASHINO, T., MIZOGUCHI, T. & MIZUNO, T. 2007. Arabidopsis Clock-Associated Pseudo-Response Regulators

PRR9, PRR7 and PRR5 Coordinately and Positively Regulate Flowering Time Through the Canonical CONSTANS-Dependent Photoperiodic Pathway. *Plant and Cell Physiology,* 48**,** 822-832.

NIETO, C., LOPEZ-SALMERON, V., DAVIERE, J. M. & PRAT, S. 2015. ELF3-PIF4 interaction regulates plant growth independently of the Evening Complex. *Curr Biol,* 25**,** 187-193.

NIMMO, H. G. 2018. Entrainment of Arabidopsis roots to the light:dark cycle by light piping. *Plant Cell Environ,* 41**,** 1742-1748.

NIMMO, H. G., LAIRD, J., BINDBEUTEL, R. & NUSINOW, D. A. 2020. The evening complex is central to the difference between the circadian clocks of Arabidopsis thaliana shoots and roots. *Physiol Plant*.

NIWA, Y., YAMASHINO, T. & MIZUNO, T. 2009. The circadian clock regulates the photoperiodic response of hypocotyl elongation through a coincidence mechanism in Arabidopsis thaliana. *Plant Cell Physiol,* 50**,** 838-54.

NOHALES, M. A., LIU, W., DUFFY, T., NOZUE, K., SAWA, M., PRUNEDA-PAZ, J. L., MALOOF, J. N., JACOBSEN, S. E. & KAY, S. A. 2019. Multi-level Modulation of Light Signaling by GIGANTEA Regulates Both the Output and Pace of the Circadian Clock. *Developmental Cell,* 49**,** 840-851.e8.

NOMOTO, Y., KUBOZONO, S., YAMASHINO, T., NAKAMICHI, N. & MIZUNO, T. 2012. Circadian clock- and PIF4-controlled plant growth: a coincidence mechanism directly integrates a hormone signaling network into the photoperiodic control of plant architectures in Arabidopsis thaliana. *Plant Cell Physiol,* 53**,** 1950-64.

NUSINOW, D. A., HELFER, A., HAMILTON, E. E., KING, J. J., IMAIZUMI, T., SCHULTZ, T. F., FARRE, E. M. & KAY, S. A. 2011. The ELF4-ELF3-LUX complex links the circadian clock to diurnal control of hypocotyl growth. *Nature,* 475**,** 398-402.

O'NEILL, J. S. & REDDY, A. B. 2011. Circadian clocks in human red blood cells. *Nature,* 469**,** 498-503.

OAKENFULL, R. J. & DAVIS, S. J. 2017. Shining a light on the Arabidopsis circadian clock. *Plant Cell Environ,* 40**,** 2571-2585.

ODAKA, Y., MALLY, A., ELLIOTT, L. T. & MEYERS, S. 2000. Nuclear import and subnuclear localization of the proto-oncoprotein ETO (MTG8). *Oncogene,* 19**,** 3584-3597.

OH, J., PARK, E., SONG, K., BAE, G. & CHOI, G. 2020. PHYTOCHROME INTERACTING FACTOR8 Inhibits Phytochrome A-Mediated Far-Red Light Responses in Arabidopsis. *The Plant Cell,* 32**,** 186-205.

ÖLLINGER, R., KORGE, S., KORTE, T., KOLLER, B., HERRMANN, A. & KRAMER, A. 2014. Dynamics of the circadian clock protein PERIOD2 in living cells. *Journal of Cell Science,* 127**,** 4322.

ONAI, K. & ISHIURA, M. 2005. PHYTOCLOCK 1 encoding a novel GARP protein essential for the Arabidopsis circadian clock. *Genes Cells,* 10**,** 963-72.

PARA, A., FARRE, E. M., IMAIZUMI, T., PRUNEDA-PAZ, J. L., HARMON, F. G. & KAY, S. A. 2007. PRR3 Is a vascular regulator of TOC1 stability in the Arabidopsis circadian clock. *The Plant Cell,* 19**,** 3462-73.

PARK, H. J., BAEK, D., CHA, J. Y., LIAO, X., KANG, S. H., MCCLUNG, C. R., LEE, S. Y., YUN, D. J. & KIM, W. Y. 2019. HOS15 Interacts with the Histone Deacetylase HDA9 and the Evening Complex to Epigenetically Regulate the Floral Activator GIGANTEA. *The Plant Cell,* 31**,** 37-51.

PERALES, M. & MAS, P. 2007. A functional link between rhythmic changes in chromatin structure and the Arabidopsis biological clock. *The Plant Cell,* 19**,** 2111-23.

PHAM, V. N., KATHARE, P. K. & HUQ, E. 2018. Phytochromes and Phytochrome Interacting Factors. *Plant Physiology,* 176**,** 1025-1038.

PITTENDRIGH, C. S. & MINIS, D. H. 1964. The Entrainment of Circadian Oscillations by Light and Their Role as Photoperiodic Clocks. *The American Naturalist,* 98**,** 261-294.

PRESS, M. O., LANCTOT, A. & QUEITSCH, C. 2016. PIF4 and ELF3 Act Independently in Arabidopsis thaliana Thermoresponsive Flowering. *PLOS ONE,* 11**,** e0161791.

PRESS, M. O. & QUEITSCH, C. 2017. Variability in a Short Tandem Repeat Mediates Complex Epistatic Interactions in Arabidopsis thaliana. *Genetics,* 205**,** 455-464.

PRUNEDA-PAZ, J. L., BRETON, G., PARA, A. & KAY, S. A. 2009. A functional genomics approach reveals CHE as a component of the Arabidopsis circadian clock. *Science,* 323**,** 1481-5.

QIU, Y., PASORECK, E. K., REDDY, A. K., NAGATANI, A., MA, W., CHORY, J. & CHEN, M. 2017. Mechanism of early light signaling by the carboxy-terminal output module of Arabidopsis phytochrome B. *Nat Commun,* 8**,** 1905.

QUINT, M., DELKER, C., FRANKLIN, K. A., WIGGE, P. A., HALLIDAY, K. J. & VAN ZANTEN, M. 2016. Molecular and genetic control of plant thermomorphogenesis. *Nature Plants,* 2**,** 15190.

RASCHKE, A., IBAÑEZ, C., ULLRICH, K. K., ANWER, M. U., BECKER, S., GLÖCKNER, A., TRENNER, J., DENK, K., SAAL, B., SUN, X., NI, M., DAVIS, S. J., DELKER, C. & QUINT, M. 2015. Natural variants of ELF3 affect thermomorphogenesis by transcriptionally modulating PIF4-dependent auxin response genes. *BMC plant biology,* 15**,** 197-197.

REED, J. W., NAGPAL, P., BASTOW, R. M., SOLOMON, K. S., DOWSON-DAY, M. J., ELUMALAI, R. P. & MILLAR, A. J. 2000. Independent Action of ELF3 and phyB to Control Hypocotyl Elongation and Flowering Time. *Plant Physiology,* 122**,** 1149-1160.

REED, J. W., NAGPAL, P., POOLE, D. S., FURUYA, M. & CHORY, J. 1993. Mutations in the gene for the red/far-red light receptor phytochrome B alter cell elongation and physiological responses throughout Arabidopsis development. *The Plant Cell,* 5**,** 147-157.

ROCKWELL, N. C., SU, Y.-S. & LAGARIAS, J. C. 2006. PHYTOCHROME STRUCTURE AND SIGNALING MECHANISMS. *Annual Review of Plant Biology,* 57**,** 837-858.

RODEN, L. C., SONG, H.-R., JACKSON, S., MORRIS, K. & CARRE, I. A. 2002. Floral responses to photoperiod are correlated with the timing of rhythmic expression relative to dawn and dusk in Arabidopsis. *Proc Natl Acad Sci U S A,* 99**,** 13313-13318.

ROENNEBERG, T. & MERROW, M. 2016. The Circadian Clock and Human Health. *Curr Biol,* 26**,** R432-43.

RONALD, J. & DAVIS, S. J. 2017. Making the clock tick: the transcriptional landscape of the plant circadian clock. *F1000Res,* 6**,** 951.

RONALD, J. & DAVIS, S. J. 2019. Focusing on the nuclear and subnuclear dynamics of light and circadian signalling. *Plant Cell Environ,* 42**,** 2871-2884.

RÖSLER, J., JAEDICKE, K. & ZEIDLER, M. 2010. Cytoplasmic Phytochrome Action. *Plant and Cell Physiology,* 51**,** 1248-1254.

RUGNONE, M. L., FAIGÓN SOVERNA, A., SANCHEZ, S. E., SCHLAEN, R. G., HERNANDO, C. E., SEYMOUR, D. K., MANCINI, E., CHERNOMORETZ, A., WEIGEL, D., MÁS, P. & YANOVSKY, M. J. 2013. LNK genes integrate light and clock signaling networks at the core of the Arabidopsis oscillator. *Proc Natl Acad Sci U S A,* 110**,** 12120-12125.

SAINI, R., JASKOLSKI, M. & DAVIS, S. J. 2019. Circadian oscillator proteins across the kingdoms of life: structural aspects. *BMC Biology,* 17**,** 13.

SAITO, H., OGISO-TANAKA, E., OKUMOTO, Y., YOSHITAKE, Y., IZUMI, H., YOKOO, T., MATSUBARA, K., HORI, K., YANO, M., INOUE, H. & TANISAKA, T. 2012. Ef7 Encodes an ELF3-like Protein and Promotes Rice Flowering by Negatively Regulating the Floral Repressor Gene Ghd7 under Both Short- and Long-Day Conditions. *Plant and Cell Physiology,* 53**,** 717-728.

SALOME, P. A., WEIGEL, D. & MCCLUNG, C. R. 2010. The role of the Arabidopsis morning loop components CCA1, LHY, PRR7, and PRR9 in temperature compensation. *The Plant Cell,* 22**,** 3650-61.

SAWA, M. & KAY, S. A. 2011. GIGANTEA directly activates Flowering Locus T in Arabidopsis thaliana. *Proc Natl Acad Sci U S A,* 108**,** 11698-703.

SAWA, M., NUSINOW, D. A., KAY, S. A. & IMAIZUMI, T. 2007. FKF1 and GIGANTEA complex formation is required for day-length measurement in Arabidopsis. *Science,* 318**,** 261-5.

SEO, P. J., PARK, M. J., LIM, M. H., KIM, S. G., LEE, M., BALDWIN, I. T. & PARK, C. M. 2012. A self-regulatory circuit of CIRCADIAN CLOCK-ASSOCIATED1 underlies the circadian clock regulation of temperature responses in Arabidopsis. *The Plant Cell,* 24**,** 2427-42.

SHARROCK, R. A. & CLACK, T. 2004. Heterodimerization of type II phytochromes in Arabidopsis. *Proc Natl Acad Sci U S A,* 101**,** 11500.

SHIKATA, H., HANADA, K., USHIJIMA, T., NAKASHIMA, M., SUZUKI, Y. & MATSUSHITA, T. 2014. Phytochrome controls alternative splicing to mediate light responses in Arabidopsis. *Proc Natl Acad Sci U S A,* 111**,** 18781-6.

SHIM, J. S., KUBOTA, A. & IMAIZUMI, T. 2017. Circadian Clock and Photoperiodic Flowering in Arabidopsis: CONSTANS Is a Hub for Signal Integration. *Plant Physiology,* 173**,** 5-15.

SIDDIQUI, H., KHAN, S., RHODES, B. M. & DEVLIN, P. F. 2016. FHY3 and FAR1 Act Downstream of Light Stable Phytochromes. *Frontiers in plant science,* 7.

SILVA, C. S., NAYAK, A., LAI, X., HUTIN, S., HUGOUVIEUX, V., JUNG, J. H., LOPEZ-VIDRIERO, I., FRANCO-ZORRILLA, J. M., PANIGRAHI, K. C. S., NANAO, M. H., WIGGE, P. A. & ZUBIETA, C. 2020. Molecular mechanisms of Evening Complex activity in Arabidopsis. *Proc Natl Acad Sci U S A,* 117**,** 6901-6909.

SOMERS, D. E., DEVLIN, P. F. & KAY, S. A. 1998. Phytochromes and cryptochromes in the entrainment of the Arabidopsis circadian clock. *Science,* 282**,** 1488-90.

SONG, H. R. & NOH, Y. S. 2012. Rhythmic oscillation of histone acetylation and methylation at the Arabidopsis central clock loci. *Mol Cells,* 34**,** 279-87.

SONG, Y. H., KUBOTA, A., KWON, M. S., COVINGTON, M. F., LEE, N., TAAGEN, E. R., LABOY CINTRÓN, D., HWANG, D. Y., AKIYAMA, R., HODGE, S. K., HUANG, H., NGUYEN, N. H., NUSINOW, D. A., MILLAR, A. J., SHIMIZU, K. K. & IMAIZUMI, T. 2018. Molecular basis of flowering under natural long-day conditions in Arabidopsis. *Nature Plants,* 4**,** 824-835.

SONG, Y. H., SHIM, J. S., KINMONTH-SCHULTZ, H. A. & IMAIZUMI, T. 2015. Photoperiodic flowering: time measurement mechanisms in leaves. *Annu Rev Plant Biol,* 66**,** 441-64.

SRIKANTH, A. & SCHMID, M. 2011. Regulation of flowering time: all roads lead to Rome. *Cell Mol Life Sci,* 68**,** 2013-37.

SUN, J., QI, L., LI, Y., CHU, J. & LI, C. 2012. PIF4–Mediated Activation of YUCCA8 Expression Integrates Temperature into the Auxin Pathway in Regulating Arabidopsis Hypocotyl Growth. *PLOS Genetics,* 8**,** e1002594.

TAJIMA, T., ODA, A., NAKAGAWA, M., KAMADA, H. & MIZOGUCHI, T. 2007. Natural variation of polyglutamine repeats of a circadian clock gene ELF3 in Arabidopsis. *Plant Biotechnology,* 24**,** 237-240.

TAKAHASHI, N., HIRATA, Y., AIHARA, K. & MAS, P. 2015. A hierarchical multi-oscillator network orchestrates the Arabidopsis circadian system. *Cell,* 163**,** 148-59.

TAKEUCHI, T., NEWTON, L., BURKHARDT, A., MASON, S. & FARRE, E. M. 2014. Light and the circadian clock mediate time-specific changes in sensitivity to UV-B stress under light/dark cycles. *J Exp Bot,* 65**,** 6003-12.

TAOKA, K., OHKI, I., TSUJI, H., FURUITA, K., HAYASHI, K., YANASE, T., YAMAGUCHI, M., NAKASHIMA, C., PURWESTRI, Y. A., TAMAKI, S., OGAKI, Y., SHIMADA, C., NAKAGAWA, A., KOJIMA, C. & SHIMAMOTO, K. 2011. 14-3-3 proteins act as intracellular receptors for rice Hd3a florigen. *Nature,* 476**,** 332-5.

TEPPERMAN, J. M., ZHU, T., CHANG, H. S., WANG, X. & QUAIL, P. H. 2001. Multiple transcription-factor genes are early targets of phytochrome A signaling. *Proc Natl Acad Sci U S A,* 98**,** 9437-9442.

THINES, B. & HARMON, F. G. 2010. Ambient temperature response establishes ELF3 as a required component of the core Arabidopsis circadian clock. *Proc Natl Acad Sci U S A,* 107**,** 3257.

TONG, M., LEE, K., EZER, D., CORTIJO, S., JUNG, J., CHAROENSAWAN, V., BOX, M. S., JAEGER, K. E., TAKAHASHI, N., MAS, P., WIGGE, P. A. & SEO, P. J. 2020. The Evening Complex Establishes Repressive Chromatin Domains Via H2A.Z Deposition. *Plant Physiology,* 182**,** 612-625.

UNDURRAGA, S. F., PRESS, M. O., LEGENDRE, M., BUJDOSO, N., BALE, J., WANG, H., DAVIS, S. J., VERSTREPEN, K. J. & QUEITSCH, C. 2012. Background-dependent effects of polyglutamine variation in the Arabidopsis thaliana gene ELF3. *Proc Natl Acad Sci U S A***,** 201211021.

VALVERDE, F., MOURADOV, A., SOPPE, W., RAVENSCROFT, D., SAMACH, A. & COUPLAND, G. 2004. Photoreceptor regulation of CONSTANS protein in photoperiodic flowering. *Science,* 303**,** 1003-6.

VAN BUSKIRK, E. K., DECKER, P. V. & CHEN, M. 2012. Photobodies in Light Signaling. *Plant Physiology,* 158**,** 52.

VAN BUSKIRK, E. K., REDDY, A. K., NAGATANI, A. & CHEN, M. 2014. Photobody Localization of Phytochrome B Is Tightly Correlated with Prolonged and Light-Dependent Inhibition of Hypocotyl Elongation in the Dark. *Plant Physiology,* 165**,** 595-607.

VENKATESH, S. & WORKMAN, J. L. 2015. Histone exchange, chromatin structure and the regulation of transcription. *Nat Rev Mol Cell Biol,* 16**,** 178-89.

WANG, C.-Q., SARMAST, M. K., JIANG, J. & DEHESH, K. 2015a. The Transcriptional Regulator BBX19 Promotes Hypocotyl Growth by Facilitating COP1-Mediated EARLY FLOWERING3 Degradation in Arabidopsis. *The Plant cell,* 27**,** 1128-1139.

WANG, L., FUJIWARA, S. & SOMERS, D. E. 2010. PRR5 regulates phosphorylation, nuclear import and subnuclear localization of TOC1 in the Arabidopsis circadian clock. *EMBO J,* 29**,** 1903-15.

WANG, L., KIM, J. & SOMERS, D. E. 2013. Transcriptional corepressor TOPLESS complexes with pseudoresponse regulator proteins and histone deacetylases to regulate circadian transcription. *Proc Natl Acad Sci U S A,* 110**,** 761-6.

WANG, W., BARNABY, J. Y., TADA, Y., LI, H., TÖR, M., CALDELARI, D., LEE, D. U., FU, X. D. & DONG, X. 2011a. Timing of plant immune responses by a central circadian regulator. *Nature,* 470**,** 110-4.

WANG, X., WANG, Q., HAN, Y.-J., LIU, Q., GU, L., YANG, Z., SU, J., LIU, B., ZUO, Z., HE, W., WANG, J., LIU, B., MATSUI, M., KIM, J.-I., OKA, Y. & LIN, C. 2017. A CRY–BIC negative-feedback circuitry regulating blue light sensitivity of Arabidopsis. *Plant J,* 92**,** 426-436.

WANG, X., WU, F., XIE, Q., WANG, H., WANG, Y., YUE, Y., GAHURA, O., MA, S., LIU, L., CAO, Y., JIAO, Y., PUTA, F., MCCLUNG, C. R., XU, X. & MA, L. 2012. SKIP is a component of the spliceosome linking alternative splicing and the circadian clock in Arabidopsis. *The Plant Cell,* 24**,** 3278-95.

WANG, Y., WU, J.-F., NAKAMICHI, N., SAKAKIBARA, H., NAM, H.-G. & WU, S.-H. 2011b. LIGHT-REGULATED WD1 and PSEUDO-RESPONSE REGULATOR9 Form a Positive Feedback Regulatory Loop in the Arabidopsis Circadian Clock. *The Plant Cell,* 23**,** 486.

WANG, Z., CASAS-MOLLANO, J. A., XU, J., RIETHOVEN, J. J., ZHANG, C. & CERUTTI, H. 2015b. Osmotic stress induces phosphorylation of histone H3 at threonine 3 in pericentromeric regions of Arabidopsis thaliana. *Proc Natl Acad Sci U S A,* 112**,** 8487-92.

WANG, Z.-Y. & TOBIN, E. M. 1998. Constitutive Expression of the CIRCADIAN CLOCK ASSOCIATED 1 (CCA1) Gene Disrupts Circadian Rhythms and Suppresses Its Own Expression. *Cell,* 93**,** 1207-1217.

WEBB, A. A. R., SEKI, M., SATAKE, A. & CALDANA, C. 2019. Continuous dynamic adjustment of the plant circadian oscillator. *Nat Commun,* 10**,** 550.

WU, J. F., TSAI, H. L., JOANITO, I., WU, Y. C., CHANG, C. W., LI, Y. H., WANG, Y., HONG, J. C., CHU, J. W., HSU, C. P. & WU, S. H. 2016. LWD-TCP complex activates the morning gene CCA1 in Arabidopsis. *Nat Commun,* 7**,** 13181.

XIE, Q., WANG, P., LIU, X., YUAN, L., WANG, L., ZHANG, C., LI, Y., XING, H., ZHI, L., YUE, Z., ZHAO, C., MCCLUNG, C. R. & XU, X. 2014. LNK1 and LNK2 Are Transcriptional Coactivators in the Arabidopsis Circadian Oscillator. *The Plant Cell,* 26**,** 2843-2857.

XIE, Y., TANG, Q., CHEN, G., XIE, M., YU, S., ZHAO, J. & CHEN, L. 2019. New Insights Into the Circadian Rhythm and Its Related Diseases. *Frontiers in Physiology,* 10.

XING, H., WANG, P., CUI, X., ZHANG, C., WANG, L., LIU, X., YUAN, L., LI, Y., XIE, Q. & XU, X. 2015. LNK1 and LNK2 recruitment to the evening element require morning expressed circadian related MYB-like transcription factors. *Plant Signal Behav,* 10**,** e1010888.

YAKIR, E., HILMAN, D., KRON, I., HASSIDIM, M., MELAMED-BOOK, N. & GREEN, R. M. 2009. Posttranslational regulation of CIRCADIAN CLOCK ASSOCIATED1 in the circadian oscillator of Arabidopsis. *Plant Physiology,* 150**,** 844-857.

YANOVSKY, M. J., MAZZELLA, M. A. & CASAL, J. J. 2000. A quadruple photoreceptor mutant still keeps track of time. *Curr Biol,* 10**,** 1013-5.

YEOM, M., KIM, H., LIM, J., SHIN, A. Y., HONG, S., KIM, J. I. & NAM, H. G. 2014. How do phytochromes transmit the light quality information to the circadian clock in Arabidopsis? *Molecular Plant,* 7**,** 1701-1704.

YU, J. W., RUBIO, V., LEE, N. Y., BAI, S., LEE, S. Y., KIM, S. S., LIU, L., ZHANG, Y., IRIGOYEN, M. L., SULLIVAN, J. A., ZHANG, Y., LEE, I., XIE, Q., PAEK, N. C. & DENG, X. W. 2008. COP1 and ELF3 control circadian function and photoperiodic flowering by regulating GI stability. *Mol Cell,* 32**,** 617-30.

ZAGOTTA, M. T., HICKS, K. A., JACOBS, C. I., YOUNG, J. C., HANGARTER, R. P. & MEEKS-WAGNER, D. R. 1996. The Arabidopsis ELF3 gene regulates vegetative photomorphogenesis and the photoperiodic induction of flowering. *Plant J,* 10**,** 691-702.

ZHANG, L. L., SHAO, Y. J., DING, L., WANG, M. J., DAVIS, S. J. & LIU, J. X. 2021. XBAT31 regulates thermoresponsive hypocotyl growth through mediating degradation of the thermosensor ELF3 in <em>Arabidopsis</em&gt. *Science Advances,* 7**,** eabf4427.

ZHU, J.-Y., OH, E., WANG, T. & WANG, Z.-Y. 2016. TOC1–PIF4 interaction mediates the circadian gating of thermoresponsive growth in Arabidopsis. *Nat Commun,* 7**,** 13692.

ZHU, Z., QUINT, M. & ANWER, M. U. 2020. EARLY FLOWERING 3 controls temperature responsiveness of the circadian clock. *bioRxiv***,** 2020.11.11.378307.

ZHU, Z., XU, F., ZHANG, Y., CHENG, Y. T., WIERMER, M., LI, X. & ZHANG, Y. 2010. Arabidopsis resistance protein SNC1 activates immune responses through association with a transcriptional corepressor. *Proc Natl Acad Sci U S A,* 107**,** 13960-5.

ZIELINSKI, T., MOORE, A. M., TROUP, E., HALLIDAY, K. J. & MILLAR, A. J. 2014. Strengths and limitations of period estimation methods for circadian data. *PLOS ONE,* 9**,** e96462.

ZOLTOWSKI, B. D. & IMAIZUMI, T. 2014. Structure and Function of the ZTL/FKF1/LKP2 Group Proteins in Arabidopsis. *The Enzymes,* 35**,** 213-239.

Appendix 1

Proteins sequence used in ELF3 tracheophyte alignment

>AT_AraTh_AT2G25930
MKRGKDEEKILEPMFPRLHVNDADKGGPRAPPRNKMALYEQLSIPSQRFGDHGTMNSRSNNTSTLVHPG
PSSQPCGVERNLSVQHLDSSAANQATEKFVSQMSFMENVRSSAQHDQRKMVREEEDFAVPVYINSRRS
QSHGRTKSGIEKEKHTPMVAPSSHHSIRFQEVNQTGSKQNVCLATCSKPEVRDQVKANARSGGFVISLDV
SVTEEIDLEKSASSHDRVNDYNASLRQESRNRLYRDGGKTRLKDTDNGAESHLATENHSQEGHGSPEDID
NDREYSKSRACASLQQINEEASDDVSDDSMVDSISSIDVSPDDVVGILGQKRFWRARKAIANQQRVFAVQ
LFELHRLIKVQKLIAASPDLLLDEISFLGKVSAKSYPVKKLLPSEFLVKPPLPHVVVKQRGDSEKTDQHKMES
SAENVVGRLSNQGHHQQSNYMPFANNPPASPAPNGYCFPPQPPPSGNHQQWLIPVMSPSEGLIYKPHP
GMAHTGHYGGYYGHYMPTPMVMPQYHPGMGFPPPGNGYFPPYGMMPTIMNPYCSSQQQQQQQPNE
QMNQFGHPGNLQNTQQQQQRSDNEPAPQQQQQPTKSYPRARKSRQGSTGSSPSGPQGISGSKSFRPF
AAVDEDSNINNAPEQTMTTTTTTTRTTVTQTTRDGGGVTRVIKVVPHNAKLASENAARIFQSIQEERKRYD
SSKP

>AL_AraLy_AL4G18010.t1
MKRGKDEEKILEPMFPRLHVNDADKGGPRAPPRNKMALYEQLSIPSQRFGDHGTLRSNNTSTLVHPGPS
NQPCGVERNLSAQHLDSSAANQATEKFVSQMSFMENVRSVAQHDQRKMVREEEDFAVPVYINSRRSQG
HGRNKTGIEKEKHTPLVEPSPRNSLQFQEVNRTSSKQNVRSKPEGRDQVKAKAKSGGFVISLDLSVTEEID
LEKSASSYDRVNDCNASLRQESRNRLYRDGGETRVKDTDNGAESHLETESHSEDGHCSPEDIDTGREYS
RSRGCASLQQINEEASDDVSDDSMVDSISSMDVSPDDVVGILGQKRFWRARKAIANQQRVFAVQLFELHR
LIKVQKLIAASPDLLLDEINFLGKVSAKSYPVKKLLPSEFLVKPPIPHVVVKQRGDSEKTDQHKMESSAENVV
GRFSNQGHHQQSNYMPFANNPPASPAANGYCYPPQPPPSGNQQWLIPVMSPSEGLIYKPHPGMGHTG
HYGGYYGHYMPTPMVMPQYHPGMGFPPPGNGYFPPYGIMPTMMNPYCSGQQQQQQQPNDQMNQFG
HHGNLQNTQQQQSSVNAAAALQHQQPTKSYPRARKSRQGSTGSSPSGPQGISGSKSFRPFSAVDEDSKI
NNAPEQMMTTTTTTSTTVTQTTRDGGGVTRVIKVVPHNAKLASENAARIFQSIQEERQRYDSSKP

>OS1_OrySa_Os06g05060.1
MATRGGGGGGGGKEAKGKVMGPLFPRLHVNDAAKGGGPRAPPRNKMALYEQFTVPSHRFSGGGGGG
GVGGSPAHSTSAASQSQSQSQVYGRDSSLFQPFNVPSNRPGHSTEKINSDKINKKISGSRKELGMLSSQT
KGMDIYASRSTAEAPQRRAENTIKSSSGKRLADDDEFMVPSVFNSRFPQYSTQENAGVQDQSTPLVAAN
PHKSPSTVSKSSTKCYNTVSKKLERIHVSDVKSRTPLKDKEMEAAQTSKNVEVEKSSSFHASKDMFESRH
AKVYPKMDKTGIINDSDEPHGGNSGHQATSRNGGSMKFQNPPMRRNEISSNPSSENTDRHYNLPQGGIE
ETGTKRKRLLEQHDAEKSDDVSRLLEQHDAENIDDVSDSSVECITGWEISPDKIVGAIGTKHFWKARRAIM
NQQRVFAVQVFELHKLVKVQKLIAASPHVLIESDPCLGNALLGSKNKLVEENLKAQPLLVATIDDVEPSLQQ
PEVSKENTEDSPPSPHDTGLGSGQRDQAATNGVSKSNRRATPVASDNKQNNWGVQLQPPQNQWLVPV
MSPLEGLVYKPYSGPCPPAGSILAPFYANCTPLSLPSTAGDFMNSAYGVPMPHQPQHMGAPGPPSMPM
NYFPPFSIPVMNPTAPAPVVEQGRHPSMPQPYGNFEQQSWISCNMSHPSGIWRFHASRDSEAQASSASS
PFDRFQCSGSGPVSAFPTVSAQNNQPQPSYSSRDNQTNVIKVVPHNSRTASESAARIFRSIQMERQRDD*

>OS2_LOC_Os01g38530.1
MRGGGGGGKEVEERGKVMGPLFPRLHVNDAAKGGGPRAPPRNKMALYEQFTVPSHRFSGGGGALASA
RGSLARSTSAASQSQVYGCDMPLFEPFNVPSNGPGQSVEKMNSNSVNRQINGSRKDSGMLSTQPKGID
KYGSGSRAECAPQQRVEKGIKSSSGRKLADDDEFIVPSVFSARFPQYSTKERAGVQEESTPLVALSPHKS
PPAVSKSPTKCYNTVSKNLERINVSDVKSRGSQKDKETGPAQTLKNVEVEHFSSFEASKDMFGSKHAKVC
PKTGTINDLDEPHLENSEHQATSRNGSSVKFQNPPVRRNTISAKPSPGIENTNGHCNLPQGGLKEAGTKR
KRLEAQDNAEKIDDLSDSSVECITAWEISPDEIVGAIGAKHFWKARRAIINQQRVFAAQVFELHKLVKVQKLI
AASPHVLIEGDPCLGNALLASKKKMAEENLKAQPVLVATNDDVQPSLQEPELSKENSEENPPSPRDTAPV
SGHHDQTAKIGASKSNLRATPVASDNRQNNCGVQLQPPQNQWLIPVMSPSEGLVYKPYSGPCPPAGSIL
APFYANCTPLRLPSTTGDFMNSAYGVPIPHQPQHMGAPGTPTMPMNYFPPFSVPVMNPVALASAVEQGR
HPSMPQPYGNLEQHSRMSCNMSHPSGIWRFHASRDSEAQASSASSPFDRLQCGGSGPVSAFPTASAQ
NTQPQPSSGSRDNQTNVIRVIPHNNSQTASESAARIFRSIQMERQQDDS*

>ZM1_GRMZM2G045275_T01
MTRGGGGQGGKEEPGKVMGPLFPRLHVSDAGKGGGPRAPPRNKMALYEQFTVPSNRFSSPAASARAA
GASLVPSTAAAQVYGYDRTLFQPFDVPSNEPPRSSEKFKGNTINGQSNSTRREPLRMSSQTKNKDVCAS
KSIAKCTSQHRVGNTIMSSGKKVVSDDEFMVPSICYPRFYRQSTQDHADKSKPQSTTNPHKSPAMSKSSV
ECYSTVNKHLDKINEADRRLMNSPKVKEKEAVQGSKAVEVKEKSSSFQASEKFKDKYAKLCQMRNKASNI
NHCDNNGCQPASVNGNFTEAKNPTAARNTSSCKPCTDVDSSNRKSNLLERSPREVGAKRKRGHHNGEQ
NDDLSDSSVECIPGGEISPDEIVAAIGPKHFWKARRAIQNQQRVFAVQVFELHKLIKVQKLIAASPHLLIEGD
PVLGNALTGKRNKLPKGNSKVQTLSITNKDDIQPTLEQPELSKQDTEGNLLAHSHDDGLGDNHHNQAATN
ETFTSNPPAMHVAPDNKQNNWCMNPPQNQWLVPVMSPSEGLVYKPFAGPCPPVGNLLTPFYANCAPSR
LPSTPYGVPIPHQPQHMVPPGAPAMHMNYFPPFSMPVMNPGTPASAVEQGSHAAAPQPHGHMDQQSLI
SCNMSHPSGVWRFLASRDSEPQASSATSPFDRLQVQGDGSAPLSFFPTASAPNVQPPPSSGGRDRDQQ
NHVIRVVPRNAQTASVPKAQPQPSSGGRDQKNHVIRVVPHNAQTASESAAWIFRSIQMERNQNDS*

>ZM2_AC233870.1_FGT003
MRRGATKDDAAPDKVMGPLFPRLHVNDTLKGGPRAPPRNKMALYEQFSVPSHRYSAAVPPAPSPAPPW
GAQRPASAVPSTSASQVGGGDRPIFPLFRVPSTEPVRSSDQTNANSNGQGANGTIAESGRQRQSTHLKS
KDTNAAGPPAEGNNSVGKKLANDDDFTVPSVLYSGMPPHSSQEKLTLFPTTSPCKSVPAKYSSTDKRRLE
GMDASDVKSKGPSGIKEKEPVQVRIDLEDKETTPSFQVLNDKTWSPDPKLSSHMDRLKKQHAEAESYQIR

TRNENAVETQSPPKNGVSLLSKPYVDRREQNGDSDLLGHGLRETGVKRKRSHHDVEQNDDLSDSSVESL
PGMEISPDDVVSAIGPKHFWKARRAIVNQQRVFAVQVFELHRLIKVQKLIAASPHVLIEGDPCLGKSLAVSK
KRLAGDVETQLESAKNDDGVRPTQLEHSKEKTEANQPSPSQDEQAATNGDVAASMHTPSDNKQKSWCI
PAPPSQWLIPVMSPSEGLVYKPYTGHCPPVGSLLAPPFFASYPTSSSSTAGGDFMSSACGARLMSAPVYF
PSFSMPAVSGSAVEQVSHVAASQHKRNSCSEAVLASRDSEVQGSSASSPASSETAAQPRVIRVVPHTAR
TASESAARIFRSIQMERKQNDP*

>PT1_Potri.006G233800.1
MKRGKDYDKIMGPMFPRLHVNDTDKGGPRAPPRNKMALYEQLSIPSQRFNPDVLPRNSSNTSDLAPTGS
SSQGSGLERHFPYPHYVPSPTPTDVAEKYHSRQPDGRNLNTPVAPLMQRKKVGEEDDFTVPVFVHSGK
GQGQTKMQTSAAQEKLASLCPTYLGHSSRIQNAGDNGHIGSTGLNLRPDTSNQSEDNLEVCVSSSDHIAR
HSTNLRTREKNDIPEEGNASQNQQYRNNLVSNFTRLHENDTCLQQETSARLQSNHSEHGDHVPESRRQK
EKINIFQPGNDSHLRKDCSSPNEPEIDSECFGDKTCGSLQFRNGDKSNDASETSMVDSVSVLDISPDDVV
GIIGQKHFWKARRAIANQQRVFSVQLFELHRLIKVQQLIAGSPHVLLEEEVHLAKPPMKGSPCKNLPSECA
VTPPVHVAKHKDNSENPNHKMECFAENAVGKTPFASVKNGQPPNFGPHAGPTTVPMASDTKMAPWCFH
PPPGLQWLVPVMSPSEGFVYKPYTAPGFMGSGCGGCGPFGPIPLTDNFMTSAYAIPTSHYHQGIGVSPG
APPVGNACFAPYGMPGMNPAISGSAGSGSCGQTAQFPGGILSSNMPHQSSCNERTQKSEAVLEGMKLR
ASKNTSVQGSTGSSPSGRVQGVGTVQAADGRAAFPPFPVTPPCPEGAPQHQETDQLSKVIKVVPHNGR
SATESVARIFQSIQEGRKQYDSL*

>PT2_Potri.003G045000.1
MRGAKDEEKMTSPMFPRLHVNDAEKGGPRAPPRNKMALYEQLCIPSQRFSSGSGSMLPVLPNNGSSLA
PSISSSHGTGHERSVFTPVSNSPTPLHLTEKLFYYSSGGVKSSALMTSQEEKFVEVTNDQNLNTSRPLSFS
ATCNSFQSHKVSDIKNFSWKKLGDENDSRFHSSAQSGSNLSCNNSQYSKDQENQHCLNLSFSVQFQNTS
ETQKKKTGTINVKEIDHMRIQIEDNGKVFEACQNSMEKFATVTSIKDKPSVSSSSGKISSTKSLKRTYSSSN
QEYRKNSVNVLKCLPGTNEQLNQELVTMPDKTVIGDNILVEYRVVTGKENPSKVRSELYSRALLQDDNRN
RCGLEKRSKYREDKQSGSLKAGDLERNDDAAETSMVDSVTALEITPDDVVGVIGEKQFWKARTAIVNQQR
VFAAQVFELHRLIKVQKLIAGSPHLLLEDNLYVGRASLKVSQINKVPSKCAMVDKPKDHSQKQHTSADFAG
ENVVGKLPLPSTNDETSKEPISQRSNYSGSAPPAPVATTAKPSPWCYPPPGNQWLVPVMSPSEGLVYKP
YAGPCPPVSRFMEPVYGSCGPISLAPGGGDFLNAAYSVSASNHEEIGILPGNPHFGQTFFQPFGMPVMNP
SICDSAVEQIRPRIGPQSKDNQLAVGDVNFNIPLQSSCNMSNQMSRVISCCVENFQGLKESEIQGSSAGSL
SKMPKANALPLFPMEPTLQASYPNAQTNEQQARVIKVVPHNRRSATESAARIFQSIQEERKQYD*

>MT1_Medtr3g103970.1
MKRGNDDEKVMGPLFPRLHVGDTEKGGPRAPPRNKMALYEQFSIPSQRFNLPPHHPNTSINTVPPSSSS
QGAVHERNYVFPGHLTPETLTRQSEGKNLNASLSQLEQRKKIDEDDFRVPVYIRSKIGQSNDKSHESFDG
KNLTSAGSRNFGFFKAGRINRERDLNNPRTDVRNEIDGPPQVSPNKEQPFTSARDTSNGESSNTSVRQA
KVIQNQEFQDRAVFKLSSSRQGDGCLHQDCRAESQSNGTGQRDASVESTREIGKSNDPIANQTSPTEAIN
GTEYHDTGTGSPIHSGNLNKNDNISKISRVEDLSTLKISPDDVVAIIGQKQFWKARKAIANQQRVFAVQVFE
LHRLIKVQQLIAGSPDLLFEDGAFLGKSLPDGSTPKKLALEYVVKPRLQNLKRKVDSENVNQNMECSAENA
VGKTSISSVKNGSHLSSSTPFAGNPHHGNMAAENGMGPWGFNQSPGHQWLIPVMSPSEGLVYKPYPGP
GFTGTNYGGSGPFGAPPSCGTFMNPSYGMPPPPETPPGSHAYYPPYGSMPFMKAAASESVVEHVNQFS
ARVQSRHLSEGEADCNKHNQSSCNLPVQRNGATTHVMHHQRSKEFELQMSTASSPSEMTQGMSTGQV
AEERDALPLFPMVPVEPEGVAQSIETGQQTRVIKVVPHNRRSATESAARIFQSIQEERKQYDTL*

>MT2_Medtr1g016920.1
MKRGKGGDDEKVGPMFPRLHVNDTTEKGGPRAPPRNKMALYEQFSVPFQRLNPNSHSSSSNSIPLTSSS
TMGNDLERSNIFPVRLPSQADAHRAKSYISHQSNGANLDTLSTQLEQGKKVDGDDSRAYDHSRIGQSNHK
MTNSFNGEKITLVIPSRQNTVISVKSALTGEIIDSRVRQGKKIPDEEDQECSVSNINRFPQGDSCTRQESNDI
EHSDGLLDTAMDMDNRNSFHSTVDRTMVLEAANDTEYHDANIDSPIQKGNSEGSGDLSNISTIENLSSLKL
SPDGVVQILGQQLFWKARRKITNQQRAFAVQVFELHRLIKVQHLIAGSSNLMLDAAAILEKFPLQESIPKSLS
LEVVVESQTKNHKQQDHSESLNHRLDCSAEKGVEKTSCSYQKYGSHLSNYTPFSGNSDQANVGSQYFN
QSPGHQWLIPVMSPSEGLVYKPYPGPGYTGAVYGGYRPFGQGPPDVTFMNPAYGVPDFHQAIAVPPFIP
PGGYPYFPPHGVPAMYQSASVSAVEQVNQFSAHGSRNQNGTSSLEEANFYTHNQSSCNLTNQKNGATL
HVRKPQPSRERELESSPGEKAQEIIKEKSAEERDTLSSSFTVPIVSKEVLKSLETRQKPQVIRVVPHNPRSA
TVSAARIFQSIQEERKRYDLV*

>MT_Medtr8g015480.1
MKGAIDEGKEISPMFPRLHVKDAEKGGPKAPPRNKMALYEQFSIPSQSFASSGSGSLFTLPLRNCTVPTTS
SHLGCGQSIKFYSSNASSILSEKTQAYNSRKINSTKLTASHDLEHMTPAKQVTKIQQDYFINNSKNSLKTLD
GEDAFITSGSVHVKSNPSDKDEENKLARYNLNCSLKSLSSFRKVMNSPGTIELKSAQYGKSLMKEHKDVR
QIDQNAEEKPLHSLNGFNDTTNASSNSSIKDRNSKSMNKEQRSLKEENRNISVDSLKTLQGSNGHRYEDH
VAFADKINLRDHCSEKPTMSDFQKCSRELEIGTRSSHGKRERSKDEETSKNYDALNKSSSKCRFGMDISP
DDVVGLIGEKQFWKTRRTIINQQRIFFMQVFELHRLIKVQRLIAGSPNLLFEDKLLLNKPSVEASSSNKLQSD
FISEQQPTVFKLDSKSEKATTSEDVENNAVGKISLPFVNNISKENNQLSNYGNHHLGNLALASADKSSNAK
HSPNIVYPPPPPNQWLVPVMSPSEGLVYKPIIGPCPPNSGGIMTPLYGGCSPMSFNQGSKDVVMDPSLTT
SFHQKIRLLSGSSLPQLLPPCVPSFMHRSISASSVEQMAQSNGPKNHYSSAELNSTILYQSPSNMSTQISH
VMARNFSPYQSLEDNKELQISIANSPSKRMKRDELPLFPLAPTFWSSPDRDSIDEHQEHHSRVIKALPHNP
KSASESAAKIFKSIQEERKFL*

>BR1_BraRa_Brara.D01576.1
MKRGKEEEEKKLEPMFPRLHVNDADKGGGPRAPPRNKMALYEHLTIPSHRFTDHHSSSPRHTNTLFPPP
PPVPSNQPCGVERNLTSQHLDSSASGHVTQMSSMENVTTLAHRRGDQRKTLREEDDFAVPVYDNDSST
RFQSPGRRNGEKRTTLFGDQAKGSSSSKRHGMDLEKSASGCERVNASFLLRQESTSSRLELDQDGDET
GVMETDDGVESHGDPNDVDNDDVSDDSISSVDVSPDEVVGVIGQKRFWRARKAIANQQRIFAVQLFELH
RLIKVQRLIASSSDVLLDEISYLGNVPVKKLLPSEFIVKPPPLPHATKHRRGDPEKTDQDKMECSAENVVGK
LSNQGQQHQPSNYMPFASNPPTAVNGCYYPPPPSGGNQQWLIPVMSPSEGLIYKPHPGPGPPVCGGYY
GHFMPAPMMMGSFMGGGPPPFHPGVGNGYFPPYGMMNPYGSGHQQQQQPSEQMNQFVHPVNTQQQ
SSVNEAISQQQPTKSYPRARKSRQRSTGSSPRGPEGISDTNSFRPFSVVDDDDNNEPEQMMTTTTTTTR
TTVTQTTRDGGAVTRVIKVVPHNAKLASENAARIFRSIQEERKHYDSFSNHS

>BR2_BraRa_Brara.I04408
MKRGKEEEKRLEPMFPRLHVKDAEKGGPRAPPRNKMALYEQLSIPSQRFTSSDRVGGSLPPNTSPLLPP
GPSSNQGTDNFVTQMPLMENVRTTSAQHDHQRKIAREEDDFAVPVFINSRRPGRGKSGLKRGVGLAANS
ATEDMDLASTSDRVDDGRINNGVESHMEASEEEGHGNLNDEYCTSGGGGYTSLQQEINNEEEASDDNS
MVDSVSSLDVSPDEVVGVLGQKRFWRARKAIAKEGHSYIVQGACRDSLWILYCVFLASACWNMSPVSVC
QQRVFAVQLFELHRLIKVQRLIAASPDVLVDDMSYVGKVAAKSYPVKKLHLPSGFLVKPPLPQVIKHRSSD
YSEKTDQHKMECSAENVVGRLPNQGQGHHHQQPSNYMMPFATNQPNANGCYYPPQPPPPSGGNQQW
LIPVMSPSEGLIYKPHPGPGPGHTGLVCGGYYGHFMPAPMFMGGGGGQPPPFHPGMGFPSHGNGYFPP
YGGIMMNPYYSGQQQQQQPNEQMNNNIQQQSSVNEATSQQQQQPTKSYPRAKKSRQEGISGKKKSFQ
PFSAVDDDDDDDNDKINNAAPPTEEMMTTTTTTTTTVTQTTRDGAGVTRVIKVVPHNANLASENAARIFRS
IQEERKQYYP

>SB1_Sobic.003G191700.1
MTRGGGGGGDGKGPLFPRLHVSDAGKGGGPRAPPRNKMALYEQLTVPSNRFSSPAPAPARAAGAKASL
VPSTSAAQVYGYDRTLFQPFNVPSNEPARSSEKFKGNCINGQSNSTRRESLRMSSQTKSKDVCASKSIAG
CTSQHRGGNTIKSSGKKVVNDDEFMVPSICSPRIYRYSTQEHADKSKPQSTTNPHKSPSMSKSSAKCYST
VNKHLDRMNEADMRLMNSPKVKEKEAVQVPKGVEVKEKDSSIQASEKFKDKYAKLCQMRNKVSNINRSD
NNSCQPTSVNGKSTEAKNPTATRNPSSCKPCTDVDSSNWNSNLLERSPREGGAKRKRQHHSGEQNDDL
SDDSVECIPGWELSPDEIAGAIGPKHFWKARRAIQNQQRVFAVQVFELHKLIKVQKLIAASPHLLIEGDPVL
GNALMGKRNKLPKGNLKVQTLSITNKDDIQPTLEQPELSKQNTEGNPSHHSRDDGLDDNHHDQAAANET
FTSNPPAIPVAPDNKQNNWCMNPPQNQWLVPVMSPSEGLVYKPYAGPCPPVGNLLTPFYANCTPLRLPS
TPYGVPMPHQPQQMVPPGAPAMHMNYFPPFSMPVMNPGTPASAVEQGSHAAAPQPQGHMEQQSLISC
NMSHPSGIWRFLASRDSEPQASSASSPFDRLEAQGDGSGPVSFFPKASVLNAQPQPSSGGRDQQNHVI
RVVPRNAQTASVPNAQPQPSSGGRDQQNHVIRVVPRNAQTASVANAQTQPSSGGQDQWNHVIRVVPH
NAQTASESAARIFRSIQMERKQNDS*

>SB2_Sobic.009G257300.1
MRRGGAKDDAAPDKVMGPLFPRLHVNDTLKGGPRAPPRNKMALYEQFSVPSHRYSAAAAAPPPPSAPA
PSPAPPWRAQRPVPATSASQVGGSDRPLFPSFCVPSTEPVRSSDQMNANSNGRAANGTRAESGRQSTH
LKSKDTNAAGPTAECSSRQRENGNKNSSGKKLANDDDFTVPSVLYSGVPPHSSQEKLTLFPTTSPCKSVP
AKYSSNGKRHLEGIDVSDVKSKGRSGIKDTEPVQVRIDLEDEETTPSFQILKDKTGRPDPKVSPFMDRLKK
YNVADKQYSEAESYQMRTRNEDAVKTQNPPKNGSVLLSKPYDDREQNGDSDILKHGLRDTGEKRKRSH
HGVEQNDDLSDSSVEFLAGMEISPDDVVGAIGPKHFWKARRAIVNQQRVFAVQVFELHRLIKVQKLIAASP
HLLIEGDPCLGKSLAASKKKLAGDVEKQLQSAKNNDEVQPTQQQQLEHSKENTEANQPSPSQDDAAGVQ
HNNQAAINGAVSSNPPSMPTPSDNKQNSWCIPPPPSQWLVPVMSPSEGLVYKPYSGHCPPAGSFMAPP
FFASCGPVSLPSTAGDFMNSAYGVAMPHQPQHMGVPGPPPMPPMYFPPFSMPVMNPAVSASAVEQVS
HVAASQRNGHIEQHTRNSCNASHLRSEAVSAGVWRVHASRDSELQGSSASSPFDRQQGEGRGPAPPFP
ASSVGNRQAQAQAQASSGSRENPSRVIRVVPHTARTASESAARIFQSIQMERKQNDP*

>SL1_Solyc08g065870.2.1
MKRGKGEEKVMGPMFPRLHVNDTDKGGPRAPPRNKMALYEQLSIPSQRFNSGVLPLDPNNTSKMAPPS
SSQGSGHDRSGYLPIQHPPSRRLADKPPGHSSDPSTLLQQYELKKRTEEDDFTVPIFVNSKLGQAHGSHN
VNMEKLSPSGQLFCPNKELEGVTHLTLRQQRNSQNKENLKCTLARREKTTSNSASKECRLDPQVGCSSIP
EPVKGTYDGSSYPRKEFVSEEQLTANDLVNDTESQEDRAHKSLQTGNLDRGDDLSETSRVESISGTDISP
DDIVGIIGLKRFWKARRAIVNQQRVFAIQVFELHRLIKVQRLIAGSPNSSLEDPAYLGKPLKSSSIKRLPLDCI
VRESQSVLKRKHDSEKPHFRMEHTAESNVGKASLSTVQNGSQLSSHKPFSGTPLPTPVTNDSNAGPWCF
QQPPGHQWLIPVMSPSEGLVYKPFPGPGFTSPICGSGPPGSSPTMGNFFAPTYGVPAPNPHYQGMGVP
FAPPTGHGYFRQYGMPAMNPPISSTASEESNQYTMPGLQHQFSGVVDDVNIQHQDSSNVLNQKKENVP
DVVRYQSTKDNEVQASSASSPIETAGRNMLSLFPTSPVTDNRDGSPQACVPDNPARVIKVVPHNARSATE
SVARIFQSIQQERNNMT*

>SL2_Solyc12g095900.1.1
MKRGKGEEKLMGPMFPRLHVNDTEKGGPKAPPRNKMALYEQLSIPSQRFKYGISNNRNNADIQGNGREN
DDFFSVQLPPSRHPAENPHSCSSNSKTPLLPVESNKKTEEDDFRVPIFVKSKASQGNGKLYSTLDGRKLS

ASTAVISGHSRKDLNDENFKQIAVGREISCNSTSIPSMDKLDDLLKKADVQLQYEPRNDPDNTLGILCKNDL
LQPECRVDPQVGGTMLSEPVRVVDIGDSSLLVKDVASKEHIIPNNNQSNDKESKEDKASESLQTKIVNQDD
DLSETSMVESIFGMYISPDDVVAIIGQKHFWNARRAIATQQRAFAVQVFELHRLIKVQRLIASSQSMLEDSA
YLSKAVKDSSPKKLPLEYIARDGHNVPKQRKNFEKPNTRMECSAENTEGKPVKDSSAKRLLLEYIPRDGH
NVSKQKKDFEKPNISMECSAENTVGKGSFSSVQNNSQSSSYSLFSGHPIANDSTMGGPWSFNQPSGHQ
WLIPVMTPSEGLVYKPYLGPGVTSSICGGYGPPGSTPIIGNHSAPSYGIPASHHQYQGVRMPFTPPAGHN
YFPSYGIPAINPAISSSAVDQSSLFVAQGLQGQLSGGGANFSVQRQNSSNMPSNKNGTFPEVKSRSCRDA
EMQASTASSPSGTANKITVDNATERRNVLPLFPTSPATKNLDISSQPQLPSHHARVIKVVPRNARSATESA
ARIFQSIQEERKQYDSVVN*

>SL3_Solyc11g070100.1.1
MKRGTGEEKVMGPMFPRLNVNDTEKGGPRAPPRNKMALYEQLSIPSQRYNPGDLPHNSSNSANLVLPH
PSQENEHERGVLFSRQLPALRHPVEKPYGRSSGSNTPLREVKSKRQTEKEDFRVPTFDNSKERAVNTED
YSKGTSDIDKRDSTLKRTDQLSHVTPRENLVNTFGESHKTNIVQLEFRSDCQVDCTVFSGSVIDVDNDSQE
DKTCKSSQTGEMAHSDELSETSMVEYVSEMDISPDNVVRMIGQKHFWKARRAIANQQRTLALQVFELHRL
LKVQKLIAGSPNLNLEDNAYLGKPLKRLSAKRVCLEHSVKAPEIVSRPKNDSEKPKGRMECNAENDVGKT
SLSSVRQPSSCNPLSEKQLPTPVKHDSLMSPWYFNQPPGHQWLIPMMSPSEGLVYKPHSGPAVMSPVY
GGCGPPGSTPMTGNFLASAYGLPFAPPTGHGYFRPFGMPVTNPAIPSPTQNQSNQVVASHSKGQLSGG
RASFNIQHPNSSNVGSESDGTLPEVVRLYPSRDSELHASTAGSPSEITRAVDMGNSTRGRSAFHHFPTSP
AVDNPILRPQPHFPERPARAIKAIPHNARSATESVARIFQSIQEERKQY*

>EG1_Eucgr.C02997.1
MKRGKDDDKIMGPMFPRLHVNDTEKGGPRAPPRNKMALYEQLSIPSQRFGSGMLPLNPNNSSNLVSPAS
SNQGTGSARNLYFPRHLPPSTPTHLSERLNAGKSGGTSPANSLARVEQRKNAGDGDDFMVPVYVQSGT
GQGKNKNSKAGDNATNYTAKMQSSCSDDPRRSSSVGLSSRQESNLDGSIRSYRNIATAENGRRSLKEAD
APRNPVLASFSTSRGTDAQLRQGNEDGSQSDEHAQDFENEETSRDIEKGISSWSSRDPRLGETQRCPPE
PNSFGKENLNETCGALLMVDAGRNDDASEVSIADSVSGFDISPDDVVGIIGQKHFWKARRAIVNQQRVFA
VQVFELHRLIKVQKLIAGSPHLLIEDVSGLGKTSLVNSPAKKFSEDHNGGYPSQTTNHKEEQEKPGHQMEC
SAENAVGKTSISSVKSANQLSDYGPGMRNPPLAPIVPDVKMGPWGYPQPSGQQWLIPVMSPSEGLVYKP
YPVPGLTGTACGGCGPYNSSPMMANIPNPAYGVPLHPHHQGFGFPSGVPPPGHSYFPTYGMPVMSFNV
SGSSVEQTNRFSRPVQYGQTGQLSGGEVNNLQHQNSSNLPKQRKGSVAQIKFQANKDSELQVSTASSP
SEKPPEGLGNVQSSDGKEALPLFPVAPAVSEGGSQLREAEQPTRVIRSVPHNARSATESVARIFRSIQEER
KQFDSI*

>EG2_Eucgr.F03094.1
MNTSPMFPRFHVNDTEKGGPRAPPRNKMALYEQLSIPSQSFNSPMTSLLPLPLDQGGSLASSAPLLFGGA
NQRYALTPLCSSAVTHLARKAELHASAGVKLNSLMETREINLMQARGSLHFKRVAPRKHRDADDFTIPALV
KRVLTPHSDRKCNKNLKLNPDLHMDDSSQSKSSREKQIDPTRSTSMNSRQCARNPLLDNQEVSSASHER
PVTLCRENTDASFPPSSKDKISETSKGSHASIIGECRSSSVDGLACSNTSMGDGCHVQQDISVVRGEVLEE
LSKGNASRLRSRLRSKPLIENGKRGANGTKCDNKDHEDGEYPIQAAEGNGCNVLDSLEESPSSLYLLPDD
VVGVIGEKHYWNARKAIVNQQRIFAAQVFELHRLIRVQRLLSRSPHLLGSSLYFGNPLVEHHAIKSVPSECLI
EATTLLKSNSLSTQERNPTPMVKLPLPPIDSDFSKKLIGERPEQSHYSETSNPAACEPTLRCFPRIGNQWL
VPMMSPSEGLIYKSYSAVCPPRGGTVGPLYGGCAPISFESMGNDVGMTFGIPASQRQAMGILPRTSVAG
QTFFLPWGIPLTNPSVASSAIEPMSNPFILGSQSNPQVNQRSTGEVNISRTHQSSCNVSTQVSRVISCDGL
KSPTLKENELQGSTGSNPSEKLGGAALPLFPIDPTKSDQKVQVHSSNRLEKVIKVVPHNPRSAAESAARIF
QSIQEERKRHE*

>BD_Bradi2g14290.1
MRRGGGGPAPAGKEDKVMGPLFPRLHVNDTLKGGPRAPPRNKMALYEQFSVPSQRFTPHRASSSALSS
ASPGQIGGSDRPLFPSFCVPSNEPARSSEHINTNSNGRDGNATRVESGRHSTQLKSKDTYAAGSTAECS
SQRRENSVKNSSGKKLTNDDDFTVPSVFCSGVPPHSTQEVVRIQEKSTAFPSTSPYKSGPTMSKSSAKCS
NTDKRYLEGTNVSDMRSRDSPSIKDKAPLKTMTNLDVEERSSSFQISKEKAGKADDKISSHRDKLSDLNVF
DKQHARTEVHQARRTNENAAESQNAPKAGNGPSSTNVERNGASNLLEKGLRVTGEKRKRSEGHHNVQK
DDSSDLSVESLPGLEISPDDVVGAIGPKHFWKARRAIVNQQRVFAVQVFELHRLIKVQKLIAASPHLLIEGD
PCLGSALATSKKKLAAGNVEKQPPSAKNKDDAQLTLQQVEYSKDNIEGNQASPSQDDVVVVQHNNQAAS
NGGDTSNPPAIPAAPDNKQSNWCTPPQNQWLVPVMSPSEGLVYKPYTGPCPPAGSFLAPFYASCAPLSL
PSTAGDFMNSPYGIHMPHQPQHMGLGGPPPMPPMYFPPFSMPVMNPVVSASAVEQVSRIAPARPNAHV
EHYSRNSCNMRNEAMSAGIWRFHASRDSELQASSAASSPFDRQQGEARGPAAPPPIPTSSAGNGQPQP
STGSKENPAGVIRVVPHTARTASESAARIFRSIQMERQQNDP*

>SM1_411196
MTSKGSSREGRGESSRSSHSNHHGKGQSRANAAVAEPLFPRVHVSDTRNGPKAPPRNKMALYEQLTVP
SQHFLQRQTSGLVWPPMNPAYASQYAPFASNCFTPCFAPPGLSFHHHASSTDGGTASQSMGAPLGSQK
SMVMDSEVDKELQRVPRVVDENNPVGGGGNAATPTTPCAARPVPCAKSSSQQQQQQHPSANTITAATA
NVVNTTMANATLANVNKRVRNEDDFAVPTYCFPKDGKGVEAGSGSKQQQQQHSNTRSEMNASKSSAAE
IVERTVPSSAGVSSSPAAVAGVTAPAAGRGGGGGAAATAAPGVISPHKGHTEHISSSNICESAAGSDNQS
DDFFQSLHEEQVSGDGDSNASIVDPFGKIAARDVVGAVGEKEFWKTRKTILRQQRIFETQVFELHRVVKV
QHLLAESPKLLLEPDHARFHLAQPLPITHEIATPAEGRQLAHPPVAVRGSNKDQTTNFTTAQASKPLYNPK
DQHRQQRSYSTAPADISPREAPPPPPAVTATLINTCSSSPAPPPPPPPPEMNSSSTTTTQGMTYQTFPGA

ANSWGYATFPAGNQWAMLPPSCQPYVFQPPPNAAQMLPGYGAAYQPVFHNGAGSYELFPMVPRPPRM
QTAEMQPVYWQQPMYPSVHSSGWYAFPPQFFDSSSVQTPQPSKLPKSANSTQQEQQEKRGPEMTQR
WIEGERQQHGVSYSLPFSYVPPSERHEQQQQQGGGGGAGFNGNNGAMKVVPRAVMATPESAAGILKSI
QRERR*

>SM2_415241
MEDKNAPPGGALFPRLHVKETKNAGPRAPPRNKMALYEQLTIPSHRFQQQQSDGAPPQPFVPQVCKFEP
MISPALNRGYYFPYYMVPSPVAFQPMNVVLGQHSQSVANETEQRELQQVPGDGGSNRQLARIPSLHSRA
GSGKTKTRAPRVDDVAAVPTYPSKPAAVPARSSKQEHFASASVAPSNASTSATKSQRQVEVRETTQARK
DSRPRNRAPGDLGDQENGSEVRVMASSSPSHSYESNEDNGRIDNQSDEELEGRCSPEEVEASDDSATS
VVENNAAPSAITSKEIMSAVGDEEFWKMRKAMQRQQTIFQKQLFELHRLTKVQHLMANSKISDPSKTQDE
KTDKRVGSEPTHCGEAPKTSKPGPKPDQAPAPKTPSQTQPLSTTPYAYTTHPRPIQAANTINYATSHPAY
NQWYAPLPFQFPFQQPFPVTAQVFNTPYYPAPLYGGGAAPPFLPPPDPRQFMSPPIQLQPWPQHPGSLY
SDPAALQWMGFVNPPGGATYRPPAAESSLQASSIHDDHQSRKDRGIHLRSQGSSSGFSLIQRADSSSPA
PAPSPSPAAENRRQQHQEPRQKLVGRFCGEKQSGGESEHGVSPYSRPSGFQSVKNSSSSSKEQRSSQ
GSHKAIKVTPRAAPVTAESAAEILHSIQKERPS*

Appendix 2

Sequences used in monocotyledon ELF3 alignment

>OS1_OrySa_Os06g05060.1
MATRGGGGGGGKEAKGKVMGPLFPRLHVNDAAKGGGPRAPPRNKMALYEQFTVPSHRFSGGGGGG
GVGGSPAHSTSAASQSQSQSQVYGRDSSLFQPFNVPSNRPGHSTEKINSDKINKKISGSRKELGMLSSQT
KGMDIYASRSTAEAPQRRAENTIKSSSGKRLADDDEFMVPSVFNSRFPQYSTQENAGVQDQSTPLVAAN
PHKSPSTVSKSSTKCYNTVSKKLERIHVSDVKSRTPLKDKEMEAAQTSKNVEVEKSSSFHASKDMFESRH
AKVYPKMDKTGIINDSDEPHGGNSGHQATSRNGGSMKFQNPPMRRNEISSNPSSENTDRHYNLPQGGIE
ETGTKRKRLLEQHDAEKSDDVSRLLEQHDAENIDDVSDSSVECITGWEISPDKIVGAIGTKHFWKARRAIM
NQQRVFAVQVFELHKLVKVQKLIAASPHVLIESDPCLGNALLGSKNKLVEENLKAQPLLVATIDDVEPSLQQ
PEVSKENTEDSPPSPHDTGLGSGQRDQAATNGVSKSNRRATPVASDNKQNNWGVQLQPPQNQWLVPV
MSPLEGLVYKPYSGPCPPAGSILAPFYANCTPLSLPSTAGDFMNSAYGVPMPHQPQHMGAPGPPSMPM
NYFPPFSIPVMNPTAPAPVVEQGRHPSMPQPYGNFEQQSWISCNMSHPSGIWRFHASRDSEAQASSASS
PFDRFQCSGSGPVSAFPTVSAQNNQPQPSYSSRDNQTNVIKVVPHNSRTASESAARIFRSIQMERQRDD

>OS2_OrySa_Os01g38530.1
MATRGGGGGGGKEAKGKVMGPLFPRLHVNDAAKGGGPRAPPRNKMALYEQFTVPSHRFSGGGGGG
GVGGSPAHSTSAASQSQSQSQVYGRDSSLFQPFNVPSNRPGHSTEKINSDKINKKISGSRKELGMLSSQT
KGMDIYASRSTAEAPQRRAENTIKSSSGKRLADDDEFMVPSVFNSRFPQYSTQENAGVQDQSTPLVAAN
PHKSPSTVSKSSTKCYNTVSKKLERIHVSDVKSRTPLKDKEMEAAQTSKNVEVEKSSSFHASKDMFESRH
AKVYPKMDKTGIINDSDEPHGGNSGHQATSRNGGSMKFQNPPMRRNEISSNPSSENTDRHYNLPQGGIE
ETGTKRKRLLEQHDAEKSDDVSRLLEQHDAENIDDVSDSSVECITGWEISPDKIVGAIGTKHFWKARRAIM
NQQRVFAVQVFELHKLVKVQKLIAASPHVLIESDPCLGNALLGSKNKLVEENLKAQPLLVATIDDVEPSLQQ
PEVSKENTEDSPPSPHDTGLGSGQRDQAATNGVSKSNRRATPVASDNKQNNWGVQLQPPQNQWLVPV
MSPLEGLVYKPYSGPCPPAGSILAPFYANCTPLSLPSTAGDFMNSAYGVPMPHQPQHMGAPGPPSMPM
NYFPPFSIPVMNPTAPAPVVEQGRHPSMPQPYGNFEQQSWISCNMSHPSGIWRFHASRDSEAQASSASS
PFDRFQCSGSGPVSAFPTVSAQNNQPQPSYSSRDNQTNVIKVVPHNSRTASESAARIFRSIQMERQRDD*

>HV_HORVU1Hr1G094980.6
MRRAGGGGGGGSGEDKVMGPLFPRLHVNDTTLKGGGPRAPPRNKMALYEQFSVPSQRFAANTAPAAH
RPAASFAAVSSASAGQIGGIDRPLFPSFCVPSNEPVPLPQHINTNSSGHATSGRLSTQLKSKDAYAAGSTA
ECTSSHGRDNNAKNSSGNKLTNDDDFTVPSVFCSGVRPRSNHEEARIQENSTHLPATSPYKSGPTVSKP
TAKFPNTDKRYLEGRNPSDTRSRDSPNIIRDKAPANTTTNFLEAEERTSSFQFSADKTMGKRDDKGSSYR
DKPSSINVSDKQQSRNEGHQARTRNENAAESQNAPKAGNGPYSTDIACNGASNLSEKGLRETGEKRKRS
TGHHDVQRDDSSDSSVESLPELEISPDDVVGAIGPKHFWKARRAIVNQQRVFAVQVFELHRLIKVQKLIAA
SPHLLIEGDPCLGSALVTSKKKTAAANVEKQLLSAKSKDDDDAQLTLQQVEYSKDNTEGNQASPSQDNDL
VEVRHENQAASNGAVSSNPPAMPAPTDNKQNNWCAPPPQNQWLVPVMSPSEGLVYKPYTGPCPPAGS
FLAPFYASCAPLSLPSTAGEFMNSPYGIPMPHQPQHMGVGGPPAMPPMYFPPFSVPVMNPVVSSSAVEQ
VSRVAAARPNTHLEHHSRSSCNMRNEAVSVGGVWRFHSSRGSKLQGSSAASSPFDRQQGQGEARGHA
AAAPAAPPPTSSSAGNGNGNAAQHGPCDPGGTAHGTHRVGVGGAHLSVDPDGEAAERPV

>ZM1_AC233870.1_FGT003
MRRGATKDDAAPDKVMGPLFPRLHVNDTLKGGPRAPPRNKMALYEQFSVPSHRYSAAVPPAPSPAPPW
GAQRPASAVPSTSASQVGGGDRPIFPLFRVPSTEPVRSSDQTNANSNGQGANGTIAESGRQRQSTHLKS
KDTNAAGPPAEGNNSVGKKLANDDDFTVPSVLYSGMPPHSSQEKLTLFPTTSPCKSVPAKYSSTDKRRLE
GMDASDVKSKGPSGIKEKEPVQVRIDLEDKETTPSFQVLNDKTWSPDPKLSSHMDRLKKQHAEAESYQIR
TRNENAVETQSPPKNGVSLLSKPYVDRREQNGDSDLLGHGLRETGVKRKRSHHDVEQNDDLSDSSVESL
PGMEISPDDVVSAIGPKHFWKARRAIVNQQRVFAVQVFELHRLIKVQKLIAASPHVLIEGDPCLGKSLAVSK
KRLAGDVETQLESAKNDDGVRPTQLEHSKEKTEANQPSPSQDEQAATNGDVAASMHTPSDNKQKSWCI
PAPPSQWLIPVMSPSEGLVYKPYTGHCPPVGSLLAPPFFASYPTSSSSTAGGDFMSSACGARLMSAPVYF
PSFSMPAVSGSAVEQVSHVAASQHKRNSCSEAVLASRDSEVQGSSASSPASSETAAQPRVIRVVPHTAR
TASESAARIFRSIQMERKQNDP*

>ZM2_GRMZM2G045275_T01
MTRGGGGQGGKEEPGKVMGPLFPRLHVSDAGKGGGPRAPPRNKMALYEQFTVPSNRFSSPAASARAA
GASLVPSTAAAQVYGYDRTLFQPFDVPSNEPPRSSEKFKGNTINGQSNSTRREPLRMSSQTKNKDVCAS
KSIAKCTSQHRVGNTIMSSGKKVVSDDEFMVPSICYPRFYRQSTQDHADKSKPQSTTNPHKSPAMSKSSV
ECYSTVNKHLDKINEADRRLMNSPKVKEKEAVQGSKAVEVKEKSSSFQASEKFKDKYAKLCQMRNKASNI
NHCDNNGCQPASVNGNFTEAKNPTAARNTSSCKPCTDVDSSNRKSNLLERSPREVGAKRKRGHHNGEQ
NDDLSDSSVECIPGGEISPDEIVAAIGPKHFWKARRAIQNQQRVFAVQVFELHKLIKVQKLIAASPHLLIEGD
PVLGNALTGKRNKLPKGNSKVQTLSITNKDDIQPTLEQPELSKQDTEGNLLAHSHDDGLGDNHHNQAATN
ETFTSNPPAMHVAPDNKQNNWCMNPPQNQWLVPVMSPSEGLVYKPFAGPCPPVGNLLTPFYANCAPSR
LPSTPYGVPIPHQPQHMVPPGAPAMHMNYFPPFSMPVMNPGTPASAVEQGSHAAAPQPHGHMDQQSLI
SCNMSHPSGVWRFLASRDSEPQASSATSPFDRLQVQGDGSAPLSFFPTASAPNVQPPPSSGGRDRDQQ
NHVIRVVPRNAQTASVPKAQPQPSSGGRDQKNHVIRVVPHNAQTASESAAWIFRSIQMERNQNDS*

>BD_Bradi2g14290.1
MRRGGGGPAPAGKEDKVMGPLFPRLHVNDTLKGGPRAPPRNKMALYEQFSVPSQRFTPHRASSSALSS
ASPGQIGGSDRPLFPSFCVPSNEPARSSEHINTNSNGRDGNATRVESGRHSTQLKSKDTYAAGSTAECS
SQRRENSVKNSSGKKLTNDDDFTVPSVFCSGVPPHSTQEVVRIQEKSTAFPSTSPYKSGPTMSKSSAKCS
NTDKRYLEGTNVSDMRSRDSPSIKDKAPLKTMTNLDVEERSSSFQISKEKAGKADDKISSHRDKLSDLNVF

DKQHARTEVHQARRTNENAAESQNAPKAGNGPSSTNVERNGASNLLEKGLRVTGEKRKRSEGHHNVQK
DDSSDLSVESLPGLEISPDDVVGAIGPKHFWKARRAIVNQQRVFAVQVFELHRLIKVQKLIAASPHLLIEGD
PCLGSALATSKKKLAAGNVEKQPPSAKNKDDAQLTLQQVEYSKDNIEGNQASPSQDDVVVVQHNNQAAS
NGGDTSNPPAIPAAPDNKQSNWCTPPQNQWLVPVMSPSEGLVYKPYTGPCPPAGSFLAPFYASCAPLSL
PSTAGDFMNSPYGIHMPHQPQHMGLGGPPPMPPMYFPPFSMPVMNPVVSASAVEQVSRIAPARPNAHV
EHYSRNSCNMRNEAMSAGIWRFHASRDSELQASSAASSPFDRQQGEARGPAAPPPIPTSSAG
NGQPQPSTGSKENPAGVIRVVPHTARTASESAARIFRSIQMERQQNDP*

>SI1_Seita.3G121000.1
MRRGAGKDEAPDKVMGPLFPRLHVNDTVKGGPRAPPRNKMALYEQFSVPSHRFSAAAAAPAAPAPAPP
WHAHRPAPGAATSAVPSTSASQAGGSDRPLFPSYCVPSTEPVRSSDHMNANSNGRAGNATRTESGRLS
THLKSKDTNAAGLTAECSSKHRENTTKNSSGKKLTNDDDFTVPSVLYSGIPPHSTQEKFTPFPTKSPYKSM
PAMYKSSAKCSNTDRTHLEGMKVSDAISMGSPGIKEKEPTKVRIDLEIEERTSSFQTSKEKSGRLDPKVSS
YRDKLNKYNVADKQSSEIASYQTRNRKENAGETQNPPEAEMAPSAKPYAGMEQNGNSDLLELGLRETGE
KRKRSHHGVEHNDDLSDSSVESLPEMEISPDDVVSAIGPKHFWKARRAIVNQQRVFAVQVFELHRLIKVQ
KLIAASPHLLIEGDPCLDKALAASKKKLAGGDAEKQHQSAKYKDDVQQTLQQLEHSKDNTEADQPSPTQD
DVVAVQHNNQAAATAAVNSNPPTMPTPSDNKQNSWCIPPPPNQWLVPVMSPSEGLVYKPYAGHCPPAG
SFLAPFYPSCAPVSLPSTAGDFMSSPYGIPMPHQPQHMGVPGPPPPMPPMYFPPFSMPVMNTAVSASAV
EQVSHVAASRPNGHIEQHSRSSCNMSNLRSEALSADIWRFHASKDSELQGSSASSTFDRQ
QGEGRGPAQPFPSSSVGNGQPQPSSGSRENPGRVIRVVPHTSRTASESAARIFESIKMERQQND*

>SI2_Seita.5G204600.1
MTRGGAAGGGGREEQGKVMGPLFPRLHVSDAGKGGGPRAPPRNKMALYEQFTVPSNRFSSSAASTRA
AGGSLVTSTSASQVYSYDRPLFQPFDVPSNGPAHSSEKFKGNSINGQSNSTRRESGRMPTQTKNNDVYA
SKSIAESTSQHRVGNINKNSSGKKVANNDEFMVPSICSPRFSRYSTQEHAGVQDKSNPLSATNPHKSPSA
MPKSSAECYSAVNRHLERIDESDMRSMSSSKVKEKESVQGSKIVEVEEKSLPVQAFKEKFKNKDAKACQ
MRDNANNIDSYDNPHFGNSRRQPTSMNGSSMEAKNPTTTRNTVSCKPCTDLNDCNKNSNLLDRSLREA
GSKRKRGHQDVEQNDDLSDSSVECIPGWEVSPDEIVGAIGPKHFWKARKAIQNQQRVFAVQVFELHKLIK
VQKLIAASPHLLIEGDPVLGSALVGKKTKLPKGNLKVQTLSIANKDDIQPTPEQPELSKQNTEGNPPSPCRD
DGLGGNGHDQAATNETFTSNPPVMPAAPDNKQNNWCMNPPQNQWLVPVMSPSEGLVYKPYAGPCPPV
GSLLAPFYANCTPLKLPSTPYGVPMPHQPQHMAPPGAPAMHMNYFPPFSVPVMNPGAPASAVEQGSHA
AVPQPHGRAEQQSLISCNMSHPSGIWRFHASRDSEPQASSASSPFDRIQVQGDGSGPVSVFPSAPAQNA
QPQPSSGSRDQQNHVIRVVPHNAQTASESAARIFRSIQMERRQNDP*

>SB1_Sobic.009G257300.1
MRRGGAKDDAAPDKVMGPLFPRLHVNDTLKGGPRAPPRNKMALYEQFSVPSHRYSAAAAAPPPPSAPA
PSPAPPWRAQRPVPATSASQVGGSDRPLFPSFCVPSTEPVRSSDQMNANSNGRAANGTRAESGRQSTH
LKSKDTNAAGPTAECSSRQRENGNKNSSGKKLANDDDFTVPSVLYSGVPPHSSQEKLTLFPTTSPCKSVP
AKYSSNGKRHLEGIDVSDVKSKGRSGIKDTEPVQVRIDLEDEETTPSFQILKDKTGRPDPKVSPFMDRLKK
YNVADKQYSEAESYQMRTRNEDAVKTQNPPKNGSVLLSKPYDDREQNGDSDILKHGLRDTGEKRKRSH
HGVEQNDDLSDSSVEFLAGMEISPDDVVGAIGPKHFWKARRAIVNQQRVFAVQVFELHRLIKVQKLIAASP
HLLIEGDPCLGKSLAASKKKLAGDVEKQLQSAKNNDEVQPTQQQQLEHSKENTEANQPSPSQDDAAGVQ
HNNQAAINGAVSSNPPSMPTPSDNKQNSWCIPPPPSQWLVPVMSPSEGLVYKPYSGHCPPAGSFMAPP
FFASCGPVSLPSTAGDFMNSAYGVAMPHQPQHMGVPGPPPMPPMYFPPFSMPVMNPAVSASAVEQVS
HVAASQRNGHIEQHTRNSCNASHLRSEAVSAGVWRVHASRDSELQGSSASSPFDRQQGEGRGPAPPFP
ASSVGNRQAQAQAQASSGSRENPSRVIRVVPHTARTASESAARIFQSIQMERKQNDP*

>SB2_Sobic.003G191700.1
MTRGGGGGGDGKGPLFPRLHVSDAGKGGGPRAPPRNKMALYEQLTVPSNRFSSPAPAPARAAGAKASL
VPSTSAAQVYGYDRTLFQPFNVPSNEPARSSEKFKGNCINGQSNSTRRESLRMSSQTKSKDVCASKSIAG
CTSQHRGGNTIKSSGKKVVNDDEFMVPSICSPRIYRYSTQEHADKSKPQSTTNPHKSPSMSKSSAKCYST
VNKHLDRMNEADMRLMNSPKVKEKEAVQVPKGVEVKEKDSSIQASEKFKDKYAKLCQMRNKVSNINRSD
NNSCQPTSVNGKSTEAKNPTATRNPSSCKPCTDVDSSNWNSNLLERSPREGGAKRKRQHHSGEQNDDL
SDDSVECIPGWELSPDEIAGAIGPKHFWKARRAIQNQQRVFAVQVFELHKLIKVQKLIAASPHLLIEGDPVL
GNALMGKRNKLPKGNLKVQTLSITNKDDIQPTLEQPELSKQNTEGNPSHHSRDDGLDDNHHDQAAANET
FTSNPPAIPVAPDNKQNNWCMNPPQNQWLVPVMSPSEGLVYKPYAGPCPPVGNLLTPFYANCTPLRLPS
TPYGVPMPHQPQQMVPPGAPAMHMNYFPPFSMPVMNPGTPASAVEQGSHAAAPQPQGHMEQQSLISC
NMSHPSGIWRFLASRDSEPQASSASSPFDRLEAQGDGSGPVSFFPKASVLNAQPQPSSGGRDQQNHVI
RVVPRNAQTASVPNAQPQPSSGGRDQQNHVIRVVPRNAQTASVANAQTQPSSGGQDQWNHVIRVVPH
NAQTASESAARIFRSIQMERKQNDS*

>PV1_Pavir.J05026.1
MRRGLGKDEAPDKVMGPLFPRLHVNDTVKGGPRAPPRNKMALYEQFSVPSHRLSAAAPAPAPAPPWHA
HRPAAGAATSGAPSTSATQAGGSDRPLFPSFCVASTEPVRSSDHMNANSNGNATRAESGRQSTHFKNK
DTNAAGPTADCSSKHRENINRTSSGKKLTNDDDFTVPSVLYSVMPPHSTQEKVTPFPTTSPYNNVAAISKS
STKYSNTDKRHLEGMKVSDAKSRESPGIKEKESAQVRIDLEIEERTSSFQKSKEKLGRQDPKVSSFRDRLN
KYNVVDTKNSEIESYHSKSRKENAVEPQNPPKAKMAPSSKPYADMEQNGNSNMLEHGLRETGEKRKRSP
HGVDQNDDLSDSSVESLPEMEISPNDVVGAIGPNHFWKARRAIVNQQRVFAVQVFELHRLIKVQKLIAASP
HLLIEGDPCLGKSLVTSKKKLPGEDAEKQLQSAKNKDDVQPTLQQLEHTKDNTEANQPSPTQDDVVGVQ

HNNQAAANGAVTSNPPTIPTPDNRQNSWCVPPPPPNQWLVPVMSPSEGLVYKPYTGHCPPAGSFLAPFY
ASCAPVSLPSTAGDFMSSPYGIPMPNQPQHMGVPGPPPMPPMYFPPFSMPVMNTAVSASQQVSHVAAS
RPNGHVEQHSRSSCNMSNLRSEALSAGIWRFHASKGSELQGSSASSPFDRQQGEGRGPAPPFPSSSAG
NVQPQPSTGIRENPGRVIRVVPHTSRTASESAARIFKSIQRERQQNDS*

>PV2_Pavir.Ea01714.1
MTRGGAGGAGEGDASLFPRLRVSDAGRGGGPRAPPRNKMALYEQFTVPPSRFSSSARAAGGSFVPSTS
AGQVYSYDWRLFQPFGAPSNEPARSSEKFKGNSINGQSNSTRRESGRMSSQTKNNDACASKSIAECTSQ
HRVGNVTKNSSAKKLANNDQFMVPSICSPIFSPCSTQGKAGVKDKSRPLSATNPHKNPSMPKSYAECYSA
VNRHLERIDKSDMRSMSCPRAKEKEPVEGSKNVEVQEKSSSKDAKTCQMGGNASHINSSDNPHLGNSE
RQPARMNGSSIEAKSTTKNTVPCKPFTDLNNSNQNSNLLERSLREAGAKRKRGHHDVEQSDHLSDDSVE
CIPSWEVSPDEIVGAIGPKHFWKARRAIQNQQRVFAVQVFELHKLIKVQKLIAASPHLLIEGDPVLGSALVG
KKTKLPKGNLKVQAVAVANKDDIQLTLEQPELSNKNTDANPPSPSRDDGLGGNCQDHAATEETFTRNPPA
MPAAPDNKQNNWCMNPPQNQWLVPVMSPSEGLVYKPYAGPCPPVGSLLTPFYANCTPLRPSSTPYGVP
MPQQPQHMAPPGAPAMHMNYFPPFSMPVMNPGAPASAVKQGRHPAAPQPHGRMEQQSLISCNKSHPS
GIWRFHASRDSEPQASSTSSPFDRIQVQADGSGSVSVFPTATARNARPQPSSGNRDQQNIVIRVVPHNA
QTASESAARIFQSIQKERQQNDL*

>OT1_Oropetium_20150105_04072A
MKRGGCKDEAPDKVMGPLFPRLHVNDTVKGGPRAPPRNKMALYEQFSVPSHRFTTTAPAPAPPWKPHR
PAGGPGSGASSAVPSTSTSQVGGNERPLFPSFCVPSTEPVRSSDHKTTYSNWRTGHAARAESCRKSTQ
LKSRDTYATGPTAGCSSQHRENNLQNSSGKEMTNDDDFTVPSVLYAGMPPHSTQENVRIQEKITPCPPTA
PYKSDSAMSKPSSKCSNTNRRYLEGMIVSDAKSRESPSLKEKEPAKTMRDMDSEERTSSFQISKDKLGRL
DTNVSLYTDRLNNFSYADKQRSDIEGYQAERRKENATETQKHPPKNGTTLSSTPHMDMEQNDSSTLLEH
GLREAGEKRKMSYQDVERKGDLSDSSVDSLPELEISPDDVVSAIGLAQFWKARRAIVHQQKVFAVQIFELH
RLIKVQKSIAASPHVLIEGDPCFGKALVVSKKKLAGGSLGKHLLSSPKSKDDAQPTLQQQEYSKGNTDGKQ
PSPSPDDVAAGVRHDGHCTTNDAVSSNPPVMSTASENKQNSWCIPPPPNQWLVPIMSPSEGLVYKPYTG
PCPPGGSFMAPFYAGCTPVSLPSTAGDFMHSAYGIPMPHQPQHMGVPAGPPMAPMYFPPFSMPVMNH
AASASAVEQVSHVAAWPNGHREQQHSRSSCNMSHLRSEALSAGIWRFHASRDSELQGSSASSPLDRHQ
QGEGRGPAVAPRLAEPSGGNQPLSENRDNIGRVIRVVPHTARTASESAARIFQSIQMERQQSDL*

>OT2_Oropetium_20150105_23950A
MTRVGGGAKGDEATGKVMSPLFPRLHVSDAGRGGGPRAPPRNKMALYEQFTVPSSRFSSSASAGAGGG
GGGLEPSTSASQVYGYERPMFQPFDAPSNVPANSYKRIHGNSMNRQVSSTRNESGRLSSQTNNNGVDA
AGSTVECTPRNRGENVTKNFSGKILAYGDQFMVPSMNSPRCPQLSTQEHAEVQQKLNTLHATSPQRRNP
PATSKSSGKYYSAGNKHLERINISDIRSVTSPNVKEKEQALKNMEAEEIPSIHVSKEKFGSKVAKVCLMTDE
AINSYNSGKPHLEIVGRQSSSMDGCSTKTQNTTASKDTASCNPCSDWDTTNRNSCLPKENLKESGSKRK
KSLEHHDAKQNDDLSDSVESVPGWEIRPEQIVAAIGQKYFWKARGAIQNQQRIFAVQVFELHKLIKVQKSIA
ASPHVLTEGDPCLGNALVGKKLPDGNLKAQTLSIRNKDVIHPSTDQPDLSKENTEGNMRSPSHDDELDGN
RHGPVATNRAFTSNPTTIPTAPGNKQKNWCVNPPQNQWLVPVMSPSEGLVYKPYSGPCPPAGSLLTPFY
ANFAPLSLPSAAFGVPIPHQQQYMALPGTPAMPMNYFPPFTVPVVNPAAPASAVEQGSHAGASQPNGNV
QSRISCNMSNPSGIWKFYASRDSEPQASSASSPSDGLQGDGNGSVSFLPASSIQNAQPHPSSGSRDKQS
HVIRVVPHNAQTASESAARIFRSIQMERRQSDL*

>PH1_Pahal.H01171.1
MTRGGAGPGGGREEQGKVMGPLFPRLHVSDAGRGGGPRAPPRNKMALYEQFTVPSSRFSSSAASARA
AGGSLVPSTSASQVYSYDRPLFQPFDAPSNEPARSSEKFKGNSINGQSNNSTRRESGRMSSQTKNNDAC
ASKSIAACTSQYRVGNVIKNSSVKKVANNDEFMVPSICSPIFSQCSTQGNAGVQDKSRPLSATNPHKNPS
MPKSYAECYNAVNRHLERIDESDMRSMSYPKAKEKEPVEGSKNVEVQEKSSSVQASKEKFKKKDAKTCQ
MGDNASHTNSSDNPNLGNSGRQPARMNGSSIAAKKSTTRNTVPCKPSTDLNNSNQNSNLLERSLREAGA
KRKRGHRNVEQNDDLSDDSVECMPSWEVSPDELVGAIGPKHFWKVRRAIQNQQRVFAVQVFELHKLIKV
QKLIAASPHLLIEGDPVLGSALVGKKTKLPKGNLKVQAVSIANKDDIQLTLEQPELSKQNTDSNPPSPSCDD
GLGGNCQDQAATDETFTRNPLAMPAAPDNKQNDWGMNPPQNQWLVPVMSPSEGLVYKPYAGPCPPVG
SLLTPFYANCTPLRLPSSPYGVPMPQQPQHMAPPGAPAMHMNYFPPFSMPVMNPGAPASAVEQGRHPG
APQPHGRMEQQSLISCNTSHPSGIWRFHASRDSEPQASSASSPFDRIQVQADGSGPVSVFPTAPARNAQ
PQPSYGSRDQQNIVIRVVPHNAQTASESAARIFQSIQMERQQNDL*

>PH2_Pahal.C01693.1
MRRGPGKDEAPDKVMGPLFPRLHVNDTVKGGPRAPPRNKMALYEQFSVPSHRFSAAAPAPAPAPPWHA
HMPAAGVANSGVPSTSASQAGGSDRPLFPSFCVPSTEPVRSSDHMNANSNGLAGNATRAESGRQSTHL
KNKDTNAAGPTADCSSKHRENMNRTSSGKKLTNDDDFTVPSVLYSRMPPHSTQEKVTHFPTTSPYKNVA
AISKSATKCSNTDKRHLEGMKVSDAKSRESPGVKEKEPAKARIDLEIKERTSSFQTSKEKSGRQDPKVSSF
RDRPNKYNVADKQHSEIESYHSKSRKENAVETENPPKAKMAPSSKPYADMEQNGNSDMLEHDLRETGE
KRKRSHHGVEQNDDFSDSSVESLPEMEISPDDVVGAIGPKHFWKARRAIVNQQRVFAVQVFELHRLIKVQ
KLIAASPHLLIEGDPCLGKSLVTSKKKLPGGDDAEMQLQSAKNKDDMQPTLQQLEHTKDNTEANQPSPTQ
DDVVGVQRNNQSAANGAVTSNPPTMPTPDNRQNSWCVPPPSNQWLVPVMSPSEGLVYKPYTGHCPPA
GSFLAPFYASCAPVSLPSTAGDFMGSPYGIPMPHQPQHMGIPGPPPMPPMYFPSFSMPVMNTAVSSSAV
EQVSHVAAKRPNGHVEQHSRTSCNMSNLRSEALSAGIWRFHASKDSELQGSSASSPFDRQQGEGRGPA
PPFPSSSVGNVQPQPSTGSRENPGRVIRVVPHTSRTASESAARIFESIQMERQQNDS*

Appendix 3

Additional figures to accompany chapter 3

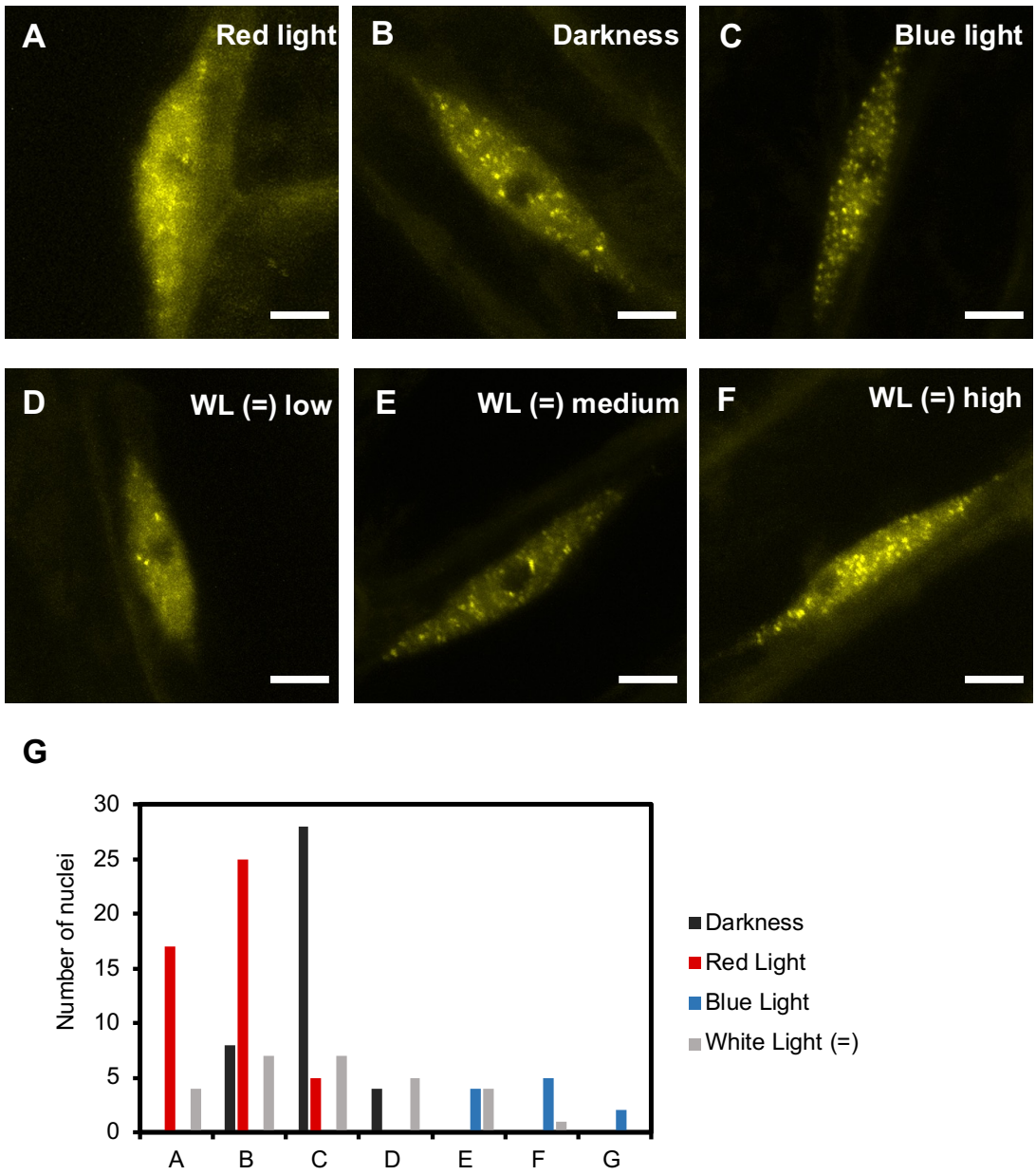

Appendix 3 Figure 1 – Equal ratio red and blue light pulse induce a wide range of foci responses

Nuclei of seven day old seedlings expressing *35S::YFP:ELF3* (*elf3-4*) were imaged at ZT10 after various light pulses that were started at ZT7. Nuclei were pulsed with **(A)** 25 μmol/m^{-2}/s^{-1} of red light (RL) **(B)** transferred to the dark, **(C)** pulsed with 25 μmol/m^{-2}/s^{-1} of blue light (BL) or **(D-F)** pulsed with white light (25 μmol/m^{-2}/s^{-1} of RL and 25 μmol/m^{-2}/s^{-1} of BL). (**D-F**) The spectrum of foci responses seen under WL: **(D)** similar foci response to RL, **(E)** similar to response to samples in the dark and **(F)** similar response to samples pulsed with blue light. **(G)** Histogram plot of the number of foci under the respective light treatment. Bins on the X axis represent: A = 0 – 4, B = 5 – 9, C = 10 – 14, D = 15 – 19, E = 20 – 24, F = 24 – 29, G 30 – 35 foci per nucleus. Data for darkness and RL is the same as in Figure 3.2 of the main text, the data for BL is the same as in Figure 3.3 of the main text and the WL data is the same as presented in Figure 3.4 of the main text.

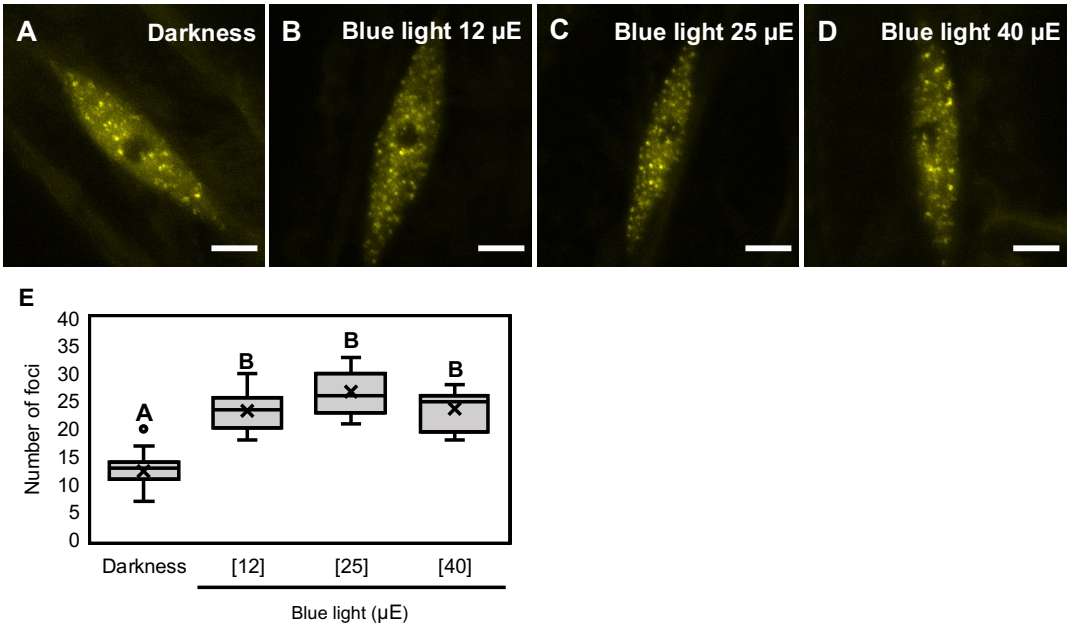

Appendix 3 Figure 2 – Blue light promotes ELF3 sub-nuclear localisation.

Nuclei of seven day old seedlings expressing *35S::YFP:ELF3* (elf3-4) were imaged at ZT10 after being either transferred to the (**A**) dark or pulsed with **(B)** 12 μmol/m^{-2}/s^{-1}, **(C)** 25 μmol/m^{-2}/s^{-1} or **(D)** 40 μmol/m^{-2}/s^{-1} of blue light (BL) for three hours starting at ZT7 (1-hour before dawn, short day photoperiods). **(E)** The number of foci per nucleus. For all treatments, nuclei were counted on at least two separate occasions with multiple biological samples imaged each time. In total, foci were counted in eight images for BL12 and BL40, nine images for BL25 and 40 images for darkness. Significance was determined by a one-way ANOVA with a tukey HSD posthoc test. Different letters signify a significant difference of $p < 0.001$. Scale bars in all images are 5 μm. The darkness data is the same as first presented in figure 3.1, while the BL25 data is the same as presented in figure 3.3.

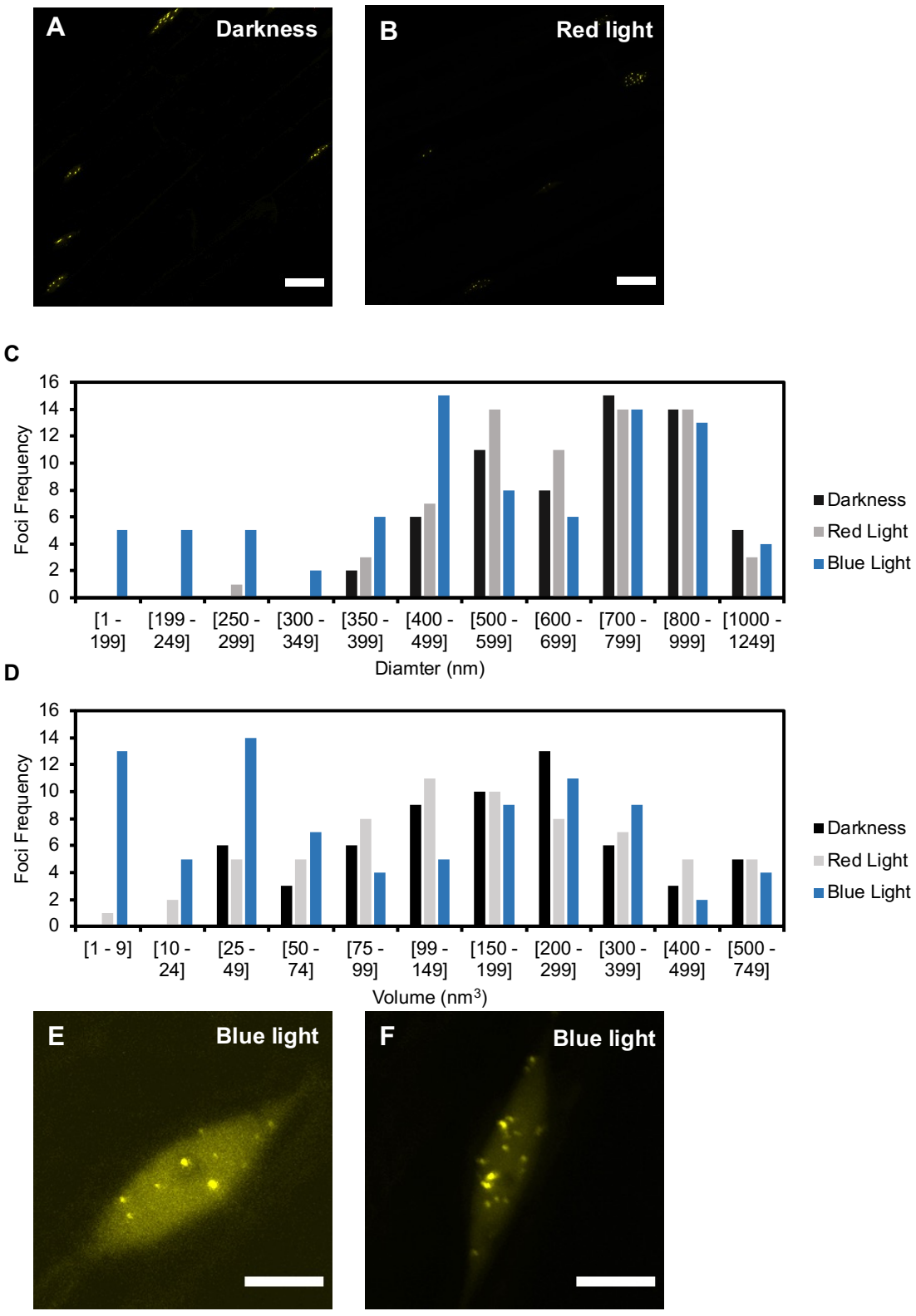

Appendix 3, figure 3 – The cellular and sub-nuclear localisation of ELF3-C under different light treatments

The cellular distribution of *35S::YFP:ELF3C* in 7-day old seedlings either transferred to (**A**) the dark or **(B)** pulsed with 25 μmol/m^{-2}/s^{-1} pulse of red light. Histogram plots of **(C)** diameter or **(D)** volume of ELF3-C foci distribution in the dark (black bars), red light (light grey bars) or blue light (blue bars). Bins on the x-axis state the size distribution of diameter (nm) or volume (nm^3).

Appendix 3, Figure 3 (continued) – A minimum of 60 foci were measured for each respective light treatment in (C-D). **(E-F)** Some ELF3-C nuclei after a 25 μmol/m^{-2}/s^{-1} BL pulse would exhibit nucleoplasmic signal. All light pulses were started at ZT7 (short-day photoperiods, 8/16) and applied for three hours before seedlings were immediately imaged. Scale bars in (A, B) are 25 μm and in (E, F) 5 μm.

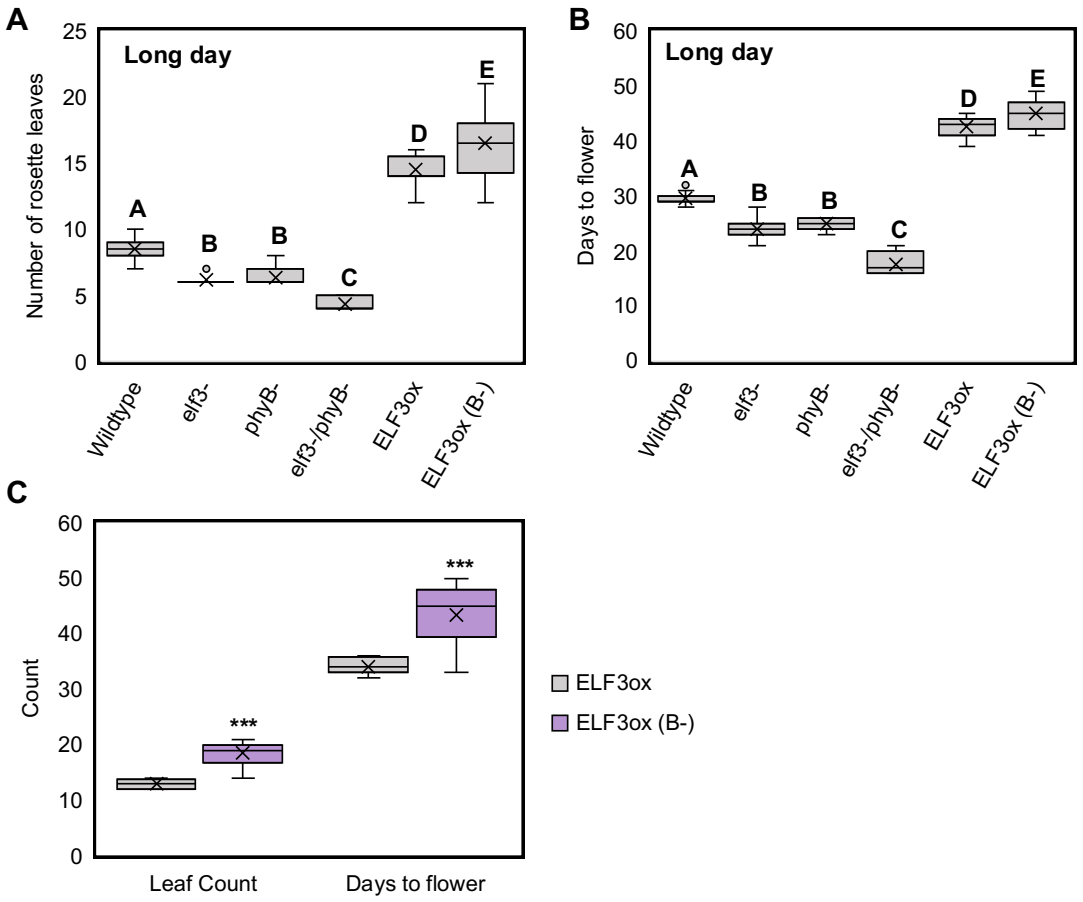

Appendix 3, figure 4 – phyB regulates ELF3's effect on flowering time under long days.

Flowering time of Ws-2, *elf3-4*, *phyB-10*, *elf3-4/phyB-10*, *35S::YFP:ELF3 elf3-4 (ELF3ox)* and *35S::YFP:ELF3 elf3-4/phyB-10* (ELF3ox B-) in long day photoperiods For (**A-B**), plants were first grown under neutral-days (12/12 photoperiod) for 12-days before being transferred to long-day photoperiods, while in **(C)** *ELF3ox* (light grey) and *ELF3ox* (phyB-) (light purple) were directly transferred to long-day photoperiods as seeds in P40 inserts that had been prior stratified for three-days. Flowering was determined as the point at which the floral stem was approximately one centimetre above the rosette. For (A-B), a minimum of 15 plants were analysed for each genotype, while in (C) a minimum of 19 plants were analysed. Significance in (A, B) was determined by a one-way ANOVA with a tukey HSD posthoc test. Different letters signify a significant difference of $p < 0.05$. Significance in (**C**) was determined by a two-way T test, *** = $p < 0.001$. The data in (A, B) forms repeat two and (C) repeat three for the data presented in Figure 3.15D of the main text.

Appendix 4

Additional figures to accompany chapter 4

A

A_thaliana	578	P	A	P	Q	Q	Q	Q	Q	P	T	K	-	-	S	Y	P	R	A	R	K	S	-	-	R	Q
A_lyrata	570	A	A	A	L	Q	H	Q	Q	P	T	K	-	-	S	Y	P	R	A	R	K	S	-	-	R	Q
B_Rapa1	485	A	I	S	-	-	Q	Q	Q	P	T	K	-	-	S	Y	P	R	A	R	K	S	-	-	R	Q
B_Rapa2	516	A	T	S	Q	Q	Q	Q	Q	P	T	K	-	-	S	Y	P	R	A	K	K	S	-	-	R	Q
P_trichocarpa1	608	R	T	Q	K	S	E	A	V	L	E	G	M	-	K	L	R	A	S	K	N	T	-	S	V	Q
P_trichocarpa2	671	S	N	Q	M	S	R	V	I	S	C	C	V	E	N	F	Q	G	L	K	E	S	-	E	I	Q
S_lycopersicum1	549	L	N	Q	K	K	E	N	V	P	D	V	V	-	R	Y	Q	S	T	K	D	N	-	E	V	Q
S_lycopersicum2	614	P	S	N	K	N	G	T	F	P	E	V	-	-	K	S	R	S	C	R	D	A	-	E	M	Q
S_lycopersicum3	499	G	S	E	S	D	G	T	L	P	E	V	V	-	R	L	Y	P	S	R	D	S	-	E	L	H
E_grandis2	593	P	K	Q	R	K	G	S	V	A	Q	I	-	-	K	F	Q	A	N	K	D	S	-	E	L	Q
E_grandis2	623	S	T	Q	V	S	R	V	I	S	C	D	G	L	K	S	P	T	L	K	E	N	-	E	L	Q
M_truncatula1	583	P	V	Q	R	N	G	A	T	T	H	V	M	-	H	H	Q	R	S	K	E	F	-	E	L	Q
M_truncatula2	553	T	N	Q	K	N	G	A	T	L	H	V	R	-	K	P	Q	P	S	R	E	R	-	E	L	E
M_truncatula3	633	S	T	Q	I	S	H	V	M	A	R	N	F	S	P	Y	Q	S	L	E	D	N	K	E	L	Q
O_sativa1	668	S	H	-	-	-	-	-	-	P	S	G	I	W	R	F	H	A	S	R	D	S	-	E	A	Q
O_sativa2	648	S	H	-	-	-	-	-	-	P	S	G	I	W	R	F	H	A	S	R	D	S	-	E	A	Q
Z_mays1	628	S	H	-	-	-	-	-	-	P	S	G	V	W	R	F	L	A	S	R	D	S	-	E	P	Q
Z_mays2	586	S	E	A	-	-	-	-	-	-	-	-	-	-	-	V	L	A	S	R	D	S	-	E	V	Q
S_bicolor1	625	N	M	S	H	-	-	-	-	P	S	G	I	W	R	F	L	A	S	R	D	S	-	E	P	Q
S_bicolor2	642	S	H	L	R	S	E	A	V	S	A	G	V	W	R	V	H	A	S	R	D	S	-	E	L	Q
B_distachyon	635	R	N	-	-	-	E	A	M	S	A	G	I	W	R	F	H	A	S	R	D	S	-	E	L	Q
S_moellendorffii1	657	Q	T	P	Q	P	S	K	L	P	K	S	A	N	S	T	Q	Q	E	Q	Q	E	-	K	-	-
S_moellendorffii2	566	R	Q	Q	H	Q	E	P	R	Q	K	L	V	G	R	F	C	G	E	K	Q	S	-	G	G	E

B

O_sativa1	335	H	Y	N	L	P	Q	G	G	I	E	E	T	G	T	K	R	K	R	L	L	E
O_sativa2	330	H	C	N	L	P	Q	G	G	L	K	E	A	G	T	K	R	K	R	L	E	A
S_bicolor1	326	D	S	D	I	L	K	H	G	L	R	D	T	G	E	K	R	K	R	S	-	-
S_bicolor2	317	N	S	N	L	L	E	R	S	P	R	E	G	G	A	K	R	K	R	Q	-	-
S_italica1	335	N	S	D	L	L	E	L	G	L	R	E	T	G	E	K	R	K	R	S	-	-
S_italica2	332	N	S	N	L	L	D	R	S	L	R	E	A	G	S	K	R	K	R	G	-	-
P_virgatum1	332	N	S	N	L	L	D	R	S	L	R	E	A	G	S	K	R	K	R	G	-	-
P_virgatum2	334	N	S	D	L	L	E	L	G	L	R	E	T	G	E	K	R	K	R	S	-	-
P_halli1	331	N	S	N	L	L	E	R	S	L	R	E	A	G	A	K	R	K	R	G	-	-
P_halli2	331	N	S	D	M	L	E	H	D	L	R	E	T	G	E	K	R	K	R	S	-	-
Z_mays1	309	G	D	S	D	L	L	G	H	L	R	E	T	G	V	K	R	K	R	S	-	-
Z_mays2	320	K	S	N	L	L	E	R	S	P	R	E	V	G	A	K	R	K	R	G	-	-
H_vulgare	328	A	S	N	L	S	E	K	G	L	R	E	T	G	E	K	R	K	R	S	T	G
B_distachyon	320	A	S	N	L	L	E	K	G	L	R	V	T	G	E	K	R	K	R	S	E	G
Oropetium_T1	339	S	S	T	L	L	E	H	G	L	R	E	A	G	E	K	R	K	M	S	-	-
Oropetium_T2	329	N	D	C	L	P	K	E	N	L	K	E	S	G	S	K	R	K	K	S	L	E

Appendix 4, Figure 1 – Protein alignments of ELF3 nuclear localisation signals

(A) Protein alignment of ELF3 sequences from across the tracheophyte plant clade. Colouration highlights the previously reported nuclear localisation signal (NLS) first reported in Liu *et al*., 2001. **(B)** Protein alignment of the ELF3 monocotyledon NLS signal identified using the NLS database tool (https://rostlab.org/services/nlsdb/). Colouration highlights the residues predicted by the NLS database to form an NLS motif in the respective protein sequence. Protein sequences were either accessed from TAIR (www.arabidopsis.org) or Phytozome (www.phytozome.jgi.doe.gov/pz/portal.html) and subsequently aligned with MAFFT as described in chapter 2, section 10. The numbers in the image reference the position of the first listed amino acid in each respective protein sequence.

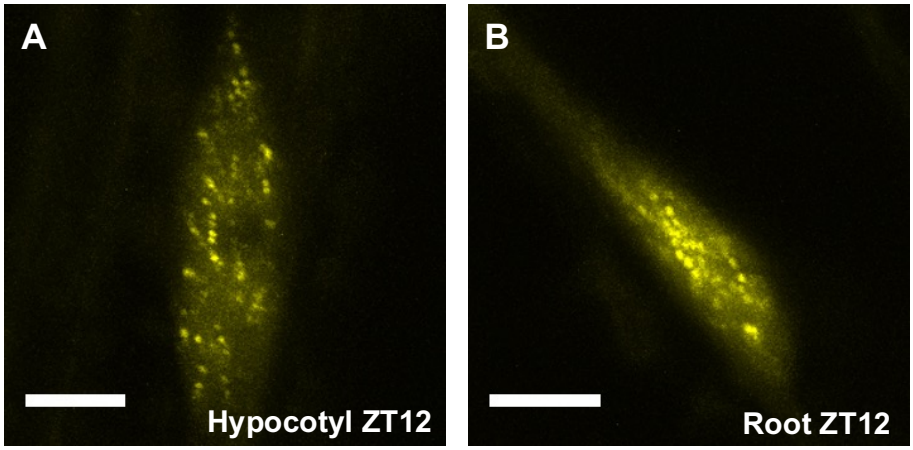

Appendix 4, Figure 2 – The sub-nuclear localisation of ELF3 at ZT12

The localisation of *35S::YFP:ELF3* (*elf3-4*) at ZT12 in (**A**) hypocotyl or (**B**) root nuclei at ZT12. Images are representative of data that is presented in chapter 4, figure 8. Scale bars are equal to 5 μm.

Abbreviations

Aa	Amino acid
ACE	ACGT-containing element
amiRNA	artifical microRNA
BBX	B-BOX PROTEIN
BIODARE	Biological Data Respository
BL	BLUE LIGHT
BLASTP	Basic local alignment search tool protein
BOA	BROTHER OF LUX ARRYTMO
BRASS	Biological Rhythm Analysis Software
CCA1	CIRCADIAN CLOCK ASSOCIATED1
CBF1	C-REPEAT/DRE BINDING FACTOR1
CBS	CCA1 binding site
CCR2	CLOCK AND COLD REGULATED2
CDFS	CYCLING DOF FACTORS
CFP	Cyan fluorescent protein
CHE	CCA1-HIKING EXPEDITION
CO	CONSTANS
CORE	COLD RESPONSIVE ELEMENT
COP1	CONSTITUTIVELY PHOTOMORPHOGENIC1
CRY	CRYPTOCHROME
CWL	Constant white light
DEB	DNA extraction buffer
EAR	Ethylene amphiphilic repression
EE	Evening element
ELF3	EARLY FLOWERING3
ELF3 (4+)	35S::YFP:ELF3 (elf3-4)
ELF3 (4-)	35S::YFP:ELF3 (elf3-4/elf4-1)
ELF3 (B+)	35S::YFP:ELF3 (elf3-4)
ELF3 (B-)	35S::YFP:ELF3 (elf3-4/phyB-10)
ELF3C	35S::YFP:ELF3C
ELF3F	35S::YFP:ELF3
ELF3MC	35S::YFP:ELF3MC
ELF4	EARLY FLOWERING4
EC	Evening complex
FAR1	FAR-RED IMPAIRED RESPONSE1
FHY3	FAR-RED ELONGATED HYPOCOTYL3
FKF1	FLAVIN BINDING, KELCH REPEAT F-BOX1
FRL	Far-red light
FT	FLOWERING LOCUS T
GFP	Green fluorescent protein

GI	GIGANTEA
GL	Green light
H3Ac	Acetlyation of histone 3
H3K4me3	Tri-methylation of lysine 4 on HISTONE 3
H3K6me2	Di-methylation of lysine 6 on HISTONE 3
H3K9Ac	Acetylation of lysine 9 on HISTONE 3
H3K9me3	Tri-methylation of lysine 9 on HISTONE 3
H3K14Ac	Acetlyation of lysine 14 on HISTONE 3
H3K27me3	Tri-methylation of lysine 27 on HISTONE 3
H3K56Ac	Acetylation of lysine 56 on HISTONE 3
H3T3	Phosphorylation of threonine 3 on HISTONE 3
HDA	HISTONE DEACETYLASE
HOS15	HIGH EXPRESSION OF OSMOTICALLY RESPONSIVE GENES15
HSP90	HEAT SHOCK PROTEIN90
HY5	ELONGATED HYPOCOTYL5
HYH	HY5-HOMOLOG
LBS	LUX binding site
LD	Long days
LDL	LYSINE DEMETHALYSE
LHCB	LIGHT HARVESTING CHLOROPHYLL A/B-BINDING PROTEIN1.1
LHY	LATE ELONGATED HYPOCOTYL
LKP2	LOV KELCH PROTEIN2
LOV	LOV KELCH
LNK	LIGHT-INDUCIBLE AND CLOCK REGULATED
LUC	LUCIFERASE
LUX	LUX ARRYTHMO
LWD	LIGHT REGULATED WD
MES	2-(*N*-morpholino)ethanesulfonic acid.
MS	Murashige and Skoog
MLK	MUT9 LIKE KINASE
N/C	Nuclear/cytoplasmic ratio
NLS	Nuclear localisation signal
NRTCs	No reverse-transcriptase controls
NTCs	No template controls
OX	Over-expressor
PCH1	PHOTOPERIODIC CONTROL OF HYPOCOTYL1
PCHL	PCH1-LIKE
PIF	PHYTOCHROME INTERACTING FACTOR
PML	Promyelocytic leukemia bodies
PPK	PHOTOREGULATORY PROTEIN KINASES
Phy	PHYTOCHROME
PRR	PSEUDO RESPONSE REGULATOR

PPT	Phosphinothricin
Pro	Promoter
PTFLs	Post-translational feedback loops
R.A.E	Relative amplitude error
RFP	Red fluorescent protein
RL	Red light
RT	Reverse transcriptase
RVE	REVEILLE
SCF	Skp/Cullin/F-box
SD	Short days
SEF1	SERRATED LEAVES AND EARLY FLOWERING1
SWR1	SWI2/SNF2-RELATED
TBE	Tris borate EDTA
TCP	TEOSINTE BRANCHED CYCLOPEDIA-PCF
TF	Transcription factor
TFL1	TERMINAL FLOWER1
TOC1	TIMING OF CAB EXPRESSION1
TPL	TOPLESS
TTFL	Transcriptional-translational feedback loops
TZP	TANDEM ZINC KNUCKLE PROTEIN
UBP	UBIQUITIN BINDING PROTEIN
UVR8	UV RESISTANCE LOCUS8
WL	White light
YFP	Yellow fluorescent protein
ZT	*Zeitgeber* time
ZTL	ZEITLUPE